Toxic Chemical and Biological Agents

Detection, Diagnosis and Health Concerns

Edited by
Giovanni Sindona
Joseph H. Banoub
Maria Luisa Di Gioia

Springer

NATO
OTAN

This publication is supported by: The NATO **Science** for **Peace** and **Security** Programme

Toxic Chemical and Biological Agents

NATO Science for Peace and Security Series

This Series presents the results of scientific meetings supported under the NATO Programme: Science for Peace and Security (SPS).

The NATO SPS Programme supports meetings in the following Key Priority areas: (1) Defence Against Terrorism; (2) Countering other Threats to Security and (3) NATO, Partner and Mediterranean Dialogue Country Priorities. The types of meeting supported are generally "Advanced Study Institutes" and "Advanced Research Workshops". The NATO SPS Series collects together the results of these meetings. The meetings are co-organized by scientists from NATO countries and scientists from NATO's "Partner" or "Mediterranean Dialogue" countries. The observations and recommendations made at the meetings, as well as the contents of the volumes in the Series, reflect those of participants and contributors only; they should not necessarily be regarded as reflecting NATO views or policy.

Advanced Study Institutes (ASI) are high-level tutorial courses to convey the latest developments in a subject to an advanced-level audience.

Advanced Research Workshops (ARW) are expert meetings where an intense but informal exchange of views at the frontiers of a subject aims at identifying directions for future action.

Following a transformation of the programme in 2006, the Series has been re-named and re-organised. Recent volumes on topics not related to security, which result from meetings supported under the programme earlier, may be found in the NATO Science Series.

The Series is published by IOS Press, Amsterdam, and Springer, Dordrecht, in conjunction with the NATO Emerging Security Challenges Division.

Sub-Series

A.	Chemistry and Biology	Springer
B.	Physics and Biophysics	Springer
C.	Environmental Security	Springer
D.	Information and Communication Security	IOS Press
E.	Human and Societal Dynamics	IOS Press

http://www.nato.int/science
http://www.springer.com
http://www.iospress.nl

Series A: Chemistry and Biology

Toxic Chemical and Biological Agents

Detection, Diagnosis and Health Concerns

edited by

Giovanni Sindona

Department of Chemistry and Chemical Technology
University of Calabria
Arcavacata di Rende, Italy

Joseph H. Banoub

Special Projects Science Branch
Fisheries and Oceans Canada
St. John's, Newfoundland and Labrador, Canada

and

Maria Luisa Di Gioia

Department of Pharmacy, Health and Nurture Science
University of Calabria
Rende, Italy

Dedicated to the Memory of Professor Giovanni Sindona

Professor Giovanni Sindona

Professor Giovanni Sindona, Department of Chemistry, University of Calabria (Italy), died on Thursday, January 16, 2020. We have lost a dear friend, a scholar, and a gentleman. Giovanni was born in Messina, Italy, on April 9, 1949, and graduated with a B.Sc. (Hons) Chemistry in 1972 from the University of Messina. After completing his Ph.D., Professor Sindona applied for bioanalytical chemistry (mass spectrometry).

In 1978, he was awarded the "Alexander von Humboldt Foundation Fellowship" by the renowned Institute für Physikalische Chemie at Bonn University. At the beginning of the 1980s, Professor Sindona became a NATO scholar at King's College London under the direction of Professor Colin B. Reese where he developed new strategies for the synthesis of nucleic acids.

In 1990, he became Full Professor of Organic Chemistry at the University of Calabria and the University of Magna Graecia Catanzaro teaching organic chemistry. Throughout his academic career, he held important management positions: Dean of Mathematics, Physics, and Natural Sciences faculty from 1994 to 1997. Professor Sindona directed the Department of Chemistry from 1997 to 2003 and from 2007 to 2015 during the establishment of the former Department of Chemistry and Chemical Technologies.

Between 1990 to 2019, Professor Sindona organized and directed five NATO International Schools for young researchers on the application of mass spectrometry to biomolecular chemistry in Italy and abroad. In 2009, he became Co-director of NATO-ASI, Science for Peace and Security Programme for experts on the Detection of Biological Agents and Toxins for the Prevention of Bioterrorism in Homeland Security.

Professor Sindona has been a member of the Italian Society of Chemistry (SCI), where he was President of the Mass Spectrometry Division and coordinator of the interdivisional group of proteomic. He was

President of the SCI Calabria section, and from 1979 he was permanent member of the Alexander von-Humboldt Foundation. Professor Sindona was member of the American Society of Mass Spectrometry since 1990. He was awarded the "Piria Award for research" in 2008, and in 2011 he received the international award "Il Bergamotto" for his studies on the research activity linked to Calabria region.

Rest in peace old friend and travel safely through the universe.

Joseph H Banoub (Canada)
Leonardo Di Donna (Italy)

Preface

This new book entitled *Detection, Diagnosis and Health Concerns of Toxic Chemical and Biological Agents: Mass Spectrometry and Allied Topics* represents the main lectures given at the NATO ASI (Advanced Study Institute), which was held successfully at the Grand Hotel San Michele, Cetraro, Italy, from September 29 to October 5, 2019.

First of all, this NATO-ASI would have not been possible without the excellent help and coordination from the NATO Science Committee of the Science for Peace and Security (SPS) Programme. This NATO-ASI was organized by the two Co-directors—Professor Giovanni Sindona (Univ. of Calabria) and Professor Marc Suter (EAWAG)—and members of the Organizing Committee—Joseph Banoub (Fisheries & Oceans Canada), Richard Caprioli (Vanderbilt Univ.), Maria Luisa Di Gioa (Univ. Calabria), and Gianluca Giorgi (Univ. of Siena).

We all were truly saddened by the untimely death of Professor Giovanni Sindona, several months after this NATO-ASI. We decided to dedicate this NATO-ASI to the memory of Professor Sindona, who, besides being one of the best scientist in Italy, was also a real pioneer in organizing similar NATO-ASI meetings in the last decades.

This NATO-ASI meeting opening session was presented by the "Al Maginifico" Rettore, Della Universita Di Calabria, the Professor Gino Cressi and the General Commander Gerardo Sica Della Assozione Nationale Carabinieri Di Cozenza. This meeting began with a presentation by Dr. Joseph Banoub (Fisheries and Oceans Canada) describing the NATO Science for Peace and Security Programme to the audience, a quick tour in the history of the NATO-ASI Scientific Programme and its past and present successes. We are indebted to Professor Caprioli who was instrumental in inviting the best lecturers and to avail secured funding from the manufacturers.

The topics to be covered include detection and effect of exposure of biological agents and new innovative molecular detection technologies. In general, the main topics discussed involved the following: risks and consequences of chemical and biological agents to human health in general with special emphasis on all the biochemical and metabolic pathways including the productive systems. The exposome, genetic risk, and environment, the various health hazard agents, risk assessment,

environmental assessment and preparedness, and analysis of sublethal effects at the molecular level were examined.

The participants were introduced to the state-of-the-art biological agent detection systems using soft-ionization mass spectrometry, tandem mass spectrometry, and biological sensors and their efficacy in measuring very low concentrations (pico- to femtomoles). Primary considerations in quantitative analysis with a focus on MS and MS/MS and the role of MS and ion mobility on metabolomics were also presented.

A discussion on several types of food bacteria, such as *Salmonella, Campylobacter*, and *Enterohemorrhagic Escherichia coli*, which are among the most common food-borne pathogens that could be used as a terror agent, took place. Their detection and disease treatment were also defined.

In addition, the participants were also introduced to the different modes of tandem mass spectrometry such as DDA and DIA scans.

Furthermore, a general description of the category A bacterial bioagents *Bacillus anthracis* (anthrax) *Yersinia pestis* (plague) *Francisella tularensis* (tularemia), which are responsible for the transmission, dissemination and causing high mortality rates and create panic in the public will be presented. Medical treatment was conferred for symptoms. Considering that these biological agents may be engineered to have multi-antibiotic resistance, prevention using synthetic neoglyconjugate vaccines was also examined.

Finally, the participants were initiated to the novel field of imaging mass spectrometry, which allows for the mapping of disease biomarkers and metabolic changes in tissue and single cells.

All the participants who attended this NATO-ASI were graduate students, postdoctoral fellows and faculty, and military scientists. The participants presented short oral presentations and posters. In addition, all participants were given the opportunity to have their contribution ready for publishing in *NATO Science for Peace and Security Series A: Chemistry and Biology* (Springer) as short note.

St Johns, NL, Canada   Joseph H. Banoub
Cosenza, Calabria, Italy   Maria Luisa Di Gioa

Contents

Contents

Chapter 1
Evaluation of Quality and Safety of Foods by Tandem Mass Spectrometry

Giovanni Sindona and Leonardo Di Donna

Abstract Mass spectrometry (MS) is one of the most interesting analytical approaches in food analysis. Its application in food research is addressed to authenticity assessment (geographic origin, adulterations). In this chapter we discuss the modern applications of mass spectrometry for the correct evaluation of quality and safety parameters of foodstuff. Specific applications in food chemistry are presented which allow the identification of origin, quality and safety of foodstuffs. We also reiterate the uses of tandem mass spectrometry as a powerful tool for the determination of molecular quality markers in food, which is a very powerful analytical tool for the analysis achieved. When used in conjunction with stable isotope dilution analysis, it becomes the landmark between the analytical techniques used in food analysis.

Keywords Tandem mass spectrometry · Stable isotope dilution analysis · Quality markers in food · Selected reaction monitoring

1.1 Introduction

Mass spectrometry (MS) is one of the most interesting analytical approaches in food analysis. Its application in food research is addressed to authenticity assessment (geographic origin, adulterations) [1, 2], quality control (nutritional value, product traceability, sensory control) [3] and safety control (toxins formed during food processing, fungal and bacterial toxins, foodborne pathogens, pesticides, biopesticides etc.) [4, 5].

G. Sindona · L. Di Donna (✉)
Dipartimento di Chimica e Tecnologie Chimiche, Università della Calabria, Rende, CS, Italy
e-mail: l.didonna@unical.it

The analysis of complex mixtures is often facilitated by tandem mass spectrometry (MS/MS). The importance of multiple-stage mass spectrometry is well established for characterization of particular compounds using product ion scans [6], for recognizing members of families of compounds using neutral loss [7] and precursor ion scans [8], for the determination of chemical-physical properties [9] and certainly for quantification purposes [10].

The current logic of market safety and quality control is often based on the application of old, and frequently useless, analytical approaches that do not provide complete and well-meaning responses. The identification and dosage of micro and semi micro active principles present even in routine foods, requires methods that allow the correct determination of molecules in often very complex mixtures. Unfortunately, methods such those based on mass spectrometry are often still not applied since they are considered too expensive; one pretext for this not-scientific attitude is, apparently, related to the costs of recent developed new instrumentation. Nowadays, methodologies such as mass spectrometry have reached a degree of performance which allows a real and full characterization of the samples. It can be demonstrated that the cost of a full and complete analysis can be carried out on milligrams of samples and the results extended to large amounts, thus putting the cost at the very low level when spread on the entire batch. The aims of this contribution is therefore to favour the creation worldwide of proper analytical laboratory that could provide scientific methods to guarantee environmental control and suitable and safety protocols to those industries active in this field.

This chapter deals with modern applications of mass spectrometry which describe the correct evaluation of quality and safety parameters of foodstuff. Each single contribution was presented at the NATO ASI 9845535, held in Cetraro (Italy) at the beginning of October 2019. Specific applications in food chemistry are presented which allow the identification of origin, quality and safety of foodstuffs.

1.2 Results and Discussion

1.2.1 Determination of Oleuropein in Olive Oil

The first example of food quality assessment is given by the determination of Oleuropein (OLP) in extra virgin olive oil by APCI-MS/MS performed on a triple quadrupole system [11]. Oleuropein is a secoiridoid belonging to the family of phenols present in olive oil. It is believed to have some health and pharmacological activities [12, 13]. The method is based on a classical approach used in mass spectrometry, and relies on the use of flow injection analysis aided by selected reaction monitoring (SRM) analysis and labelled internal standard. The main advantage of this approach is the lack of on-line chromatographic steps, which speeds up the time of analysis. In particular, the analyte oleuropein is extracted, together with a known amount of trideuterated synthetic oleuropein, from the olive oil matrix by a solid

phase extraction step performed through a C_{18} cartridge. The recovered methanol solution containing both OLP and d_3-OLP is then injected directly in the APCI source and analyzed in SRM, monitoring the appropriate fragmentation. The key points of this approach are:

(i). the use of a suitable labeled internal standard:

Regarding this point, it is important (even in the perspective of a possible wide application of the method) to easily obtain the labeled molecule by simple synthetic procedures. The method describes the synthesis of d_3-OLP starting from demethyoleuropein (previously recovered and purified by a polar extract of olives) and CD_2N_2 (Fig. 1.1).

It is important to achieve the highest grade of isotopic purity of the labelled internal standard in order to avoid inaccurate quantification of the analyte. Figure 1.2 shows the comparison between the high resolution signals from protonated OLP and d_3-OLP. It can be seen that the isotopic purity of the internal standard is above 97%.

(ii). The selection of the appropriate fragmentation reaction:

The fragmentation pattern of oleuropein is rather straightforward (Fig. 1.3). The molecule is composed of three moieties: the glucose ring, whose loss generate the ions at m/z 361, 379 (364, 382 for d_3-OLP), the hydroxytyrosol portion which generates the ion at m/z 137, and the elenolic acid which is the core of the molecule. The most responsive ion in both analyte and internal standard MS/MS spectra is the tyrosyl ion (m/z 137) which is particularly stable due to its aromatic character. The fragmentation energy may be optimized to maximize the signal intensity.

(iii). the determination of analytical parameters.

In this type of approach the most important analytical parameters to test are of course the accuracy, the limit of quantitation (LOQ) and the limit of detection (LOD). These aspects may be verified by using an artificially fortified matrix which

Fig. 1.1 Synthesis of d3-Oleuropein
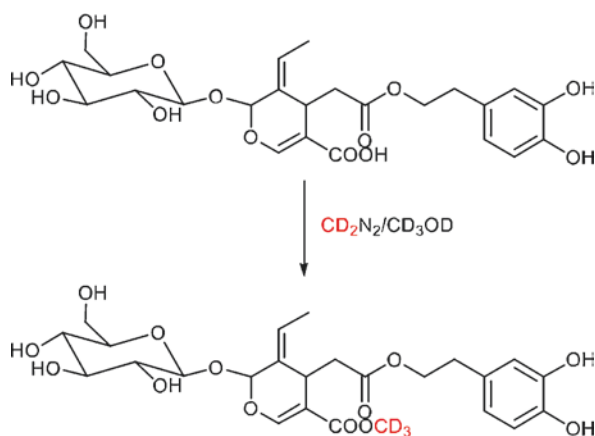
Fig. 1.2 High resolution pseudomolecular ion signal of OLP (A) and d_3-OLP (B)
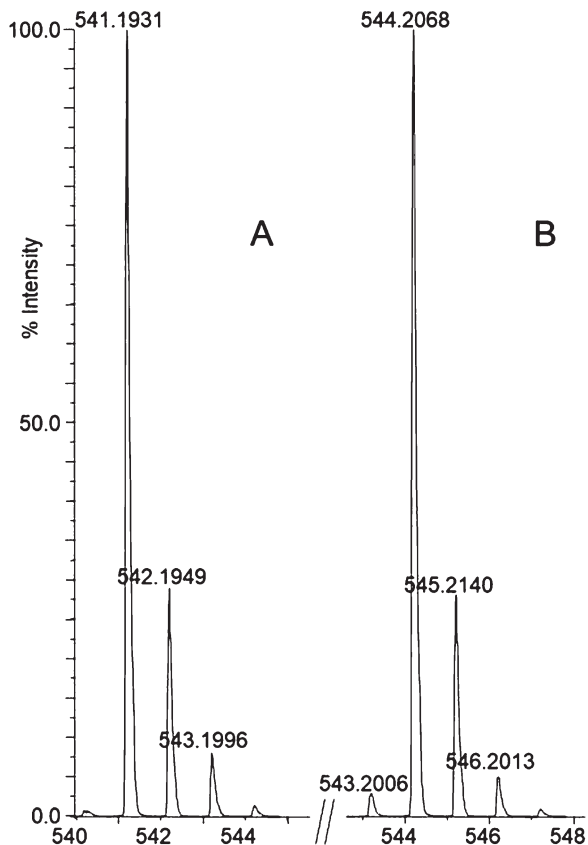
should be as much as similar to the real sample. In the determination of oleuropein the matrix test used was the corn oil which is substantially identical to extra virgin olive oil except for the absence of phenols; fortifying this matrix with a known amount of analyte and internal standard and submitting the sample to all the experimental steps, a value near the theoretical amount added should be obtained. Accuracy values in the range 85–115% are generally accepted.

1.2.2 Assessment of Resveratrol Amount in Red Wine

The use of labelled internal standard, in conjunction with tandem mass spectrometry, represents a big improvement of analytical performances in the determination of quality markers in food. On the other hands, there are cases in which combining this two techniques may create some complications. The determination of resveratrol performed by Di Donna et al. [14] has been performed using the labelled
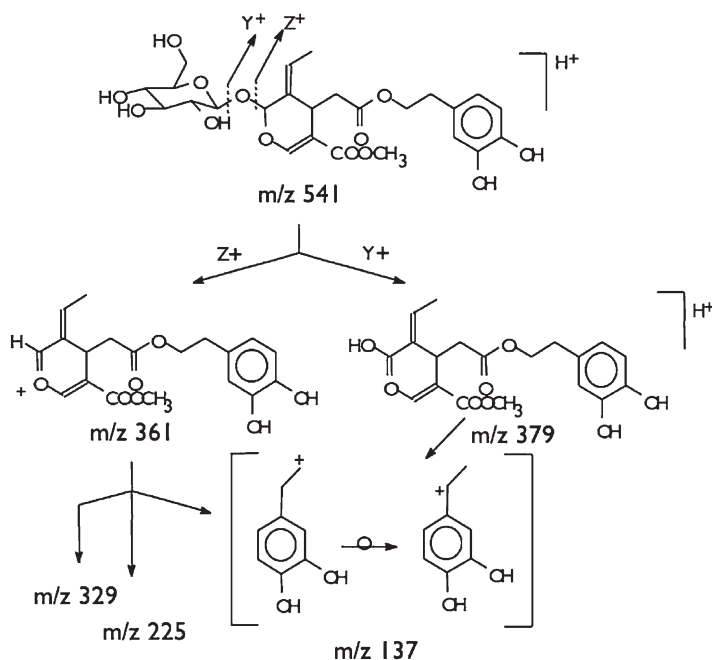
Fig. 1.3 Fragmentation of oleuropein

d_4-reveratrol as internal standard, synthesized "ad hoc" by a simple coupling reaction starting from synthons properly prepared (Fig. 1.4).

The purpose of the authors was to assay the amount of resveratrol in red wine in a triple quadrupole instrument working in SRM mode. Surprisingly, the authors realized that d_4-reveratrol could not be used in the analysis because of an unusual gas-phase fragmentation behavior of the internal standard respect to d_0-reveratrol (Fig. 1.5).

The fragmentation pattern of labelled resveratrol was ascribed to hydrogens hopping through the carbon skeleton of the highly conjugated resveratrol molecular ion prior the fragmentation. This is obviously not visible in the MS/MS spectrum of d_0-reveratrol, while it became evident when deuteria are placed on one of the two rings. The problem can be overcome by using a different type of internal standard, i.e. resveratrol enriched by ^{13}C on the carbon backbone as reported recently for the determination of resveratrol by PS-MS/MS [15].
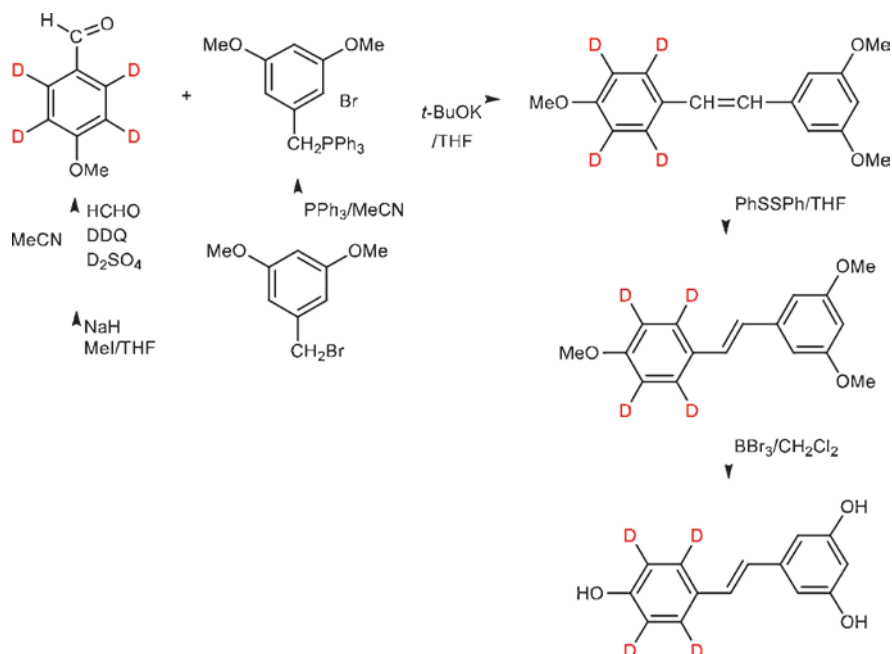
Fig. 1.4 Synthesis of d_4-reveratrol

1.2.3 Determination of Phenylethanoids in Extra Virgin Olive Oil

Sometimes it may be challenging to develop a method based on isotope standard dilution analysis, simply because of the lack of commercial suitable isotopic standards and/or because their synthesis is very tedious, if not impossible. This is the case of the determination of hydroxytyrosol and tyrosol derivatives in extra virgin olive oil [16]. According to a recent international regulation [17], these compounds may be considered molecular quality markers which increase the value added of the oil. The regulation states, in fact, that the presence of these compounds, above the concentration threshold of 5 mg per 20 g, allows the producer to report on the main label of the food a sentence which summarizes the health effect concerning its antioxidant effects. The family of this phenols comprises the free alcohols tyrosol and hydroxytyrosol, and their ester dialdehydic derivatives; although it is quite easy to synthesize the deuterated analogues of the free alcohols, the structural complexity of the esters makes difficult to obtain stable isotopomers. Bartella et al. [16] proposed the MS/MS analysis of the simple tyrosol and hydroxytyrosol using the homologue deuterated compounds as internal standards, after a simple and fast hydrolytic step. The method relies on a two-steps analysis performed on the polar extract of extra virgin olive oil (Fig. 1.6): in the first step the extract is analyzed "as is" in the presence of the internal standards using an electrospray triple quadrupole
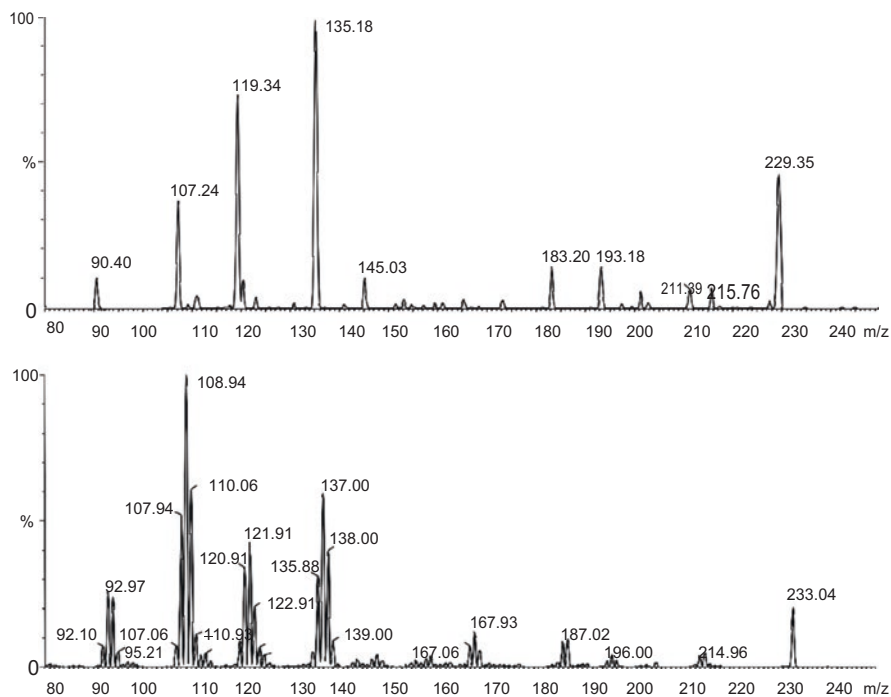
Fig. 1.5 Comparison of ESI (+)-MS/MS spectra from d_0-resveratrol (top) and d_4-reveratrol (bottom) pseudomolecular ion
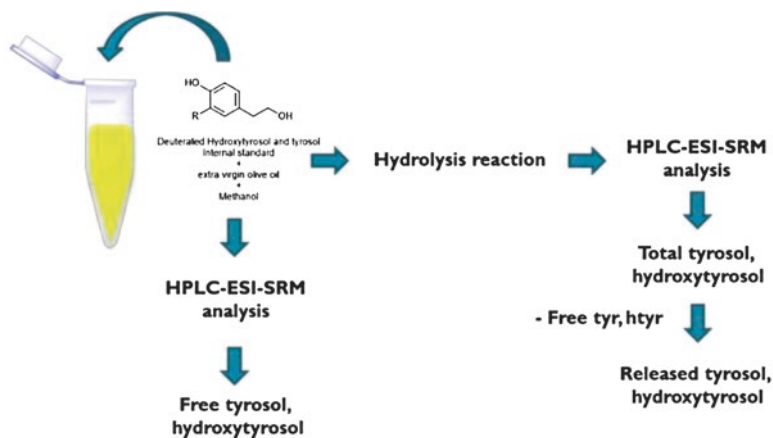
Fig. 1.6 Proposed methodology for the assay of tyrosol and hydroxytyrosol derivatives in olive oil

mass spectrometer working in SRM mode. This step allows the determination of the free fraction of the alcohols. In the second step, the polar fraction is submitted to a simple hydrolytic step in a microwave oven under standardized conditions and strong acidic conditions; the resulting reaction mixture containing the amount of alcohols released by the esters, together with the free content, is submitted to the HPLC-ESI-SRM experiment. Combining the data of the two steps, it is possible to calculate the amount of phenols as requested by the regulation. In this way, the drawback of the absence of appropriate internal standards is overcome by the hydrolytic reaction step.

1.2.4 Application of PS-MSMS for the Determination of Quality Markers in Foodstuff

A new interesting approach for the determination of quality markers in food is based on the use of paper spray tandem mass spectrometry (PS-MS/MS). The main advantage of this relatively new type of ionization source is the possibility to avoid tedious purification steps prior the mass spectrometric analysis. PS source is rather easy to set-up: it consists of a stainless steel clip on which a high voltage of some kV is applied; the clip is connected to a triangular piece of porous paper (usually filter paper) soaked with the dried sample. By spotting few microliters of a polar solvent, usually methanol, the ions are generated at the tip of the paper and directed towards the analyzer. The main drawback of this methodology is the poor reproducibility of the signal, due to the presence of a high background ions level. Tandem mass spectrometry in SRM mode lowers strongly the noise providing good analytical performances. On the other hand, the use of isotopic standards surely increases either the accuracy and LOQ and LOD values. PS-MS/MS has been applied with good results for the determination of vitamin E in extra virgin olive oil [18], resveratrol in wine [15] and methylxanthines alkaloids in coffee, cocoa products and drugs [19, 20], but also for the determination of phenylethanoids in olive oil [21]. All the above methodologies are very rapid, having time of analysis reduced to two/four minutes only.

1.3 Conclusions

Tandem mass spectrometry is a powerful tool for the determination of molecular quality markers in food. The superior capacity of MS/MS is due to the high specificity of analysis achieved. When used in conjunction with stable isotope dilution analysis, it becomes the landmark between the analytical techniques used in food analysis. The criticism usually reported, which describes the technique as too expensive is, in effect, groundless if one considers that usually the samples analyzed belongs to large production batches, and the cost of a single analysis is diluted in the price of the final product.

References

1. Herrero M, Simõ C, García-Cañas V, Ibáñez E, Cifuentes A (2012) Foodomics: MS-based strategies in modern food science and nutrition. Mass Spectrom Rev 31(1):49–69. https://doi.org/10.1002/mas.20335

2. Benabdelkamel H, Di Donna L, Mazzotti F, Naccarato A, Sindona G, Tagarelli A, Taverna D (2012) Authenticity of PGI "clementine of Calabria" by multielement fingerprint. J Agric Food Chem 60(14):3717–3726. https://doi.org/10.1021/jf2050075

3. Ibáñez C, Simó C, García-Cañas V, Cifuentes A, Castro-Puyana M (2013) Metabolomics, peptidomics and proteomics applications of capillary electrophoresis-mass spectrometry in foodomics: a review. Anal Chim Acta 802:1–13. https://doi.org/10.1016/j.aca.2013.07.042

4. de Koster CG, Brul S (2016) MALDI-TOF MS identification and tracking of food spoilers and food-borne pathogens. Curr Opin Food Sci 10:76–84. https://doi.org/10.1016/j.cofs.2016.11.004

5. Mazzotti F, Di Donna L, Macchione B, Maiuolo L, Perri E, Sindona G (2009) Screening of dimethoate in food by isotope dilution and electrospray ionization tandem mass spectrometry. Rapid Commun Mass Spectrom 23(10):1515–1518. https://doi.org/10.1002/rcm.4011

6. Di Donna L, Mazzotti F, Salerno R, Tagarelli A, Taverna D, Sindona G (2007) Characterization of new phenolic compounds from leaves of olea europaea L. by high-resolution tandem mass spectrometry. Rapid Commun Mass Spectrom 21(22):3653–3657. https://doi.org/10.1002/rcm.3262

7. Schwartz JC, Wade AP, Enke CG, Graham Cooks R (1990) Systematic delineation of scan modes in multidimensional mass spectrometry. Anal Chem 62(17):1809–1818. https://doi.org/10.1021/ac00216a016

8. De Hoffmann E (1996) Tandem mass spectrometry: a primer. J Mass Spectrom 31(2):129–137. https://doi.org/10.1002/(SICI)1096-9888(199602)31:2<129::AID-JMS305>3.0.CO;2-T

9. Di Donna L, Napoli A, Sindona G, Athanassopoulos C (2004) A comprehensive evaluation of the kinetic method applied in the determination of the proton affinity of the nucleic acid molecules. J Am Soc Mass Spectrom 15(7):1080–1086. https://doi.org/10.1016/j.jasms.2004.04.027

10. Di Donna L, Bartella L, Napoli A, Sindona G, Mazzotti F (2018) Assay of lovastatin containing dietary supplement by LC-MS/ MS under MRM condition. J Mass Spectrom 53(9):811–816. https://doi.org/10.1002/jms.4202

11. De Nino A, Di Donna L, Mazzotti F, Muzzalupo E, Perri E, Sindona G, Tagarelli A (2005) Absolute method for the assay of oleuropein in olive oils by atmospheric pressure chemical ionization tandem mass spectrometry. Anal Chem 77(18):5961–5964. https://doi.org/10.1021/ac050545h

12. Bulotta S, Celano M, Lepore SM, Montalcini T, Pujia A, Russo D (2014) Beneficial effects of the olive oil phenolic components oleuropein and hydroxytyrosol: focus on protection against cardiovascular and metabolic diseases. J Transl Med 12(1). https://doi.org/10.1186/s12967-014-0219-9

13. Hassen I, Casabianca H, Hosni K (2015) Biological activities of the natural antioxidant oleuropein: exceeding the expectation - a mini-review. J Funct Foods 18:926–940. https://doi.org/10.1016/j.jff.2014.09.001

14. Di Donna L, Mazzotti F, Benabdelkamel H, Gabriele B, Plastina P, Sindona G (2009) Effect of H/D isotopomerization in the assay of resveratrol by tandem mass spectrometry and isotope dilution method. Anal Chem 81(20):8603–8609. https://doi.org/10.1021/ac9015243

15. Di Donna L, Taverna D, Indelicato S, Napoli A, Sindona G, Mazzotti F (2017) Rapid assay of resveratrol in red wine by paper spray tandem mass spectrometry and isotope dilution. Food Chem 229:354–357. https://doi.org/10.1016/j.foodchem.2017.02.098

16. Bartella L, Mazzotti F, Napoli A, Sindona G, Di Donna L (2018) A comprehensive evaluation of tyrosol and hydroxytyrosol derivatives in extra virgin olive oil by microwave-assisted hydro-

lysis and HPLC-MS/MS. Anal Bioanal Chem 410(8):2193–2201. https://doi.org/10.1007/s00216-018-0885-1

17. Commission Regulation (EU) (2012) No 432/2012 of 16 May 2012 establishing a list of permitted health claims made on foods, other than those referring to the reduction of disease risk and to children's development and health. Off. J. Eur Comm. No L136/1. https://eur-lex.europa.eu/legal-content/EN/TXT/HTML/?uri=CELEX:32012R0432&from=IT

18. Bartella L, Di Donna L, Napoli A, Sindona G, Mazzotti F (2019) High-throughput determination of vitamin E in extra virgin olive oil by paper spray tandem mass spectrometry. Anal Bioanal Chem. https://doi.org/10.1007/s00216-019-01727-z

19. Bartella L, Di Donna L, Napoli A, Siciliano C, Sindona G, Mazzotti F (2019) A rapid method for the assay of methylxanthines alkaloids: theobromine, theophylline and caffeine, in cocoa products and drugs by paper spray tandem mass spectrometry. Food Chem 278:261–266. https://doi.org/10.1016/j.foodchem.2018.11.072

20. Taverna D, Di Donna L, Bartella L, Napoli A, Sindona G, Mazzotti F (2016) Fast analysis of caffeine in beverages and drugs by paper spray tandem mass spectrometry. Anal Bioanal Chem 408(14):3783–3787. https://doi.org/10.1007/s00216-016-9468-1

21. Bartella L, Mazzotti F, Napoli A, Sindona G, Di Donna L (2020) Rapid assay of the free and total hydroxytyrosol and tyrosol content in extra virgin olive oil by stable isotope dilution analysis and paper spray tandem mass spectrometry. Food Chem Toxicol 136:11110. https://doi.org/10.1016/j.fct.2019.111110

Chapter 2
Detection of Biological Warfare Agents Using Biosensors

Joseph H. Banoub and Abanoub Mikhael

Abstract This chapter surveys the current detection technologies used in commercially available biosensors for identifying biological warfare agents (BAs). Much of the content presented was obtained from the open-source literature and is an introduction to biosensor fundamentals. A glance at these technologies is presented with emphasis placed on the principles of detection.

2.1 Introduction

Biological agents include a series of different virulent bacteria, viruses, fungi (yeasts and moulds), and parasites. [1, 2]. All of these agents possess an irreversible threat to potentially cause ill health and death to soldiers/humans. The incidents of anthrax-laced letters, the emergence of Severe Acute Respiratory Syndrome (SARS), and repeated occurrences of illnesses caused by food-borne pathogens highlight the need for rapid and sensitive identification of the responsible biological agents [3, 4].

Biological agents (BAs) are widely found in the natural environment (workplace, hospitals, HVAC, etc.) and as a result of the voluntary release of biological warfare or terrorism agents [1, 2]. Biological agents are usually invisible and possess the ability to infect in tiny doses [1, 2]. They also have the cunning ability to replicate rapidly and require minimal resources to survive. For these reasons, it is impossible to feel their presence initially or to predict the risks they present. Recently, it has been demonstrated that bioterrorism raises the specter of exposure to toxins by

J. H. Banoub (✉)
Department of Fisheries and Oceans Canada, Science Branch, Special Projects,
St John's, NL, Canada

Department of Chemistry, Memorial University of Newfoundland, St John's, NL, Canada
e-mail: joe.banoub@dfo-mpo.gc.ca

A. Mikhael
Department of Chemistry, Memorial University of Newfoundland,
St John's, NL, Canada

devising new deliveries by which BAs can be weaponized [5–7]. It has become apparent that BAs weapons pose a real and potentially immediate threat as they are relatively cheap to manufacture and employ, and they have a tremendous potential impact as terror weapons [2]. These properties make biological weapons attractive to terrorist organizations.

2.1.1 Classification of Biological Agents

Recently, biological Agents were categorized according to the Code of Practice, Safety, Health and Welfare at Work Regulations, 2013 [8]. This classification system is founded on whether: the biological agent is pathogenic to humans, represents a hazard to soldiers, is transmissible to the nearby community, and if there is a possible effective treatment available [8–11]. Consequently, BAs are classified into four risk groups (RG), namely, RG1, RG2, RG3, and RG4, as follows:

RG1 includes BAs not linked with diseases in healthy adult humans. Examples of RG1 agents include *Bacillus subtilis* or *Bacillus licheniformis*, *Escherichia coli*-K12, and adeno-associated virus (AAV) types 1 through 4 [9, 10].

RG2 includes BAs connected with human diseases, which is rarely serious and for which preventive or therapeutic interventions are often available. Examples of RG2 agents include *Salmonella* sp., *Chlamydia psittaci*, measles virus, and hepatitis A, B, C, D, and E viruses [9, 10].

RG3 contains BAs associated with serious or lethal human diseases for which preventive or therapeutic solutions may be available (high individual risk but low community risk). Examples of RG3 agents include *Brucella*, *Mycobacterium tuberculosis*, *Coccidioides immitis*, yellow fever virus, and human immunodeficiency virus (HIV) types 1 and 2 [9, 10].

RG4 includes BAs that are expected to cause dangerous human disease for which preventive or therapeutic solutions are *not usually* available (high individual risk and high community risk). RG4 agents only include viruses. Examples of RG4 agents consist of Crimean-Congo hemorrhagic fever virus, Ebola virus, and herpesvirus simiae (B-virus). Under the classification system, these Risk Group 1 agents are the least hazardous, whilst Group 4 is the most hazardous [9, 10].

2.1.2 Analytical Measurement of Biological Agents

Field BAs and urban public health surveillance systems usually provide a rapid determination of the presence of BAs in the atmosphere and may, in time, indicate when and where the biological agent was released [11–15]. Once, the point source is revealed, and the BA identified, rapid clean-up effort could be initiated, after the release of the compound. Moreover, it is essential to monitor the presence of BAs in

the environment, to provide people at risk with the means of rapidly identifying contaminated air, water, food, and equipment [11–15].

It is well known that antibodies specifically targeting proteins or pathogens, can be generated to a wide variety of target cell bacterial analytes and are the most popular choices for the recognition element in many biosensors. Typical immunoassay formats include competitive, displacement, sandwich, and enzyme-linked immunosorbent assays (ELISA) [14]. ELISA, for example, uses colorimetric or chemiluminescent enzyme substrates for signal transduction and is more suited to automated instruments because of the multiple incubations and washes required.

The classical approach to detect the bacteria species type or microbe involves the use of differential metabolic assays, monitored colorimetrically, and on immuno-chemical routine tests.

In addition, the use of cell culture and electron microscopy are vital for the diagnosis of viruses, bacteria, and intracellular parasites. Consequently, all samples retrieved from the affected environment must be cultured to obtain enough numbers of different cell types for reliable identification. Unfortunately, one of the major drawbacks is that the time required for the microbial outgrowth is long, and some bacteria obtained cannot be cultured as a result of genetic mutation.

This chapter has been drafted as a quick summary of the novel biodetection approaches using luminescence biosensing approaches, published recently, for the detection of warfare potential BA weapons; it will exclude all the conventional approaches. The readers are encouraged to peruse the references included within the text, to search for the applied commercial used biosensors, that for simplification reasons, we did not discuss herewith.

2.2 What Is the Definition of Biosensors?

The IUPAC definition of a biosensor is "a self-contained integrated device that is capable of providing specific quantitative or semi-quantitative analytical information using a biological recognition element (biochemical receptor) which is in direct spatial contact with a transducer element [15]. A biosensor should be clearly differentiated from a bioanalytical system, which requires additional processing steps, such as reagent addition. The term "biosensor" is the short form of "biological sensor." The device is made up of a transducer and a biological element that can be an enzyme, an antibody, or a nucleic acid. The bioelement interacts with the analyte under investigation, and the biological response is converted into an electrical signal by the transducer (Fig. 2.1) [16, 17].

Fig. 2.1 Schematic representation of the detection of a bioelement using a biosensor

2.3   Overview of Predominant Sensing Techniques

Sensing can be explained as the use of recognition elements (biological in origin) for binding to the biothreat molecule of interest. The binding event must be transduced in a manner that signals the presence of the targeted analyte. Biosensor probes are becoming increasingly complicated, mainly owing to the combination of advances in two technological fields: microelectronics and biotechnology. Biosensors are highly valuables devices in measuring a wide spectrum of BA analytes [18, 19].

Ideally, each sensing detection technology should contain the following characteristics:

Specific and able to discriminate between closely related pathogenic and nonpathogenic organisms or toxins.

Sensitive and able to detect small amounts of the target within a high background matrix. Possess high affinity and being able to maintain binding even through repeated washing steps.

Stable enough to allow long-term use.

It should be understood that luminescence biosensing technology is totally distinct from other physicochemical methods, such as mass spectrometry (MS) or Fourier transform infrared spectroscopy (FTIR) and Raman based analysis. These methods, of course, have their merits and are very sensitive and specific. Therefore, in the following sections, we will provide an overview of the state-of-the-art prime molecular sensing technologies for the detection of BAs.

2.3.1   Pathogenic Bacteria Electrical Detection Via Immobilized Antimicrobial Peptides

It is well known that the current methods for detecting pathogenic bacteria, which include ELISA and PCR [20, 21], are assays that exploit antibodies as molecular recognition elements due to their highly specific targeting of antigenic sites. Nonetheless, these antibodies lack the stability needed to detect pathogenic species under harsh environments and necessitate a one-to-one pairing of antibody-based sensors for each analyte to be detected. Whereas nucleic acid probe-based techniques such as PCR can reach single-cell detection limits, they still need the extraction of nucleic acids and are limited in portability [21, 22].

It should be noticed that the synthesis of antimicrobial peptides (AMPs) and their resulting intrinsic stabilities render them to be commonly selected for their use as molecular recognition elements in electronic biosensing platforms [23–25]. AMPs do exist in nature and are located either in the skin of higher organisms and/or in the extracellular milieu of bacteria [25]. The replacements of current antibody-based affinity probes, with more stable and durable AMPs in biological sensors, have a

major advantage as recognition elements. This advantage stems from the AMPs semi-selective binding nature to target cells of a variety of pathogens.

The bioactivity of AMPs toward microbial cells can be classified according to their secondary structures [24, 25]. Many AMPs adopt amphipathic conformations that spatially shield the hydrophobic group of the cationic amino acids so it can target the anionic head groups of lipids in the bacterial membrane. On the other hand, the membranes of plants and animals separate negative charges to the inner leaflet and contain cholesterols that decrease the activity of the AMP [25]. The AMPs, linear cationic peptides such as magainins, are in particular, attractive for the microbial sensing applications due to their small molecular size and intrinsic stability [26, 27] Especially, the positively charged AMP magainin I (GIGKFLHSAGKFGKAFVGEIMKS) binds most selectively to the bacterial cell *E. coli* O157:H7 as a precursor to bactericidal activity [25–27].

2.3.1.1   Development of an AMP-Based, Label-Free Electronic Biosensor

A robust and portable biosensor for the pathogenic bacteria detection that could impact water quality monitoring for bacterial contamination was developed by McAlpine and coworkers [23–25]. The particular interest of the developed biosensor was that it combined the natural specificity of biological recognition to label-free sensors providing sensitive electronic readout. Accordingly, McAlpine et al. reported the selective and sensitive detection of infectious agents via electronic detection based on antimicrobial peptide-functionalized micro capacitive electrode arrays [25].

The semi-selective antimicrobial peptide magainin I, which occurs naturally on the skin of African clawed frogs, was immobilized on gold microelectrodes via a C-terminal cysteine residue. Remarkably, exposing the sensor to different pathogenic Escherichia coli concentrations showed detection limits of approximately 1 bacterium/μL, a clinically acceptable detection limit. The peptide-micro capacitive hybrid device was additionally able to exhibit both Gram-selective detection as well as interbacterial strain discrimination, while maintaining recognition capabilities toward pathogenic strains of *E. coli* and *Salmonella* [25].

The first step toward the development of an AMP-based, label-free electronic biosensor is to target the microbial cells by using magainin I through the use of the impedance spectroscopy. It should be noted that electrical impedance measures the total opposition to a circuit or a part of the circuit presented to an electric current. Usually, the impedance is the results for both resistance and reactance. It is important to remember that the resistance component is formed from collisions of the current-carrying charged particles with the internal structure of the conductor. Furthermore, the reactance component is an additional opposition to the movement of the electric charge that results from the changing magnetic and electric fields in circuits carrying alternating current.

Figure 2.2 outlines the sensing platform. First, the AMPs are immobilized on the micro-fabricated interdigitated gold electrodes (Fig. 2.2a). It should be specified
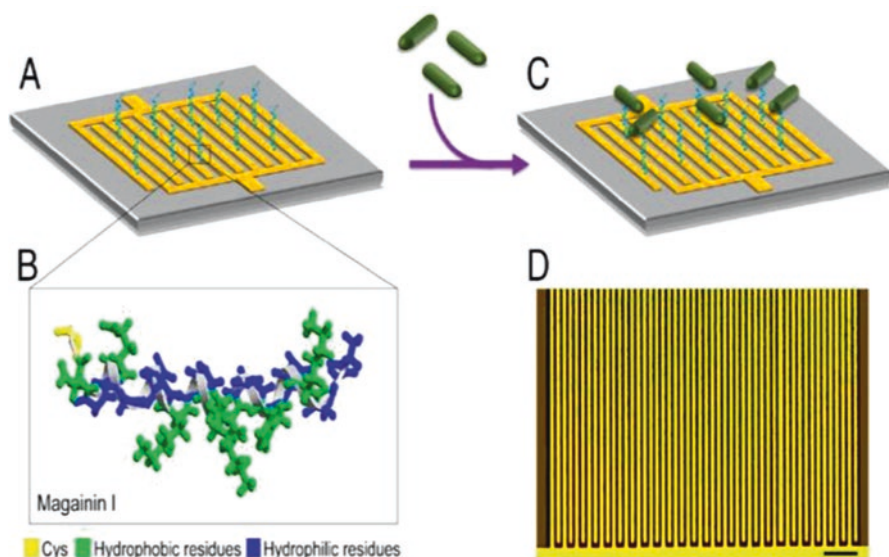
Fig. 2.2 AMP-based electrical detection of bacteria. (Adapted from Ref. [25])

that magainin I contains a cysteine residue on the C terminus (Fig. 2.2b), which allows its covalent attachment to the gold electrodes. Next, the heat-killed bacterial cells are injected and incubated on the AMP-modified electrodes [25]. When the bacteria are recognized by the AMPs, the binding will ensue (Fig. 2.2c), causing the dielectric property to changes that can be monitored by a spectrum analyzer. Usually, the impedance is measured over a frequency range of 10 Hz to 100 kHz. Figure 2.2d shows an optical micrograph of the device, which is made using standard microfabrication techniques.

The results of the measurements performed after incubation of the immobilized AMPs with pathogenic E. coli O157:H7 cell concentrations ranging from 10^3 to 10^7 cfu/mL are shown in Fig. 2.3. When a blank device with no immobilized AMPs was also tested for comparison, it was found that there was no change in the impedance of the blank device without immobilized AMPs, upon exposure to various bacterial concentrations.

Figure 2.3a demonstrates that at low frequencies, the various concentrations of bacterial cells have the effect of increasing the impedance, which is proportional to to the number of cells present in the sample. As the frequency increases, the input to the impedance from the bacterial cells decreases. This leaves only the dielectric relaxation of small dipoles, including water molecules in the buffer solution, to affect the measured impedance.

Figure 2.3b represents the impedance change at a fixed frequency of 10 Hz. The change in the impedance is directly proportional to the number of bacterial cells attached to the immobilized AMPs and displayed in a logarithmic increase with respect to a series of diluted bacterial concentrations. Remarkably, the detection

Fig. 2.3 Impedance spectra and sensitivity of the AMP electronic biosensor. (Adapted from Ref. [25])
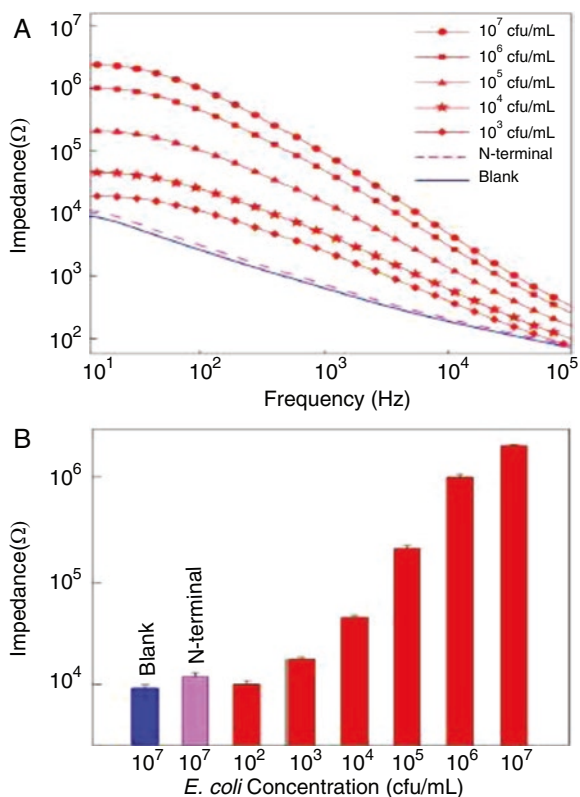
limit of the response of the hybrid AMP-microelectrode device to *E. coli* was established to be 10^3 cfu/mL (1 bacterium/μL). This lowest limit of detection seems to be limited by the presence of impedance due to the electrical double layer formed from the electrode polarization effect at low frequencies. Notably, these sensitivity limits are clinically relevant and compare favorably to AMP-based fluorescent assays [26], antibody-based impedance sensors [27], and to the LAL test [25].

2.3.1.2   Real-Time Detection of Pathogenic Bacteria

To mimic the usage of the AMP microelectrodes in daily applications like direct water sampling, the biosensor response was studied in real-time, as presented in Fig. 2.4. First, a microfluidic cell was attached to the interdigitated biosensor chip (Fig. 2.4a), to make the electrodes perpendicular to the direction of the sample flow (Fig. 2.4b) [25].

Next, the fluid was introduced by using a syringe pump attached to the inlet port and was let to flow through to the outlet port at a flow rate of 100 μL/min. The flow cell was first flushed with the buffer to establish a baseline. This was followed by
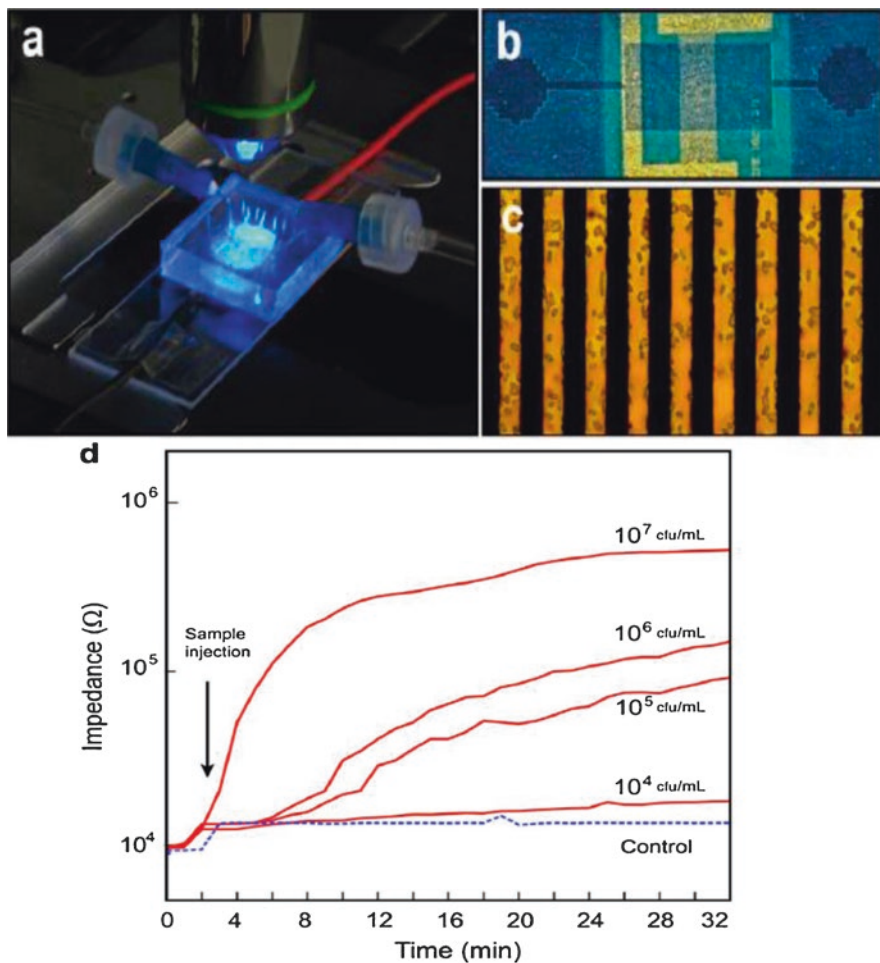
Fig. 2.4 Real-time binding of bacteria to AMP biosensors. (Adapted from Ref. [25])

injection of various dilutions (104–107 cfu/mL) of the pathogenic *E. coli* cells in phosphate-buffered saline (PBS) to the channel at a reduced flow rate of 5 μL/ min for 30 min. For example, Fig. 2.4c demonstrates the microelectrode array after exposure to 107 cfu/mL bacterial cells. Simultaneously, the impedance response was continuously monitored during the sample flow-through process (Fig. 2.4d).

All samples generated a measurable response with respect to the control sample within 5 min, with the highest concentration sample producing a response within 30 s; the responses saturated after 20 min. These results augured well for the implementation of this sensor in continuous monitoring of flowing water supplies.

2.3.1.3 Selectivity Measurements

McAlpine also examined the selectivity of the AMP-functionalized biosensors toward the following various bacterial species (*1*) Gram-negative pathogenic *E. coli* O157:H7, (*2*) the nonpathogenic *E. coli* strain American Type Cell Culture (ATCC) 35218, (*3*) Gram-negative pathogenic *Salmonella typhimurium*, and (*4*) the Gram-positive *Listeria monocytogenes*. The selectivity was first studied by using methods of fluorescent microscopy. This was done by staining bacterial cells and optically mapping their binding density to gold films hybridized with AMPs. The discriminative binding patterns of immobilized magainin I and the surface density of the different bacterial cells (all 10^7 cfu/mL) stained with propidium iodide (PI) nucleic acid stain are showed in Fig. 2.5. In summary, the coupling of AMPs with micro capacitive biosensors leads to the implementation of a portable, label-free
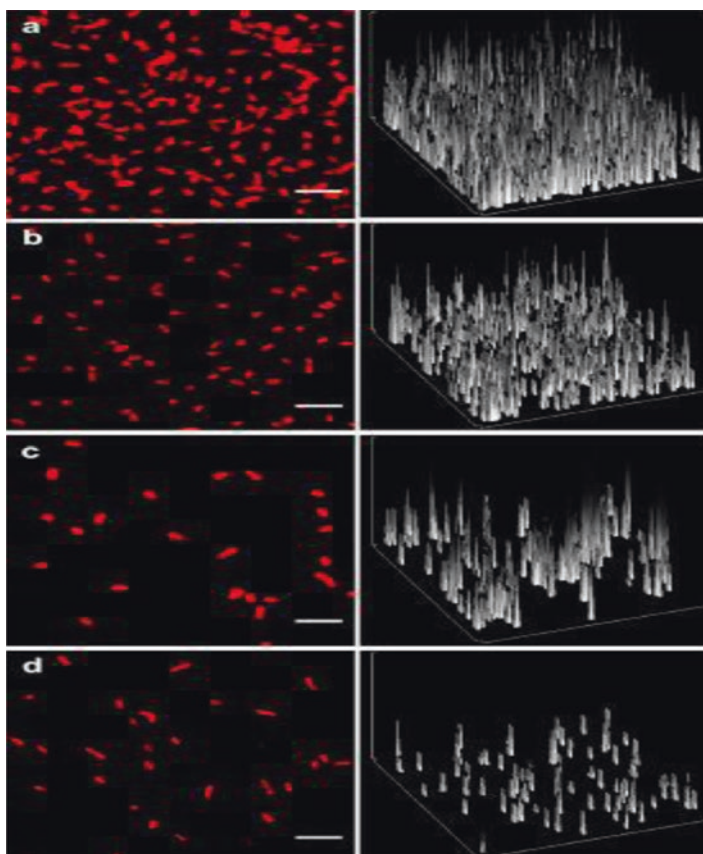
Fig. 2.5 Optical microscopy of the selectivity of AMPs. (Left) Demonstration of selective binding of the immobilized AMP to various stained bacterial cells (107 cfu/mL), including (**a**) E. coli O157:H7, (**b**) S. typhimurium, (**c**) E. coli ATCC 35218, and (**d**) L. monocytogenes. (Right) The corresponding surface density of the bound cells. Scale bars are 10 μm. (Adapted from Ref. [25])

sensing platform for the sensing of infectious agents. The obtainable sensitivity approached 1 bacterium/μL-a clinically acceptable limit-and the AMPs allowed for sufficient selectivity to differentiate pathogenic and Gram-negative bacteria while retaining broadband detection capabilities [25–28]. In addition, the simulated water sampling chip, which consisted of a microfluidic flow cell integrated onto the hybrid sensor, demonstrated the potential of real-time on-chip monitoring of the interaction of *E. coli* cells with the antimicrobial peptides [25].

2.3.2 NRL Array Biosensor for Toxin Detection

This following part discusses the progress made with the NRL Array Biosensor, which is a portable device for rapid and simultaneous detection of multiple targets, which was developed, automated and miniaturized for operation at the point-of-use by the US Navy Research Laboratories. This Array Biosensor has been used for the quantitative immunoassays versus a broad number of toxins, and for its usefulness as semi-selective molecules which can be used as alternative recognition moieties [29–31]. In this sensor, the antibodies or other capture molecules are immobilized in a 2-D arrangement on an optical waveguide, and then a standard fluoroimmunoassays are donewithin the channels of a multi-channel flow cell, which is placed on the waveguide surface (Fig. 2.6, left). In the NRL array biosensor, the spots are interrogated using evanescent wave technology that is specifically: a light issued from a 635 nm diode laser that is focused into the edge of the patterned waveguide and after propagation and mixing within the waveguide, the confined beam generates an evanescent field in the sensing portion of the waveguide [29, 32]. The definition of an evanescent field or wave is a vibrating electric and/or magnetic field, which does not spread as an electromagnetic wave but whose energy is spatially concentrated in the proximity of the source (oscillating charges and currents) [32].
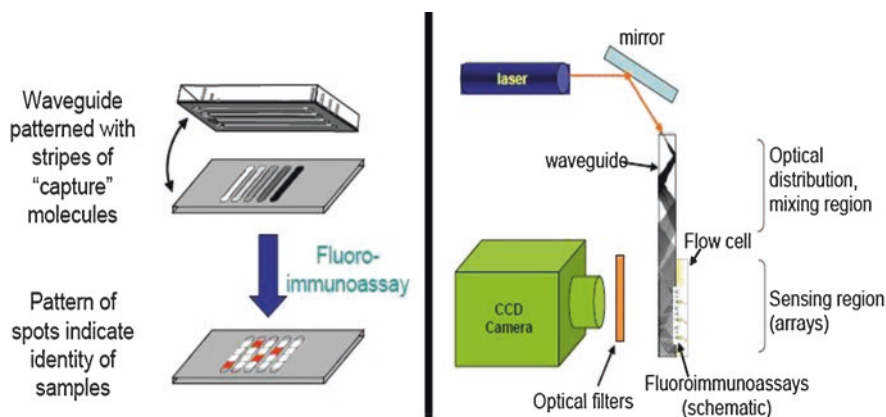
Fig. 2.6 NRL Array Biosensor. (Adapted from Ref. [29])

The surface attached molecules marked with fluorophore are excited by this evanescent field, generating a fluorescence signal, which is then detected using a CCD camera fitted with appropriate bandpass and longpass filters (Fig. 2.6, right). Because of the limitation of the penetration depth of the evanescent field, only surface-attached fluorophores are excited, allowing the analysis of heterogenous or turbid samples. The position and intensities of the fluorescent spots express the identity and concentration of the target sample in each lane [29, 32].

The NRL Array Biosensor was used successfully for the detection of toxins and for multiple toxins simultaneously in multiple samples, it could also detect toxin levels as low as 500 pg/mL and quantify the toxin concentration, and finally, it could perform toxin assays in clinical, food, and environmental samples [29]. Furthermore, both sandwich immunoassays for protein toxins (e.g., staphylococcal enterotoxin B [SEB] and ricin) and competitive immunoassays for low molecular weight toxins (e.g., trinitrotoluene and fumonisin B1) were reported. [29] A schematic of the sandwich immunoassay format is shown in Fig. 2.7 [16].

2.3.2.1 Toxins Environmental Testing in Food and Air

Determination of bacteria and large toxins in foods and air by the NRA Array Biosensor Assays normally employ a sandwich immunoassay format. However, mycotoxins are smaller in size and are therefore better assayed using an indirect competitive immunoassay [32–35].
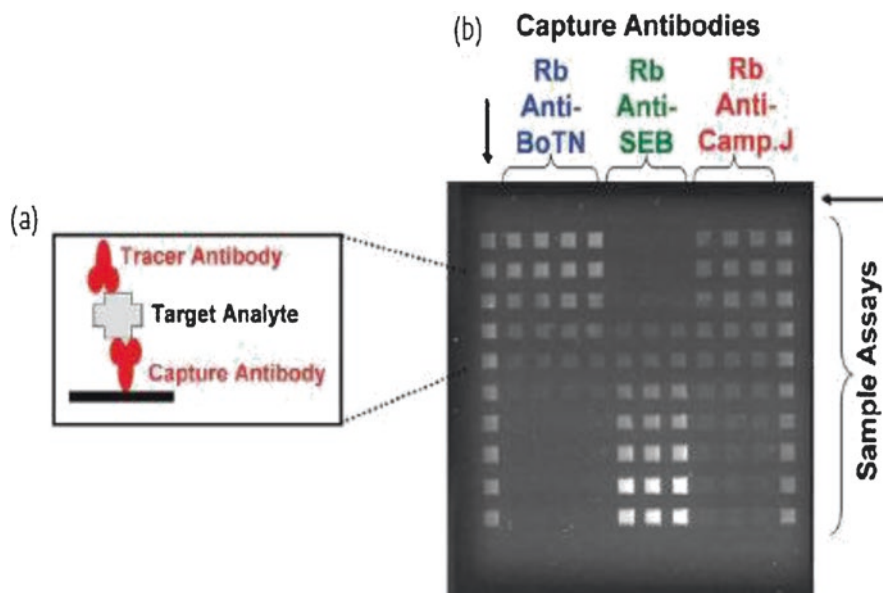
Fig. 2.7 Immunoassay with the NRL array biosensor using the sandwich immunoassay format. (Adapted from Ref. [16])

The validity of the NRL Array Biosensor was demonstrated for the detection of mycotoxins (ochratoxin A, deoxynivalenol, and aflatoxin B1) in various food matrices and air [32–35].

This competitive assay protocol involved attaching the biotinylated mycotoxin derivatives onto the waveguide, this was followed by incubating the test sample with cyanine 5 (Cy5)-labeled anti-toxin antibodies and then passing the pre-incubated mix over the immobilized mycotoxin derivatives. Since the immobilized mycotoxin derivatives competed with the toxin in the test sample for binding to the fluorescent antibodies; it was found that the resulting fluorescent signal of the immunocomplex on the waveguide surface was inversely proportional to the concentration of toxin in the sample (decrease in signal with increasing concentration [32–35].

This type of Array Biosensor has been automated and miniaturized for operation as point-of-use quantitative immunoassay arrays. This methodology was utilized to measure an expanded number of toxins and toxin indicators in food and clinical fluids. In addition, semi-selective recognition molecules were also used to expand the repertoire of toxins that can be detected on a single array. In the automated system, up to 6 samples can be analyzed simultaneously while the non-automated system can test up to 12 samples [30].

2.3.2.2   Use of Antimicrobial Peptides for Toxin Detection

Taitt and coworkers investigated the possibility of using antimicrobial peptides (AMPs) for the detection of inactivated botulinum toxins A, B, and E as well as other toxins in assays analogous to the AMP-based bacterial assays [36]. They observed apparent differences in the patterns of binding between botulinum neurotoxoids A, B, and E. It was found that the detection limits were improved when immobilized AMPs were used for target capture [36].

2.3.3   Surface Acoustic Wave (SAW) Sensors

The Love wave (LW) physical effect was firstly revealed by the mathematician Augustus Edward Hough Love [37, 38]. Typically, LW sensors consist of two components, which are the transducing area and the sensing area. The transducing area consists of the interdigital transducers (IDTs), which are metal electrodes, sandwiched between the piezoelectric substrate and the guiding layer [39–41]. The input IDT is excited through the application of an rf signal and introduces a mechanical acoustic wave into the piezoelectric substrate, which is directed across the guiding layer up to the output IDT, then it is converted back to a measurable electrical signal (Fig. 2.8) [40].

It should be understood that the sensing area is the part of the sensor surface, positioned between the input and output IDT, which is exposed to the analyte.
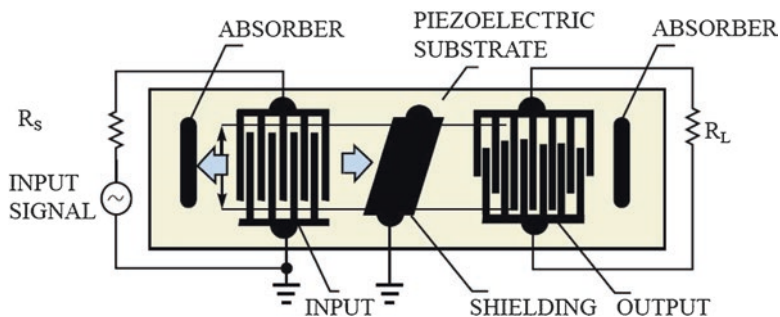
Fig. 2.8 Surface Acoustic Wave Sensor (SAW). (Adapted from Ref. [40])

Consequently, to permits the use of a SAW device as a biosensor, the device has to be coated with a biospecific layer corresponding to the analyte. The immobilization chemistry strongly depends upon the underlying SAW substrate with or without a guiding layer and hence on the chemical environment available. Gold surfaces, for example, allow the use of functionalized thiols, whereas quartz or SiO2 surfaces enable the use of various silanes [42]. Analyte-specific molecules (e.g., antibodies) are immobilized on the SAW device to catch analyte molecules (e.g., antigens) from the sample stream. Analytes binding to the immobilized capture molecules will affect the speed of the SAW and hence the output signal generated by the driving electronics [39].

SAW detectors can identify and measure many BAs simultaneously and are relatively inexpensive, making them a popular choice amongst civilian response units [39–42]. SAW detectors detect changes in the properties of acoustic waves as they travel at ultrasonic frequencies in piezoelectric materials. The basic transduction mechanism involves the interaction of these waves with surface-attached matter. Multiple sensor arrays with multiple coatings and pattern recognition algorithms provide the methods to identify agent classes and reject interferant responses that could cause false alarms [39–43].

Recently, SAW immunosensors were successfully applied to detect *E. coli*, *Legionella*, the anthracis simulant B8 *Bacillus thuringiensis* (B8), and M13 bacteriophage (M13) acting as model analyte for bacteria or viruses. Tamarin et al. used Love wave sensors based on a quartz substrate with a SiO2 wave-guiding layer. Antibodies against M13 were immobilized on the sensor surface to detect the bacteriophage directly [43].

Stubbs et al. developed a SAW immunoassay for the detection of analytes in the gas phase, e.g., cocaine plumes [44]. For this purpose, SAW devices based on quartz were used. Antibodies were coupled to the SAW device via adsorbed protein A and coated with a hydrogel layer to overcome the problem of hydration of the biomolecule [44]. Benzoylecgonine, the major metabolite of cocaine, could be detected in vapor [45]. In general, it can be specified that SAW-based biosensors offer the possibility of observing real-time binding events of proteins at appropriate sensitivity levels [45, 46].

2.3.4 Biosensing with Luminescent Semiconductor Quantum Dots

Recently, luminescent semiconductor nanocrystals or quantum dots (QDs) have become a successful novel nanomaterial possessing unique photophysical fluorescent properties, which have helped create a new generation of robust fluorescent biosensors [47–53]. It should be stated that the fluorescent properties of QDs have overcome most of the liabilities of conventional organic and protein-based fluorophores. The biosensing QD properties of interest include high quantum yields, broad absorption spectra coupled to narrow size-tunable photo-luminescent emissions, and exceptional resistance to both photo-bleaching and chemical degradation. In this section, we will investigate the advancement in using QDs for many invitro biosensing applications, including their use in immunoassays, as generalized probes [47–53].

2.3.4.1 Immunoassays Using Quantum Dots

The unique advantages of using QDs are owed to their inherent photostability, their improved sensitivity, and size-tunable photoluminescence coupled to their broad absorption spectra. These unique advantages have allowed them to serve as multi-color or multiplexed immunoassays. It should be mentioned that in terms of coupling QDs to antibodies, the most common method reported in the literature utilizes biotin-avidin interactions [48]. The avidin/streptavidin-coated QDs are commercially available, while biotin-labeling of antibodies are usually prepared in-house. The QDs containing free carboxylic acid groups from their capping agents may also be covalently attached to the epsilon amine of an antibody's lysine residues by using EDC/NHS coupling chemistry [47–53]. Instead, simple electrostatic interactions can be used depending on the overall protein charge at the pH of conjugation [48]. For example, sandwich immunoassays were used by Goldman et al. for the simultaneous recognition of four toxins in a single microtiter well, as shown in Fig. 2.9 [47, 48, 53].

In this assay, antibodies immobilized in a microtiter well plate were first subjected to the mixed toxin sample. Antibodies particular for each of the toxins linked to a different color QD were then put in the microtiter well plate. The subsequent signal from the mixed toxin samples was then deconvoluted using a simple algorithm. Similarly, QD-antibody bioconjugates were used to detect and distinguish between diphtheria toxin and tetanus toxin proteins, which were generally immobilized onto poly-L-lysine coated coverslips and for the simultaneous detection of *Escherichia coli* O157:H7 and *Salmonella typhimurium* bacteria using various colored QDs as immunoassay labels [54].

Fig. 2.9 QD multiplexed
biosensing. (Adapted from
Ref. [53])
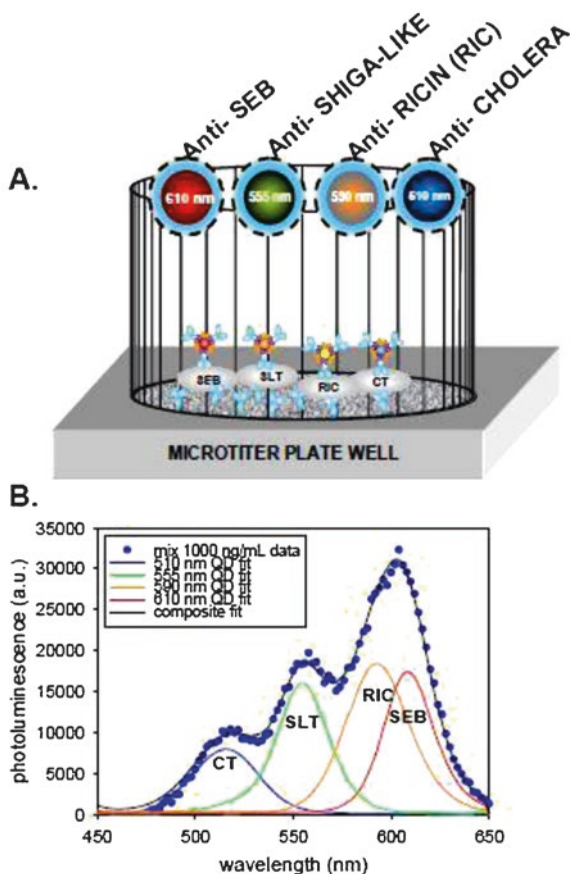
2.3.4.2 Nucleic Acid Detection

Liang et al. utilized QDs to miRNA microarray assays by using streptavidin QDs probes to label biotinylated miRNA targets derived from rice, as shown in Fig. 2.10 [52]. Initially, miRNAs were oxidized with sodium periodate to oxidize the ribose 2′- and 3′- hydroxyl groups into aldehydes. The resulting dialdehyde was then reacted with biotin-X-hydrazide resulting in biotinylated miRNA. This was followed by immobilizing the 5′ amine-modified oligonucleotide probes antisense to miRNAs on the amine-reactive glass slides. The biotinylated miRNAs were captured on the microarray by oligonucleotide probes in hybridization. QDs were labeled on the captured miRNAs through the strong specific interaction of streptavidin and biotin. Since the QDs have a high extinction coefficient and quantum yield, so tiny amounts of miRNAs can be detected easily with a laser confocal scanner. In addition, as an alternative, the colorimetric gold–silver detection method was used in which captured miRNAs were labeled with streptavidin-conjugated gold followed by silver enhancement. During silver enhancement, the gold nanoparticles bound to
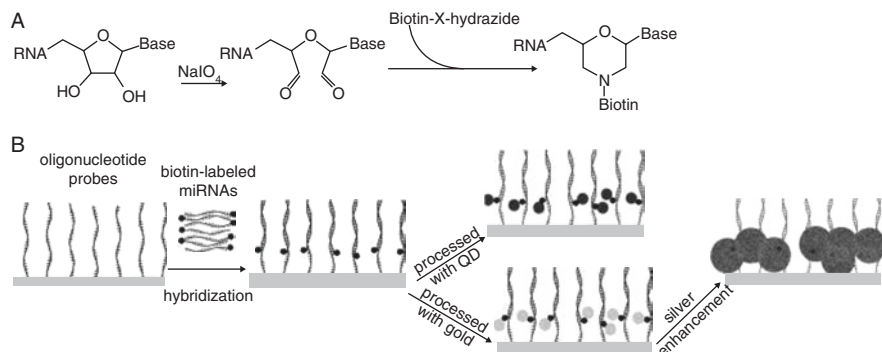
Fig. 2.10 Schematic principles of the miRNA profiling microarray. (Adapted from Ref. [52])

miRNAs catalyzed the reduction of silver ions to metallic silver, which further autocatalyzed the reduction of silver ions to form metallic silver precipitation on gold, resulting in a signal enhancement [52]. This process allowed straightforward detection of the microarray with an ordinary charge-coupled device (CCD) camera mounted on a microscope.

They found that QD probes offered decent sensitivity down to sub-femtomolar concentrations and dynamic range above several orders of magnitude. This was significantly better than other dye-based methods and further hindered the use of amplification while allowing a semi-quantitative comparison of the amount of miRNA in different samples [53].

Figure 2.11 displays a set of images for various concentrations of miRNA (21 nt siRNA) detected by QD [53]. It should be noted that the signals become gradually weaker with the decrease in miRNA concentration (Fig. 2.11a). When the miRNA concentration was as low as 39 pM, the fluorescence signal could be detected, indicating that the lower detection limit of miRNA microarrays is at least 0.4 fmol. As shown in Fig. 2.11b, the fluorescence intensity of the spots is linear to the model miRNA in a logarithmic fashion from 156 to 20,000 pM, and the dynamic range is about two orders of magnitude. This implies that this method can be used to quantify miRNAs with a broad concentration range [53].

2.3.4.3   Sensing Based on FRET with Quantum Dot Bioconjugates

Fluorescence Resonance Energy Transfer (FRET) is a physical process in which radiationless transmission of energy phenomena occurs depending on the distance-dependent transfer of energy from a donor molecule to an acceptor molecule. FRET has been extensively used in biophysical and biochemical studies to probe ligand-receptor binding and molecular structural changes [55–57]. In the following example, the authors incubated the dye-labeled DNA targets with biotinylated capture DNA probes, which were allowed to be conjugated to streptavidin QDs, only when the two DNA sequences hybridize. The resulting hybridization was then detected
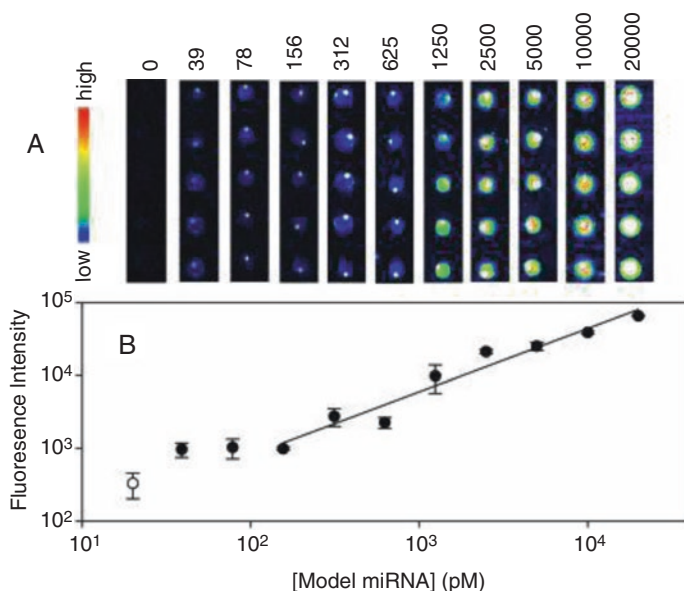
Fig. 2.11 Detection limit and dynamic range of the model miRNA detection microarray. (**a**) Image sets of microarrays hybridize with various concentrations of miRNAs from 20 nM to 39 pM and the background. The 50 μM concentration of oligonucleotide probes printed on slides pentaplicately. The volume of model miRNA needed to hybridize with microarray was 10 μl. (**b**) Correlation between the fluorescence intensity of spots and concentrations of model miRNA. The values were calculated from the image in (**a**). The open circle represents the background. (Adapted from Ref. [53])

via FRET between the QD and the dye acceptor (Fig. 2.12) [53]. It should be noted that the additional background caused by the direct acceptor excitation is virtually eliminated through the choice of an appropriate excitation wavelength; this led to a 100-fold improvement in sensitivity compared to single organic dye molecular beacon-based detection. This type of sensing schemes can also be amenable to use in a multiplex format. The narrow and symmetric QD emissions allow easy spectral deconvolution, and the most straightforward configuration relies on several QD populations interacting with the same dye acceptor rather than the opposite [53].

2.3.5   Engineered Cell-Based Sensors: The CANARY System

Petrovick et al. have developed a novel inexpensive, genetically engineered white-blood cell biosensor for the rapid identification of warfare BA pathogens and toxins [58]. This new sensor was named and abridged as CANARY for "Cellular Analysis and Notification of Antigen Risks and Yields." CANARY sensors are capable of detecting soluble protein toxins, which are an important class of potential bioweapon, and can also be used for sequencing DNA and RNA [58].
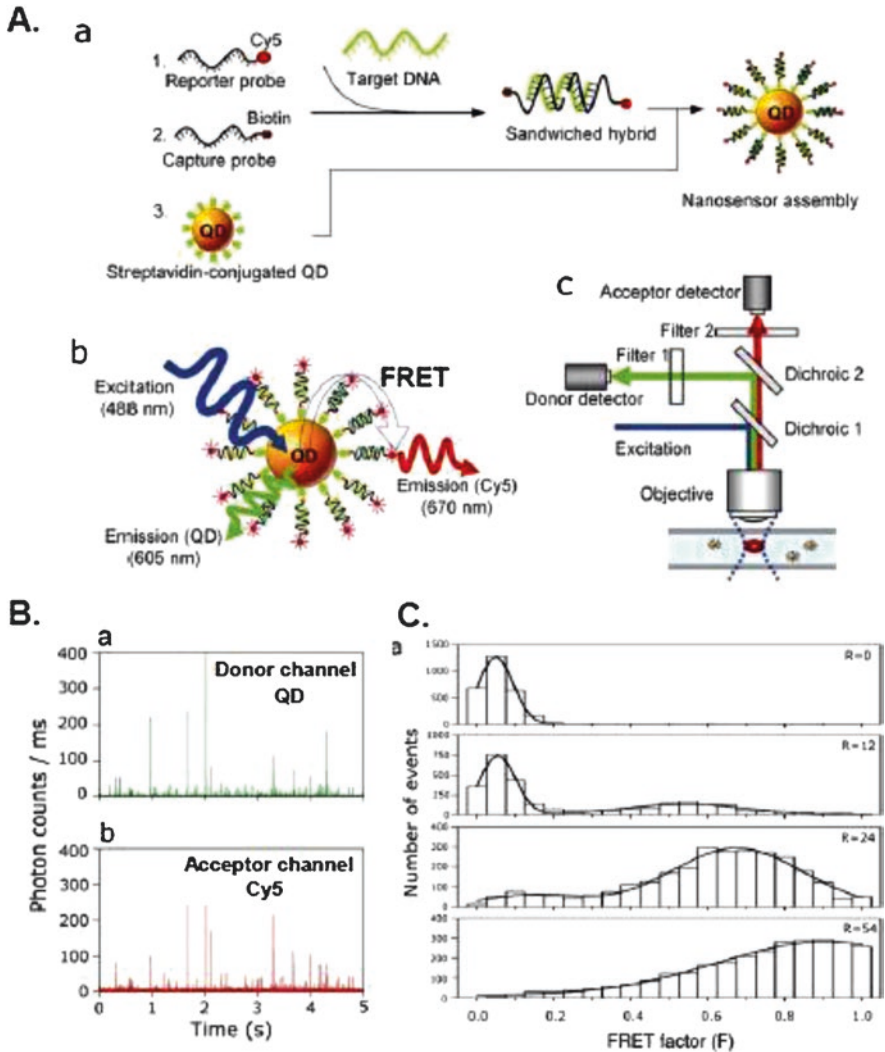
Fig. 2.12 Single QD-Based DNA nanosensor. (Adapted from Ref. [53])

2.3.5.1 CANARY Bioelectronic Sensor

The CANARY technology is based on genetically engineered white blood B cells, which can bind to and to recognize pathogens quickly and assists other parts of the immune system in fighting the infection. It is well known that B cells are the fastest known pathogen identifiers (intrinsic response less than 1 s). The B-lymphocytes recombinantly express cytosolic aequorin, a Ca-sensitive bioluminescent protein from the jellyfish *Aequoria victoria,* which emits light in response to elevations of intracellular Ca, along with the antibodies bound to the membrane. Binding of the
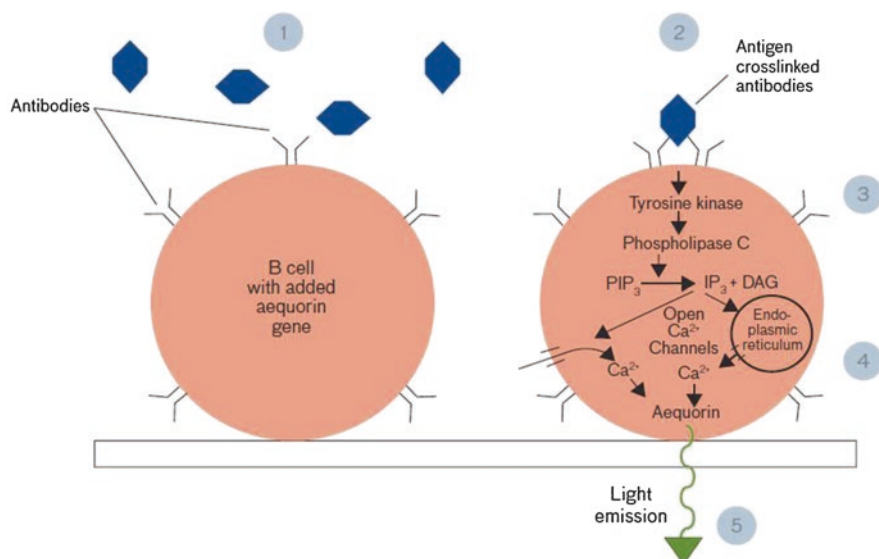
Fig. 2.13 The CANARY bioelectronic sensor. (Adapted from Ref. [58])

pathogen to the cell surface antibodies causes an increase in intracellular Ca levels, resulting in the emission of light from the cytosolic aequorin [59–63].

Two regular genetic modifications enable engineered B-cell lines to express cytosolic aequorin, as well as membrane-bound antibodies specific for pathogens of interest [62, 63]. This was achieved by crosslinking the membrane-bound antibodies to a polyvalent antigen that induces a signal-transduction cascade. This latter, sequentially involves tyrosine kinases, phospholipase C, and inositol triphosphate (IP3). The IP3 activates calcium channels, thereby increasing cytosolic calcium from both internal stores and the extracellular medium, which stimulates the aequorin, causing it to emit light (Fig. 2.13) [58, 59, 62–64].

The CANARY sensor can detect less than 50 colony-forming units (cfu) of the pathogen in less than 3 min, which include the time required to concentrate the sample [64]. It should be mentioned that state-of-the-art immunoassays take at least 15 min, whereas the polymerase chain reaction (PCR) takes longer than 30 min. The novel genetic-engineering system developed by Petrovick et al. have consisted of the efficient production of B-cell lines that can react specifically and rapidly to a variety of pathogens [58]. The antibody genes were cloned from hybridomas and inserted into expression vectors. These were transfected into a parental B cell line that expresses active aequorin, and the cells are screened for their response to the pathogen. The genetically modified CANARY cells can be applied separately in a particular identification assay, or as many as three can be linked to accomplish a multiplexed assay. Instead, several antibodies can be expressed in a single cell line to provide a classification assay [59]. It is also possible to establish B cells that emit at various wavelengths of light, allowing multiplexed assays that simultaneously discriminate among several targets [58].
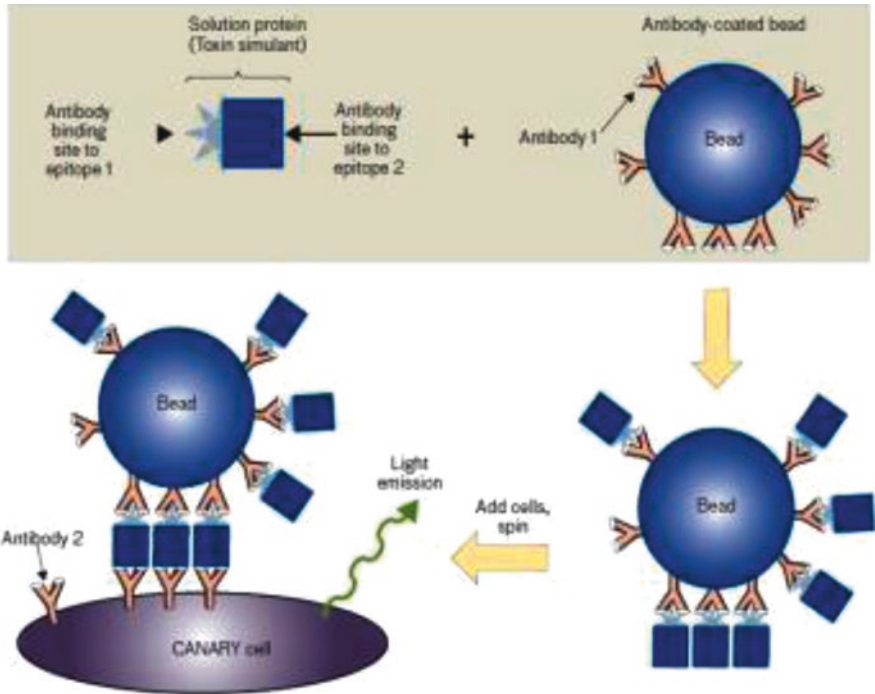
Fig. 2.14 Two antibodies assay for toxins detection. (Adapted from Ref. [58])

2.3.5.2 Toxin Detection

A novel effective method described by Petrovick et al. for the immobilization of a toxin was to obtain it on beads coated with antibodies against that specific toxin [58]. The antibody-coated beads were then incubated in a solution containing the suspected toxin and washed to remove the contaminating proteins and other materials. The toxin- obtained decorated beads are excellent candidates for the purification and immobilization of toxin analytes by the CANARY cells, as illustrated in Fig. 2.14 [58].

It should be mentioned that the CANARY cells should express an antibody that attaches to the toxin at another site different from that of the capture antibody. Since the toxin is immobilized on the bead, the antibodies on the CANARY cell that attaches to the toxin are as well immobilized, and therefore light emission is stimulated [59]. This method has been used to develop a very effective CANARY assay for botulinum neurotoxin type A (BoNT/A), which is the most poisonous toxin known to man, with an LD50 of about 550 ng by inhalation for a 55 kg adult. Under best conditions, the assay sensitivity is currently 16 pg (1.6 ng/mL) [58].

2.3.5.3   Detection of the DNA Sequence

The detection of soluble macromolecules has another remarkable application, which is the identification of DNA and RNA sequences. The capability to identify nucleic acid (NA: DNA or RNA) sequences is central in the deduction of the first hard NA sequence information, concerning a new or genetically modified pathogen [58]. It is crucial to develop assays that have the flexibility to respond quickly to new threats. For this reason, developing NA probes allow for the rapid and quick examination of the actual genetics of the target organism [58]. When the NA sequence of a pathogen is revealed, multiple short probes are created that bind adjacent to each other along a specific sequence on the target NA [59]. Consequently, Petrovick et al. developed a novel assay that uses a single CANARY cell line that expresses an antibody against digoxigenin. Each of these probes is marked with a single digoxigenin molecule. If these probes are added to the solution containing the target NA sequence, the binding of multiple digoxigenin-containing probes produces a tight cluster of immobilized digoxigenin molecules, which will stimulate light production from the CANARY cell (see Fig. 2.15) [58].

In the absence of target NA, every digoxigenin-labeled probe stays monomeric, and therefore cannot crosslink antibodies on the surface of CANARY cells. There are more benefits to detect RNA compared to DNA because there is only one copy of genomic DNA per bacterium, but on the other hand, there can be thousands of copies of a single RNA strand, so the number of target molecules per bacterium is much higher. Furthermore, since probe binding demands that the target NA must be
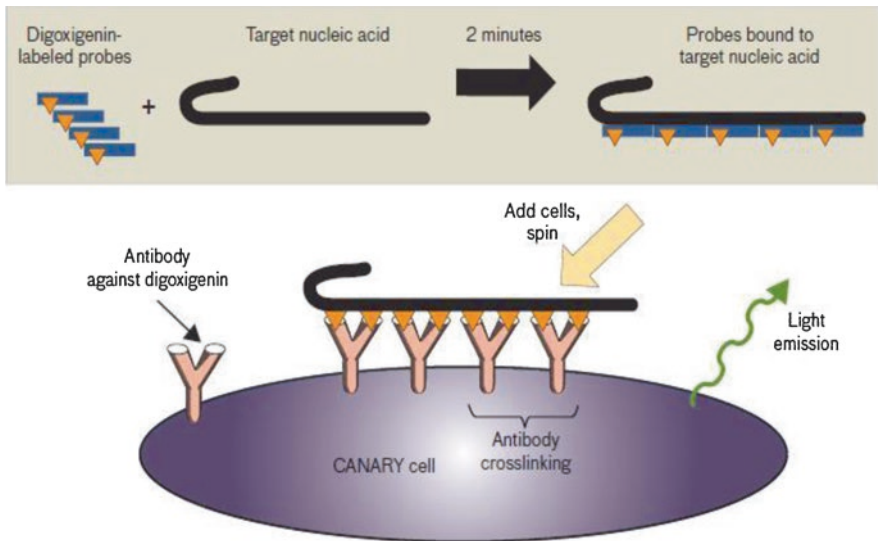
Fig. 2.15 DNA probes designed that bind to a specific region on a single-target nucleic acid (NA). (Adapted from Ref. [58])
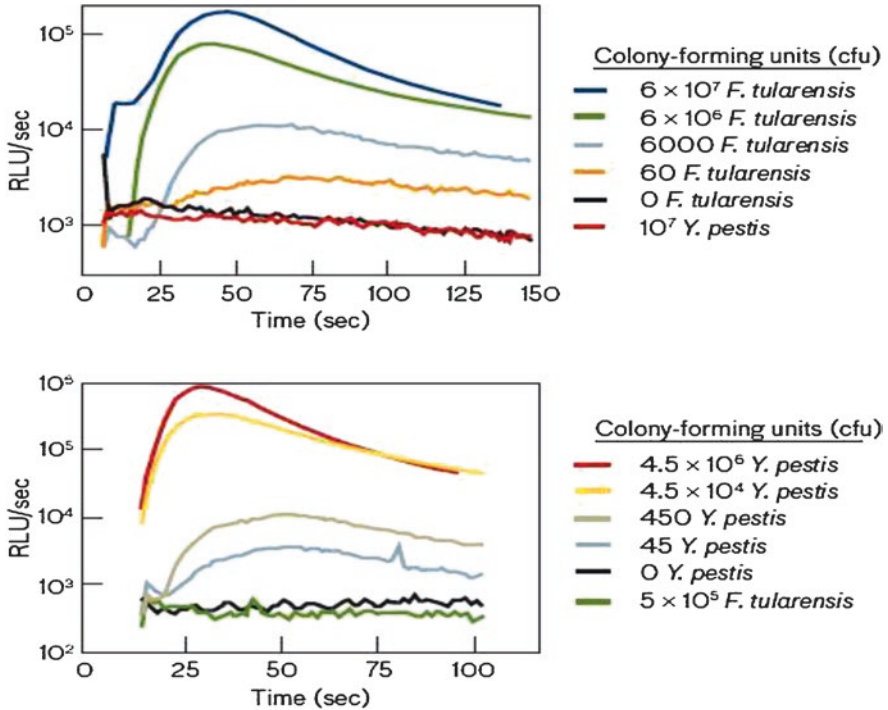
Fig. 2.16 The dose-response curves for inactivated *Francisella tularensis* (top) and *Yersinia pestis* (bottom). (Adapted from Ref. [58])

a single-strand, a denaturing step must be done to separate the two constituent strands of DNA. RNA, however, is normally single-stranded [58].

2.3.5.4   **CANARY Detections of *Francisella tularensis* and *Yersinia pestis***

The CANARY approach takes advantage of a receptor that binds to the constant part of the antibodies and leaves the antigen-binding part of the antibody free. After the binding of the bacteria with the captured antibodies, the receptor initiates a signal cascade, similar to the one induced by the crosslinking of membrane-bound antibodies on B cells, which activates aequorin [58].

The excellent combination of speed and sensitivity of the CANARY system was shown with cell lines expressing an antibody that specify for the F1 antigen of *Yersinia pestis (Yp)*, shown in Fig. 2.16 [58]. When concentrated in the centrifuge luminometer, as little as 45 cfu of formalin-inactivated Yp are detected. However, there was no response to relatively large numbers of *F. tularensis* [58].

For biological defense applications, the CANARY technology was added into a flexible biological-aerosol sensor platform called PANTHER that can create the core of a family of mission-specific bio-aerosol identification sensors useful as

standalone sensors for the site/building protection, emergency response, rapid screening, and environmental monitoring [58].

To summarize, the CANARY's capabilities open possible applications in pathogen genotyping, virulence testing, antibiotic resistance screening, and viability assessment. Moreover, using these cells demonstrate the best-known combination of speed and sensitivity. Other applications of CANARY technology comprise biological aerosol sampling, point-of-care diagnostics, pre-symptomatic diagnosis in the outcome of a biowarfare attack, finding of agricultural pathogens at ports of entry, or screening of perishable food supplies medium [62], which activates the aequorin, causing it to emit light [59, 60].

2.3.6 High-Density Microsphere-Based Fiber-Optic DNA Microarrays

It is well known that an optical fiber is a flexible, translucent fiber produced by drawing glass (silica) or plastic to a diameter slightly thicker than that of a human hair [65, 66]. Optical fibers consist of an inner core that is surrounded by a clad material of a lower refractive index. Because of the differences in refractive index, light is totally reflected. A fiber optic bundle consists of thousands of individual fibers fused together, such that each fiber retains its ability to transmit light independently of its neighbors (Fig. 2.17) [67].

Pantano and Walt showed that by selectively etching the fiber core, an array of microwells could be formed [68, 69]. These microwells can be filled with oligonucleotide-functionalized microspheres. The array dimensions can be tailored to suit any size of the oligonucleotide-functionalized microsphere. The well diameters are equal to those of the fiber cores, and the depths are dependent on the etchant concentration, the exposure time, and the fiber composition. Because each microsphere is optically wired to fiber, the specific interactions on each microsphere surface can be independently monitored. Walt and coworkers developed a high-density fiber-optic DNA microarray containing oligonucleotide-functionalized, 3.1-m-diameter microspheres haphazardly distributed on the etched face of an imaging fiber bundle [68, 69].

Usually, these fiber bundles are composed of around 6000–50,000 fused optical fibers, in which each fiber contains an etched well [70]. The desired oligonucleotide sequences are attached to individual microspheres, then added to each etched wells on the fiber optic bundle face. The produced microwell arrays are capable of casing complementary-sized microspheres, each containing thousands of copies of a unique oligonucleotide probe sequence. Walt and coworkers showed that the array fabrication process resulted in random microsphere placement. It should be understood that the determination of the position of microspheres in the random array, essentially required an optical encoding scheme. The detection schemes, which are combined the intrinsic recognition abilities of nucleic acids, are usually measured

Fig. 2.17 (**a**) Individual optical fiber is a flexible, transparent fiber and a fiber optic bundle consists of thousands of individual fibers fused bundle. (**b**) Scanning force images of the etched face of an optical fiber imaging bundle. The first (left) is empty, and the second (right) contains complementary-sized microspheres. Each well diameter is approximately 3.1 μm. [67]
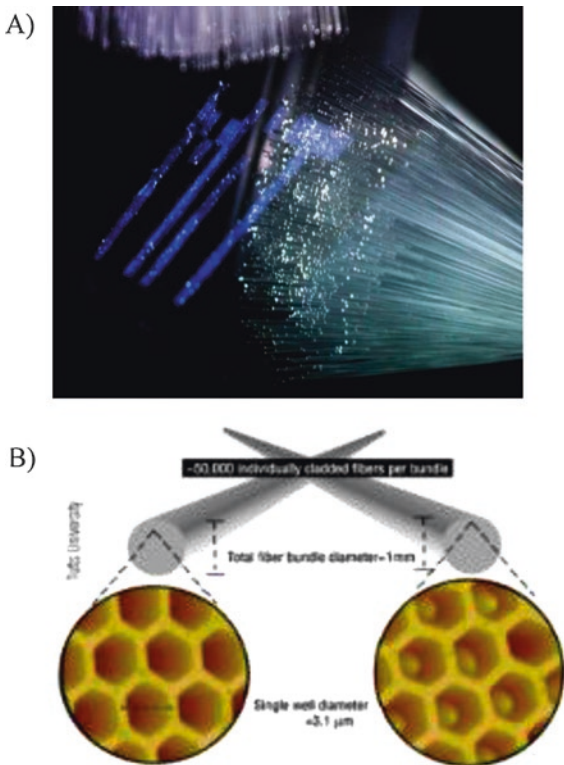
with fluorescence-based detection methods. This "optical bar code" obtained is simply a combination of fluorescent dyes with different excitation and emission wavelengths and intensities that allow each bead to be independently identified [70].

Nonetheless, additional degrees of freedom are available in the fiber-optic format, which allows an additional number of excitation and emission wavelengths that can be used. It should be mentioned that the optically bar-coded arrays, can be decoded in a matter of seconds. This occurs by conventional image processing software that collects a series of fluorescence images at different excitation and emission wavelengths and then analyzes the relative intensities of each bead. Alternatively, preformed oligonucleotides may be added directly to surface-activated microspheres [70].

Needless to say, those fluorescence-based assays are more desirable than traditional radiolabeled methods due to their increased safety and experimental versatility. Fluorescence can be incorporated into microarray assays by fluorescent intercalating dyes, fluorescently labeled targets, or label-less methods employing fluorescence resonance energy transfer (FRET). Fluorescence-based assays enable the measurement of multiple wavelengths independently and simultaneously. The use of multiple fluorophores enables parallel interrogation schemes [70–73].

2.3.6.1 Fiber Optic DNA Biosensors

A general array protocol entails immobilizing a probe sequence (primer) that can hybridize to its fluorescently-labeled complementary target. The fluorescent tag is commonly incorporated into the target molecules via polymerase chain reaction (PCR) [73]. This primer labeling method is convenient when amplification is needed for detection, or when it is used to construct a cDNA library from a genomic RNA pool via reverse transcription. In addition, the derivatized fiber core experiments can detect unlabeled (non-fluorescent) target solutions [66]. This is achieved by competitive hybridization with fluorescent target samples. In this method, the fluorescent synthetic target complements are synthesized and initially hybridized to the array to saturate the array probe elements [66]. The unlabeled target solution is then hybridized to the same array, competing with the prehybridized synthetic targets. The presence of the unlabeled target is determined by a fluorescence decrease caused by the displacement of the fluorescent synthetic target by the unlabeled species. This procedure eliminates the need to incorporate fluorescence into the target and allows quantitative measurements to be performed. These fiber optic platforms are the basis for microsphere array designs that improved array fabrication and allowed extremely high-density sensor placement [66].

2.3.6.2 Analysis Setup and Protocol

The imaging system consists of a light source, an inverted microscope, and a modified Olympus epifluorescence microscope/charge-coupled device camera (Photometrics PXL). A fiber chuck carried the imaging fiber in a fixed position while electronically controlled filter wheels switched between the analytical wavelength and the encoding wavelengths, enabling complete analysis and identification of the microspheres within minutes. Excitation light is sent into the proximal tip of the imaging fiber, and emission from the fluorescing molecules captured and directed onto the CCD camera detector (Fig. 2.18) [72A].

The multiplex analysis images were acquired for 1 and 0.5 s at wavelengths specific to each encoding dye. A 365-nm excitation filter and a 600-nm long-pass emission filter were used for the Eu-dye. A 620-nm excitation filter and a 670-nm emission filter were used for the Cy5 dye. A 530-nm excitation filter and a 580-nm emission filter were used for TAMRA. That is the detection of amplified DNA fragments that were incubated with a fluorescein-labeled sequencing primer in the existence of the two allelic ROX-ddNTP or TAMRA-ddNTP terminators. All targets were labeled with fluorescein. It was shown that the fluorescence intensity was proportional to the extent of hybridization at each probe position [72A]. In addition, the camera was equipped with an internal chip that provides megapixel resolution (1280/1024). This megapixel chip was able to resolve the arrays miniatured feature sizes (3 mm) and provided multiple pixels for each optical channel in the fiber bundle (Fig. 2.19).
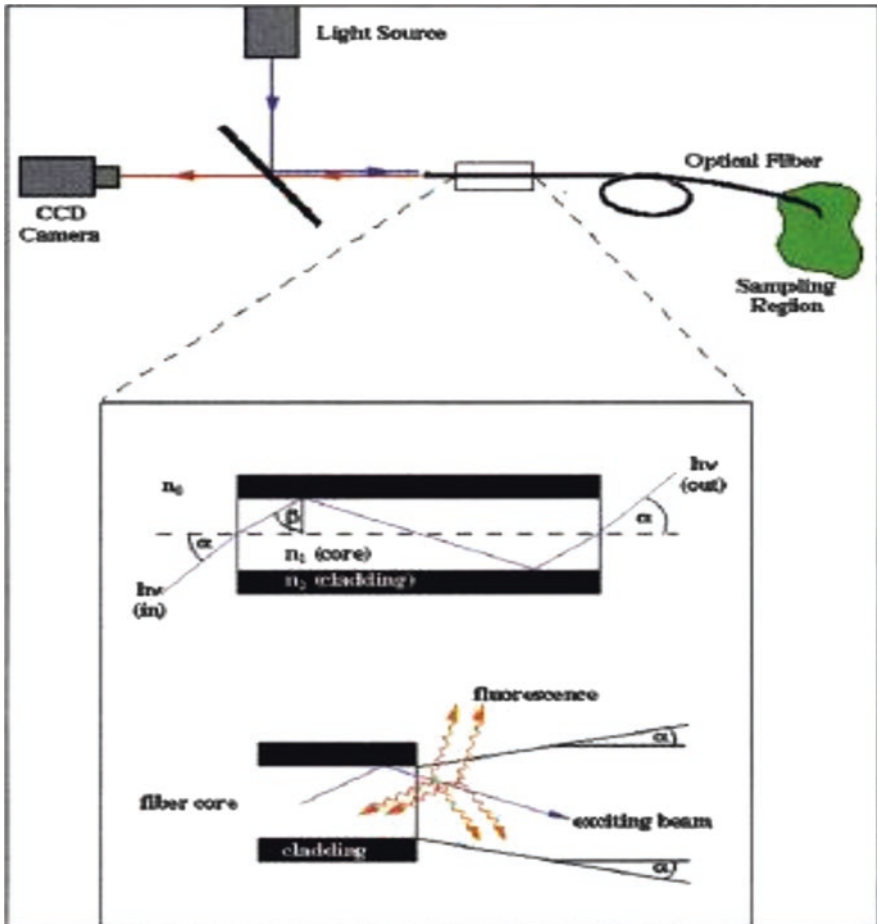
Fig. 2.18 Schematic diagram of the fiber optic imaging system. (Adapted from Ref. [72B])

This entire array is about the size of a single spot on a traditional spotted array. (Adapted from Ref. [72B]).

Finally, it can be surmised that the described fiber optic microsphere-based bio-sensor is a versatile platform that possesses micro-scale features and an overall array size that enables rapid analysis and extremely low detection limits. Redundant detection elements in the array increase the signal-to-noise ratio and avoid the potential for false-positive and false-negative results. Microsphere-based arrays are reusable and are easy to fabricate. The fiber optic platform has also been applied to other applications, including artificial olfaction and cell-based array sensing [66].
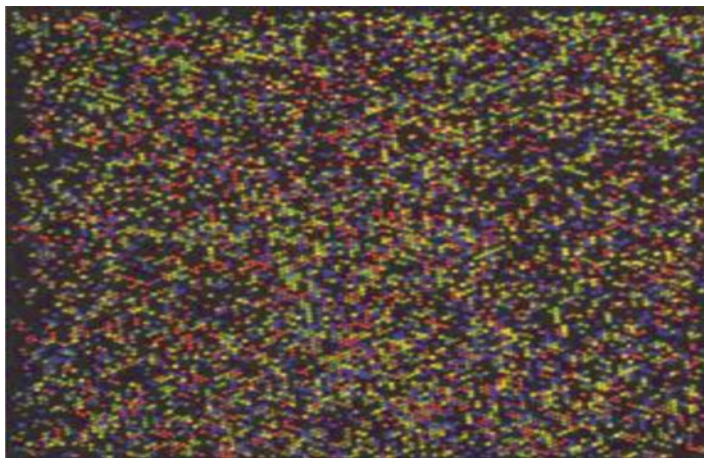
Fig. 2.19 An image of a 13,000-well square fiber bundle microarray, with a diameter of −1.2 mm

2.3.7 *Surface Plasmon Resonance*

Recently, numerous strategies for protein labeling were developed, and they allowed the characterization of proteins concerning their composition, folding, or interaction with other proteins [74]. Surface plasmon resonance (SPR) is a label-free detection procedure which is a suitable and reliable platform in clinical analysis for biomolecular interactions. Undeniably, SPR has been proven to be one of the most powerful technologies to determine the specificity, affinity, and kinetic parameters displayed during the binding of macromolecules. These binding of macromolecules include, but are not limited to, protein-protein, protein-DNA, enzyme-substrate or inhibitor, receptor-drug, lipid membrane-protein, protein-polysaccharide, and cell or virus-protein [75–84]. SPR is an optical technique that measures the refractive index changes in the vicinity of thin metal layers (i.e., gold, silver, or aluminum films) in response to biomolecular interactions.

2.3.7.1 SPR Principle

When the photon of an incident light strikes a metal surface, typically a gold surface, surface plasmon resonance occurs. When a portion of the light energy excites the electrons of the metal surface layer, at a certain angle of incidence, it creates electron movements which propagate parallel to the metal surface. This electric oscillation is termed as a "plasmon." This oscillation, in turn, makes an electric field whose range is approximately 300 nm from the border between the metal surface and sample solution [76, 79]. In a commercial SPR biosensor configuration, the incident light employed is generated by a high-reflective index glass prism of the
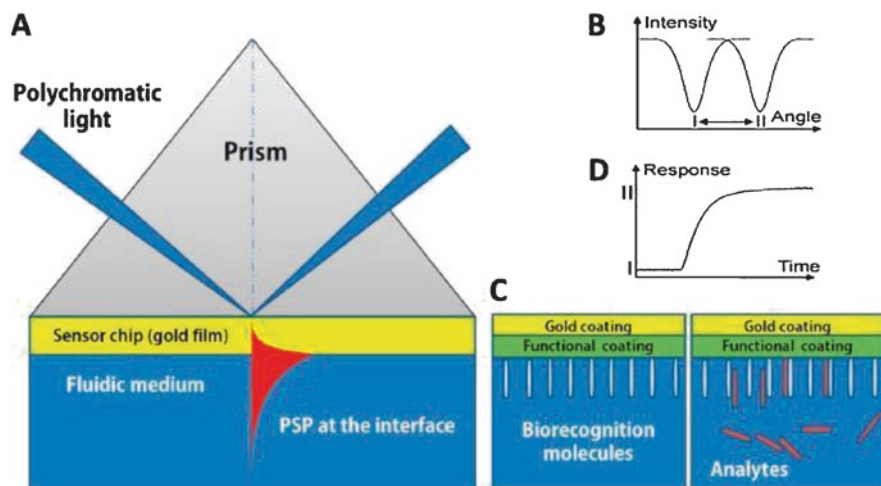
Fig. 2.20 Concept of a surface plasmon resonance (SPR) biosensor: (**a**) Kretschmann geometry of the ATR method; (**b**) spectrum of reflected light before and after refractive index change; (**c**) analyte-biorecognition elements binding on SPR sensor surface and (**d**) refractive index changes caused by the molecular interactions in the reaction medium. (Adapted from Ref. [74])

Kretschmann geometry of the attenuated total reflection (ATR) method (Fig. 2.20) [74].

The defined SPR angle, at which resonance happens, relies on the refractive index of the material coating the metal surface, and the constant light source wavelength. When there is no change in the reflective index of the sensing medium, the plasmon oscillation cannot be formed (Fig. 2.20a). In addition, it should be noted that when the surface of the sensing material has been coated through biomolecule attachment only, there will be perhaps an unnoticed small change in the reflective index of the sensing medium, and as a result, the plasmon oscillation cannot be formed (Fig. 2.20c, left side) [74]. However, when the metal surface has been coated with an analyte-biorecognition couple of biomolecules, detection is achieved by measuring the changes in the reflected light obtained on a detector (Fig. 2.20c, right side). In addition, the amount of surface concentration can be quantified by monitoring the reflected light intensity or tracking the resonance angle shifts. Typically, an SPR biosensor has a detection limit of 10 pg/mL [76–79].

In all commercial SPR biosensors, probe molecules are initially immobilized on to the surface of the sensor. Once the solution of target molecules is flown into contact with the surface, a probe-target binding via affinity interaction happens, which consequently induces an increase in the refractive index at the SPR sensor surface (Fig. 2.20d) [74]. Resonance or response units.

(RU) in SPR experiments are employed to explain the signal change, where 1 RU is equal to a critical angle shift of 10^{-4} degrees [80–84]. At the beginning of the

experiment, whereas probe-target interactions have not happened, the initial RU value relates to the initial critical angle. The difference in refractive index Δ_{nd} arise from within a layer of thickness h can be computed as:

$$\Delta nd = \left(dn \, / \, dc\right) vol \Delta\Gamma \, / \, h \tag{2.1}$$

where $(dn/dc)_{vol}$ is the increase of refractive index n with the volume concentration of analyte c, and $\Delta\Gamma$ is the concentration of the bound target on the surface [76].

2.3.7.2 High-Throughput Screening (HTS)

There are numerous different formats of SPR biosensors. These comprise the array format, multi-channel unit format, and SPR imaging format, which permit simultaneous and continuous detection to evaluate the performance of hundreds to thousands of affinity binding events on a chip surface [81–83]. In SPR imaging, the incidence angle remains constant, and the attachment of biomolecules on a gold surface is measured as the change in reflectivity (or reflectance) in relation to the incident ray intensity, unlike SPR sensors that depend on the measurement of the absorption dip in the SPR angle or SPR wavelength [80–84]. Recently, it was shown that SPR imaging technology using a multi-analyte biosensor allows the measurement of a high-throughput methodology, and it achieves a similar degree of sensitivity of conventional SPR biosensors (Fig. 2.21) [82].

Consequently, SPR imaging systems without any labeling requirements can be used for high-throughput screening (HTS), specifically in drug discovery, more than any other optics-based detection methods [83, 84].

2.3.7.3 Surface Plasmon Resonance Sensing of Biological Warfare Agent Botulinum Neurotoxin A

Dhaked and coworkers developed a label-free real-time method for the detection and quantification of botulinum neurotoxin A (BoNT/A) using surface plasmon resonance (SPR) [84]. The authors used an antibody against rBoNT/A-HCC fragment, and synaptic vesicles (SV), which were immobilized on a carboxymethyl dextran modified gold chip. The immobilization of BoNT/A antibody and interaction of BoNT/A with immobilized antibody were characterized in-situ by SPR and electrochemical impedance spectroscopy. A sample solution containing BoNT/A antigen in concentrations ranging from 0.225 fM to 4.5 fM and 0.045 fM to 5.62 fM was interacted with the immobilized antibody and immobilized SV, respectively [84].

Fig. 2.21 High-throughput drug screening using an SPR imaging protein chip system. The bright image indicates protein-protein interaction on a gold surface. Upon the binding of an inhibitor to the target protein, protein-protein interactions are disrupted, resulting in changes in SPR imaging signal intensity and a darker image. (Adapted from Ref. [82])
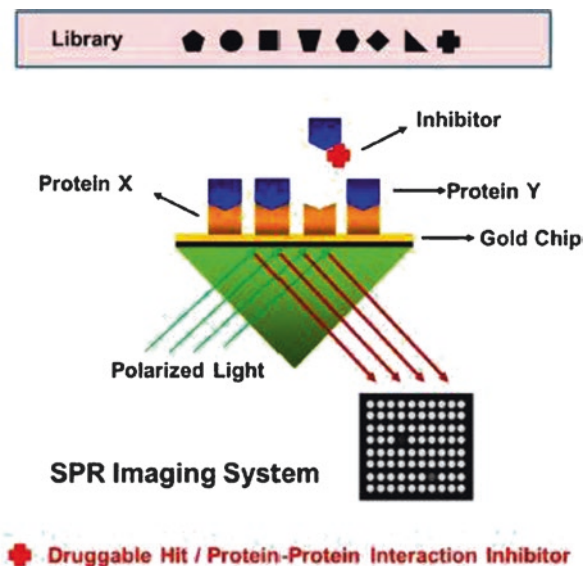
2.3.7.3.1 Immobilization of BoNT/A Antibody and SV Protein on CM5 SPR Sensor Chip

Dhaked and coworkers described the stepwise immobilization of BoNT/A antibody and SV protein on a CM5 chip, respectively, in nine steps. These steps involved the stabilization of the baseline, the activation of carboxyl groups on the CM5 chip, and converting them into activated carboxymethylated groups on the sensor chip for future bounding to the free amino groups of BoNT/A antibody. This was followed by washing with PBS and measuring the SPR angle that has shifted nearly to the baseline [84]. When the BoNT/A antibodies are injected on the CM5 chip, an increase in the SPR angle was observed. Finally, washing with 1000 mM ethanolamine was performed to prevent non-specific binding and to block the unreacted NHS-ester groups on CM5 chip. From Figs. 2.22 and 2.23, a net angle change of 95.44 m° and 48 m° are observed, and this ascribes the attachment of 0.79 ng/ mm2 of antibody and 0.4 ng/mm2 SV protein on CM5 chip, respectively [84].

2.4 Conclusion

Most of the sensing measuring devices used for the detection of biological warfare agents are based on luminescence immunoassay signal transduction mechanisms, which are optical. In this chapter, we have discussed the following subjects: impedance spectroscopy, evanescent wave technology and internal reflection fluorescence (TIRF) excitation, surface acoustic wave sensors, fluorescent biosensors, Fluorescence Resonance Energy Transfer (FRET), light emission (CANARY),
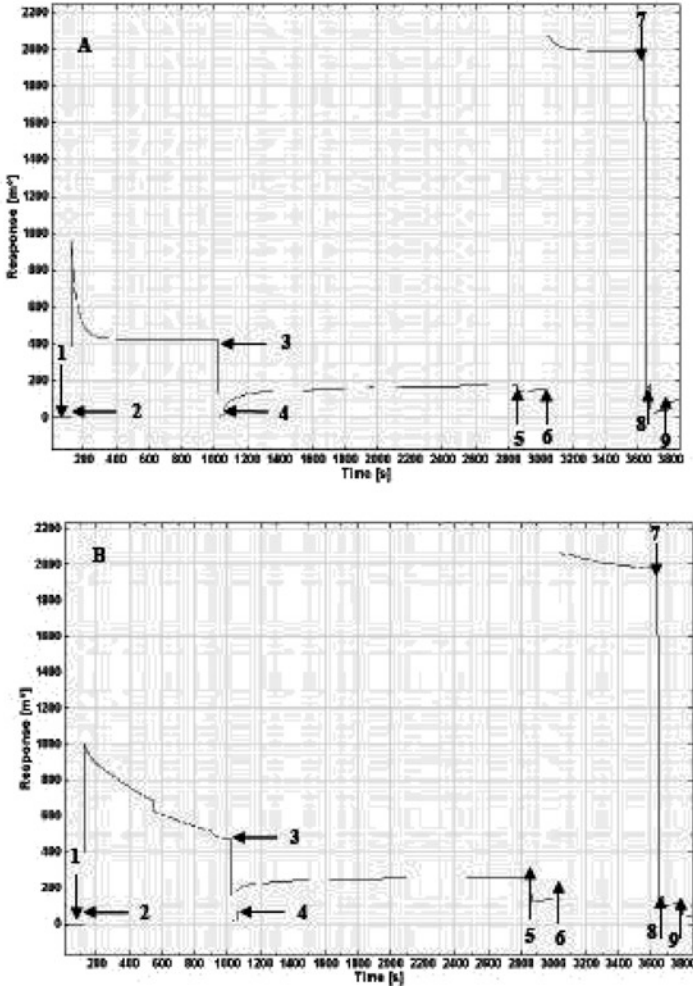
Fig. 2.22 Sensorgram showing different steps [(1) Baseline (2) EDCNHS activation (3) Washing (4) Antibody coupling (5) Washing (6) Deactivation (7) Washing (8) Regeneration and (9) Back to baseline] involved in the (**a**) immobilization of BoNT/A antibody (1: 500 dilution); (**b**) immobilization of SV on CM5 chip [84]

microsphere-based fiber-optic biosensors, and surface plasmon resonance. It should be noted that although fluorescence detection is the most popular, surface plasmon resonance (SPR)-based immunoassay formats with surface imaging capabilities are growing in popularity [80–86]. Multiplexing, or simultaneous detection of multiple analytes, is one of the most important prerequisites for biothreat agent detection. As mentioned in our introduction, the presented work is more a "Comptes Rendus" and an introduction to this series of sensing measuring devices used for the detection of biological warfare agents that were presented to the participants of this NATO-ASI meeting.
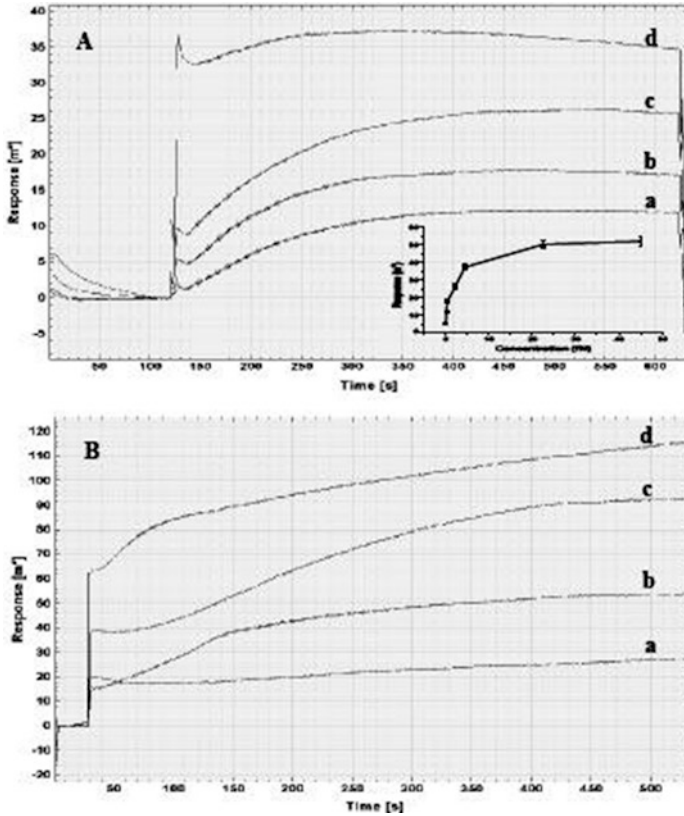
Fig. 2.23 SPR sensor response for the interaction of different concentration of BoNT/A antigen with (**a**) immobilized BoNT/A antibody (a) 0.225 fM, (b) 0.45 fM, (c) 2.25 fM and (d) 4.5 fM (**b**) immobilized SV (a) 0.045 fM, (b) 0.225 fM, (c) 1.12 fM and (d) 5.62 fM Temperature: 25o C and pH: 7.5 [84]

References

1. Eitzen EM Jr, Takafuji ET (1997) Historical overview of biological warfare. In: Sidell FR, Takafuji ET, Franz DR (eds) Medical aspects of chemical and biological warfare. Office of the Surgeon General, Borden Institute, Walter Reed Army Medical Center, Washington, DC, pp 415–423
2. Ridel R (2004) Biological warfare and bioterrorism: a historical review. Proc Bayl Univ Med Cent 17(4):400–406
3. WHO (2003) Severe acute respiratory syndrome (SARS). Wkly Epidemiol Rec 78. 86.92
4. Gray C (2007) Another bloody century: future warfare, Phoenix, pp 265–266
5. Heymann DL (2001) Strengthening global preparedness for defense against infectious disease threats. Committee on Foreign Relations, United States Senate. Hearing on the threat of bioterrorism and the Spread of Infectious Diseases
6. Hoffman RE, Norton JE (2000) Lessons learned from a full-scale bioterrorism exercise. Emerg Infect Dis 6:652–653

7. US Commission on National Security in the 21st Century (1999) New World Coming: American Security in the 21st Century, supporting research and analysis. September 15, 1999
8. Szinicz L (2005) History of chemical and biological warfare agents. Toxicology 214(3):167–181
9. CDC. Biological and Chemical Terrorism: Strategic Plan for Preparedness and Response (2005) Recommendatons of the CDC strategic planning workgroup. MMWR Recomm Rep 49.(RR-4:1–26
10. Cenciarelli O, Rea S, Carestia M, D'Amico F, Malizia A, Bellecci C, Gaudio P, Gucciardino A, Fiorito R (2013) Bioweapons and bioterrorism: a review of history and biological agents. Defence S&T Tech Bull 6(2):111–129
11. Barrett JA , Bowen GW, Golly SM, Hawley C, Jackson WM, Laughlin L, Lynch ME, (1998) Assessment of biological agent detection equipment for emergency responders, June 1, 1998. Chemical Biological Information Analysis Center (CBIAC), P.O. Box 196, Gunpowder, MD 21010-0196
12. Chemical and Biological Terrorism: Research and Development to Improve Civilian Medical Response to Chemical and Biological Terrorism Incidents, National Academy of Sciences (1999) National Academy Press, Washington, DC 2005
13. Barrett JA, Bowen GW, Golly SM, Hawley C, Jackson WM, Laughlin L, Lynch ME, (1998) Final Report on the Assessment of Biological Agent Detection Equipment for Emergency Responders, U.S. Army Chemical and Biological Defense Command (CBDCOM), CBIAC, P.O. Box 196, Gunpowder, MD 21010-0196
14. Marquette CA, Blum LJ (2006) State of the art and recent advances in immunoanalytical systems. Biosens Bioelectron 21(8):1424–1433
15. IUPAC (1992), 64: 143
16. Sapsforda KE, Bradburneb C, Delehantyb JB, Medintzb I (2008) Sensors for detecting biological agents. Mater Today 11(3):38–49
17. Thevenot R, Toth K, Durst RA, Wilson GS (1999) Electrochemical biosensors: recommended definitions and classification. Pure Appl Chem 71:2333–2348
18. Thevenot R, Toth K, Durst RA, Wilson GS (2010) Electrochemical biosensors: recommended definitions and classification. Biosens Bioelectron 16:121–131
19. Thevenot R, Toth K, Durst RA, Wilson GS (2001) Electrochemical biosensors: recommended definitions and classification. Anal Lett 34:635–659
20. Daly P, Collier T, Doyle S (2002) PCR-ELISA detection of Escherichia coli in milk. Lett Appl Microbiol 34:222–226
21. Tsai W-L, Miller CE, Richter ER (2000) Determination of the sensitivity of a rapid *Escherichia coli* O157:H7 assay for testing 375-gram composite samples. Appl Environ Microbio 66(9):4149–4151
22. Nicolas P, Mor A (1995) Peptides as weapons against microorganisms in the chemical defense system of vertebrates. Annu Rev Microbiol 49:277–304
23. Zasloff M (2002) Antimicrobial peptides of multicellular organisms. Nature 415:389–339
24. Meng H, Kumar K (2007) Antimicrobial activity and protease stability of peptides containing fluorinated amino acids. J Am Chem Soc 129:15615–15622
25. Mannoor MS, Zhang C, Link J, McAlpine MS (2010) Electrical detection of pathogenic bacteria via immobilized antimicrobial peptides. Proc Natl Acad Sci U S A 107(45):19207–19212
26. Zasloff M, Martin B, Chen HC (1988) Antimicrobial activity of synthetic magainin peptides and several analogues. Proc Natl Acad Sci U S A 85:910–913
27. Zasloff M (1987) Magainins, a class of antimicrobial peptides from Xenopus skin: isolation, characterization of two active forms, and partial cDNA sequence of a precursor. Proc Natl Acad Sci U S A 84:5449–5453
28. Matsuzaki K, Sugishita KI, Harada M, Fujii N, Miyajima K (1997) Interactions of an antimicrobial peptide, magainin 2, with outer and inner membranes of Gram-negative bacteria. BBA-Biomembranes 1327:119–130
29. Taitt CR, Shriver-Lake LC, Ngundi MM, Ligler FS (2008) Array biosensor for toxin detection: continued advances. Sensors 8:8361–8377

30. Ligler FS, Taitt CR, Shriver-Lake LC, Sapsford KE, Shubin Y, JPb G (2003) Array biosensor for detection of toxins. Anal Bioanal Chem 377(3):469–477

31. Feldstein MJ, Golden JP, Ligler FS, Rowe CA (2001) Reflectively coated optical waveguide and fluidics cell integration. U.S. Pat. 6: 192,168

32. Golden JP, Taitt CR, Shriver-Lake LC, Shubin YS, Ligler FS (2005) A portable automated multianalyte biosensor. Talanta 65(5):1078–1085

33. Ngundi MM, Qadri SA, Wallace EV, Moore MH, Lassman ME, Shriver-Lake LC, Ligler FS, Taitt CR (2006) Detection of deoxynivalenol in foods and indoor air using an array biosensor. Environ Sci Technol 40(7):2352–2356

34. Sapsford KE, Taitt CR, Fertig S, Moore MH, Lassman ME, Maragos CA, ShriverLake LC (2006) Indirect competitive immunoassay for detection of aflatoxin B-1 in corn and nut products using the array biosensor. Biosens Bioelectron 21(12):2298–2305

35. Ngundi MM, Taitt CR (2006) An Array biosensor for detection of bacterial and toxic contaminants of foods. In: Diagnostic bacteriology protocols. Humana Press, Totowa, pp 53–68

36. Shriver-Lake LC, Erickson JS, Sapsford KE, Ngundi MM, Shaffer KM, Kulagina NV, Hu JE, Gray SA, Golden JP, Ligler FS, Taitt CR (2007) Blind laboratory trials for multiple pathogens in spiked food matrices. Anal Lett 40(16–18):3219–3323

37. Milne EA (1941) Augustus Edward Hough love. 1863–1940. Obituary Notices of Fellows of the Royal Society 3(9):466

38. O'Connor JJ, Robertson EF Augustus Edward Hough love. In: MacTutor history of mathematics archive. University of St Andrews, St. Andrews

39. Länge K, Rapp BE, Rapp M (2008) Surface acoustic wave biosensors: a review. Anal Bioanal Chem 391:1509–1519

40. https://www.mccoycomponents.com/blog/view/anatomy-of-baw-saw-and-fbar-filters

41. Weinheim E, Wohltjen H, Dessy R (1979) Anal Chem 51:1458–1464

42. Collings AF, Caruso F (1997) Rep Prog Phys 60:1397–1445

43. Tamarin O, Comeau S, Déjous C, Moynet D, Rebière D, Bezian J, Pistré J (2003) Biosens Bioelectron 18:755–763

44. Stubbs DD, Hunt WD, Lee SH, Doyle DF (2002) Biosens Bioelectron 17:471–477

45. Stubbs DD, Lee SH, Hunt WD (2003) Anal Chem 75:6231–6235

46. Sapsford KE, Berti L, Medintz IL (2005) Fluorescence resonance energy transfer concepts, applications and advances. Minerva Biotech 16:253–279

47. Goldman ER, Medintz IL, Mattoussi H (2006) Luminescent quantum dots in immunoassays. Anal Bioanal Chem 384:560–563

48. Goldman ER, Balighian ED, Mattoussi H, Kuno MK, Mauro JM, TranPT AGP (2002) Avidin: a natural bridge for quantum dot-antibody conjugates. J Am Chem Soc 124:6378–6638

49. Wang SP, Mamedova N, Kotov NA, Chen W, Studer J (2002) Antigen/antibody immunocomplex from CdTe nanoparticle bioconjugates. Nano Lett 2:817–822

50. Sun BQ, Xie WZ, Yi GS, Chen DP, Zhou YX, Cheng J (2001) Microminiaturized immunoassays using quantum dots as fluorescent label by laser confocal scanning fluorescence detection. J Immunological Methods 249:85–89

51. Hoshino A, Fujioka K, Manabe N, Yamaya S, Goto Y, Yasuhara M, Yamamoto K (2005) Simultaneous multicolor detection system of the single-molecular microbial antigen with total internal reflection fluorescence microscopy. Microbiology & Immunology 49:461–470

52. Liang RQ, Li W, Li Y, Tan CY, Li JX, Jin YX, Ruan KC (2005) An oligonucleotide microarray for microRNA expression analysis based on labeling RNA with quantum dot and nanogold probe. Nucleic Acids Res 33:e17

53. Sapsford KE, Thomas P, Medintz IL, Hedi M (2006) Biosensing with luminescent semiconductor quantum dots. Sensor 6:925–953

54. Yang L, Li Y (2006) Simultaneous detection of Escherichia coli O157: H7 and Salmonella Typhimurium using quantum dots as fluorescence labels. Analyst 131(3):394-401

55. Jares-Erijman E, T b J (2003) FRET Imaging. Nature Biotech 21:1387–1395

56. Sapsford KE, Berti L, Medintz IL (2005) Fluorescence resonance energy transfer concepts, applications and advances. Minerva Biotech 16:253–279

57. Sandros MG, Shete V, Benson DE (2006) Selective, reversible, reagentless maltose biosensing with core-shell semiconducting nanoparticles. Analyst 131:229–235

58. Petrovick MS, James D, Harper JD, Frances E, Nargi FE, Eric D, Schwoebel ED, Mark C, Hennessy MC, Todd H, Rider TH, Hollis MA (2007) Rapid sensors for biological-agent iden-tification. LINCOLN LABORATORY JOURNAL (17):63–84

59. Cormie MJ, Prasher DC, Longiaru M, McCann RO (1989) The enzymology and molecular biology of the Ca2+-activated photoprotein, Aequorin. Photochem Photobiol 49(4):509–512

60. Shimomura O, Musicki B, Kishi Y (1989) Semi-synthetic Aequorins with improved sensitivity to Ca2+ ions. Biochem J 261:913–920

61. Wilson HA, Greenblatt D, Poeni M, Finkelman FD, Tsien RY (1987) Cross-linkage of B lymphocyte surface immunoglobulin by anti-Ig or antigen induces prolonged oscillation of intracellular ionized calcium. J Exp Med 166:601–606

62. Tsuji FJ, Inouye S, Goto T, Sakaki Y (1983) Site-specific mutagenesis of the calcium-binding photoprotein aequorin. Proc Natl Acad Sci U S A 83:8107–8111

63. Shimomura O, Johnson FH (1978) Peroxidized coelenterazine, the active group in the photo-protein aequorin. Proc Natl Acad Sci U S A 75(6):2611–2615

64. Rider TH, Petrovick MS, Nargi FE A B cell–based sensor for rapid identification of pathogens. Science 301:213–215

65. Senior JM, Yousif JM (2009) Optical fiber communications: principles and practice. Pearson Education

66. Epstein JR, Leung APK, Kyong-Hoon L, Walt DR (2003) High-density, microsphere-based fiber optic DNA microarrays. Biosens Bioelectron 18:541–546

67. http://spie.org/newsroom/decoding-dna

68. Pantano P, Walt DR (1996) Ordered nanowell arrays. Chem Mater 8:2832–2835

69. Fodor SPA, Read JL, Pirrung MC, Stryer L, Lu AT, Solas D (1991) Light-directed, spatially addressable parallel chemical synthesis. Science 251:767–773

70. Epstein JR, Lee M, Walt DR (2002) High-density fiber-optic genosensor microsphere array capable of zeptomole detection limits. Anal Chem 74:1836–1840

71. Schena M, Shalon D, Davis RW, Brown PO (1995) Quantitative monitoring of gene expression patterns with a complementary DNA microarray. Science 270:467–470

72. (A) Ferguson JA, Steemers FJ, Walt DR (2000) High density fiber optic DNA random micro-sphere array. Anal Chem 72:5618–5624; (B) Walt DR (2000) Bead-based fiber-optic arrays. Science 287(5452):451–45

73. Mullis KB (1994) Polymerase chain reaction (Nobel prize). Angew Chem 106:1271–1276

74. Nguyen HH, Park J, Sebyung Kang S, Kim M (2013) Surface plasmon resonance: a versatile technique for biosensor applications. Sensors 15:10481–10510

75. Stephanopoulos N, Francis MB (2006) Choosing an effective protein bioconjugation strategy. Nat Chem Biol 7:876–884

76. Tugarinov V, Kanelis V, Kay LE (2006) Isotope labeling strategies for the study of high-molecular-weight proteins by solution NMR spectroscopy. Nat Protoc 1:749–754

77. Phelan ML, Nock S (2003) Generation of bioreagents for protein chips. Proteomics 3:2123–2134

78. Šípová H, Homola J (2013) Surface plasmon resonance sensing of nucleic acids: a review. Anal Chim Acta 773:9–23

79. De Feijte JA, Benjamins J, Veer FA (1978) Ellipsometry as a tool to study the adsorption behavior of synthetic and biopolymers at the air-water interface. Biopolymers 17:1759–1772

80. Smith EA, Corn RM (2003) Surface plasmon resonance imaging as a tool to monitor biomo-lecular interactions in an array based forma. Appl Spectrosc 57:320A–332A

81. Steiner G (2004) Surface plasmon resonance imaging. Anal Bioanal Chem 379:328–331

82. Jung SO, Ro HS, Kho BH, Shin YB, Kim MG, Chung BH (2005) Surface plasmon resonance imaging-based protein arrays for high-throughput screening of protein-protein interaction inhibitors. Proteomics 5:4427–4431
83. Kim M, Han SH, Shin Y (2007) Surface plasmon resonance biosensor chips. Biochip J 1:81–89
84. Tomar A, Gupta G, Singh MK, Boopathi M, Singh B, Dhaked RK (2016) Surface plasmon resonance sensing of biological warfare agent botulinum neurotoxin A. J Bioterror Biodef 7(2):142–154
85. Tsai WC, Li IC (2009) SPR-based immunosensor for determining staphylococcal enterotoxin a. Sens Actuators B Chem 136:8–12
86. Stenberg E, Persson B, Roos H, Urbaniczky C (1991) Quantitative determination of surface concentration of protein with surface plasmon resonance using radiolabeled proteins. J Coll Interf Sci 143:513–526

Chapter 3
Mass Spectrometry Methods for Food Safety/Detection of Toxins in Food

Gianluca Giorgi

Abstract In this chapter, a brief overview of fundamentals in mass spectrometry (MS) and on methods for food safety and detection of toxins in food is described. It is focused on ionization techniques, analyzers, high resolution MS, tandem MS and on different methodologies and approaches that modern mass spectrometry offers in this field.

3.1   Mass Spectrometry: An Overview

Mass spectrometry (MS) is an important and very powerful methodology for structurally characterizing, identifying, and for quantifying wide classes of unknowns, ranging from apolar low molecular weight (MW) analytes to polar big molecules with MW of millions of Daltons [1–3].

MS finds applications in many fields, such as food, biomedicine, environment, archaeology, forensics, *omics* sciences, etc. Its most important features are high specificity and selectivity, high sensitivity and high speed. Its coupling with separative techniques, such as gas chromatography (GC) and high performance liquid chromatography (HPLC), lets possible to carry out analysis of very complex mixtures with high sensitivity and specificity. The scheme of a mass spectrometer is reported in Fig. 3.1.

Mass spectrometry studies ions in the gas phase. As we are generally dealing with molecules, the first event which must occur in a mass spectrometer, and in particular in the ion source, is the ionization, *i.e.* transformation of a molecule into an ion. Once formed, ions are driven towards the analyzer, which separates them according to their mass-to-charge (*m/z*) ratios, and finally to the detector.

G. Giorgi (✉)

Department of Biotechnology, Chemistry & Pharmacy, University of Siena, Siena, Italy
e-mail: gianluca.giorgi@unisi.it
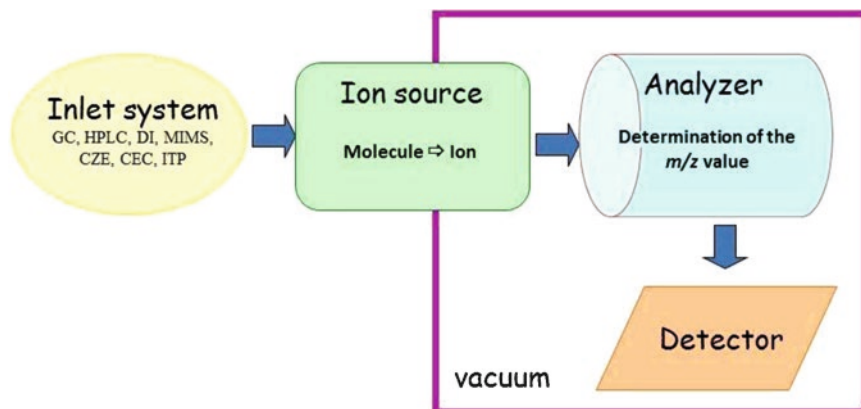
Fig. 3.1 The diagram of a mass spectrometer

3.2 Ionization Techniques

Ionization is the crucial event in every MS experiment: if ions are not formed, no any datum will be obtained.

Mass spectrometry can study wide classes of molecules with different chemico-physical properties. Having different properties, they cannot be ionized with the same ionization technique. So there are ionization techniques for volatile molecules and many others for ionizing polar analytes. All of them can be used for ionizing different toxins [4].

3.2.1 Volatile Molecules

Ionization techniques for ionizing volatile molecules are mostly limited to electron ionization and chemical ionization. The former is the first ionization technique used in MS more than one century ago and it is based on gas phase interactions between a molecule with an energetic electron beam. Chemical ionization has been introduced around the middle of the previous century and it is based on gas-phase ion-molecule reactions between the neutral analyte and a gas introduced in the ion source.

Both these ionization techniques can be coupled to gas chromatography (GC-MS) for the analysis of complex mixtures.

As an example, volatile toxins, such as polychlorinated dibenzo-*p*-dioxins (PCDDs), poly-chlorinated dibenzofurans (PCDFs), polychlorinated biphenyls (PCBs) [5] and mycotoxins [6] can be ionized by electron ionization and chemical ionization.

3.2.2   *Polar Analytes*

The real revolution in ionization methods for polar compounds is represented by Fast Atom Bombardment (FAB) introduced in 1981 by Barber and Bordoli [7]. FAB overcame the previous methods as it was easy, sensitive, reproducible, fast and able to ionize relatively big molecules.

But few years after its introduction, other ionization techniques, and in particular electrospray (ESI) and matrix-assisted laser desorption (MALDI), owing to their higher versatility, replaced FAB. Soon other atmospheric pressure ionizations were introduced, *i.e.* atmospheric pressure chemical ionization (APCI), atmospheric pressure photo ionization (APPI). More recently an increasing plethora of ambient mass spectrometry methods [8], such as desorption electrospray ionization (DESI) [9], direct analysis in real time (DART) [10], low temperature plasma (LTP) [11], rapid evaporative ionization mass spectrometry (REIMS) [12], paper spray ionization (PSI) [13], electrospray laser desorption ionization (ELDI) [14] and many others, which ionize analytes in their ambient, reducing or eliminating extraction and purification steps, have been introduced. As an example, ambient conditions using DART ionization coupled to high resolution mass spectrometry have been used in the analysis of multiple mycotoxins in cereals [15], while ELDI has been used for a rapid identification of herbal toxins emergency care [16].

3.3   Analyzers

Once the ions are formed in the ion source, they are accelerated towards the mass analyzer where their separation occurs according to their *m/z* ratios.

Analyzers can be divided into two main groups: those based on ion separation *in space* (or ion-beam analyzers: sectors, quadrupole, time of flight) and those separating ions *in time* (ion traps, Orbitrap, FT-ICR) (Table 3.1).

For ion separation, analyzers can use a magnetic field (B), an electric field (E) and a radiofrequency. As an example, quadrupoles use an electric field and a radiofrequency while with Orbitrap only an electric field is used.

Analyzers differ each other for some features, such as coverage of *m/z* range and resolving power. While time-of-flight has not restriction on *m/z* range, routinely all the others can analyze ions up to *m/z* 4000÷6000.

Actually, analyzers with high resolving power are: sectors (EB, BE), time of flight, FT-ICR and Orbitrap. A high resolving power allows to obtain some advantages, such as an increase of selectivity due to isobaric ion differentiation, elimination of interfering species and measurement of accurate mass from which the elemental composition of an ion can be obtained. On the other hand, an increase of resolving power implies a decrease of sensitivity and an increase of scan time.

Analyzers are involved not only in obtaining a full scan mass spectrum but also in tandem mass spectrometry experiments. Briefly, tandem mass spectrometry uses

Table 3.1 Analyzers and their main features

Analyzer	Force	Separation based on	*m/z* range	Resolving power	Mass accuracy
Ion separation *in space*					
Sectors (EB, BE, ….)	Magnetic and electrostatic fields	Ion momentum and kinetic energy	10,000	10,000	1–3 ppm
Quadrupole (Q)	Electric field and radiofrequency	Stability/instability	4000	Unit	No
Time of flight (ToF)	Electric field	Speed	>100,000	>30,000	1–3 ppm
Ion separation *in time*					
3D and 2D ion trap (IT)	Electric field and radiofrequency	Frequency of the orbits	4000	<500	No
Fourier transform ion cyclotron resonance (FT-ICR)	Electric field, radiofrequency, magnetic field	Frequency of the orbits	10,000	>1,000,000	<1 ppm
Orbitrap	Electric field	Frequency of the harmonic oscillations	<6000	>300,000	1–3 ppm

two (MS/MS or MS^2) or more (MS^n) sequential stages of mass analysis (which can be spatially or temporally separated) in order to examine selectively the dissociations of given ions in a mixture of ions. For small molecules, ion dissociation can be induced by collision with a gas, such as nitrogen, argon, helium, occurring in a collision cell (q) located after the first analyzer, or inside an ion trap.

Different instrumental setup can be used in tandem mass spectrometry, such as sectors (B,E; E,B), triple quadrupoles (QqQ), ion traps, QqToF, Q-Orbitrap, FT-ICR, ToF/ToF.

3.4 Study of Complex Mixtures by MS

In the study of complex mixtures by MS, the classical approach consists in an extraction, a preliminary purification of the sample and a coupling of MS with gas chromatography (GC) for volatile compounds or with high performance liquid chromatography (HPLC) for polar compounds. Thus GC-MS(/MS) and HPLC-MS(/MS) couplings are extensively used when complex mixtures have to be analyzed. This approach increases specificity and selectivity of the analysis, because, for each compound, in addition to its mass spectrum, its retention time is also obtained. So, even if different compounds might yield the same mass spectrum, they will have different retention times.

A new tendency is to reduce at minimum or remove at all the extraction and purification steps and to introduce the entire sample inside the ion source. This can

be done in classical atmospheric pressure ionizations, such as ESI, by direct infusion, or by using ambient mass spectrometry techniques, such as DESI, DART, LTP, REIMS, PSI, etc.

The simultaneous introduction of many analytes in the ion source gives a molecular fingerprint of the sample and it is very effective for rapid screening analyses. On the other hand, it can have some drawbacks, such as ion suppression phenomena, presence of isobaric species, need of a high dynamic range, difficulty to detect trace molecules.

3.5   Identification, Confirmation and Quantitation of Analytes by Mass Spectrometry

Depending on the information we are interested in, different mass spectrometry approaches and strategies, using MS, high resolution mass spectrometry and tandem mass spectrometry, can be followed for identification, confirmation and quantitation of different compounds in complex matrices.

3.5.1   Structural Characterization and Identification of Unknowns: Untarget Analysis

In a discovery phase of a study in many fields, such as metabolomics [17], proteomics [18], toxicology [19], and many others, for structurally characterize and identifying unknowns without any preliminary information, an untarget analysis has to be performed.

An untargeted profiling shows the presence of all ionizable and detectable analytes and it can be advantageous for novel marker and toxin discovering. Further, this approach permits retrospective analysis of data based on a-posteriori hypothesis.

On the other hand, low abundance compounds might be likely missed because ion suppression or obscuration by background signals from the matrix.

In mass spectrometry untarget analysis, two main methods can be used: Data Dependent Acquisition or Data Independent Acquisition methods.

3.5.1.1   Data Dependent Acquisition (DDA)

 In Data Dependent Acquisition a full MS scan is performed and ions are ranked by their intensities and/or charges. Then, according to user defined criteria, software applies automated real-time decisions for subsequent HRMS/MS^n analysis (Fig. 3.2).

A user-defined criterion might be: for ions exceeding a signal threshold, a high-resolution mass spectrum in a narrow m/z range followed by MS^2 or MS^n product ion scans have to be performed. To avoid repeating the same experiment for the
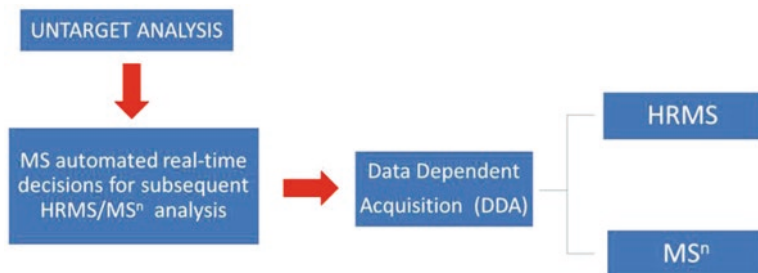
Fig. 3.2 Scheme of untarget and data dependent acquisition analysis
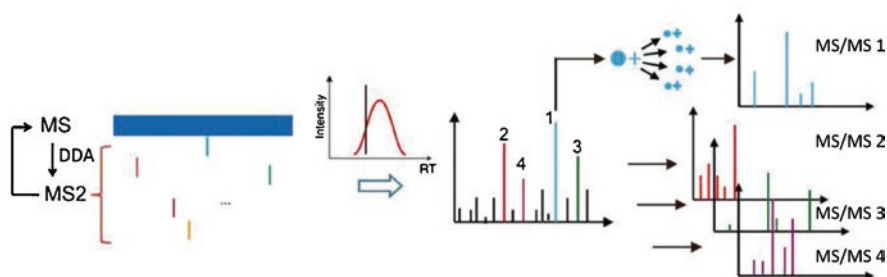
Fig. 3.3 A scheme of data dependent acquisition analysis. A MS full scan is acquired followed by MS^2 product ion scans of automated real-time selected ions. (Adapted from Ref. [17]. Copyright 2019, Springer)

same ions, a dynamic exclusion criterion (*i.e.* in the next 50 s doesn't select the same *m/z* value more than one time) has also to be defined (Fig. 3.3).

Different instrumental setup can be used for DDA analysis, such as sector instruments, ion traps, triple quadrupoles, Q-Orbitrap, QToF, FT-ICR.

DDA technique suffers from some limitations derived by low MS^2 spectral coverage due to its biased selection of high abundant precursor ions and to the undefined MS^2 spectral quality as the MS/MS spectra are not always acquired at the apex of a chromatographic peak.

High resolution mass spectrometry can be also used for a full mass spectrum acquisition in the *m/z* range defined by the operator.

3.5.1.2 Data Independent Acquisition (DIA)

Data independent acquisition methods have been generally used for target analysis. Some of them, and in particular those based on MS^{All}, MS^E, SWATH, PAcIFIC and MSX scan modes, are currently used for both target and untarget analysis (Fig. 3.4).

These approaches are not strictly MS^2 acquisition methods as no precursor ion selection is performed. In particular, ions in a narrow/wide *m/z* range are submitted all together to collision induced dissociations. Thus the resulting product ion
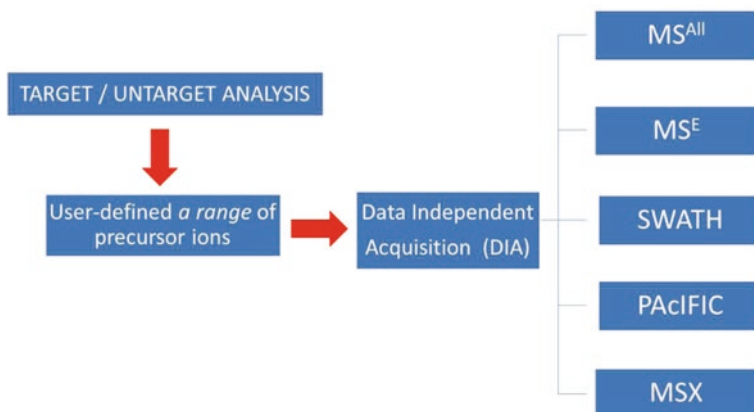
Fig. 3.4 Data independent acquisition modes based on user-defined ranges of precursor ions

spectrum contains all product ions, regardless of what the precursor ion is. It follows that the MS^2 spectrum is nonselective and it may lack specificity if more than one compound enters the ion source at the same time. It follows that these techniques generally require efficient chromatographic separations.

The produced data sets are very large, including a huge number of ions produced by also a huge number of analytes, which have to be entirely processed with appropriate algorithms and data analysis strategies.

The MS^{All} scan mode, also referred as MS^E [20], or All Ion Fragmentation (AIF) [21, 22] consists of two parallel alternating scan functions operating in a QqToF mass spectrometer: in the first, all ions coming from the ion source within a wide mass range (*e.g. m/z* 100–1000) are transmitted all together through a quadrupole, operating in a wide pass mode, to the collision cell, which has a low collision energy, so to avoid fragmentation, and finally to the ToF mass analyzer. All these ions form the precursor ion spectrum. The second scan function acquires data over the same mass range, but the collision energy is high (20–40 eV, for example) so to obtain product ions which are analyzed by the ToF analyzer. The result is a nonselective product ion spectrum of all precursor ions. By using a ToF analyzer, high resolution spectra are obtained for both the precursor ion and the product ion spectra.

If an efficient separative system, such as GC, HPLC or ion mobility, is coupled to MS, in most cases, the predominant fragment ions are produced by a single precursor ion.

The entire data set is then mined post-acquisition by assigning product ion spectra to their associated precursor ion peaks. This is done by aligning the precursor ion spectrum of each component with its corresponding product ion spectrum by retention time.

A scheme of the LC-MS^E method is depicted in Fig. 3.5.

SWATH (sequential window acquisition of all theoretical fragment-ion spectra) analysis is implemented on a QqToF instrumentation [24, 25]. In this technique, the
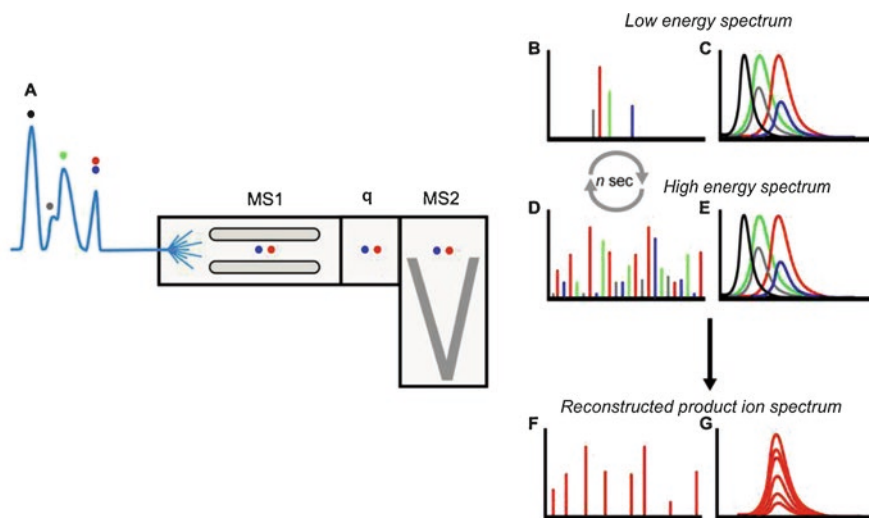
Fig. 3.5 An overview of LC–MS^E. Molecules coming from a separative system enter the mass spectrometer (**A**). They are ionized and ions pass through the quadrupole, operating in a wide pass mode (MS1), enter the collision cell (q) and then the ToF analyzer. When the collision energy is low, spectra of all precursor ions are obtained (**B**) together with their retention times (**C**); when the collision energy is switched to high, spectra of all product ions are obtained (**D**) together with their retention times (**E**). An ion-accounting algorithm compares the retention time profiles and intensity of all individual precursor ions (**C**) to all individual product ions (**E**) matching them on the basis of retention time profile and intensity (**G**) and creating a reconstructed product ion spectrum linked to a single precursor ion (**F**) that can be used by search engines to identify compounds. (Adapted from Ref. [23])

quadrupole analyzer is stepped continuously across the whole selected *m/z* range with a medium width mass window (20–30 Da) for precursor ion selection. Precursor ions are then transmitted to the collision cell, submitted to collision-induced dissociations and the resulting product ions are analyzed sequentially in high resolution by the ToF analyzer (Fig. 3.6).

The quadrupole isolation window can be (*i*) fixed (*e.g.* 25 Da width) (Fig. 3.6A); (*ii*) variable, with different isolation width based on equalizing the distribution of either the precursor ion population or the total ion current (Fig. 3.6B) [26], (*iii*) sequentially shifted with a small overlapping mass range (*e.g.* 5 Da), referred to as shift or offset SWATH, typically requiring five repetitive injections so to reconstruct more accurately the precursor/product ion relationship and improve the accuracy of compound identification and quantification (Fig. 3.6C) [27].

Other DIA methods are PAcIFIC and MSX, both applied in proteomics.

PAcIFIC, referred as precursor acquisition independent from ion count, has been developed on a LTQ-Orbitrap instrument and requires multiple injections for one sample analysis [28].

In the first injection, the ion trap performs MS^2 spectra at every *m/z* value at each of ten continuous intervals (each with a 1.5 Da width) across a range of 15 Da using
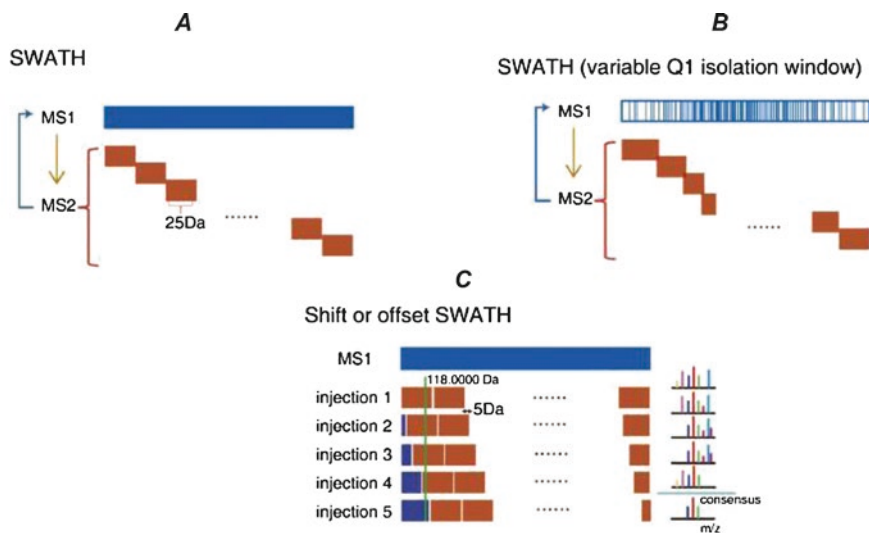
Fig. 3.6 Different SWATH scan modes. (Adapted from Ref. [17])

a 2.5 Da isolation width. The injections are repeated, in each shifting the *m/z* range 15 Da up, until the whole *m/z* range has been covered. This has the advantage to decrease the complexity of acquired MS^2 at cost of repeating multiple injections for each sample.

MSX is another data independent acquisition method mainly applied in proteomics and set up in the Q Exactive mass spectrometer [29]. It is developed by multiplexing five isolation mass ranges (4 Da each), randomly chosen from the predefined *n* possible non overlapping windows, and combined in one multiplexed MS^2 spectrum. The random selection is repeated until the whole *m/z* range is covered. MSX technique maintains the acquisition efficiency similar to SWATH technique, but higher selectivity similar to PAcIFIC, which is a good combination of data acquisition efficiency and computational deconvolution [17].

3.5.2 Confirm Presence/Absence of Known Analytes and Quantitation: Target Analysis

In the case of confirmation of presence/absence/suspicion of known analytes and/or for their quantitation, a target analysis can be performed (Fig. 3.7). In this case, the gas phase behavior of each analyte is known, so distinctive single ions or reactions are monitored.

A target analysis has advantages of high sensitivity, wide dynamic range, high reproducibility and allowing quantitative reproducibility. On the other hand, it is limited by the number of compounds which can be analyzed in a single experiment.
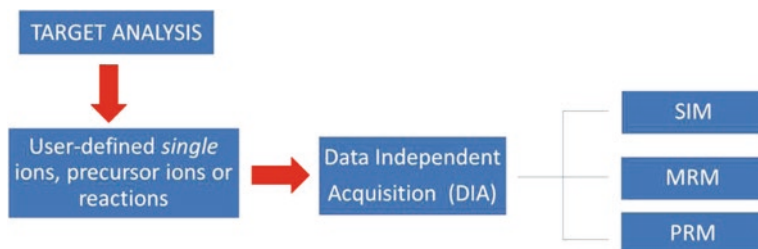
Fig. 3.7 Scheme of a MS and MS/MS data independent acquisition target analysis
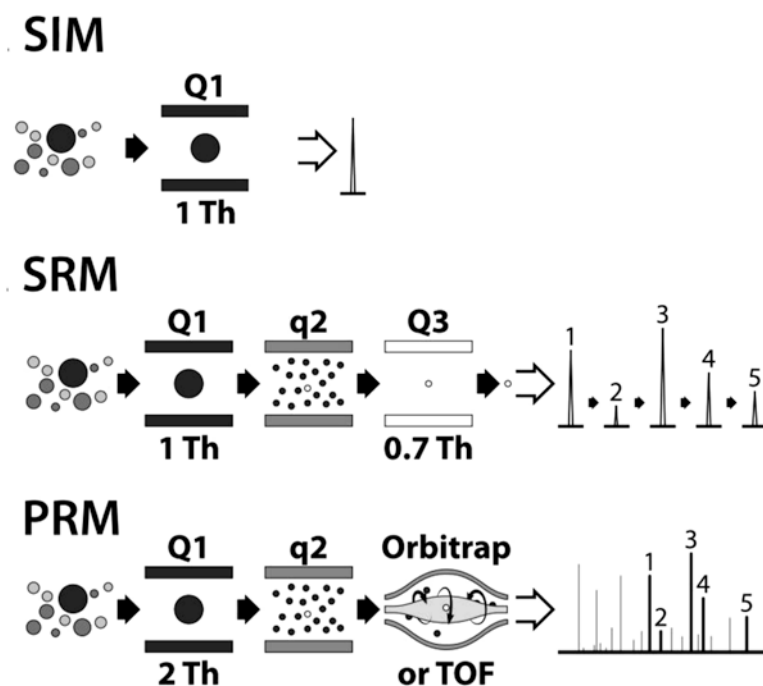
Fig. 3.8 Scheme of MS scan mode in selected ion monitoring (SIM), and of MS/MS scan modes in selected reaction monitoring (SRM) and parallel reaction monitoring (PRM). (Modified from Ref. [30])

In target analysis a *data independent acquisition* can be performed with single ions, precursor ions or reactions set by the user before the experiments starts.

The classical *selected ion monitoring* (SIM) approach is a MS method, requiring one analyzer and consisting in monitoring selected ions, one or more, of each analyte. It can be performed in low or high resolution mode. In SIM the analyzer is not scanning but fixed so to acquire only the ions of interest (Fig. 3.8). As more than one ion can be monitored, the analyzer "jumps" from one *m/z* value to the next. This ensures high sensitivity but scarce selectivity as a given ion might be produced by

different molecules. Combining SIM with retention time increases selectivity as very few molecules, if not one, will yield the same ions and will have the same retention time. Owing to the large diffusion of tandem mass spectrometry instruments, the use of SIM is actually limited in low resolution analysis but it is widely used in high resolution MS.

Tandem mass spectrometry methods, and in particular selected reaction monitoring (SRM), also known as multiple reaction monitoring (MRM), are widely used in target analysis. In selected reaction monitoring, typically occurring in triple quadrupole mass spectrometers, both analyzers don't make any scan but are fixed at given *m/z* values: the first at the *m/z* value of the precursor ion, the latter at *m/z* value of the product ion (Fig. 3.8). By monitoring one or more reactions for a single analyte, a SRM analysis is much more specific and selective than monitoring just single ions as it occurs in SIM. Furthermore SRM offers highly sensitive, and cost-effective analysis for simultaneous quantitation of several hundreds of targeted compounds in a single experiment.

Parallel reaction monitoring (PRM) [30] is also included in this group, being related to SRM, even if it can be used also in untarget analysis (Fig. 3.8).

As in a SRM assay, also in parallel reaction monitoring the first analyzer selects specific ions of interest for fragmentation. Unlike SRM/MRM, the second analyzer is not fixed on a given *m/z* value, but it scans over a wide *m/z* range so to detect all fragment ions at once (Fig. 3.8). Parallel reaction monitoring has been firstly set up on Q Exactive mass spectrometer having a quadrupole followed by an Orbitrap analyzer [30], but it has been used also with a ToF as a second analyzer.

So in PRM no any reaction pathway has to be defined, saving time in method development, and the use of high resolution and accurate mass measurements is an advantage when analyzing analytes in complex mixtures.

3.6 Food Safety/Detection of Toxins in Food

Toxins are represented by wide classes of molecules with different chemico-physical properties, ranging from volatile small molecules to polar big molecules, such as proteins. Among other analytical methods, mass spectrometry plays a key role and it is widely applied in the field of food safety for detecting and quantifying contaminants, residues and toxins in food [16, 31–35].

A targeted approach with data independent acquisition mode is aimed to detect the presence/absence of already known and well characterized contaminants, residues and toxins in food and it is limited to a user built compound list.

As an example, liquid chromatography coupled to mass spectrometry operating in multiple reaction monitoring with triple quadrupole instruments has been traditionally selected for mycotoxin analysis, monitoring in parallel quantitative and qualitative ion transitions. This approach provides both high sensitivity and high selectivity, and achieves limits of regulatory requirements for the official control methods. Anyway the method set-up is tedious and time-consuming when wanting to determine a large number of substances [36].

A targeted approach by using PRM has been developed for the characterization of six bacterial protein toxins of *Clostridium perfringens* of potential warfare significance [37].

Similarly an immuno-LC-MS/MS method, using PRM, for the simultaneous and specific quantification of the three potential biological warfare agents, ricin, staphylococcal enterotoxin B, and epsilon toxin, in complex human biofluids and food matrices has been setup [38].

On the other hand, an untarget analysis is able to detect both unexpected compounds, true unknowns, such as new emerging pesticides and toxins not yet integrated into current monitoring plans, and already known compounds. Among many others, some examples of untarget analysis are the use of the SWATH method for the identification and quantitation of pesticide residues in food [39]; a screening method based on a GC-APCI-MS^E approach for around 130 pesticides in fruit and vegetable samples; identification and quantification of domoic acid by UHPLC-QTOF MS^E tandem mass spectrometry, with simultaneous identification of non-target photodegradation products [40].

Looking for unknown and known analytes, high resolution should be used both in analysis of small molecules, such as contaminants and pesticides [41, 42] offering in this case the possibility to determine the accurate mass and the chemical formula, and in the case to big molecules, such as proteins, for a better certainty of identification and for the ability to detect polymorphisms and post-translational modifications.

References

1. Gross JH (2017) Mass spectrometry. A textbook, 3rd edn. Springer Verlag, Berlin/Heidelberg
2. Cole RB (2010) Electrospray and MALDI mass spectrometry: fundamentals, instrumentation, practicalities, and biological applications, 2nd edn. Wiley, Hoboken
3. Cifuentes A (2013) Foodomics: advanced mass spectrometry in modern food science and nutrition. Wiley, Hoboken
4. Witczak A, Sikorski ZE (eds) (2017) Toxins and other harmful compounds in foods, 1st edn. CRC Press, Boca Raton
5. L'Homme B, Scholl G, Eppe G, Focant J-F (2015) Determination of PCDD/Fs and dioxin-like PCBs in food and feed using gas chromatography-triple quadrupole mass spectrometry. J Chromatogr A 1376:149–158
6. Melchert HU, Pabel E (2004) Reliable identification and quantification of trichothecenes and other mycotoxins by electron impact and chemical ionization-gas chromatography–mass spectrometry, using an ion-trap system in the multiple mass spectrometry mode: candidate reference method for complex matrices. J Chromatogr A 1056:195–199
7. Barber M, Bordoli RS, Sedgwick RD, Tyler AN (1981) Fast atom bombardment of solids as an ion source in mass spectrometry. Nature 293:270–275
8. Ambient ionization mass spectrometry. New developments in mass spectrometry. (2014) Domin M, Cody R (eds). Royal Society of Chemistry
9. Ifa DR, Wiseman JM, Song QY, Cooks RG (2007) Development of capabilities for imaging mass spectrometry under ambient conditions with desorption electrospray ionization (DESI). Int J Mass Spectrom 259:8–15

10. Cody RB, Laramée JA, Durst HD (2005) Versatile new ion source for the analysis of materials in open air under ambient conditions. Anal Chem 77:2297–2302

11. Zhang Y, Ma XX, Zhang SC, Yang CD, Ouyang Z, Zhang XR (2009) Direct detection of explosives on solid surfaces by low temperature plasma desorption mass spectrometry. Analyst 134:176–181

12. Balog J, Szaniszlo T, Schaefer K-C, Denes J, Lopata A, Godorhazy L, Szalay D, Balogh L, Sasi-Szabo L, Toth M, Takats Z (2010) Identification of biological tissues by rapid evaporative ionization mass spectrometry. Anal Chem 82:7343–7350

13. Liu J, Wang H, Manicke NE, Lin J-M, Cooks RG, Ouyang Z (2010) Development, characterization, and application of paper spray ionization. Anal Chem 82:2463–2471

14. Huang M, Jhang S, Chan Y, Cheng S, Cheng C, Shiea J (2014) Electrospray laser desorption ionization mass spectrometry. In: Domin M, Cody R (eds) Ambient ionization mass spectrometry. New developments in mass spectrometry. Royal Society of Chemistry, pp 372–388

15. Vaclavik L, Zachariasova M, Hrbek V, Hajslova J (2010) Analysis of multiple mycotoxins in cereals under ambient conditions using direct analysis in real time (DART) ionization coupled to high resolution mass spectrometry. Talanta 82:1950–1957

16. Su H, Liu K-T, Chen B-H, Lin Y-P, Jiang Y-M, Tsai Y-H, Chang F-R, Shiea J, Lee C-W (2019) Rapid identification of herbal toxins using electrospray laser desorption ionization mass spectrometry for emergency care. J Food Drug Anal 27:415–427

17. Wang R, Yin Y, Zhu Z-J (2019) Advancing untargeted metabolomics using data-independent acquisition mass spectrometry technology. Anal Bioanal Chem 411:4349–4357

18. Fiorino GM, Fresch M, Brümmer I, Losito I, Arlorio M, Brockmeyer J, Monaci L (2019) Mass spectrometry-based untargeted proteomics for the assessment of food authenticity: the case of farmed versus wild-type salmon. J AOAC Int 102:1339–1345

19. Wu AHB, Colby J (2016) High-resolution mass spectrometry for untargeted drug screening. In: Garg U (ed) Clinical applications of mass spectrometry in drug analysis. Methods in molecular biology, vol 1383. Humana Press, New York

20. Plumb RS, Johnson KA, Rainville P, Smith BW, Wilson ID, Castro-Perez JM, Nicholson JK (2006) UPLC/MS^E; a new approach for generating molecular fragment information for biomarker structure elucidation. Rapid Commun Mass Spectrom 20:1989–1994

21. Geiger T, Cox J, Mann M (2010) Proteomics on an orbitrap benchtop mass spectrometer using all-ion fragmentation. Mol Cell Proteomics 9:2252–2261

22. Naz S, Gallart-Ayala H, Reinke SN, Mathon C, Blankley R, Chaleckis R, Wheelock CE (2017) Development of a liquid chromatography-high resolution mass spectrometry metabolomics method with high specificity for metabolite identification using all ion fragmentation acquisition. Anal Chem 89:7933–7942

23. Kramer G, Moerland PD, Jeeninga RE, Vlietstra WJ, Ringrose JH, Byrman C, Berkhout B, Speijer D (2012) Proteomic analysis of HIV–T cell interaction: an update. Front Microbiol 3:240

24. Gillet LC, Navarro P, Tate S, Rost H, Selevsek N, Reiter L, Bonner R, Aebersold R (2012) Targeted data extraction of the MS/MS spectra generated by data-independent acquisition: a new concept for consistent and accurate proteome analysis. Mol Cell Proteomics 11:O111.016717

25. Bonner R, Hopfgartner G (2019) SWATH data independent acquisition mass spectrometry for metabolomics. TrAC Trends Anal Chem 120:115278

26. Zhang Y, Bilbao A, Bruderer T, Luban J, Strambio-De-Castillia C, Lisacek F, Hopfgartner G, Varesio E (2015) The use of variable Q1 isolation windows improves selectivity in LC-SWATH-MS acquisition. J Proteome Res 14:4359–4371

27. Ludwig C, Gillet L, Rosenberger G, Amon S, Collins BC, Aebersold R (2018) Data-independent acquisition-based SWATH-MS for quantitative proteomics: a tutorial. Mol Syst Biol 14:e8126

28. Panchaud A, Scherl A, Shaffer SA, von Haller PD, Kulasekara HD, Miller SI, Goodlett DR (2011) PAcIFIC: how to dive deeper into the proteomics ocean. Anal Chem 81:6481–6488

29. Egertson JD, Kuehn A, Merrihew GE, Bateman NW, MacLean BX, Ting YS, Canterbury JD, Marsh DM, Kellmann M, Zabrouskov V, Wu CC, MacCoss MJ (2013) Multiplexed MS/MS for improved data-independent acquisition. Nat Methods 10:744–746

30. Peterson AC, Russell JD, Bailey DJ, Westphall MS, Coon JJ (2012) Parallel reaction monitoring for high resolution and high mass accuracy quantitative, targeted proteomics. Mol Cell Proteomics 11:1475–1488

31. Hird SJ, Lau BP-Y, Schuhmacher R, Krska R (2014) Liquid chromatography-mass spectrometry for the determination of chemical contaminants in food. Trends Anal Chem 59:59–72

32. Tevell Åberg A, Björnstad K, Hedeland M (2013) Mass spectrometric detection of protein-based toxins. In: Biosecurity and bioterrorism: biodefense strategy, practice, and science. Vol. 11(Suppl. 1): S215–S226

33. Duriez E, Armengaud J, Fenaillec F, Ezand E (2016) Mass spectrometry for the detection of bioterrorism agents: from environmental to clinical applications. J Mass Spectrom 51:183–199

34. Andjelkovic M, Tsilia V, Rajkovic A, De Cremer K, Van Loco J (2016) Application of LC-MS/MS MRM to determine Staphylococcal enterotoxins (SEB and SEA) in milk. Toxins 8:118

35. Johnson RC, Kalb SR, Barr JR (2011) Toxin analysis using mass spectrometry. In: Budowle B, Schutzer SE, Breeze RG, Keim PS, Morse SA (eds) Microbial Forensics, 2nd edn. Academic Press, pp 405–420

36. Righetti L, Paglia G, Galaverna G, Dall'Asta C (2016) Recent advances and future challenges in modified mycotoxin analysis: why HRMS has become a key instrument in food contaminant research. Toxins 8:361

37. Duracova M, Klimentova J, Myslivcova Fucikova A, Zidkova L, Sheshko V, Rehulkova H, Dresler J, Krocova Z (2019) Targeted mass spectrometry analysis of clostridium perfringens toxins. Toxins 11:177

38. Dupré M, Gilquin B, Fenaille F, Feraudet-Tarisse C, Dano J, Ferro M, Simon S, Junot C, Brun V, Becher F (2015) Multiplex quantification of protein toxins in human biofluids and food matrices using immunoextraction and high-resolution targeted mass spectrometry. Anal Chem 87:8473–8480

39. Parrilla Vázquez P, Lozano A, Ferrer C, Martínez Bueno MJ, Fernández-Alba AR (2018) Improvements in identification and quantitation of pesticide residues in food by LC-QTOF using sequential mass window acquisition (SWATH®). Anal Methods 10:2821–2833

40. Gagez A-L, Bonnet A, Pineau P, Graber M (2017) Identification and quantification of domoic acid by UHPLC/QTOF tandem mass spectrometry, with simultaneous identification of non-target photodegradation products. Int J Environ Anal Chem 97:1192–1205

41. Kaufmann A (2012) The current role of high-resolution mass spectrometry in food analysis. Anal Bioanal Chem 403:1233–1249

42. Wong JW, Wang J, Chow W, Carlson R, Jia Z, Zhang K, Hayward DJ, Chang JS (2018) Perspectives on liquid chromatography–high-resolution mass spectrometry for pesticide screening in foods. J Agric Food Chem 66:9573–9581

Chapter 4
Fundamentals of Mass Spectrometry-Based Metabolomics

Emilio S. Rivera, Marissa A. Jones, Emma R. Guiberson, and Jeremy L. Norris

Abstract Metabolomics involves the study of a complex and diverse array of compounds that can be thought of as the ultimate end products of the complex systems that are characteristic of molecular biology. The compounds that constitute the metabolome are small in size relative to the genome and proteome and include amino acids, carbohydrates, organic acids, lipids, and nucleotides with a mass less than 1800 Da. Understanding the role of these metabolites and the way in which changes in these important molecules impact biological processes has great potential to improve public health through better understanding of disease mechanisms. A comprehensive understanding of the metabolome will ultimately lead to better candidate biomarkers and drug targets enabling improvements in patient care. Metabolomics experiments can be divided primarily into two experimental strategies: targeted and untargeted. This monograph details these two approaches and the specific considerations for sample preparation, analytical separations, instrumental considerations, and data analysis that are required in the practice of these important technologies. Furthermore, selected applications of targeted and untargeted experiments are showcased to demonstrate the role of metabolomics as part of multi-omics studies and how metabolites can be spatially mapped in biological systems using imaging mass spectrometry.

E. S. Rivera · J. L. Norris (✉)
Mass Spectrometry Research Center, Vanderbilt University, Nashville, TN, USA

Department of Biochemistry, Vanderbilt University, Nashville, TN, USA
e-mail: emilio.s.rivera@vanderbilt.edu

M. A. Jones · E. R. Guiberson
Mass Spectrometry Research Center, Vanderbilt University, Nashville, TN, USA

Department of Chemistry, Vanderbilt University, Nashville, TN, USA
e-mail: marissa.a.jones@vanderbilt.edu; emma.r.guiberson@vanderbilt.edu

4.1   Introduction

Metabolomics is a field which studies the chemically diverse set of biological molecules that are essential components of living systems. These include molecules such as amino acids, carbohydrates, organic acids, lipids, and nucleotides. The compounds that make up the metabolome typically have molecular weights less than 1800 Da. The metabolites in this mass range are of special interest to the scientific community due to their dynamic nature and their close relation to phenotype. Metabolomics differs from its -omic counterparts (genomics, transcriptomics, and proteomics) in that metabolites are typically the final expression of a complex series of molecular events that make up system's biology [1]. Through the study of metabolomics, there is great potential to not only expand our fundamental understanding of cellular processes, but these discoveries hold the promise to change human health. The understanding of the end point of disease mechanisms could lead to improved treatment and detection through the discovery of biomarkers and drug targets which would improve patient outcomes [2]. As a result, the field of metabolomics research has expanded greatly. Publications have correspondingly increased exponentially, for example citations related to metabolomics research as increased 665 times from 1992 to 2017 [3].

With this rise in interest, a variety of technologies have been developed and are currently being applied to the study of metabolites. The principal methods include NMR (nuclear magnetic resonance) [4], GC-MS/MS (gas chromatography tandem mass spectrometry) [5], LC-MS/MS (liquid chromatography tandem mass spectrometry) [6], and IMS (imaging mass spectrometry) [7]. NMR-based methods, which have steadily been increasing for the past 15 years, have a few distinct differences from MS-based platforms: they are largely non-destructive, quantitative, and require minimal sample preparation (no derivitization, sample treatment or chromatographic separation). However, NMR is 10 to 100 times less sensitive than LC-MS and GC-MS [8]. Although each method has applications for which it is best suited, LC-MS and GC-MS methods account for ~80% of all published metabolomics studies. Due to the popularity of these methods, this review will focus primarily on mass spectrometry based methods.

4.1.1   Targeted Vs. Untargeted Assays

In general, metabolic experiments can be characterized by one of two possible experimental approaches: targeted and untargeted assays (Fig. 4.1). Targeted approaches probe a specific hypothesis, monitoring a limited number of known metabolites. Alternatively, untargeted approaches are often used for hypothesis generation and focus on broad coverage of diverse metabolites to identify both known and unknown metabolic changes.
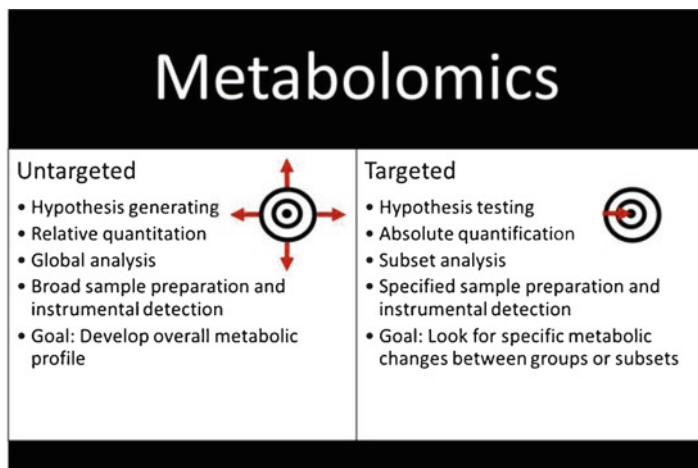
Fig. 4.1 Untargeted Vs. Targeted Metabolomics. A list of attributes of untargeted metabolomics in contrast to targeted metabolomics [9]

The targeted approach to metabolomics requires many considerations in order to produce an assay that is suitable for the biological question under consideration. The type of quantitation (*i.e.*, absolute or relative), sample preparation, separation strategy, mass spectrometer parameters, and data analysis approach all must be implemented to satisfy the ultimate experimental goal. One major advantage of targeted metabolomics is that it allows for absolute quantitation. With known analytes of interest being investigated, the necessary steps to obtain absolute quantitation are limited, only requiring the creation of a calibration curve for each analyte to be run in parallel with samples [9]. Relative quantitation is even easier to obtain experimentally as it entails comparing intensities among samples.

In targeted metabolomics, characteristics of analytes such as solubility, polarity, and pH can be used to determine the optimal assay parameters. Analytes that can be grouped together such as amino acids, or short chain fatty acids, can be processed together for all downstream steps such as extraction, derivatization, and chromatography. For example, amino acids can be extracted in aqueous solvent, as they all contain a primary amine, which allows for derivatization by dansyl chloride to aid in chromatography [10]. In addition, these derivatized products can all be separated by C18 reverse phase chromatography and require similar instrument parameters.

When taking the untargeted approach to a metabolomics experiment, the objective is to broaden the effectiveness of the workflow for simultaneous analysis of a wide variety of metabolites [11]. As the goal of an untargeted experiment is to develop an overall metabolic profile of a biological system, it is critical that methods of extraction and separation chosen be broadly inclusive of a diverse range of metabolites. To achieve these goals, metabolite experiments are comprised of an experimental design, sample preparation, separation method, mass spectrometric analysis, data processing and data interpretation (Fig. 4.2).
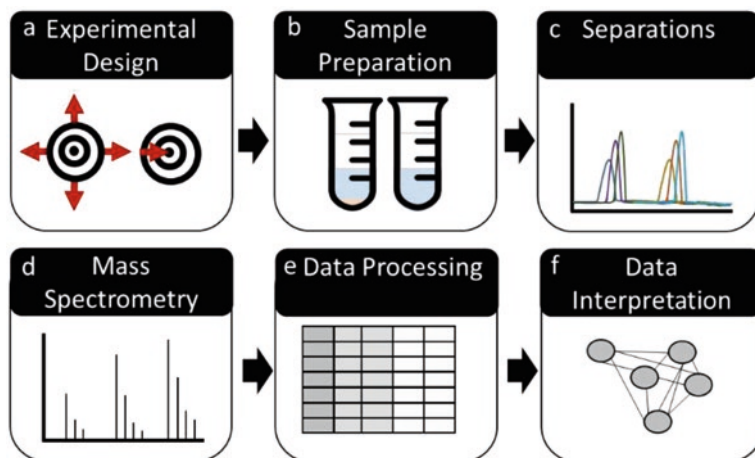
Fig. 4.2 All metabolomics experiments consist of the following: (**a**) Experimental design (targeted or untargeted experiments), (**b**) sample preparations (metabolite extraction and reconstitution), (**c**) separations (liquid chromatography), (**d**) mass spectrometry, (**e**) data processing (preprocessing and metabolite identification), and (**f**) data interpretation (metabolic network mapping)

4.2 Sample Preparation

The method by which an analyte is obtained and processed for analysis is crucial. Several considerations must be made for both targeted and untargeted extraction approaches.

For targeted metabolomics, the extraction method is dependent upon the sample matrix and class of analytes to be measured. The sample preparation process could be as simple as dilution of the sample with solvent prior to analysis [12], or as complicated as a multistep extraction involving sample preparation columns and buffer exchanges followed by a multistep derivatization. The goal of sample preparation is to mitigate any interference in the measurement of the analytes of interest that may arise from the complex biological matrix with minimal sample manipulation. Before choosing an extraction method, it is important to consider necessary down-stream manipulations. To continue with the above example, amino acids may need to be extracted from a complex matrix such as cell culture and may require derivatization for effective reverse phase chromatography. In this case, the extraction can be accomplished effectively with a mix of methanol, water and formic acid [13], which are ideal for downstream reverse phase chromatography. Regardless of the extraction method, one major consideration is loss of analyte during sample processing [14]. To address this problem, a known internal standard is introduced at or near the beginning of sample preparation to account for loss of analyte as well as any inconsistency such as pipetting error, retention time drifts in chromatography, or instrumental drift [15]. Internal standards can be utilized for normalization of analytes, where abundances are often reported as 'response ratios' to their respective internal

standard [16]. Resuspension is also a consideration, as the solvent chosen can have effects on downstream chromatography such as reproducibility of retention times or peak shape [17].

The optimal extraction method in untargeted approaches depends on the complexity of the sample matrix as well as the class of analytes. Having little to no information about the metabolites of interest, however, it can be difficult to discern the optimal extraction protocol. For this reason, straightforward and versatile techniques such as protein precipitation [18], Folch extraction [19], and Bligh-Dyer extraction [20] involving multiple immiscible solvents are often employed in untargeted metabolomics. Here, different classes of biomolecules are separated into isolated liquid fractions; polar metabolites suspend in the aqueous layer while lipids separate into a hydrophobic fraction such as chloroform. This phenomenon allows for simple, broad extractions of metabolites and even lends itself to multiomics workflows as each different class of biomolecules from a single sample can be easily taken for class-specific sample preparation [21].

The addition of internal standards in untargeted workflows is also common practice [22]. In this context, an internal standard could be used for normalization purposes where each analyte is reported relative to the internal standard, or it could provide a retention time reference point to provide insight on chromatographic drift over the course of an experiment [22]. More common, however, is the practice of sample pooling [23]. This involves pooling equal volumes from each sample for downstream quality control. This approach operates on the premise that a pooled sample contains every possible analyte from an entire untargeted experiment in a single injection and can thus be used to gauge both chromatography and instrumental efficiency. While analytes may in some cases be diluted in the pooled sample, this methodology works to provide qualitative insight to an experiment. Quality control of chromatographic and instrumental drift can be determined by periodically injecting the pooled sample mix between samples (after every 10 injections), over the course of the experiment.

Again, as with targeted metabolomics, the last major consideration for sample preparation is the composition of the final resuspension solvent. Trying to use generic solvents which are broadly compatible with any unknown analytes present in the sample will help to avoid analyte precipitation or having sample conditions incompatible with chromatography. Some biases can be made however, tailoring the resuspension solvent to the analytes being measured. For example, if measuring lipids, a solvent that will minimize lipid precipitation is necessary. Most lipids have been found to be soluble in chloroform making it an attractive choice for resuspension; however, chloroform would not be compatible with most reversed-phase or HILIC methods, and therefore cannot be used for resuspension in most applications. Instead, methanol, which solubilizes most lipids could serve as a substitute resuspension solvent.

4.3 Separations

Analytical separation of metabolites prior to mass analysis provide a means for more comprehensive analysis metabolites, enabling greater depth of coverage. There are analytical tasks that do not require separations for the analysis of metabolites; however, these approaches sacrifice broad metabolite coverage in favor of other important performance characteristics of the assay. For example, direct-infusion high-resolution MS (DI-HRMS) allows for the analysis of metabolites without the need for chromatographic alignment and extensive sample preparation [24]. In addition, direct-infusion methods also allow for maximum sample throughput [2]. Many imaging mass spectrometry techniques also do not use any chromatographic separations. However, these technologies allow for the unique ability to spatially localize specific m/z to regions of a sample, which can be of unique importance in clinical applications [25]. Although separation-free techniques can be used for metabolomics analysis, isomeric compounds cannot be separated and ion suppression effects must be mitigated [2]. To address these challenges, typically liquid chromatography, gas chromatography, capillary electrophoresis, and ion mobility are used.

4.3.1 Liquid Chromatography

One of the first widely accepted types of liquid chromatography in a column format was normal-phase chromatography which was derived from thin layer chromatography (TLC) [26]. Normal phase separations employ a polar stationary phase, often consisting of silica [26, 27]. This polar stationary phase is ideal for retaining and separating polar molecules in highly nonpolar solvents such as hexanes, which can be incompatible with downstream components and not provide the necessary polarity for efficient electrospray ionization [28]. While normal phase has lost much of its popularity due to its major limitations, it is still used in limited capacities due to its effective class separations of analytes such as lipids, as well as its compatibility with organic solvents which are necessary for the stability of some molecules [29].

In contrast to normal-phased chromatography, reversed-phase chromatography is defined by a nonpolar stationary phase which retains and separates nonpolar, hydrophobic analytes very effectively [30]. Historically, reversed-phase chromatography has been the gold standard in LC-MS, which has percolated into LC-MS based metabolomics [31]. Reversed-phase chromatography offers versatility in mobile phase/sample composition and can be used in flow regimes from nanoflow (< 1 μL/min) to analytical flow (>100 μL/min < 1 mL/min). Furthermore, reversed-phase chromatography produces highly reproducible retention times and peak shapes [32, 33]. One large hurdle associated with the use of reversed-phase chromatography for metabolites, however, is the inherently polar properties of the majority of endogenous small molecules. As discussed above, this problem has led to the

development of many derivatizing strategies for small molecules to make them less polar and aid in reversed-phase retention.

Hydrophilic interaction chromatography (HILIC) is a relatively new chromatography technique which is a variation of normal phase chromatography [34]. Briefly, HILIC relies on a thin layer of water which surrounds the polar stationary phase, allowing for analytes to interact with the water layer rather than the stationary phase directly [34]. This interaction with water lends to the retention of polar, hydrophilic molecules without the need for mobile phases which are incompatible with mass spectrometry. This normal-phase variant has increased opportunities for performing metabolomics without concern for analyte hydrophobicity. In addition, HILIC provides a method of separation capable of retaining and effectively resolving polar metabolites without the need for derivatization as with reversed-phase chromatography or incompatible solvents like normal-phase. Despite its clear advantages over reversed-phase and normal-phase in the context of metabolites, it does have limitations. Retention time and peak shape have been observed to be less robust than reversed-phase requiring a great deal of care in buffering of mobile phases as well as long re-equilibration periods between injections [35]. All of these factors and others have led to hesitance in the field towards adopting HILIC, with some asserting that a new method of separating polar molecules is still needed [36].

Because reversed-phase and HILIC techniques offer complementary coverage of the metabolome, they are often used together to provide a more comprehensive analysis of sample analytes [21]. Many common extraction methods such as the Folch extraction or the Bligh-Dyer extraction afford separations of metabolite classes into distinct sample fractions [19, 20]. This fractionation allows for non-polar to be analyzed by downstream reversed-phase, and polar metabolites from the same sample to be analyzed by HILIC [21]. While this approach can significantly increase analysis time, it provides a much more comprehensive view of the metabolites in a given sample set.

4.3.2 Gas Chromatography

Gas chromatography (GC) has also been shown to provide a high degree of sensitivity and reproducibility for volatile analytes. Rather than using changes in solvent composition to separate analytes as in LC, GC takes advantage of analytes having different boiling points by ramping temperature [37]. When coupled to a mass spectrometer, GC offers reliable platform for metabolomics [38]. One consideration when integrating these techniques is an ionization source. In most GC experiments, electron-impact (EI) or chemical ionization (CI) are used for ionization before mass analysis [39]. Much like LC-MS, GC-MS can be used to effectively separate and analyze complex mixtures and is effective in both targeted and untargeted experiments. However, there are certain limitations associated with GC-based metabolomics. As GC relies on analyte volatility, it is vital that analytes be volatile enough to transition into the gas phase easily in order for GC-based methods to be effective

[40]. Historically, in the event that analytes of interest are not sufficiently volatile, derivatizations such as alkylation have been necessary to increase volatility for effective analysis by GC [40]. While effective, these derivatization techniques can be laborious and complicate data [41]. For these reasons, GC is not as widely used in metabolomics workflows as LC.

4.3.3   Capillary Electrophoresis

Another form of separation which has been gaining popularity in the field of metabolomics is capillary electrophoresis (CE). CE is not a form of chromatography because it lacks a stationary phase, a defining component of all chromatography [42]. Instead, CE separation is achieved by applying high voltage to a capillary, inducing an electrophoretic migration of ions. The electrophoretic mobility of the analytes is dependent upon the ions charge-to-size ratio [42], wherein separation of ions with differing electrophoretic mobilities is achieved. One strength of CE is its high resolution, which is directly correlated to the potential applied to the column as well as narrow peak widths provided in part by the inherent electroosmotic flow, rather than laminar flow as in traditional chromatography [43, 44]. This resolution coupled to mass spectrometry is conducive to both targeted and untargeted metabolomics. In the past, the integration of these two technologies was a limiting factor [45]. In recent years however, advancements have been made which allow for easy coupling of CE to mass spectrometry [46]. Current limitations of CE include a lack of robustness, especially related to clogging [47].

4.3.4   Ion Mobility

Another separation technology which has been demonstrated to be effective for the analysis of metabolites is ion mobility (IM) [48]. By applying a high voltage gradient opposing a gas flow, charged analytes are driven by the voltage gradient in one direction, and by the gas flow the opposite direction. These competing forces allow gas-phase separation of ions based on differing size-to-charge [49]. Because IM operates in the gas phase, it is frequently coupled with mass spectrometry, often being integrated within the mass analyzers of an instrument [50]. Ion mobility provides a degree of separation which can be comparable to that of LC-MS or GC-MS, on a much shorter timescale. Where chromatographic methods separate metabolites in a matter of minutes to hours, [51, 52] IM operates on the order of milliseconds [53]. IM is usually measured in drift time, and can be used to calculate an ion's collision cross section with proper calibration [54]. When coupled to mass spectrometry, IM provides a high degree of separation, having been shown to separate isobaric species, as well as offering this orthogonal drift time information for each analyte. Moreover, IM can be utilized in conjunction with chromatography

up-stream of a mass spectrometer, providing a second level of separation as well as affording higher peak capacity [9]. Ion mobility is not without shortcomings however, especially that the addition of ion mobility in a metabolomics experiment has been shown to reduce overall sensitivity [53].

4.4 Mass Spectrometry

In metabolomics, the instrument of choice is dependent on the experiment being conducted, where different mass spectrometer platforms are ideal for different types of assays. For targeted experiments, an instrument capable of interrogating many known molecules on a time-scale that is compatible with the chromatographic time-scale is critical. Targeted assays are commonly quantitative; therefore, it is important that the instrument selected has good quantitative capabilities and sensitivity. Usually this type of work is done by a triple-quadrupole or QTRAP system [15]. Untargeted experiments have different needs, as unknown molecules must be selected for fragmentation in a manner that permits broad coverage of the analytes. Orbitrap-based and quadrupole time-of-flight (QTOF) systems have proven themselves optimal for these types of workflows [6, 55]. There are many other types of mass spectrometers which can be used for LC-MS-based metabolomics, but this chapter will focus specifically on these as they are the platforms that play a central role in the field.

Triple quadrupole and QTRAP platforms are the dominant mass spectrometers used in the field of targeted metabolomics [55]. These instruments are very similar in design, sharing an electrospray source followed by optics for the transmission of ions to an initial quadrupole capable of isolating specific *m/z* windows. A second quadrupole is then used as a collision cell for collision-induced dissociation (CID) to fragment precursor ions for MS/MS analysis [56]. These two instruments differ in their final stage where a triple quadrupole is equipped with a third quadrupole used to isolate a particular *m/z* of the fragments created in the collision cell for transmission to the detector. The QTRAP is equipped with a ion trap rather than a conventional quadrupole, which is capable of not only of performing subsequent fragmentation events on product ions but also accumulating ions for increased sensitivity [57]. This instrument can also be operated as a conventional triple quadrupole instrument. Both systems are capable of isolating a precursor ion, fragmenting, and monitoring the presence of specific fragments on the order of milliseconds [58]. The monitoring of a specific fragment of a specific parent ion is referred to as a selected reaction monitoring (SRM), and this approach can be multiplexed so that multiple analytes can be monitored in the same assay with high specificity. This approach is referred to as multiple reaction monitoring (MRM), and is paramount for targeted LC-MS techniques [59]. Practically, these mass spectrometers are capable of quantitatively monitoring upwards of 50 unique transitions within milliseconds [58]. This level of speed allows for dozens of metabolites to be measured with

sufficient coverage over a chromatographic peak, producing quantitative, reproducible data for each metabolite.

Untargeted metabolomics comes with a different set of requirements due to the chemical diversity of analytes that are characterized in a single analysis. Here, an instrument's ability to quickly and efficiently identify a molecule which may be of interest for further investigation by MS/MS is critical. There exist two main methods of addressing this problem: data-dependent-acquisition (DDA) and data-independent-acquisition (DIA). Various vendors have different names for these processes, but in general these two techniques prevail in untargeted metabolomics workflows [9]. DDA has proven to be effective in the field of proteomics for years [60]. For DDA, tandem mass spectra are collected for *m/z* values selected from a previously acquired MS spectrum; where the instrument is set to perform an initial MS scan, determine the N most abundant ions, and isolate those for MS/MS analysis [61]. This entire process must take place in milliseconds [62], and is repeated several times over the course of a peak for effective and reliable MS/MS data.

DIA has grown more prominent recently, where independent of the MS data, the instrument indiscriminately isolates mass windows (which in some cases can be chosen by the operator) across the entire MS mass range [63]. Each of these windows is sequentially isolated for fragmentation, meaning that ions within each window will proceed to the collision cell, producing fragments that are subsequently analyzed [64]. One exception to this generalization is in Waters platforms, which refer to their version of DIA as 'MS^E' and fragments all precursor ions simultaneously following an initial MS scan. Regardless of the how the DIA is carried out, as with DDA, this entire process must be repeated several times within a peak width for reliable fragmentation and quantitation [64]. The difficulty in this approach is pairing fragment ions with their parent ion counterparts. This requires sophisticated software programs for data annotation [65]. Thus, the specific data analysis approach must be carefully considered before acquiring data to ensure success.

It should be noted that fragmentation, while integral to both workflows, serves a slightly different purpose for targeted and untargeted metabolomics. In a targeted experiment, fragmentation is used as validation of the previously known identity of a given molecule. The resulting fragment is measured, meaning that quantitation is based solely on the abundance of fragment ions [66]. In untargeted metabolomics, MS/MS is used to extract more information about the possible identity of a given molecule [11]. In this case, any quantitative measurements are most frequently made using MS data [11]. Lastly, the mass resolving power of the instrument tends to differ between targeted and untargeted workflows. Untargeted metabolomics benefits from higher mass resolving power as exact mass measurements in the MS data can aid in identifying a metabolite [67]. For this reason, Orbitrap-based and QTOF systems have prevailed as the ideal platforms for an untargeted experiment. Orbitraps offer varying levels of mass resolving power, ranging from 15,000–240,000 [68], and can be modulated by the operator to suit an experiment. While not as high performance, QTOF instruments offer mass resolving powers of up to 60,000 on current platforms [69]. In contrast, a targeted experiment relies on specific fragmentation and retention time for identification of a metabolite, rather than mass

resolving power [9]. A targeted metabolomics experiment is also greatly affected by the speed of the mass spectrometer being used. For this reason, most instrument platforms used in targeted workflows are low resolution mass spectrometers capable of rapid scan rates that enable high-speed MRM analyses. Both targeted and untargeted workflows require high levels of data management and processing, which can often prove to be the most cumbersome and time-intensive component of a metabolomics experiment.

4.5   Data Analysis

The validity of identifications in metabolomics studies are crucial for making biological conclusions. A useful framework for considering the confidence in the identification of a specific metabolite has been established [9]. In this framework, there are five levels of validation ranging from a unique feature such as an accurate mass measurement at level five (the lowest level of validation), to a validated identification which is measured against a reference standard with a confirmed structure at level one (the highest level of validation) (Fig.4.3).

One universal challenge between targeted and untargeted experiments is determining which spectra in these large data sets are representative of a real metabolite. In order to make confident identifications, informative features relevant to
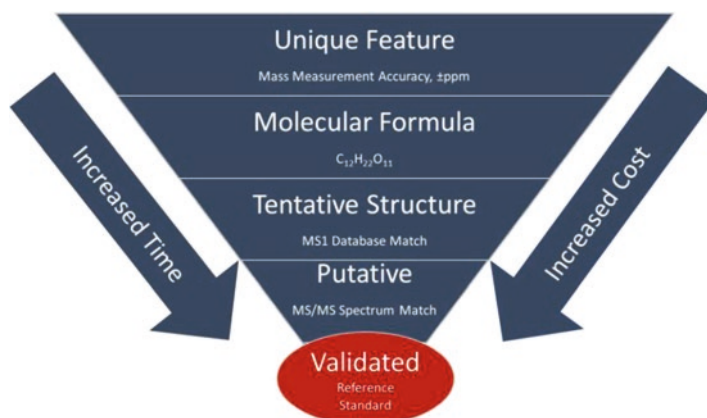
Fig. 4.3 Levels of Confidence for Metabolite Validation. From top to bottom the least validated level 5 to validated level 1 is shown. With increased level of validation comes increased time and cost. A level five validated feature is a unique feature with accurate mass measurement. A level four validation is a unique molecular formula. A level three validated feature includes tentative structure and matches a precursor to an MS1 data based. A level two validated feature, a putative identification matches MS/MS spectra to a database. Level two and three validations utilize orthogonal measurements and can be techniques other than mass spectrometry such as NMR, collisional cross section, spectroscopy, or retention time. A completely validated metabolite, a level one validation matches a metabolite to a reference standard [9]

biological processes must be differentiated from extraneous ones. For example, Mahieu et al. showed that although a dataset had over 25,000 features, with the subtraction of isotopes, adducts, artifacts, and contaminants, less than 1000 were metabolites [70]. Preprocessing methods facilitate recognition of data as either meaningful or irrelevant.

There are a variety of tools for data preprocessing such as noise filtering, spectral deconvolution, chromatogram alignment, and retention time correction. Data processing such as peak detection, peak alignment, metabolite identification, quality control, normalization, statistical analysis, metabolite quantification, and *in silico* fragmentation are also used [71]. Both targeted and untargeted metabolomics methods share similar data preprocessing. With targeted methods such as MRM, chromatographic features linked to specific MS/MS transitions are often used. A variety of commercial software, such as LCQuan (ThermoFisher Scientific), allow for the identification of internal standards for relative quantitation or the import of calibration curves for absolute quantitation [72].

To reduce the dimensionality of the data, classification and clustering tools are used [73]. Once metabolites are identified, relative or absolute quantitation can be performed to determine the overall role of observed metabolic changes in a global framework. There are a variety of commercially available tools for targeted and untargeted LC-MS data analysis including LCQuan, Agilent Masshunter, Bruker's Profile Analysis, Thermo SIEVE, Waters' Progensis QI and more [72, 74–77]. In addition there are a number of open source, vendor-independent tools including XCMS/XCMS Online, Mzmine 2, and MS-DIAL [78–80].

After data preprocessing, metabolite identification remains challenging owing to incomplete spectral libraries and incompatibility between databases and data types. For example, some databases are compatible with MS^n data while others are only designed to search compounds. Table 4.1 provides a list of relevant spectral libraries and databases to assist in the identification of metabolites. When determining which database best fits an experiment, it is important not only to consider the total number of compounds and the data type, but also the original data used to build the data base. For example, it is possible to limit false identifications for a human-based experiment by selecting HMDB rather than an *in silco* prediction-based database.

Once metabolites are identified, pathways become integral in identifying the collective role metabolites play in relation to a scientific question. Table 4.2 lists a few metabolic pathway analysis tools, their number of reference pathways and the number of organisms on which they are based. Using these tools, data sets can be mapped into known biological networks to aid in the interpretation of the results and provide context that will help generate future hypotheses. Although pathway analysis can often bring about answers to a variety of biological questions, it is important to note that many experiments are temporal and looking at the accumulation of metabolites or the change between experimental groups. In order to directly follow a metabolic pathway, heavy labeling experiments are needed [87].

Table 4.1 A variety of spectral libraries and databases are available for metabolite identification. From left to right the database or spectral library, the number of total compounds, target data types, organism base/ Focus and a brief description are shown [71, 81–86]

Spectral Library/ database	Total Compounds	Targets	Organism Base/ focus	Description
MoNA	>200,000	EI, MS/MS, MSn	Multiple species, Curated	Curated Spectra
Metlin	>500,000	CID-MS/MS	Multiple species	Commonly used, Original use QTOF
NIST	>574,000	EI-MS, CID-MS/MS	Multiple species	Curated database
m/z cloud	8904	MSn	Multiple species	Multiple stage MSn
KEGG	18,612	Metabolites	Multiple species	Pathway database
HMDB	114,100	Metabolites	Human	Spectra, physical and biological properties
ChemSpider	67,000,000	All small molecules	Curated data, compounds	Curated data
Mass Bank	>38,000	EI, MS/MS, MSn	Multiple species	Long standing community database
MINE	>571,000	Metabolites	In silico predicted metabolites	Predicted database

Table 4.2 Pathway analysis databases provide the biological context for individual metabolite measurements within a system. From left to right the database, number of reference pathways, and organisms included are shown

Database	Reference Pathways	Organisms
KEGG[88]	372	>700
MetaCyc[89]	1100	1500
WikiPathways[90]	100	20

4.6 Other Approaches to Metabolomics

Pathway analysis introduces a unique view of identified metabolites and their biological relevance. Metabolomics offers a plethora of biological significance through the metabolites identified, but many times metabolomics through routine LC-MS lack dimensions of information. There are highly complementary approaches that can be used in the study of metabolism. Three specific examples are described below: multiomic sample preparation methodologies, imaging MS for the addition of spatial information, and NMR for high reproducibility [88–90].

4.6.1   Combining Metabolomics with Other Omics Technolgies

LC-MS has been successfully utilized for metabolomics, but previous sample preparation methods made metabolomics incompatible with proteomic and lipidomic analysis. In order to maximize the data extracted from a sample, a new method known as sample preparation for multi-omics technologies (SPOT) has been developed for high-throughput multi-omics analysis by various collaborations at Vanderbilt University [25, 91]. This technology allows for proteomic, transcriptomic, and metabolomic analysis from the same sample, with common sample preparation methodology. This common preparation allows for high-throughput sample analysis, which would be optimal for applications such as rapid threat assessment. This LC-MS based method allows for temporally resolved data sets in addition to multi-omics analyses, optimal for addressing complex bio-logical questions.

   This novel multi-omics sample preparation method utilizes cells but can be applied to tissue samples as well. Cells are lysed, undergo a freeze-thaw cycle, and then are sonicated in an ice bath. Aliquots are then lysed and precipitated with 75:25 Acetone: Ethanol for 2 h, then spun down. The resulting supernatant is then collected for metabolomic analysis while the precipitate is used for proteomics analysis. SPOT applied to metabolomics is best utilized for untargeted analysis. 50 microliters of supernatant extracted from SPOT sample preparation were analyzed through either reverse phase LC or HILIC in a global untargeted analysis with simultaneous analysis of molecular fragmentation. This approach showed reproducible results comparable to traditional metabolomic methods and is efficient with the ability to take cells from pellets to desalted samples ready for MS analysis within 9 h. Additionally, this method led to the extraction of changing metabolites key for biological information. SPOT was applied to human acute promyelocytic leukemia (HL-60) cells that were exposed to zinc intoxication. Additionally, data was collected at various time points throughout the analysis from 6 h to 24 h.

   This investigation highlighted three pathways that appeared significantly modified with zinc treatment: tryptophan metabolism, purine metabolism, and eicosanoid signaling. Metabolomics allowed for the discovery of cellular responses not found with proteomics and transcriptomics on the same sample. These pathways were previously identified with genomic technologies and are supported by these metabolomic data sets extracted using SPOT. The continued use of the SPOT protocol will answer many biological questions, through the incorporation of high-throughput, time-resolved, large-scale data sets for untargeted multi-omics analysis.

4.6.2   Metabolomic Analysis with Imaging Mass Spectrometry

IMS has been used with high success for metabolomic analysis. Although LC-MS is more suitable for absolute quantitation, IMS maintains the spatial information from a tissue section. A paper from 2018 utilized IMS, in coordination with immunohistochemistry, qPCR, western blotting and enzyme assays, to elucidate the

regional differences in glucose metabolism in the brain [91]. IMS is an untargeted, label-free technology, but can also be used to visualize the localization of targeted metabolites such as those related to glucose metabolism. In this paper ATP, ADP, HP and HBP were all identified to determine regional differences in metabolism within the brain. This approach allows for direct measurement of metabolites generated through specific pathways and in specific brain regions. Then, using immuno-histochemistry and Nissl staining, these regional differences can be visualized a high spatial resolution.

MALDI IMS sample preparation differs from LC-MS methods, due to its retention of spatial information. Tissue can be sectioned and mounted onto glass slides, then sprayed with matrix to improved ionization efficiency. This maintains the relationship of the robust chemical information provided by MS with spatial location in the tissue, offering new correlations between the molecular makeup of the tissue and the various regions and substructures. Overall this approach allowed for the identification of key metabolites and gives insight into the relationship between brain regions and pathways. Metabolites are tentatively identified by exact mass, and then confirmed by MS^3 fragmentation experiments.

IMS showed the regional variations between areas that use glucose for glycolysis versus areas that use glucose primarily for the pentose phosphate pathway (PPP). For example, more of the glucose in the thalamus is entering the PPP over other regions such as the amygdala where more glucose is utilized in other pathways such as glycolysis. However, in white matter tracts and regions with low glycolysis and PPP, ATP production is high. Additionally, this investigation showed an increase in lactate during fasting that shows regional localization to specific brain substructures. Overall IMS allows for spatially resolved metabolomics, also showing the ability to conduct high resolution metabolomics with the addition of spatial information in regions of interest to study specific pathways.

4.6.3 Other Metabolomics Methods: Nuclear Magnetic Resonance

Previous methods described for metabolomics utilize mass spectrometry for analysis. While MS is higher in sensitivity by orders of magnitude, other technologies such as nuclear magnetic resonance (NMR) have been growing in their applicability to metabolomic research. NMR has a variety of advantages over MS [8]. The sample preparation for NMR is relatively easy compared to LC-MS, high experimental reproducibility, and NMR is nondestructive for samples. One of the major benefits of NMR, however, is the ability to quantify the metabolite levels explicitly. Due to these advantages and the high automatability, NMR-based metabolomics has been increasing over the last 15 years. With NMR technologies such as MRI and ssNMR, living cells and entire organs can be analyzed due to the nondestructive nature of NMR, applications that are currently inaccessible for MS. Ultimately the choice between NMR and MS relies on the priorities of the experiment: high sensitivity and more identifications, or nondestructive analysis.

NMR suffers from limited spectral bandwidth when analyzing complex metabolomics samples, however, which can make untargeted complex mixtures difficult to analyze. 2D NMR spectra allows for more information at overlapping resonances, helping with further separation of peaks. 2D NMR involves the plotting of two frequency axes against each other, allowing for visualization of correlation be-tween different peaks using either homonuclear or heteronuclear correlations [92]. While 2D NMR applied to metabolomics can be cumbersome, the Gi-raudeau group has recently described a fast quantitative 2D NMR workflow for metabolomics and lipidomics [93]. This approach specifically mentions UF COSY (ultrafast correlation spectroscopy), ^{1}H-^{13}C HSQC (heteronuclear single-quantum correlation spectroscopy), and ZF-TOCSY (Z-filter total correlation spectroscopy) as their approaches, but their workflow can be applied to any 2D NMR approach. Previously 2D NMR experiments required long acquisition, up to several hours per spectrum, as well as difficulties in quantitation. This new fast 2D NMR workflow reduces acquisition time and allows for quantitation for both targeted and untargeted approaches. For targeted approaches, standard additions or calibration are incorporated into the sample design, which untargeted approaches utilize involved data processing and statistics.

4.7   Conclusion

Metabolomics is a growing field with a variety of analytical and computational tools for analyzing a broad, dynamic, and diverse chemical and biological spaces. Strategies exist for analyzing the metabolome for both hypothesis generation and hypothesis testing. Specifically, mass spectrometry enables the interrogation of this chemical space to answer a biological question. However, the experimental design including design (targeted/untargeted), sample preparation, separations, data acquisition, and data analysis tailored towards the ultimate question is integral to a successful experiment. As the endpoint of biochemical processes, the metabolome is uniquely suited to provide a broad, yet specific view biologically processes that closely relate to phenotype, especially for biological and medicinal applications.

References

1. Ryan D, Robards K (2006) Metabolomics: the greatest omics of them all?. https://doi.org/10.1021/AC0614341
2. Ren J-L, Zhang A-H, Kong L, Wang X-J (2018) Advances in mass spectrometry-based metabolomics for investigation of metabolites. RSC Adv 8(40):22335–22350. https://doi.org/10.1039/C8RA01574K
3. Guo S, Tian J, Zhu B, Yang S, Yu K, Zhao Z (2018) Trends in metabolomics research: A Scientometric analysis (1992–2017). Curr Sci 114(11)
4. Markley JL, Brüschweiler R, Edison AS, Eghbalnia HR, Powers R, Raftery D, Wishart DS (2017) The future of NMR-based metabolomics. Curr Opin Biotechnol 43:34–40. https://doi.org/10.1016/J.COPBIO.2016.08.001

5. Papadimitropoulos M-EP, Vasilopoulou CG, Maga-Nteve C, Klapa MI (2018) Untargeted GC-MS metabolomics. Humana Press, New York, pp 133–147. https://doi.org/10.1007/978-1-4939-7643-0_9

6. Zhou B, Xiao JF, Tuli L, Ressom HW (2012) LC-MS-based metabolomics. Mol BioSyst 8(2):470. https://doi.org/10.1039/C1MB05350G

7. Dueñas ME, Larson EA, Lee YJ (2019) Toward mass spectrometry imaging in the metabolomics scale: increasing metabolic coverage through multiple on-tissue chemical modifications. Front Plant Sci 10(860). https://doi.org/10.3389/fpls.2019.00860

8. Emwas A-H, Roy R, McKay RT, Tenori L, Saccenti E, Gowda GAN, Raftery D, Alahmari F, Jaremko L, Jaremko M et al (2019) NMR spectroscopy for metabolomics research. Meta 9(7):123. https://doi.org/10.3390/metabo9070123

9. Schrimpe-Rutledge AC, Codreanu SG, Sherrod SD, McLean JA (2016) Untargeted metabolomics strategies—challenges and emerging directions. J Am Soc Mass Spectrom 27(12):1897–1905. https://doi.org/10.1007/s13361-016-1469-y

10. Gray WR (1967) Dansyl Chloride Procedure. *Methods Enzymol* 11(C):139–151. https://doi.org/10.1016/S0076-6879(67)11014-8

11. Vinayavekhin N, Saghatelian A Untargeted metabolomics. In: Current protocols in molecular biology. Wiley, Hoboken, p 2010. https://doi.org/10.1002/0471142727.mb3001s90

12. Enders JR, McIntire GL (2015) A dilute-and-shoot LC-MS method for quantitating opioids in Oral fluid. J Anal Toxicol 39(8):662–667. https://doi.org/10.1093/jat/bkv087

13. Ser Z, Liu X, Tang NN, Locasale JW (2015) Extraction parameters for metabolomics from cultured cells. Anal Biochem 475:22–28. https://doi.org/10.1016/j.ab.2015.01.003

14. Boyd RK (1993) Quantitative trace analysis by combined chromatography and mass spectrometry using external and internal standards. Rapid Commun Mass Spectrom:257–271. https://doi.org/10.1002/rcm.1290070402

15. Roberts LD, Souza AL, Gerszten RE, Clish CB Targeted Metabolomics. *Curr Protoc Mol Biol* 2012:1. (SUPPL.98. https://doi.org/10.1002/0471142727.mb3002s98

16. Dunn WB, Ellis DI (2005) Metabolomics: current analytical platforms and methodologies. TrAC Trends Anal Chem 24(4):285–294. https://doi.org/10.1016/j.trac.2004.11.021

17. Cajka T, Fiehn O (2014) Comprehensive analysis of lipids in biological systems by liquid chromatography-mass spectrometry. TrAC Trends Anal Chem:192–206. https://doi.org/10.1016/j.trac.2014.04.017

18. Jiang L, He L, Fountoulakis M (2004) Comparison of protein precipitation methods for sample preparation prior to proteomic analysis. J Chromatogr A 1023(2):317–320. https://doi.org/10.1016/j.chroma.2003.10.029

19. Folch J, Lees M, Sloane GH (2019) A simple method for the isolation and purification of total Lipides from animal tissues* Downloaded From; 2019

20. Bligh EG, Dyer WJ A rapid method of total lipid extraction and purification

21. Gutierrez DB, Gant-Branum RL, Romer CE, Farrow MA, Allen JL, Dahal N, Nei YW, Codreanu SG, Jordan AT, Palmer LD et al (2018) An integrated, high-throughput strategy for Multiomic systems level analysis. J Proteome Res 17(10):3396–3408. https://doi.org/10.1021/acs.jproteome.8b00302

22. Gertsman I, Barshop BA (2018) Promises and pitfalls of untargeted metabolomics. J Inherit Metab Dis:355–366. https://doi.org/10.1007/s10545-017-0130-7

23. Broadhurst D, Goodacre R, Reinke SN, Kuligowski J, Wilson ID, Lewis MR, Dunn WB (2018) Guidelines and considerations for the use of system suitability and quality control samples in mass spectrometry assays applied in untargeted clinical Metabolomic studies. *Metabolomics*. https://doi.org/10.1007/s11306-018-1367-3

24. Haijes HA, van der Ham M, Gerrits J, van Hasselt PM, Prinsen HCMT, de Sain-van der Velden MGM, Verhoeven-Duif NM, Jans JJM (2019) Direct-infusion based metabolomics unveils biochemical profiles of inborn errors of metabolism in cerebrospinal fluid. Mol Genet Metab 127(1):51–57. https://doi.org/10.1016/J.YMGME.2019.03.005

25. Norris JL, Caprioli RM Analysis of tissue specimens by matrix-assisted laser desorption/ ionization imaging mass spectrometry in biological and clinical research. https://doi.org/10.1021/cr3004295

26. Jandera P (2005) Liquid chromatography | normal phase. In: Encyclopedia of analytical science. Elsevier, pp 142–152. https://doi.org/10.1016/b0-12-369397-7/00324-1
27. Scott RPW (2000) Chromatography: Liquid | mechanisms: normal phase. In: Encyclopedia of separation science. Elsevier, pp 706–711. https://doi.org/10.1016/b0-12-226770-2/00301-x
28. Jiang P, Lucy CA (2016) Coupling normal phase liquid chromatography with electrospray ionization mass spectrometry: strategies and applications. Anal Methods:6478–6488. https://doi.org/10.1039/c6ay01419d
29. Abbott SR (1980) Practical aspects of normal-phase chromatography. J Chromatogr Sci 18(10):540–550. https://doi.org/10.1093/chromsci/18.10.540
30. Patti GJ, Yanes O, Siuzdak GI (2012) Metabolomics: the apogee of the omics trilogy. Nat Rev Mol Cell Biol:263–269. https://doi.org/10.1038/nrm3314
31. Dettmer K, Aronov PA, Hammock BD Mass spectrometry-based metabolomics. Mass Spectrom Rev 26(1):51–78. https://doi.org/10.1002/mas.20108
32. Patterson RE, Ducrocq AJ, McDougall DJ, Garrett TJ, Yost RA (2015) Comparison of blood plasma sample preparation methods for combined LC-MS lipidomics and metabolomics. J Chromatogr B Anal Technol Biomed Life Sci 1002:260–266. https://doi.org/10.1016/j.jchromb.2015.08.018
33. Cutillas P (2005) Principles of nanoflow liquid chromatography and applications to proteomics. Curr Nanosci 1(1):65–71. https://doi.org/10.2174/1573413052953093
34. Alpert AJ (1990) Hydrophilic-interaction chromatography for the separation of peptides, nucleic acids and other polar compounds. J Chromatogr A 499(C):177–196. https://doi.org/10.1016/S0021-9673(00)96972-3
35. Simon R, Enjalbert Q, Biarc J, Lemoine J, Salvador A (2012) Evaluation of Hydrophilic Interaction Chromatography (HILIC) versus C18 reversed-phase chromatography for targeted quantification of peptides by mass spectrometry. J Chromatogr A 1264:31–39. https://doi.org/10.1016/j.chroma.2012.09.059
36. Naser FJ, Mahieu NG, Wang L, Spalding JL, Johnson SL, Patti GJ (2018) Two complementary reversed-phase separations for comprehensive coverage of the semipolar and nonpolar metabolome. Anal Bioanal Chem 410(4):1287–1297. https://doi.org/10.1007/s00216-017-0768-x
37. Martin AJP, Synge RLM (1941) A new form of chromatogram employing two liquid phases. Biochem J 35(12):1358–1368
38. Roessner U, Wagner C, Kopka J, Tretheway RN, Willmitzer L (2001) Simultaneous analysis of metabolites in tuber by gas chromatography-mass spectrometry. Plant J 23:1
39. Castrillo JI, Hayes A, Mohammed S, Gaskell SJ, Oliver SG (2003) An optimized protocol for metabolome analysis in yeast using direct infusion electrospray mass spectrometry. Phytochemistry 62:929–937
40. Halket JM, Waterman D, Przyborowska AM, Patel RKP, Fraser PD, Bramley PM (2005) Chemical derivatization and mass spectral libraries in metabolic profiling by GC/MS and LC/MS/MS. J Exp Bot 56(410):219–243. https://doi.org/10.1093/jxb/eri069
41. Jonsson P, Johansson AI, Gullberg J, Trygg J, A J, Grung B, Marklund S, Sjöström M, Antti H, Moritz T (2005) High-throughput data analysis for detecting and identifying differences between samples in GC/MS-based metabolomic analyses. Anal Chem 77(17):5635–5642. https://doi.org/10.1021/ac050601e
42. Monnig CA, Kennedy RT (2014) Capillary electrophoresis. Food Toxic Anal Tech Strateg Dev 1997(12):561–597. https://doi.org/10.1021/acs.analchem.5b04125
43. Ewing AG, Wallingford RA, Olefirowicz TM (1989) Capillary electrophoresis. Anal Chem 61(4):292A–303A. https://doi.org/10.1021/ac00179a002
44. VanOrman BB, Liversidge GG, McIntire GL, Olefirowicz TM, Ewing AG (1990) Effects of buffer composition on electroosmotic flow in capillary electrophoresis. J Microcolumn Sep 2(4):176–180. https://doi.org/10.1002/mcs.1220020404
45. Olivares JA, Nguyen NT, Yonker CR, Smith RD (1987) On-line mass spectrometric detection for capillary zone electrophoresis. Anal Chem 59(8):1230–1232. https://doi.org/10.1021/ac00135a034

46. Soga T, Ohashi Y, Ueno Y, Naraoka H, Tomita M, Nishioka T (2003) Quantitative metabolome analysis using capillary electrophoresis mass spectrometry. J Proteome Res 2(5):488–494. https://doi.org/10.1021/pr034020m

47. Nowak PM, Woźniakiewicz M, Gładysz M, Janus M, Kościelniak P (2017) Improving repeatability of capillary electrophoresis—a critical comparison of ten different capillary inner surfaces and three criteria of peak identification. Anal Bioanal Chem 409(18):4383–4393. https://doi.org/10.1007/s00216-017-0382-y

48. Dwivedi P, Wu P, Klopsch SJ, Puzon GJ, Xun L, Hill HH (2008) Metabolic profiling by Ion Mobility Mass Spectrometry (IMMS). Metabolomics 4(1):63–80. https://doi.org/10.1007/s11306-007-0093-z

49. Miller RA, Eiceman GA, Nazarov EG, King AT (2000) Novel micromachined high-field asymmetric waveform-ion mobility spectrometer. Sensors Actuators B Chem 67(3):300–306. https://doi.org/10.1016/S0925-4005(00)00535-9

50. Kanu AB, Dwivedi P, Tam M, Matz L, Hill HH (2008) Ion mobility-mass spectrometry. J Mass Spectrom 43(1):1–22. https://doi.org/10.1002/jms.1383

51. Berm EJJ, Paardekooper J, Brummel-Mulder E, Hak E, Wilffert B, Maring JG (2015) A simple dried blood Spot method for therapeutic drug monitoring of the tricyclic antidepressants amitriptyline, nortriptyline, imipramine, clomipramine, and their active metabolites using LC-MS/MS. Talanta 134:165–172. https://doi.org/10.1016/j.talanta.2014.10.041

52. Tautenhahn R, Bottcher C, Neumann S (2008) Highly sensitive feature detection for high resolution LC/MS. BMC Bioinf 9. https://doi.org/10.1186/1471-2105-9-504

53. Zhang X, Quinn K, Cruickshank-Quinn C, Reisdorph R, Reisdorph N (2018) The application of ion mobility mass spectrometry to metabolomics. *Curr Opin Chem Biol*:60–66. https://doi.org/10.1016/j.cbpa.2017.11.001

54. Picache JA, Rose BS, Balinski A, Leaptrot KL, Sherrod SD, May JC, McLean JA (2019) Collision cross section compendium to annotate and predict multi-Omic compound identities. Chem Sci 10(4):983–993. https://doi.org/10.1039/c8sc04396e

55. Xiao JF, Zhou B, Ressom HW (2012) Metabolite identification and quantitation in LC-MS/MS-based metabolomics. TrAC Trends Anal Chem:1–14. https://doi.org/10.1016/j.trac.2011.08.009

56. Yost RA, Enke CG (1978) Selected ion fragmentation with a tandem quadrupole mass spectrometer. J Am Chem Soc 100(7):2274–2275. https://doi.org/10.1021/ja00475a072

57. Matraszek-Zuchowska I, Wozniak B, Posyniak A (2016) Comparison of the multiple reaction monitoring and enhanced product ion scan modes for confirmation of stilbenes in bovine urine samples using LC–MS/MS QTRAP® system. Chromatographia 79(15–16):1003–1012. https://doi.org/10.1007/s10337-016-3121-1

58. Hopfgartner G, Varesio E, Tschäppät V, Grivet C, Bourgogne E, Leuthold LA (2004) Triple quadrupole linear ion trap mass spectrometer for the analysis of small molecules and macromolecules. J Mass Spectrom 39(8):845–855. https://doi.org/10.1002/jms.659

59. Zhou J, Yin Y (2016) Strategies for large-scale targeted metabolomics quantification by liquid chromatography-mass spectrometry. Analyst 141(23):6362–6373. https://doi.org/10.1039/c6an01753c

60. Bateman NW, Goulding SP, Shulman NJ, Gadok AK, Szumlinski KK, MacCoss MJ, Wu CC (2014) Maximizing peptide identification events in proteomic workflows using Data-Dependent Acquisition (DDA). Mol Cell Proteomics 13(1):329–338. https://doi.org/10.1074/mcp.M112.026500

61. Mullard G, Allwood JW, Weber R, Brown M, Begley P, Hollywood KA, Jones M, Unwin RD, Bishop PN, Cooper GJS et al (2015) A new strategy for MS/MS data acquisition applying multiple data dependent experiments on orbitrap mass spectrometers in non-targeted metabolomic applications. Metabolomics 11(5):1068–1080. https://doi.org/10.1007/s11306-014-0763-6

62. Schwudke D, Liebisch G, Herzog R, Schmitz G, Shevchenko A (2007) Shotgun lipidomics by tandem mass spectrometry under data-dependent acquisition control. Methods Enzymol:175–191. https://doi.org/10.1016/S0076-6879(07)33010-3

63. Doerr A (2014) DIA mass spectrometry. Nat Methods 2014:121

64. Venable JD, Dong MQ, Wohlschlegel J, Dillin A, Yates JR (2004) Automated approach for quantitative analysis of complex peptide mixtures from tandem mass spectra. Nat Methods 1(1):39–45. https://doi.org/10.1038/nmeth705

65. Bilbao A, Varesio E, Luban J, Strambio-De-Castillia C, Hopfgartner G, Müller M, Lisacek F (2015) Processing strategies and software solutions for data-independent acquisition in mass spectrometry. Proteomics 15(5–6):964–980. https://doi.org/10.1002/pmic.201400323

66. Kondrat RW, McClusky GA, Cooks RG (1978) Multiple reaction monitoring in mass spectrometry/mass spectrometry for direct analysis of complex mixtures. Anal Chem 50(14):2017–2021. https://doi.org/10.1021/ac50036a020

67. Rathahao-Paris E, Alves S, Junot C, Tabet JC (2016) High resolution mass spectrometry for structural identification of metabolites in metabolomics. Metabolomics:1–15. https://doi.org/10.1007/s11306-015-0882-8

68. Michalski A, Damoc E, Lange O, Denisov E, Nolting D, Müller M, Viner R, Schwartz J, Remes P, Belford M et al (2012) Ultra high resolution linear ion trap orbitrap mass spectrometer (Orbitrap elite) facilitates top down LC MS/MS and versatile peptide fragmentation modes. Mol Cell Proteomics 11(3). https://doi.org/10.1074/mcp.O111.013698

69. Ghaste M, Mistrik R, Shulaev V (2016) Applications of Fourier transform ion cyclotron resonance (FT-ICR) and Orbitrap based high resolution mass spectrometry in metabolomics and Lipidomics. Int J Mol Sci. https://doi.org/10.3390/ijms17060816

70. Mahieu NG, Patti GJ (2017) Systems-level annotation of a metabolomics data set reduces 25 000 features to fewer than 1000 unique metabolites. Anal Chem 89(19):10397–10406. https://doi.org/10.1021/acs.analchem.7b02380

71. Blaženović I, Kind T, Ji J, Fiehn O (2018) Software tools and approaches for compound identification of LC-MS/MS data in metabolomics. Meta 8(2):31. https://doi.org/10.3390/metabo8020031

72. LCQuan. Thermo Fisher Scientific: Hemel Hempstead, Hetfordshire, UK

73. Depke T, Franke R, Brönstrup M (2017) Clustering of MS2 spectra using unsupervised methods to aid the identification of secondary metabolites from Pseudomonas Aeruginosa. J Chromatogr B 1071:19–28. https://doi.org/10.1016/j.jchromb.2017.06.002

74. MassHunter. Agilent: Santa Clara, CA, USA

75. Profile Analysis. Bruker

76. SIEVE. Thermo Fisher Scientific

77. Progenesis. Waters, Milford, MA, USA

78. Tautenhahn R, Patti GJ, Rinehart D, Siuzdak G (2012) XCMS online: A web-based platform to process untargeted metabolomic data. Anal Chem 84(11):5035–5039. https://doi.org/10.1021/ac300698c

79. Tsugawa H, Cajka T, Kind T, Ma Y, Higgins B, Ikeda K, Kanazawa M, VanderGheynst J, Fiehn O, Arita M (2015) MS-DIAL: data-independent MS/MS deconvolution for comprehensive metabolome analysis. Nat Methods 12(6):523–526. https://doi.org/10.1038/nmeth.3393

80. Katajamaa M, Miettinen J, Oresic M (2006) MZmine: toolbox for processing and visualization of mass spectrometry based molecular profile data. Bioinformatics 22(5):634–636. https://doi.org/10.1093/bioinformatics/btk039

81. MassBank of North America(2019). https://mona.fiehnlab.ucdavis.edu/. Accessed Sep 12, 2019

82. Wishart DS, Feunang YD, Marcu A, Guo AC, Liang K, Ázquez-Fresno RV, Sajed T, Johnson D, Li C, Karu N et al (2018) HMDB 4.0: the human metabolome database for 2018. Nucleic Acids Res 46. https://doi.org/10.1093/nar/gkx1089

83. NIST Standard Reference Database 1A v17|NIST (2019). https://www.nist.gov/srd/nist-standard-reference-database-1a-v17. Accessed Sep 12, 2019

84. Horai H, Arita M, Kanaya S, Nihei Y, Ikeda T, Suwa K, Ojima Y, Tanaka K, Tanaka S, Aoshima K et al (2010) MassBank: A public repository for sharing mass spectral data for life sciences. J Mass Spectrom 45(7):703–714. https://doi.org/10.1002/jms.1777

85. Jeffryes JG, Colastani RL, Elbadawi-Sidhu M, Kind T, Niehaus TD, Broadbelt LJ, Hanson AD, Fiehn O, Tyo KEJ, Henry CS (2015) MINEs: open access databases of computationally predicted enzyme promiscuity products for untargeted metabolomics. J Cheminform 7(1):44. https://doi.org/10.1186/s13321-015-0087-1

86. mzCloud – Statistics (2019). https://www.mzcloud.org/Stats. Accessed Sep 12, 2019

87. Huang X, Chen Y-J, Cho K, Nikolskiy I, Crawford PA, Patti GJX (2014) [13]CMS: global tracking of isotopic labels in untargeted metabolomics. Anal Chem 86(3):1632–1639. https://doi.org/10.1021/ac403384n

88. Kanehisa M, Araki M, Goto S, Hattori M, Hirakawa M, Itoh M, Katayama T, Kawashima S, Okuda S, Tokimatsu T et al (2007) KEGG for linking genomes to life and the environment. Nucleic Acids Res 36(Database):D480–D484. https://doi.org/10.1093/nar/gkm882

89. Karp PD, Riley M, Paley SM, Pellegrini-Toole A (2002) The MetaCyc database. Nucleic Acids Res 30(1):59–61. https://doi.org/10.1093/nar/30.1.59

90. Pico AR, Kelder T, van Iersel MP, Hanspers K, Conklin BR, Evelo C (2008) WikiPathways: pathway editing for the people. PLoS Biol 6(7):e184. https://doi.org/10.1371/journal.pbio.0060184

91. Kleinridders A, Ferris HA, Reyzer ML, Rath M, Soto M, Manier ML, Spraggins J, Yang Z, Stanton RC, Caprioli RM et al (2018) Regional differences in brain glucose metabolism determined by imaging mass spectrometry. Mol Metab 12:113–121. https://doi.org/10.1016/j.molmet.2018.03.013

92. Aue WP, Bartholdi E, Ernst RR (1976) Two-dimensional spectroscopy. Application to nuclear magnetic resonance. J Chem Phys 64(5):2229–2246. https://doi.org/10.1063/1.432450

93. Martineau E, Dumez JN, Giraudeau P (2019., No. February, 1–14) Fast quantitative 2D NMR for metabolomics and lipidomics: a tutorial. Magn Reson Chem. https://doi.org/10.1002/mrc.4899

Chapter 5
Direct Mass Spectrometry as a Practical Analytical Strategy for High Speed, High Throughput Testing

Mark W. Duncan

Abstract Thanks to the development of new methods and the ongoing evolution of existing approaches, there are now over thirty different ambient ionization or direct mass spectrometry (D-MS) sample introduction/ionization strategies. A critical question, however, is whether these techniques can generate faster, yet comparable results to those obtained through the application of more conventional mass spectrometric techniques. This chapter discusses the strengths and weaknesses of conventional chromatography-mass spectrometry combinations (e.g., GC-MS(/MS) and LC- MS(/MS)), introduces and presents the benefits of D-MS approaches, and illustrates the practical potential of these strategies by way of specific example applications.

Keywords Direct mass spectrometry · Ambient mass spectrometry · Quantification · Direct in real time (DART) mass spectrometry · Direct electrospray ionization (DESI) mass spectrometry

5.1 Introduction

For many applications, the marriage of a separation technology (for example, gas chromatography (GC) or liquid chromatography (LC))) with mass spectrometry (MS) is a powerful, if not the ideal analytical strategy. Typically, the system is comprised of a GC or LC chromatograph interface directly to a mass spectrometer. (See Fig. 5.1.)

M. W. Duncan (✉)
Target Discovery, Inc, Mountain View, CA, USA
e-mail: mark_duncan@targetdiscovery.com
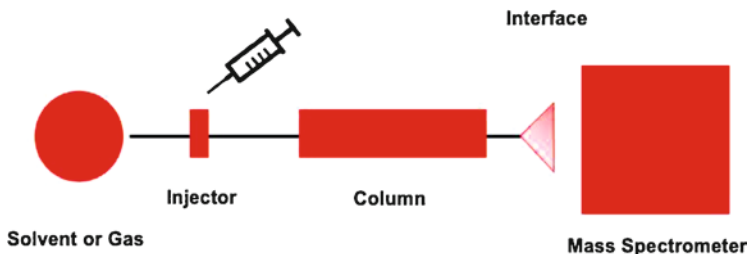
Fig. 5.1 Schematic of a convention GC/LC mass spectrometer

Following a single injection of a sample solution, this combination allows separation (in time) of the components of a complex mixture and their sequential introduction into the source of the mass spectrometer. When this strategy is combined with tandem mass spectrometry (MS/MS) an information-rich MS/MS spectrum can be generated on each component and used for structural identification. In the course of a single run, mass spectra on hundreds or even thousands of sample components can be acquired, searched against database entries, identified and/or quantified.

Although the power of these hybrid technologies is undisputed, their routine application involves significant challenges. First, the cost and complexity of hybrid systems are significant. Second, the routine operation of a GC- or LC-MS (or MS/MS) system is demanding, and so too is troubleshooting these systems. Even in the best of hands there is substantial operational downtime with an LC-MS(/MS) system. Third, method development is complex and is frequently the rate-limiting step – i.e., it can take months or even years to develop a rugged and validated procedure for a specific application. Forth, and finally, pre-analysis sample processing is typically manual, involves multiple steps, and must be performed by skilled staff. Some of these issues are discussed in more detail in the sections that follow.

Maintaining optimal or even satisfactory performance of an MS/MS is challenging. For example, system performance degrades over time because with every injection, sample components are deposited on the column, the MS interface region, and the front end of the MS (or MS/MS). Eventually, separation degrades, the interface region becomes contaminated, and the performance of the system is compromised. Spurious peaks may start to arise, retention times may shift, and degraded resolution and sensitivity are observed.

Routine operation therefore requires ongoing system suitability assessment. Specifically, when performance degrades to below acceptable limits the cause must be identified and corrected: i.e., the column needs to be changed and/or the MS vented to atmospheric pressure and components of the MS interface need to be cleaned or replaced. Changes that require venting the MS introduce substantial operational downtime (e.g., 12–24 h). Throughout the useful operational life of the instrument this cycle continues: i.e., sensitivity gradually decreases (i.e., as measured by peak height/area of a reference standard) but can be recovered when appropriate preventative maintenance steps are taken. Keeping the system operational

therefore requires a skilled operator and is associated with significant cost and downtime. In practice, problems related to LC performance and failures, combined with issues associated with the interface between the LC and MS, are more common than problems related to the MS system itself.

There are also significance challenges associated with the development of a practical analytical method. It can be a major challenge to efficiently extract the analyte(s) of interest from what is frequently a complex sample matrix containing hundreds or more abundant components. There are always losses of the target analyte(s) and to varying degrees matrix components remain in the sample extract depending on the nature of the sample and the workup steps adopted. Selecting and optimizing an extraction method – especially for multi-component analysis of low abundance components – is therefore a (very) complex endeavor. A key factor in minimizing instrument downtime and producing acceptable results is the introduction of "clean" samples into the LC-MS (or GC-MS) system. For all these reasons, developing a practical, cost-effective, robust, automated and validated analytical method for a specific application can be a very time-consuming and costly task.

The widespread adoption of LC-MS (/MS) methods has been fueled by the need for high-quality data suitable for addressing a diverse array of applications and most commonly, the LC-MS/MS work is performed on a triple quadrupole mass spectrometer operated in the selected reaction monitoring (SRM) mode. The primary strength of this instrument configuration is its ability to separate sample components, detect, identify and quantify them – all in a single run. Examples applications include the analysis of agricultural chemical residues, carcinogens, toxins (e.g., mycotoxins), veterinary drugs, additives, other environmental contaminants or endogenous components in food samples. In addition, these systems are used to measure biomarkers of disease or dysfunction in human urine, blood or tissue samples.

5.2 Direct Analysis MS Approaches as an Alternative to GC/ LC Combined with Tandem Mass Spectrometry

GC-MS/MS and LC-MS/MS have worked very well to separate the components of a complex (solution phase) sample, ionize them, and sequentially transfer the resulting ions into the vacuum system of the mass spectrometry for identification and/or quantification. As discussed above, however, the cost of the equipment, the long, complex and expensive sample preparation time, the analysis time itself (constrained by the chromatography step), the complexity of instrument operation, the time for test development, and the overall cost of test delivery mean that GC- or LC-MS/MS cannot be adopted routinely for many applications, despite their power.

There is now, however, a very long list of direct, open air surface sampling/ionization approaches available (sometimes called ambient ionization methods), and these can serve as alternatives. This list includes extractive electrospray ionization

Fig. 5.2 Schematic of a generic ambient/direct ionization mass spectrometer
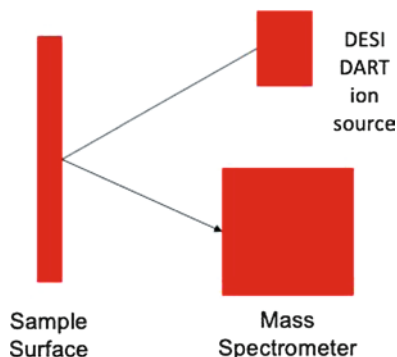
(EESI), fused droplet ESI (FDESI), direct analysis in real time (DART), desorption electrospray ionization (DESI), desorption atmospheric pressure photoionization (DAPPI) and laser ablation electrospray ionization (*LAESI*). Many of these ionization strategies have been summarized and discussed in an excellent review by Monge and colleagues [1]. These D-MS approaches not only bring the power of mass spectrometric qualitative analysis and quantification, but they also offer the significant additional advantage that samples can be analyzed without workup, rapidly, and in the open air (i.e., at atmospheric pressure). (See basic schematic included as Fig. 5.2). Several of these ambient/direct ionization techniques have been developed, refined and are now commercially available.

Two of the most widely adopted D-MS approaches are DART [2] and DESI [3], and in this chapter they alone are presented as representative of this broad class of "direct" ionization strategies. These two options are selected for discussion because, while DART-MS is the most widely adopted direct ionization approach, it is limited to the analysis of lower MW analytes. In contrast, DESI-MS is capable of analyzing proteins and protein complexes, carbohydrates, oligonucleotides and industrial polymers, together with small organic molecules [3]. Some of the primary benefits arising from the application of direct sample analysis are summarized in Table 5.1.

5.3 Direct MS Applications with an Emphasis on DART Applications

DART is a robust and versatile atmospheric pressure ionization approach that can be coupled to a wide range of mass spectrometers. The DART ion source can also be operated in several modes to provide complementary information regarding the sample and its components. For example, when a DART-MS source is coupled with a high-resolution mass spectrometer, exact mass, isotopic distributions and elemental compositions can be determined directly. On a simple, single quadrupole mass

Table 5.1 Comparison of Conventional GC/LC-MS and Direct MS Approaches

Attribute	GC- or LC-MS(/MS) Approaches	Direct MS (i.e., DART- and DESI-MS)
Practicality	Complex technology requiring complex methods and skilled staff	Sample introduction is simple. It can be performed by unskilled staff & involves minimal to no sample workup
Processes	On-line separation is required to minimize ion suppression	Works directly with "dirty" samples
Online separation	Chromatography improves selectivity, detection limits and facilitates comprehensive coverage	No chromatography markedly speeds and simplifies analysis
Analysis time	Slow – typically minutes to hours	Rapid – typically seconds to a minute
Sustainability	Environmentally unfriendly processes; organic solvents for extraction and as a mobile phase	Safe, environmentally friendly, green processes
Output	Difficult to interpret results	Fast fingerprinting. Easy-to-interpret reporting possible
Flexibility	Dedicated GC or LC required	Source can fit to many/most instruments

spectrometer (QMS), the DART-QMS combination is a compact, affordable and versatile analytical tool.

The DART ion source has been used to analyze a wide range of analytes in a diverse array of sample types and for a plethora of objectives. DART, or more specifically the DART ion source, ionizes almost anything placed in front of the source. Notably, DART can be used to sample directly from surfaces such as glass, TLC plates, concrete, paper, or currency without requiring wipes or solvent extraction. Similarly, drugs can be detected directly, in pill form, simply by placing the pill in the line of the DART source for a few seconds to minutes. Biological fluids have been analyzed directly without extraction or other processing: e.g., by dipping a glass rod in raw urine and simply placing the rod in front of the DART source. Meat, fruit and vegetables have all be analyzed directly. Analysis of synthetic materials, including reaction mixtures, polymers, adhesives, whether sticky and/or contaminated, can be carried out with little or no sample preparation [4, 5].

Just a small subset of the types of samples and applications tested through the application of DART- and DESI-MS are included in the Table 5.2 below. (Information in Table 5.2 is primarily based on references [4] and [5].)

5.4 Special Consideration in Quantitative Applications by DART and DESI

DART/DESI can also be used for quantitative analysis. In common with many other mass spectrometric techniques, the absolute abundance of ion currents produced by DART depends on multiple factors, but notably in the case of DART and DESI, on the positioning of the sample target in the gas stream, the nature of the sample

Table 5.2 Example Applications Performed by DART- and DESI-MS

Sample type	Representative analytes & analytical objectives
Human-derived samples including feces, saliva, perspiration, urine, blood, CSF, skin, and other tissues	Volatile organic compounds (VOCs) and other endogenous and exogenous components including: biomarkers of disease; prescription, over-the-counter, veterinary, illicit and counterfeit drugs; direct detection of drugs and metabolites in crude or unprocessed body fluids, including blood, urine, and saliva
Breath, atmosphere	Detection of volatile organic compounds (VOCs)
Bricks, building materials, concrete, soil …	Surface contaminants including biological residues, environmental contaminants, drugs and more
Dried (filter paper) spots prepared from urine, saliva, blood, CSF, …	Detection and quantification of endogenous components, biomarkers of disease, drugs & drug metabolites and toxins
Clothing	Residual toxins, explosives & drugs; detection and identification of biological fluids and/or stains
Plant tissue analysis including wood, bark, seeds, leaves, …	Species identification/authentication; detection and quantification of pesticides, herbicides, …
Non-human tissue and fluid samples including animal, birds, insects, marine organisms	Analysis of endogenous components; contaminants including toxins, pesticides and other environmental pollutants; species identification; detection of drugs, including prescription, over-the-counter and veterinary drugs
Water from various sources, including oceans, rivers, lakes, ponds and drinking water	Detection of contaminants including toxins, pesticides and other environmental pollutants; detection of prescription, over-the-counter, veterinary and illicit drugs
Powders, tablets, syrups and syringe contents	Active component analysis/confirmation; presence of by-products of synthesis and other impurities; detection of counterfeit drugs contains little or no actual drug content; drugs containing completely different active agents with potentially adverse/toxic consequences
Biological fluids, cultures and swabs	Analysis of swabs collected from (any) surface, including culture plates, the mouth, the skin surface, animals, ….
Currency, airline boarding passes, …	Detection and identification of drugs of abuse; explosives, detection of toxic or otherwise dangerous residues on bills.

Table 5.2 (continued)

Sample type	Representative analytes & analytical objectives
Paper and documents	Inks and dyes; residues left from fingers; detection of authentic vs. fraudulent documents; whether written entries come from a common source (i.e., same ink formula); the relative ages of entries; identification of the manufacturer and specific formula of various inks
Swabs taken from various surfaces	Detection and identification of explosives and arson accelerants; chemical weapons agents and their signatures synthetic organic or organometallic compounds including toxins and other environmentally important compounds. The detection of explosives is important for forensics and security applications. DART has been applied to the detection of nitro explosives such as nitroglycerine, TNT, and HMX, inorganic explosives such as ammonium nitrate, perchlorate, azide and peroxide explosives such as triacetone triperoxide (TATP) and hexamethylene triperoxide diamine (HMTD)
Fruits, vegetables	Pesticide residue in/on fruit and vegetables; differentiation between organically and conventionally grown products; metabolic profiling/ fingerprinting; contamination by animal products
Meat	Meat speciation/authentication and detection of adulteration; triacylglycerol (TAG), diacylglycerol (DAG) and free fatty acid (FFA) profiles of dry-cured meats; detection of mycotoxins
Fish	Profiling of caviar; analysis of trout and sardine; frozen vs. fresh differentiation; fish authentication/mislabeling; detection of toxins in seafood
Dairy and related products	Identification of melamine, dicyandiamide and cyanuric acid in milk powder, liquid milk, condensed milk and other dairy products; animal species origin; determination of butter cholesterol levels; cheese adulteration with plant oils; analysis of margarine; adulteration of buffalo milk; butter adulteration; fingerprinting of yoghurt and other dairy products; adulteration of ice cream
Herbs, spices and sauces	Addition of illegal dyes and additives; geographic discrimination; authentication of herbs and spices; contaminant analysis; pesticide residues detection/identification in herbs
Oils, nuts and condiments	Olive oil adulteration; geographic profiling of olive oil; olive oil quality; analysis of balsamic vinegar; authenticity of hazelnuts
Honey & maple syrup	Quantitative analysis of 5-hydroxymethylfurfural in honey; pesticide and toxin detection in honey; adulteration of honey and maple syrup; geographic origin; detection of the presence of added sugars
Cereals and grains	Mycotoxins and pesticides in cereals; mycotoxins in wheat; herbicides in maize; pesticides in corn, oat, rice and wheat
Alcoholic beverages	Identification of beer/spirit/wine brands; fungicides in wine; spirit authenticity/adulteration, e.g., brandy whisk(e)y adulteration, wine adulteration
Coffee and tea	Origin, type and amount of contaminants in coffee beans; ground coffee adulteration; pesticides and adulterants in coffee and tea
Drinking glasses	Residue from contents and/or handlers
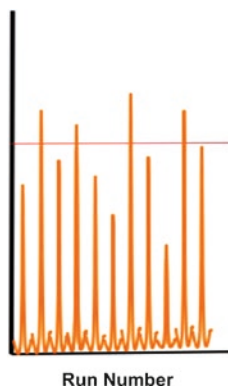
Fig. 5.3 Hypothetical Data for the Quantification of a Single Analyte (Fixed Concentration) in a Range of Samples by DART/DESI
Hypothetical data for the determination of a single specific analyte at a fixed concentration in multiple (different) samples. Note that as the sample is changed, it's positioned in the source also changes and this leads to variability in the measured signal

matrix and any sample handling/clean-up steps undertaken prior to analysis. Representative (hypothetical) data for the determination of a single specific analyte at a fixed concentration, but positioned differently in the source, and/or incorporated in different matrices, is shown in Fig. 5.3.

With the incorporation of an appropriate internal standard, however, these fluctuations can be accounted for and precise quantitative analysis (e.g., of drugs or environmental contaminants in urine, plasma, or other body fluids) is possible [4]. Further, with the incorporation of a standard curve, prepared at the same time and incorporating (pure) reference material, ion abundance ratios (i.e., analyte ion current/internal standard ion current) can be converted to accurate analyte concentrations.

The internal standard should be a good chemical mimic of the analyte and it is added to all samples and calibrators at a FIXED concentration. For optimal precision, the internal standard of choice is a stable isotope labeled form of the target analyte. The signals for the analyte (Ra) and the internal standard (Ris) are measured simultaneously in the complete sample set – i.e., all standards, controls and test samples alike. When the measured response ratio Ra/Ris is plotted against the analysis amount (i.e., the amount of reference standard incorporated into each calibration standard) for all standards in the standard curve, the relationship is typically "linearized" and precise and accurate quantification is possible. By calculating the ratio Ra/Ris for all unknowns, and by reference to the standard/calibration curve, the concentration (or amount) of analyte in each of the unknown sample can be determined. This approach to quantification, based on the use of an internal standard, is frequently used in quantitative mass spectrometry because response typically fluctuates with time and in response to other components in the matrix.

Figure 5.4 the utility of an internal standard in quantitative applications. The incorporation of a standard curve allows absolute quantification. This figure (i.e., left hand panel) shows the measured ion current (e.g., measured peak height) for
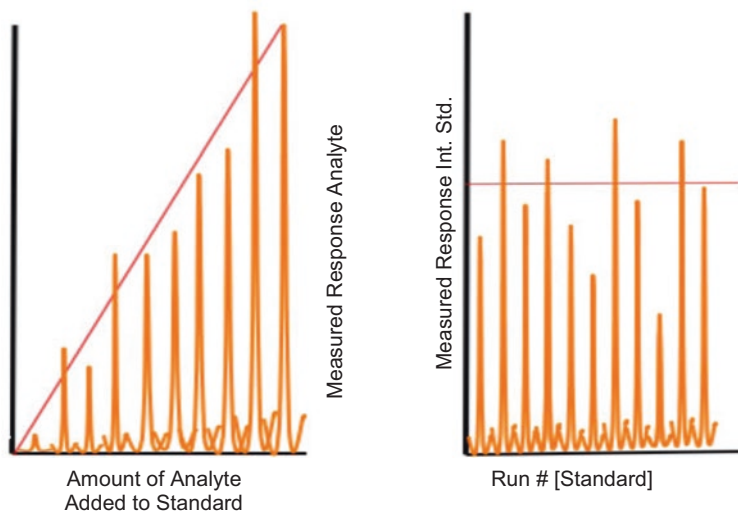
Fig. 5.4 utility of an internal standard in quantitative applications. The incorporation of a standard curve allows absolute quantification. This figure (i.e., left hand panel) shows the measured ion current (e.g., measured peak height) for increasing concentrations/ amounts of the standard reference material. Note that the relationship does not fit the ideal or predicted linear relationship. However, matching fluctuations are observed in the measured ion current (i.e., peak height) for the internal standard added at a fixed amount to each calibration sample (i.e., right hand panel). In this way, fluctuations in the measured signal over time/across samples are "normalized". Consequently, when the response ratio, Ra/Ris, is determined and plotted against the amount of standard/calibrator, precise and absolute quantification of analyte levels can be determined by DART/DESI-MS and similar strategies

increasing concentrations/amounts of the standard reference material. Note that the relationship does not fit the ideal or predicted linear relationship. However, matching fluctuations are observed in the measured ion current (i.e., peak height) for the internal standard added at a fixed amount to each calibration sample (i.e., right hand panel). In this way, fluctuations in the measured signal over time/across samples are "normalized". Consequently, when the response ratio, Ra/Ris, is determined and plotted against the amount of standard/calibrator, precise and absolute quantification of analyte levels can be determined by DART/DESI-MS and similar strategies.

5.5 Conclusions

DART-MS, DESI-MS and related direct analysis strategies are powerful tools for sample analysis, analyte identification and quantification. These ionization strategies can circumvent some of the practical complications of more convention approaches to mass spectrometric analysis, most notably, the complexities of

sample workup and inline chromatographic separation. By adoption standard quantitative strategies, most notably the incorporation of an appropriate internal standard and inclusion of a standard curve, it is possible to obtain both accurate and precise quantitative determinations. The markedly simplified sample handling requirements, combined with the opportunity to analysis samples directly, opens up new opportunities for practical, fast, high throughput analysis while retaining the inherent selectivity, sensitivity and quantitative precision of mass spectrometry.

References

1. Monge ME, Harris GA, Dwivedi P, Fernández FM (2013) Mass spectrometry: recent advances in direct open air surface sampling/ionization. Chem Rev 113:2269–2308
2. Cody RB, Laramee JA, Durst HD (2005) Versatile new ion source for the analysis of materials in open air under ambient conditions. Anal Chem 77:2297–2302
3. Takats Z, Wiseman JM, Gologan B, Cooks RG (2004) Mass spectrometry sampling under ambient conditions with desorption electrospray ionization. Science 306:471–473
4. Guo T, Yong W, Jin Y, Zhang L, Liu J, Wang S, Chen Q, Dong Y, Su H, Tan T (2017) Applications of DART-MS for food quality and safety assurance in food supply chain. Mass Spectrom Rev 36:161–187
5. Dong Y (ed) (2018) Direct analysis in real time mass spectrometry: principles and practices of DART-MS. Wiley-VCH Verlag GmbH & Co, Weinheim

Chapter 6
Mass Spectrometry in Ecotoxicology

Check for updates

Ksenia J. Groh and Marc F.-J. Suter

Abstract Risk assessment of chemical effects in the environment requires the understanding of the fate and behavior of anthropogenic chemicals in natural and technical systems, which is the focus of environmental chemistry. The exposure data obtained by environmental chemists are in turn used to evaluate the significance of toxicological effects in organisms, as studied by environmental toxicologists. Mass spectrometry-based techniques are frequently applied to monitor the exposure or investigate the effects of chemicals, particularly their mechanism of action. These techniques include, for example, targeted and non-targeted chemical analytics as well as diverse –omics methods. This chapter illustrates the application of mass spectrometry in environmental chemistry and toxicology using research projects carried out at our institute, with a particular focus on the aquatic environment.

Keywords Chemical analysis · Mass spectrometry · Search for unknowns · Environmental chemistry · Ecotoxicology · Risk assessment · –omics techniques

6.1 Evolution of Environmental Analytical Tools

Early environmental analytical chemistry monitored a limited number of anthropogenic target chemicals in various natural compartments (e.g. water, sediment, organisms) and technical or anthropogenic systems (wastewater treatment plants, drinking water production, urban runoff) in order to determine their fate and behavior. This knowledge formed the basis for assessing risks of single chemicals or chemical classes. Classical cases drawing attention to the importance of chemical monitoring in the environment include the ubiquitous contamination by e.g. polychlorinated

K. J. Groh
Food Packaging Forum Foundation, Zürich, Switzerland

M. F.-J. Suter (✉)
Eawag, Swiss Federal Institute of Aquatic Science and Technology, Dübendorf, Switzerland

ETH Zürich, Department of Environmental Systems Science, Zürich, Switzerland
e-mail: marc.suter@eawag.ch

dibenzodioxins (PCDDs) or polychlorinated biphenyls (PCBs). The former, often produced as side products of some chemical synthesis reactions carried out at high temperatures, have received wide attention particularly after the Seveso incident [1]. PCBs, before being banned, were used in many industrial products [2]. Persistence properties and long-range transport phenomena led to worldwide distribution of such compounds and culminated in their accumulation even in remote Arctic and Antarctic environments [3, 4]. As a consequence, both compound classes have been included in the Stockholm convention on persistent organic pollutants [5]. The chemical complexity of samples containing PCDDs (75 congeners) and polychlorinated dibenzofurans (PCDFs, 135 congeners) in the presence of PCBs (209 congeners) requires high resolution analysis, which in the 1970s boosted the sales of double-focusing sector field mass spectrometers, the only instruments capable of resolving powers above 20,000 at that time [6, 7].

One major limitation in chemical analysis until the 1990s was that only volatile or thermally stable target substances could be analyzed by mass spectrometry. This is because the ionization method of choice then was electron ionization (EI) or chemical ionization (CI), and sample introduction was usually performed through gas chromatography (GC), with a temperature gradient up to 300 °C. This setup limited the analytical window to mostly small and non-polar chemicals, typically below 500 Da. Consequently, all larger, thermally labile, or polar chemicals, including many pharmaceuticals, personal care products and pesticides, could not be analyzed and no standard MS methods were available for their monitoring. Hence, regulation was not possible at the time.

Only in the 1990s, with the advent of electrospray ionization (ESI) and matrix-assisted laser desorption ionization (MALDI), polar and ionic target analytes also became amenable to MS analysis. Additionally, the measured mass range could be extended by orders of magnitude, because ESI easily produces multiply charged molecules and mass spectrometers measure m/z. For instance bovine serum albumin, a protein of mass 66 kDa, could now be detected with a quadrupole MS having a mass range of up to 2000 Da, provided it was carrying 100 protons, giving a signal at m/z of 660. This new capacity provided by ESI made it possible to analyze biological macromolecules such as enzymes, allowing to investigate stress response and evolutionary adaptation of organisms on the molecular level [8–10].

Figure 6.1 illustrates the fields of application of gas chromatography (GC)-MS and liquid chromatography (LC)-MS in a biased personal representation. Of course, derivatization allows the polar part to be partially addressed with GC-MS as well [11].

6.1.1 Analyzing the "Universe of Chemicals"

With improved sample preparation and increasing sensitivity, it has now become possible to analyze very complex samples for emerging, potentially unknown, contaminants and their transformation products, present at very low concentrations. This allows understanding patterns of low dose, chronic and pulse exposure, which could be further linked with resulting toxicity and thus help explain the different effects manifesting in the exposed organisms in each case.
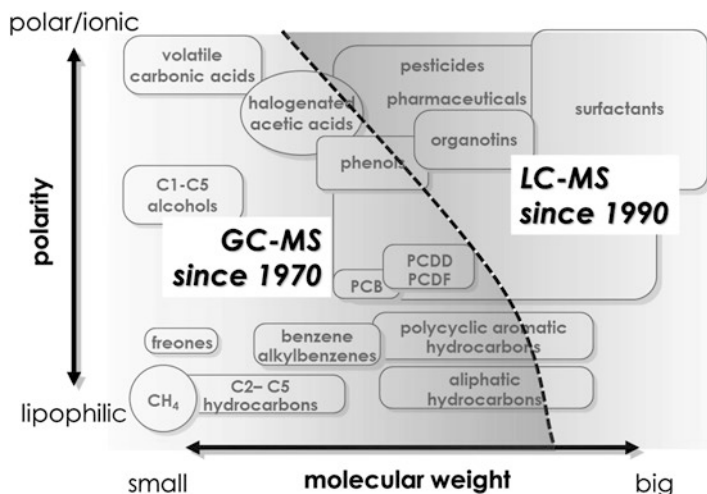
Fig. 6.1 The "Universe of Chemicals" as seen through the eyes of an environmental scientist (authors' biased personal representation). The lower left part of the diagram can be analyzed using GC-MS, while the polar and ionic high molecular weight compounds, including biologically relevant macromolecules, have only become accessible with soft desorption ionization techniques such as electrospray, typically used in LC-MS. (Reprinted with permission from Springer Nature)

However, the "Universe of Chemicals" as of July 2019 comprises over 155 million unique organic and inorganic substances as listed in the Chemical Abstracts Service (CAS – an operating division of the American Chemical Society), of which only roughly 350,000 are inventoried/regulated (see http://www.cas.org). Of course not all of these will be reaching the environment and cause adverse effects. But even so, if only a small fraction of the 350,000 inventoried substances pose a threat, monitoring them all is very likely beyond what is routinely feasible for regulatory agencies or enforcement bodies.

To further complicate the matters, these chemicals cover a wide range of physico-chemical properties, from volatile to non-volatile, from apolar with log Kow > 5, to polar and ionic. The latter group, when targeted for LC-MS analysis, comprises the so-called gap chemicals that are positively or negatively charged under natural conditions (pH 7.4). Their interaction with other charged chemicals present in the matrix will influence their speciation, and with that sorption to particles and sediments, and uptake into organisms [12, 13]. The reason why they are called gap chemicals is that classical analytical pipelines, designed with non-polar compounds in mind, will typically lose most of the polar substances in the enrichment step, particularly if reversed-phase C18 material is used. Therefore, to simultaneously capture the multitude of the "chemical universe" or "close the gap", mixed-mode enrichment [14, 15] and separation [16] methods, combining ion exchange and reversed phase, are required (Fig. 6.2).

The chemicals listed with log D_{ow} < 1 would not be captured using a C18 solid phase. However, many of these chemicals are of high environmental concern and
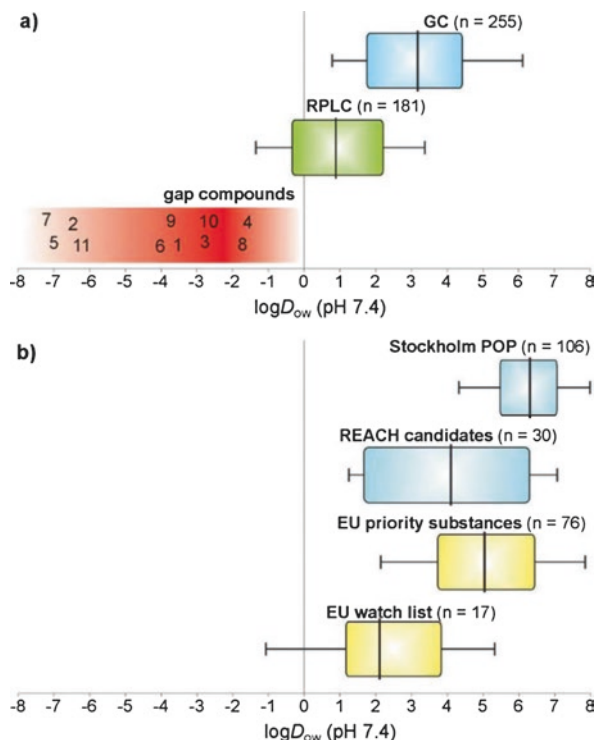
Fig. 6.2 Box and whisker plots of calculated $\log D_{OW}$ values at pH 7.4 of: (**a**) contaminants in water analyzed by either GC-MS or LC-MS (using reversed-phase column, RPLC), and examples of "gap" compounds; (**b**) contaminants regulated by the Stockholm Convention (Stockholm POP, persistent organic pollutants), Substances of Very High Concern (SVHCs) identified within EU legislation on Registration, Evaluation, Authorization and restriction of CHemicals (REACH), the list of EU priority substances according to the Water Framework Directive (WFD) and the so-called EU watch list of the WFD
Numbers in (a) refer to 1: Aminomethyl-phosphonic acid (AMPA; CAS 1066-51-9), 2: Paraquat (CAS 4685-14-7), 3: Cyanuric acid (CAS 108-80-5), 4: N,N-dimethylsulfamide (DMS; CAS 3984-14-3), 5: Diquat (CAS 85-00-7), 6: 5-Fuorouracil (CAS 51-21-8), 7: Glyphosate (CAS 1071-83-6), 8: Melamine (CAS 108-78-1), 9: Metformin (CAS 657-24-9), 10: Perfluoroacetic acid (CAS 76-05-1), 11: Ethylenediaminetetraacetic acid (EDTA; 60-00-4) [12]. (Reprinted with permission from Ref. [12]. Copyright (2016) American Chemical Society)

include, among others, the controversial herbicide glyphosate, which is a suspected carcinogen, and its microbial degradation product AMPA of likely similar toxicity, along with the herbicides paraquat (banned in the EU since 2007) and diquat, as well as the metal-chelating EDTA which has the potential to remobilize heavy metals.

After enrichment of an environmental sample, separation of the complex mixture is either done with GC for volatile and apolar compounds, or LC for polar and ionic substances (Fig. 6.3). In both cases, separation is accomplished based on partitioning between the eluent (gas for GC and liquid for LC) and the solid phase (e.g.
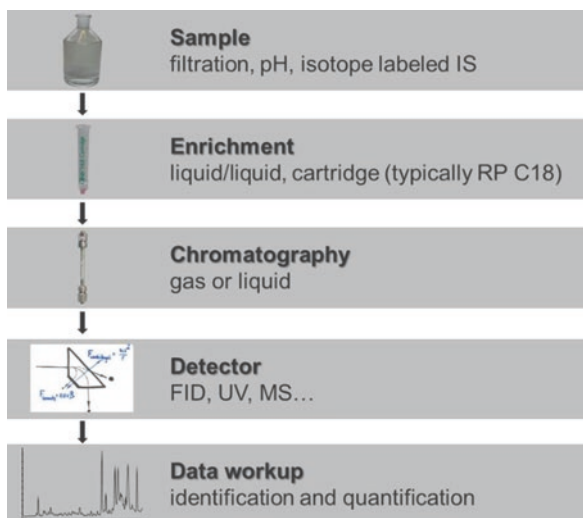
Fig. 6.3 Chemical analysis pipeline for environmental samples. In short, a typical analytical pipe-
line consists of several raw sample preparation steps, followed by enrichment (taking care to enrich
all compounds of interest), separation (realized by GC or LC), and ionization steps, concluded by
mass spectral analysis (MS and/or MS/MS). The subsequent data analysis generally comprises
matching of experimental spectra with those stored in a suitable spectral library. Abbreviations: *IS*
internal standard, *RP* reverse-phase, *FID* flame ionization detector, *UV* ultraviolet, *MS* mass
spectrometry

Table 6.1 Comparison of electron (EI) and electrospray ionization (ESI)

Advantages/disadvantages	
EI	ESI
+ Reproducible spectra (intensity, fragments)	− Ion suppression, lower reproducibility
− Signal spread over all fragments (low sensitivity)	+ Soft ionization (few peaks, high sensitivity)
+ Structural information	− Structural information only with MS/MS
	+ Increased mass range
	± Adduct ions (H^+, NH_4^+, Na^+, K^+…)
− Limited compound range (with regard to polarity, volatility, thermal stability)	+ Extended compound range (thermolabile, polar and ionized targets measurable)
+ Large spectral libraries available	± MS/MS libraries now becoming available
− Negative ions only with reactant gas	+ Easy switching between positive and negative mode

siloxane copolymers for GC and mixed mode for LC), with choice of method
depending on the specific application.

Identification and quantification then is performed using mass spectrometers,
fitted with an EI or CI source for volatiles and GC coupling, or an ESI source for
polar and ionic substances and coupling to high performance LC (HPLC). The
major analytical features of EI- and ESI-based analysis are summarized in Table 6.1.

One major advantage of EI generated spectra is their reproducibility. The fact that EI at 70 eV transfers more energy than needed for ionizing a molecule, leads to energy-release through fragmentation. The fragments generated inform about the structure of the molecule, which is ideal for subsequent library searches. Today very large curated commercial libraries are available, facilitating non-target analysis. The downside of fragmentation-based analysis is that the signal of a given analyte will be spread over all fragments, leading to a substantial reduction in the absolute intensity. Therefore, if sensitivity is the ultimate goal, CI, which produces protonated molecular ions in a gas phase reaction, can be used instead. ESI is used for coupling with LC. This is a soft ionization technique that desorbs protonated or deprotonated ions from the liquid phase into the gas phase, in the process producing few fragments if at all, but high intensity molecular ions instead. It accommodates thermolabile, polar and ionized compounds and, since mass spectrometers measure m/z, allows determining very big molecules that carry multiple charges. Depending on the instrument, positive/negative switching can be done within one run, facilitating for instance the analysis of a metabolome. Identification and structural information is only available through additional MS/MS scans. The spectra generated can then be matched against libraries that now become publicly available. Unlike in EI, ion formation is a competitive acid-base reaction and hence depends on the matrix surrounding the analyte, which can lead to ion suppression.

The most common mass spectrometers are either triple quadrupoles, typically used for high sensitivity using multiple reaction monitoring (MRM), or highly accurate mass spectrometers such as orbitraps, Fourier-transform ion cyclotron resonance (FT-ICR) or time-of-flight (TOF) instruments, which provide high resolving power. Today's state-of-the-art mass spectrometers routinely reach >100,000 resolving power, and with that unsurpassed capabilities to detect unknown contaminants in a high-throughput format either using data-dependent or data-independent MS/MS approaches.

6.1.2   Effect-Directed Analysis (EDA)

Both environmental chemists and toxicologists intending to contribute to ecotoxicological risk assessment are concerned with the question of how best to identify the chemicals present in a very complex mixture that cause adverse effects in an ecosystem. One approach is to develop a hypothesis of how this effect is caused and then focus on the chemicals known to be linked to it, an approach called *targeted analysis*.

Another popular strategy, called effect-directed analysis (EDA) [17], works by linking chemical analysis with a biological readout, which could be anything from a response in a reporter gene assay to mortality observed in a toxicity test with a model organism [18]. In this approach, chemical analysis focuses only on samples or fractions that actually are causing an effect. This allows greatly reducing the number of samples that need to be chemically analyzed. In the ideal case the measured activity can be explained by the chemicals found to be present in the sample.

One popular reporter gene assay in the field of endocrine disruption is the yeast estrogen screen (YES), which is used to determine estrogenicity of a sample [19]. This assay detects estrogenic compounds binding to the estrogen receptor; this binding activates a reporter gene, resulting in a synthesis of an enzyme which in turn then transforms its substrate into a quantifiable colored product. In a Swiss survey of rivers, estrogenicity determined in the YES was shown to correlate with estradiol equivalents calculated based on determined concentrations and relative potencies of 17ß-estrogen, estrone and 17α-ethinlyestradiol, both in grab samples and extracts from passive samplers [20]. In another study, the glucocorticoid activity [CHEM]DEQ, calculated based on chemical data and potencies relative to dexamethasone (dex equivalents DEQ) measured in an *in vitro* assay (GR-CALUX®, Fig. 6.4), was always just slightly higher than the measured [BIO]DEQ [21]. This is an indication that the entire activity could be explained by the glucocorticoids found in the sample. The only exception was the treated effluent from Switzerland (CH2ef), where the chemical data from targeted analysis could not explain the measured activity (framed data points in Fig. 6.4). This can be interpreted as an indication that glucocorticoid-like compounds were present in the sample, but not detected by the targeted analysis. Additional experiments are required to identify the unknown compound(s).

The EDA is relatively straightforward when established targeted analysis can be used to measure the presumable causative chemicals, as in the cases mentioned
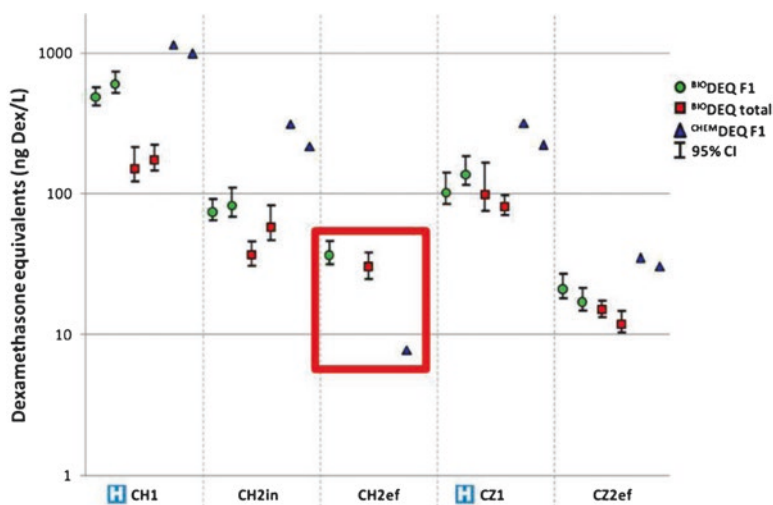
Fig. 6.4 Predicted ([CHEM]DEQ) and measured GR-CALUX® response ([BIO]DEQ), in untreated and treated wastewater samples (ng Dex/L), sampled in Switzerland (CH) or the Czech Republic (CZ) from hospital wastewater (CH1, CZ1), wastewater treatment plant influent (CH2in) or effluents (CH2ef, CZ2ef) [21]. *F1* corresponds to the slightly acidic fraction eluting from the solid phase, *total* corresponds to the merged fractions *F1-F4*, with *F2* the slightly basic, *F3* the medium polar and *F4* the lipophilic fraction. (Reprinted (adapted) with permission from Ref. [21]. Copyright (2014) American Chemical Society)

above. However, the investigation becomes much more challenging as soon as targeted analysis returns a blank and the identity of the effect-causing chemical remains unknown [22]. This then calls for a differential non-targeted analysis, which will be demonstrated using the following case study.

Around the year 2000, fishermen on Lake Thun in the Bernese Oberland, Switzerland, found that cleaning out their fish was more difficult than in previous years. This was partially caused by adhesions/fusions of the gonads to the peritoneal wall and the musculature. When the white fish (*Coregonus lavaretus*) were analyzed by veterinarians, they found additional deviations of gonadal morphology, such as asymmetry of the gonad strands, atrophy and aplasia, compartmentations, hermaphroditism and intersex [23].

Potential causes considered for this effect were biological, such as genetic factors or infectious diseases (contracted in the lake or local hatcheries), or related to environmental conditions (temperature, habitat quality, food availability or water quality). However, the intersex features observed could also have developed as a result of interactions of chemicals with the endocrine system. Therefore, sediments, lake water, muscle tissue and bile were extracted and analyzed chemically and with *in vitro* assays according to the EDA approach. The analysis of muscle (long-time storage) and bile (short-time storage) from white fish (*Corregonus lavaratus)* in Lake Thun showed that the estrogenicity determined in the YES could fully be explained by the natural estrogens estradiol (E2) and estrone (E1) [26]. Water samples taken from the lake returned blank values, but algae gave a positive response in both the YES and the additional assay used, the E-screen (Fig. 6.5). The latter is a more integrative test based on estrogen-dependent proliferation of human breast cancer cells [25]. Clearly, although the readout from these two assays differed, the sample BRI08/05 gave a consistent positive response in both, indicating that this plankton sample contains estrogens. Hence, when comparing this sample to any sample that is not estrogenic, features found in the estrogenic but absent in non-estrogenic samples could potentially be the active compound. The goal then was to identify all chemicals present in the samples and compare their relative abundance.
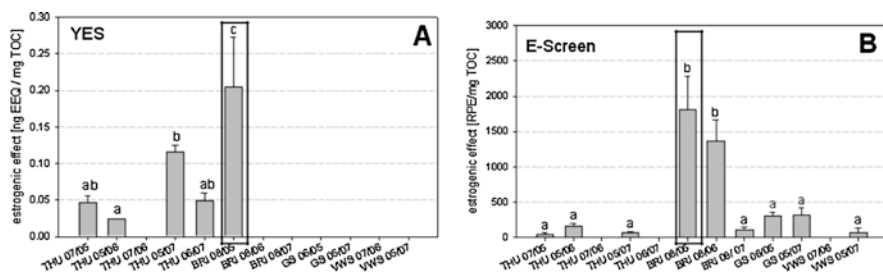
Fig. 6.5 Estrogenic activity determined in plankton extracts collected over 3 years (2005–2007) from four different lakes in Switzerland: Lakes Thun (THU), Brienz (BRI), Greifen (GS) and Lucerne (VWS) [24]. The samples were analyzed using the YES and the E-Screen assays [25]. (Reprinted with permission from Springer Nature)

Today, such screening of unknowns is done using data-dependent analysis [27, 28]. This technique, routinely used in global proteomics as well [29], produces fragment ion spectra of as many chemicals as possible that elute off the column at a given moment. The information thus obtained includes (i) retention time, related to the substance's partitioning into the solid phase of the separation column, (ii) accurate mass of the compound, (iii) the relative intensities of its isotopes and (iv) structural information through its fragments [30]. A differential analysis, e.g. using Compound Discoverer (ThermoFischer Scientific Inc., San Jose, CA, USA), then compares compounds that are present at significantly different concentrations in the active relative to an inactive sample and assignes statistical significance to the differences observed. Filtering for fold-change and *p*-value produces a list of features that could potentially be responsible for the endocrine activity detected in the sample. In the case of the Lake Thun algal extracts we found a compound that was present at very high concentration in the estrogenic sample with a mass of 180.1020 Da. The first step in identifying this unknown feature is to assign a sum formula. The Fiehn group has established rules that allow to narrow down the sum formula of a given feature, based on its accurate mass and isotopes [31]. They mined public mass spectral databases (Natural Products Data Base, Wiley) and determined the ratios of elements to carbon (elements: H, F, Cl, Br, N, O, P, S, Si) for all entries and thus likely ranges for unknown sum formulas (covering 99.7% of the entries). Of course the nitrogen rule from classical EI spectral interpretation also holds, only that in positive ESI, even ions carry an additional proton, thus they have an uneven number of nitrogens, while odd ions have zero or even numbers of nitrogens. With a 3 ppm mass accuracy, easily obtained on current state-of-the-art MS, 64 candidate sum formulas match a mass of 500 Da [31]. If the isotopic abundance is taken into account (5%), the number of candidates is reduced to 3 only. Using the rules mentioned above, we determined the sum formula to be $C_{10}H_{14}O_2N$, with a mass difference of 0.526 ppm, well within the accuracy obtainable on an Orbitrap. All elemental ratios were within the range defined by Kind and Fiehn. The double bond and ring equivalents (DBE) were determined to be 4.5, i.e. non-integer, which indicated that this ion contains an even number of electrons (M + H$^+$) and that it could be a phenolic compound (1 ring plus 3 double bonds), similar to the most important estrogenic compounds (estrone, estriol, estradiol, ethinylestradiol, nonylphenol and bisphenol A). The next best candidate ($C_6H_{17}O_2N_2P$) had a DBE of only 0.0 with a large mass difference of −1.198 ppm, and hence could be discarded.

The MS/MS spectrum, which had been acquired in a data-dependent way, showed two main fragments at m/z 138 and 121. A likely candidate that, according to the fragmentation software Mass Frontier (ThermoFischer Scientific Inc., San Jose, CA, USA), would produce these fragments, was found to be N-acetyltyramine (CAS 1202-66-0). This molecule was then synthesized and analyzed by MS. The fragments could be experimentally verified, but a test for estrogenicity in the YES returned a negative response, suggesting that N-acetyltyramine could not be the compound responsible for the estrogenic response observed in the positive sample (Fig. 6.6).
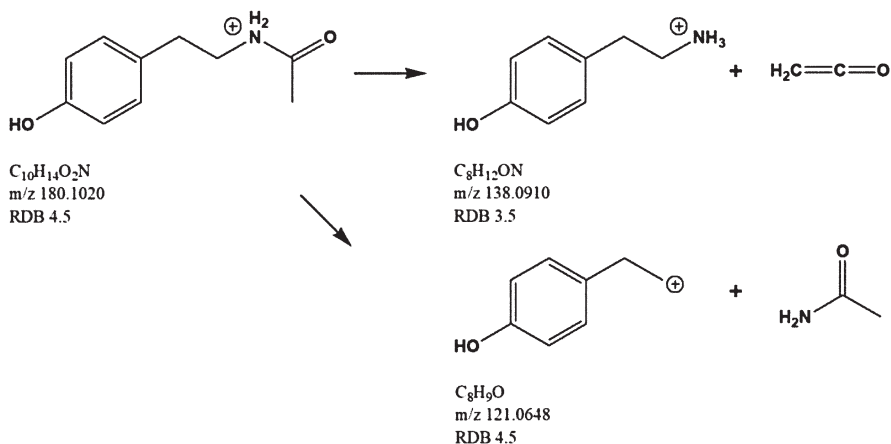
Fig. 6.6 Acetyltyramine (synthesized in house) and its predicted fragments [25]

Thus, even though the sum formula of the compound responsible for the estrogenic activity found in the plankton extract from Lake Brienz could unequivocally be determined, the correct structure remains unknown. Overall, the case study presented here nicely shows both the power and the limitations of the EDA for the discovery of unknown chemicals potentially causing adverse effects in the environment.

6.2 Mass Spectrometry for Characterizing Interactions of Chemicals with Organisms

The meaningful application of EDA in ecotoxicology relies on the availability of versatile bioassays that measure biological responses relevant to the organisms and ecosystems in focus [18]. Further, to be able to link to the apical endpoints of regulatory significance, the detected *in vitro* activity should ideally be mapped onto a particular toxicity pathway according to the adverse outcome pathways (AOP) concept [32]. The improved water status, at least in the developed countries, means that the aquatic inhabitants are now rarely if at all challenged by acute toxicity. What became much more relevant is chronic exposure to a cocktail of contaminants present at sublethal concentrations [33], whose effects might be missed by classical bioassays focused on measuring mortality. Evaluating subtle effects of chronic exposures to low concentrations requires novel bioassays that cover diverse toxicity pathways leading to relevant sublethal effects, particularly those that could negatively affect organism fitness [34]. Further needed is a better understanding of effects and mechanisms of toxicity, with a goal of ultimately being able to predict how a chemical or a chemical mixture affects an organism [35, 36].

Interactions between chemicals and living organisms are governed by toxicokinetic and toxicodynamic processes [37], and contemporary studies in both fields rely heavily on mass spectrometry [38]. Toxicokinetics describes uptake, biotransformation, distribution, and excretion of a chemical by an organism, also referred to as absorption, distribution, metabolism, and excretion (ADME) processes [39, 40]. Toxicodynamics looks at the actions of a chemical or its metabolite, carried out at the target sites where toxicity becomes manifested [32]. Such actions could include, for example, DNA adduct formation [41], oxidation of membrane lipids [9], or binding to a nuclear receptor, which in turn could trigger gene or protein expression changes and metabolite alterations [8, 40, 42–44].

Information on effective internal organismal or tissue concentrations of chemicals and their transformation products is important for toxicokinetic modeling [39] and can be obtained with the same approaches as applied to environmental compartments [14, 16, 44]. Taking samples at different time points, performing depuration experiments, or carrying out non-targeted or targeted metabolite screening allows constructing time-resolved profiles of chemical uptake, biotransformation, and excretion [39, 40, 45, 46]. MS has also been instrumental in obtaining information that sheds light on the internal distribution of chemicals. This can be done by measuring chemical contents in the dissected body parts or by using MALDI imaging to decipher chemical location on tissue sections, e.g. from zebrafish larvae [39, 46]. For example, a study of the internal distribution of cocaine in zebrafish larvae showed that cocaine was not only located at the target site, the brain, but also in the melanin-containing eye of the larvae [39], providing a better understanding of the differences in responses to psychoactive drugs observed in mammals and zebrafish larvae [46].

With regard to toxicodynamics, MS can provide data on gene expression and cellular signaling cascades, for example through looking at proteins (proteomics) and metabolites (metabolomics) [47]. The universal nature of cellular (macro)molecules and metabolites allows applying similar methods when studying organisms across the whole animal kingdom, from microorganisms [9, 43, 48] to mussels [8] to fish [29, 49–51] and other organisms [16, 38, 52].

Figure 6.7 shows that mRNA levels (studied by transcriptomics) are fast reacting and hence reflect the organism's response to the immediate challenge by a specific stressor. Changes in the proteins often reflect the more downstream changes, which could be delayed in time and are often observed to converge in a general stress response [54]. The metabolome is often as fast reacting as the transcriptome and thus can be seen as a fingerprint of the state of a cell, tissue or organism at a given moment [55, 56]. The study of metabolomics is rapidly establishing itself in ecotoxicological research [52], also because its analytical pipelines are often similar to untargeted environmental chemical analysis [16, 57].

Both global (data-dependent acquisition) and targeted (MRM) techniques can be used to investigate the proteome and metabolome. Multidimensional Protein Identification Technology (MudPIT), also referred to as global proteomics, allows the simultaneous characterization of several thousands of proteins as well as their alterations in response to toxicants [10]. This can be done for well-studied model
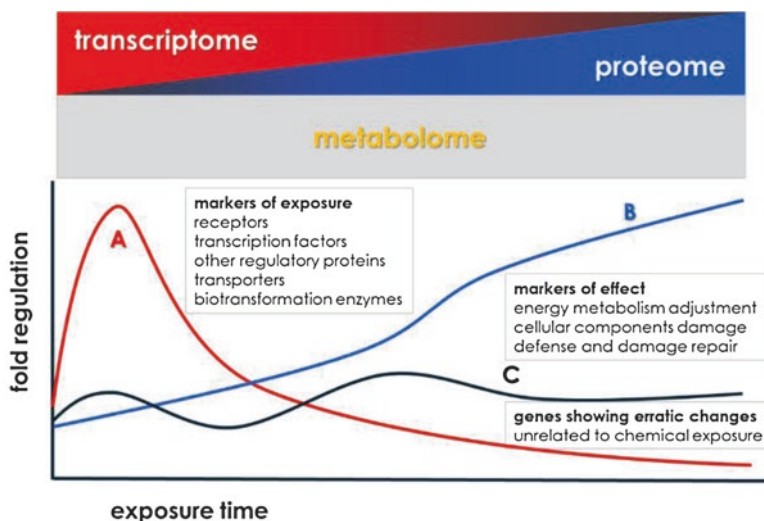
Fig. 6.7 Applicability of transcriptomics, proteomics and metabolomics for studying chemical effects on gene expression (schematic representation of gene expression trajectories adapted from Van Straalen and Feder [53])
(**a**) represents early stress-response genes, mostly indicative of exposure, (**b**) shows the late expressed genes, more informative of the effect than the nature of the chemical, and (**c**) shows genes with erratic changes with time, unrelated to chemical exposure. (Reprinted (adapted) with permission from Springer **Nature)**

organisms such as zebrafish (*Danio rerio*) or green alga (*Chlamydomonas rein-hardtii*) [9, 29, 43, 50], but also in field-relevant species such as mussels (*Mytilus galloprovincialis*) [8] or frogs (*Rana* sp.) [58]. Low sensitivity constitutes an important limitation of global proteomics, because this can hinder detection of crucial regulatory proteins, such as receptors or transcription factors, which are often present at low copy numbers. To maximize sensitivity, targeted proteomics should be used; this technique is also applied for hypothesis-driven analysis, when proteins to be studied are selected in advance [49, 51]. For instance, investigation of the ontogeny of the phase II metabolizing glutathione S-transferase (GST) enzyme family in developing zebrafish embryos demonstrated that some enzymes are maternally-transferred, some are synthesized right from the beginning of development and some appear only later, when the liver becomes functional (see Fig. 6.8) [51].

One subfield of toxicology which has received a lot of attention in recent years is nanotoxicology. Research focused on elucidation of fate and effects of nanoparticles in humans and the environment would not have been possible without the MS advances in place [59]. Inductively coupled plasma MS (ICP-MS) has been routinely applied to study metal-based nanoparticles, with dedicated separation methods such as ultrafiltration used to distinguish between ionic and nanoparticulate forms [60, 61].
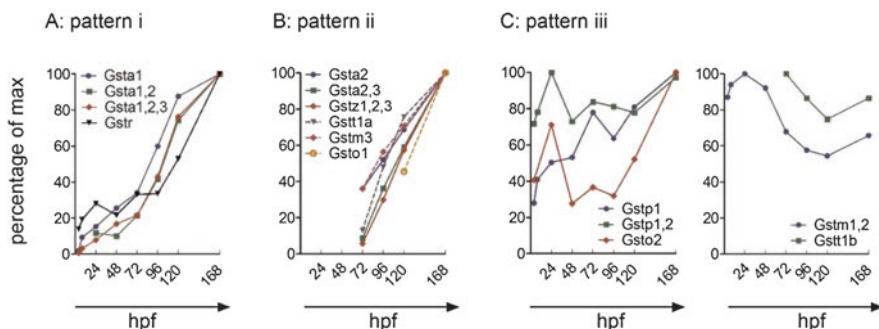
Fig. 6.8 Glutathione S-transferase (GST) expression patterns observed during zebrafish early development
(**a**) Early detection followed by continuous increase throughout the development (pattern i). (**b**) First occurrence after **72** h post fertilization (hpf), followed by an increase (pattern ii). (**c**) Variable trend with no consistent changes throughout the development (pattern iii). Median of the normalized peak area is shown as percentage of the maximal value. (Reprinted from Ref. [**51**] with permission from Oxford University Press on behalf of the Society of Tox**icology)**

The accumulation and translocation of titanium dioxide nanoparticles across placental barrier was studied in an *in vitro* model of placental transfer. Although translocation was negligible, a significant placental accumulation was observed, suggesting the need for further research to understand the nanoparticles' effects on the functionality and signaling in the placenta [62]. An important phenomenon governing the effects of nanoparticles in the cells entails the formation of nanoparticle-protein corona, which occurs when nanoparticles come in contact with biota. For example, silver nanoparticles were shown to bind to and inhibit the activity of a bacterial enzyme tryptophanase [63].

An MS-based study of corona proteins recovered from a rainbow trout gill cell line exposed to silver nanoparticles revealed several types of proteins that could be affected by nanoparticles through corona formation mechanisms, including proteins involved in endocytosis, transport, and storage, general stress response proteins, and proteins involved in ionic regulation [64].

6.3   Conclusions

In conclusion, MS plays an important role in both environmental chemistry and toxicology. MS-based techniques are used to (i) measure chemicals in environmental compartments and biota, (ii) identify unknown chemicals potentially causing adverse effects in the environment, which can be done using EDA and (iii) provide insights into the internal toxicokinetic processes and molecular mechanisms of toxicity, thus helping to elucidate AOPs leading to apical effects of interest. Thus, MS

has become essential in both fundamental and applied research in ecotoxicology, supporting risk assessment and management of chemicals.

References

1. Bertazzi PA et al (1998) The Seveso studies on early and long-term effects of dioxin exposure: a review. Environ Health Perspect 106(suppl 2):625–633
2. Beyer A, Biziuk M (2009) Environmental fate and global distribution of polychlorinated biphenyls. In: Whitacre DM (ed) Reviews of environmental contamination and toxicology, vol 201. Springer US, Boston, pp 137–158
3. Fensterheim RJ (1993) Documenting temporal trends of polychlorinated biphenyls in the environment. Regul Toxicol Pharmacol 18(2):181–201
4. Muir DCG, Norstrom RJ (2000) Geographical differences and time trends of persistent organic pollutants in the Arctic. Toxicol Lett 112-113:93–101
5. Porta M, Zumeta E (2002) Implementing the Stockholm treaty on persistent organic pollutants. Occup Environ Med 59(10):651–652
6. Cairns T, Siegmund EG (1981) PCBs. Regulatory history and analytical problems. Anal Chem 53(11):1183A–1193A
7. Djien Liem AK, Furst P, Rappe C (2000) Exposure of populations to dioxins and related compounds. Food Addit Contam 17(4):241–259
8. Oliveira IB et al (2016) Tralopyril bioconcentration and effects on the gill proteome of the Mediterranean mussel Mytilus galloprovincialis. Aquat Toxicol 177:198–210
9. Pillai S et al (2014) Linking toxicity and adaptive responses across the transcriptome, proteome, and phenotype of Chlamydomonas reinhardtii exposed to silver. Proc Natl Acad Sci U S A 111(9):3490–3495
10. Tamminen M et al (2018) Proteome evolution under non-substitutable resource limitation. Nat Commun 9(1):4650
11. Aerni H-R et al (2004) Combined biological and chemical assessment of estrogenic activities in wastewater treatment plant effluents. Anal Bioanal Chem 378(3):688–696
12. Reemtsma T et al (2016) Mind the gap: persistent and mobile organic compounds—water contaminants that slip through. Environ Sci Technol 50(19):10308–10315
13. Schwarzenbach RP et al (2006) The challenge of micropollutants in aquatic systems. Science 313(5790):1072–1077
14. Ammann AA et al (2014) LC-MS/MS determination of potential endocrine disruptors of cortico signalling in rivers and wastewaters. Anal Bioanal Chem 406(29):7653–7665
15. Kern S et al (2010) A tiered procedure for assessing the formation of biotransformation products of pharmaceuticals and biocides during activated sludge treatment. J Environ Monit 12(11):2100–2111
16. Ammann AA, Suter MJ-F (2016) Multimode gradient high performance liquid chromatography mass spectrometry method applicable to metabolomics and environmental monitoring. J Chromatogr A 1456:145–151
17. Brack W (2003) Effect-directed analysis: a promising tool for the identification of organic toxicants in complex mixtures? Anal Bioanal Chem 377(3):397–407
18. Sonavane M et al (2018) An integrative approach combining passive sampling, bioassays, and effect-directed analysis to assess the impact of wastewater effluent. Environ Toxicol Chem 37(8):2079–2088
19. Routledge EJ, Sumpter JP (1996) Estrogenic activity of surfactants and some of their degradation products assessed using a recombinant yeast screen. Environ Toxicol Chem 15(3):241–248

20. Vermeirssen ELM et al (2005) Characterization of environmental estrogens in river water using a three pronged approach: active and passive water sampling and the analysis of accumulated estrogens in the bile of caged fish. Environ Sci Technol 39(21):8191–8198
21. Macikova P et al (2014) Endocrine disrupting compounds affecting corticosteroid Signaling pathways in Czech and Swiss waters: potential impact on fish. Environ Sci Technol 48(21):12902–12911
22. Tousova Z et al (2017) European demonstration program on the effect-based and chemical identification and monitoring of organic pollutants in European surface waters. Sci Total Environ 601:1849–1868
23. Bernet D et al (2004) Frequent and unexplained gonadal abnormalities in whitefish (central alpine Coregonus sp.) from an alpine oligotrophic lake in Switzerland. Dis Aquat Org 61(1–2):137–148
24. Liedtke A et al (2009) Unpublished results
25. Soto AM et al (1995) The E-SCREEN assay as a tool to identify estrogens: an update on estrogenic environmental pollutants. Environ Health Perspect 103(suppl 7):113–122
26. Liedtke A et al (2009) Internal exposure of whitefish (Coregonus lavaretus) to estrogens. Aquat Toxicol 93(2):158–165
27. Schymanski EL et al (2014) Strategies to characterize polar organic contamination in wastewater: exploring the capability of high resolution mass spectrometry. Environ Sci Technol 48(3):1811–1818
28. Singer HP et al (2016) Rapid screening for exposure to "non-target" pharmaceuticals from wastewater effluents by combining HRMS-based suspect screening and exposure modeling. Environ Sci Technol 50(13):6698–6707
29. Groh KJ et al (2011) Global proteomics analysis of testis and ovary in adult zebrafish (Danio rerio). Fish Physiol Biochem 37(3):619–647
30. Nesatyy VJ, Suter MJ-F (2008) Analysis of environmental stress response on the proteome level. Mass Spectrom Rev 27(6):556–574
31. Kind T, Fiehn O (2007) Seven Golden rules for heuristic filtering of molecular formulas obtained by accurate mass spectrometry. BMC Bioinf 8:105–105
32. Groh KJ et al (2015) Development and application of the adverse outcome pathway framework for understanding and predicting chronic toxicity: I. Challenges and research needs in ecotoxicology. Chemosphere 120:764–777
33. Eggen RIL, Suter MJ-F (2007) Analytical chemistry and ecotoxicology—tasks, needs and trends. J Toxic Environ Health A 70(9):724–726
34. Groh KJ et al (2015) Development and application of the adverse outcome pathway framework for understanding and predicting chronic toxicity: II. A focus on growth impairment in fish. Chemosphere 120:778–792
35. Groh KJ, Tollefsen KE (2015) The challenge: adverse outcome pathways in research and regulation—current status and future perspectives. Environ Toxicol Chem 34(9):1935–1937
36. Van den Brink PJ et al (2018) Toward sustainable environmental quality: priority research questions for Europe. Environ Toxicol Chem 37(9):2281–2295
37. Ashauer R et al (2011) Toxicokinetic-toxicodynamic modeling of quantal and graded sublethal endpoints: a brief discussion of concepts. Environ Toxicol Chem 30(11):2519–2524
38. Groh KJ, Suter MJ-F (2014) Mass spectrometry in environmental toxicology. CHIMIA Int J Chem 68(3):140–145
39. Kirla KT et al (2016) From the cover: zebrafish larvae are insensitive to stimulation by cocaine: importance of exposure route and toxicokinetics. Toxicol Sci 154(1):183–193
40. Mottaz H et al (2017) Dose-dependent effects of morphine on lipopolysaccharide (LPS)-induced inflammation, and involvement of multixenobiotic resistance (MXR) transporters in LPS efflux in teleost fish. Environ Pollut 221:105–115
41. Madureira DJ et al (2014) Systems toxicology approach to understand the kinetics of Benzo(a)pyrene uptake, biotransformation, and DNA adduct formation in a liver cell model. Chem Res Toxicol 27(3):443–453

42. Nestler H et al (2012) Multiple-endpoint assay provides a detailed mechanistic view of responses to herbicide exposure in Chlamydomonas reinhardtii. Aquat Toxicol 110-111:214–224
43. Nestler H et al (2012) Linking proteome responses with physiological and biochemical effects in herbicide-exposed Chlamydomonas reinhardtii. J Proteome 75(17):5370–5385
44. Hidasi AO et al (2017) Clobetasol propionate causes immunosuppression in zebrafish (Danio rerio) at environmentally relevant concentrations. Ecotoxicol Environ Saf 138:16–24
45. Di Paolo C et al (2015) Early life exposure to PCB126 results in delayed mortality and growth impairment in the zebrafish larvae. Aquat Toxicol 169:168–178
46. Kirla KT et al (2018) Importance of toxicokinetics to assess the utility of zebrafish larvae as model for psychoactive drug screening using meta-chlorophenylpiperazine (mCPP) as example. Front Pharmacol 9:414–414
47. Sturla SJ et al (2014) Systems toxicology: from basic research to risk assessment. Chem Res Toxicol 27(3):314–329
48. Groh KJ, Nesatyy VJ, Suter MJ-F (2011) Proteomics for the analysis of environmental stress responses in prokaryotes. In: de Bruijn FJ (ed) Handbook of molecular microbial ecology I: Metagenomics and complementary approaches. Wiley-Blackwell, pp 603–625
49. Groh KJ et al (2013) Analysis of protein expression in zebrafish during gonad differentiation by targeted proteomics. Gen Comp Endocrinol 193:210–220
50. Oliveira IB et al (2017) Toxicity of emerging antifouling biocides to non-target freshwater organisms from three trophic levels. Aquat Toxicol 191:164–174
51. Tierbach A et al (2018) Glutathione S-transferase protein expression in different life stages of zebrafish (Danio rerio). Toxicol Sci 162(2):702–712
52. Viant MR et al (2017) How close are we to complete annotation of metabolomes? Curr Opin Chem Biol 36:64–69
53. van Straalen NM, Feder ME (2012) Ecological and evolutionary functional genomics—how can it contribute to the risk assessment of chemicals? Environ Sci Technol 46(1):3–9
54. Groh KJ, Suter MJ-F (2015) Stressor-induced proteome alterations in zebrafish: a meta-analysis of response patterns. Aquat Toxicol 159:1–12
55. Tufi S et al (2016) Changes in neurotransmitter profiles during early zebrafish (Danio rerio) development and after pesticide exposure. Environ Sci Technol 50(6):3222–3230
56. Taylor NS, Gavin A, Viant MR (2018) Metabolomics discovers early-response metabolic biomarkers that can predict chronic reproductive fitness in individual Daphnia magna. Meta 8(3):42
57. Viant MR, Sommer U (2013) Mass spectrometry based environmental metabolomics: a primer and review. Metabolomics 9(1):144–158
58. Shu L, Suter MJ-F, Räsänen K (2015) Evolution of egg coats: linking molecular biology and ecology. Mol Ecol 24(16):4052–4073
59. Sigg L et al (2014) Chemical aspects of nanoparticle ecotoxicology. CHIMIA Int J Chem 68(11):806–811
60. Groh KJ et al (2015) Critical influence of chloride ions on silver ion-mediated acute toxicity of silver nanoparticles to zebrafish embryos. Nanotoxicology 9(1):81–91
61. Yue Y et al (2017) Interaction of silver nanoparticles with algae and fish cells: a side by side comparison. J Nanobiotechnol 15(1):16–16
62. Aengenheister L et al (2019) Investigating the accumulation and translocation of titanium dioxide nanoparticles with different surface modifications in static and dynamic human placental transfer models. Eur J Pharm Biopharm 142:488–497
63. Wigginton NS et al (2010) Binding of silver nanoparticles to bacterial proteins depends on surface modifications and inhibits enzymatic activity. Environ Sci Technol 44(6):2163–2168
64. Yue Y et al (2016) Silver nanoparticle–protein interactions in intact rainbow trout gill cells. Environ Sci Nano 3(5):1174–1185

Chapter 7
Matrix-Assisted Laser Desorption/Ionization Imaging Mass Spectrometry: Technology and Applications

Josiah C. McMillen, William J. Perry, Kavya Sharman, Katerina V. Djambazova, and Richard M. Caprioli

7.1 Introduction

Biological imaging modalities are commonly used for characterization of health and disease, but each have trade-offs in the areas of spatial resolution, molecular coverage and specificity, and targeted or untargeted approaches. Stained tissue microscopy allows high spatial resolution to visualize tissue morphologies and cellular structure but provides little molecular information. Immunohistochemistry allows high spatial resolution similar to that of organic stains with the benefit of specific molecular information with the use of antibodies. However, molecular targets must be known in advance and antibodies may select for multiple molecular species. Matrix-assisted laser desorption/ionization (MALDI) imaging mass spectrometry (IMS) allows for the untargeted detection of hundreds to thousands of

J. C. McMillen · W. J. Perry · K. V. Djambazova
Mass Spectrometry Research Center, Vanderbilt University, Nashville, TN, USA

Department of Chemistry, Vanderbilt University, Nashville, TN, USA
e-mail: josiah.c.mcmillen@vanderbilt.edu; william.j.perry@vanderbilt.edu;
katerina.v.djambazova@vanderbilt.edu

K. Sharman
Mass Spectrometry Research Center, Vanderbilt University, Nashville, TN, USA

Program in Chemical and Physical Biology, Vanderbilt University, Nashville, TN, USA
e-mail: kavya.sharman@vanderbilt.edu

R. M. Caprioli (✉)
Mass Spectrometry Research Center, Vanderbilt University, Nashville, TN, USA

Department of Chemistry, Vanderbilt University, Nashville, TN, USA

Department of Biochemistry, Vanderbilt University, Nashville, TN, USA

Departments of Pharmacology and Medicine, Vanderbilt University, Nashville, TN, USA
e-mail: r.caprioli@vanderbilt.edu

molecular species within a single experiment [1, 2]. Although it has somewhat lower spatial resolution than microscopy, IMS enables the detection of a wide range of biological species at increased molecular coverage with high spatial resolution and sensitivity using advanced data processing techniques. Herein, we present up-to-date examples of the current technologies of MALDI IMS.

7.2 Spatial Resolution Improvements in IMS

The spatial resolution of an IMS experiment determines the level of structural detail and differentiation among regions of a sample in the resulting ion images. Most commercial IMS instruments are limited to a spatial resolution (and sampling diameter) of about 10 μm as determined by the incident spot size of a focused laser beam on a sample. Laser focusing approaches to achieve smaller ablation diameter and stage pitch reduction are important instrumental considerations for high spatial resolution IMS. Recent advances in IMS instrumentation have allowed for spatial resolution at or below 1 μm [3]. As such, molecular information using IMS can be acquired that allows comparison with common staining techniques.

A tight laser focus for high spatial resolution IMS is achieved using objective lenses placed above a sample surface. However, high power objectives can interfere with transmission of ions to the mass analyzer (Fig. 7.1, frontside geometry). An ablation diameter below 5 μm is possible with special modifications of the laser
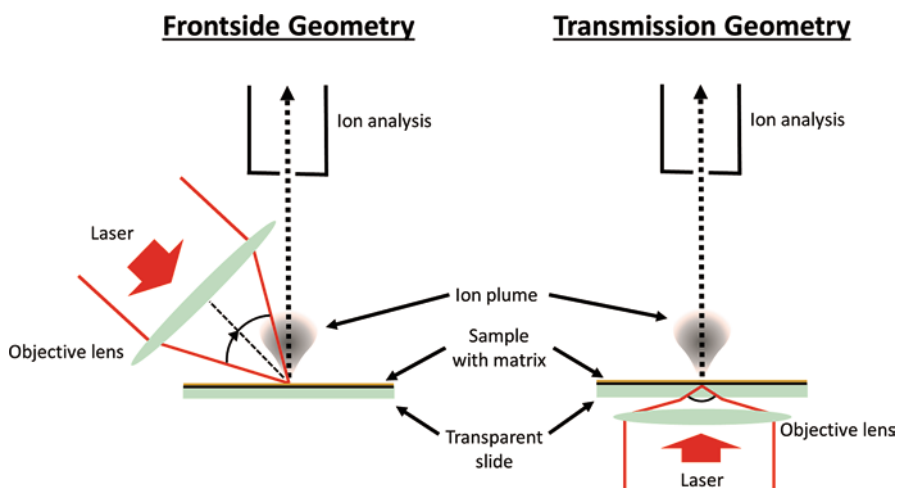
Fig. 7.1 MALDI ion sources available on commercial instruments (frontside geometry) allow for a laser ablation diameter down to 10 μm. A smaller ablation diameter can be achieved with objective lenses closer to the sample. The transmission geometry optical path allows for use of high numerical aperture lenses close to the sample such that the laser can travel through a transparent substrate and can be focused on the sample to achieve an ablation diameter of about 1 μm. (Adapted with permission from McMillen et al. [10])

optics [4, 5]. One reported approach was to drill a hole in the center of the final focusing lens and position it between the mass analyzer and the sample [6]. The lens is positioned very close above the sample while allowing ion transmission through the lens hole. Another approach to achieve a small ablation diameter is to place a high numerical aperture objective behind the sample. Thus, a sample placed on a transparent substrate results in the generation of ions unimpeded by laser optics, and this arrangement is termed transmission geometry (Fig. 7.1) [3, 7]. Transmission geometry for high spatial resolution IMS has achieved an ablation diameter of 1 μm. It has been subsequently used by other groups for high spatial resolution IMS [8, 9].

7.3 Increasing Ion Intensity for High Spatial Resolution IMS

High spatial resolution IMS brings multiple challenges including long acquisition times, large data files, and relatively low ion intensities. As the sampling area decreases, data size and length of acquisition increases as a square function. Also, ion intensities are decreased. While MALDI is a relatively "soft" ionization technique, the ratio of neutral molecules to ions is considerable (estimated to be 1:10000) [11]. While high spatial resolution increases the regiospecificity within an ion image, ion intensities are decreased due to the smaller amount of material sampled. This challenge is not unique to IMS –biological imaging using SIMS is routinely performed at 1–2 μm spatial resolution even though the liquid metal ion beams can be focused to the low nm range.

One approach to increase ion intensity for high spatial resolution IMS is to accumulate ions from a narrow mass-to-charge window. This approach is termed continuous accumulation of selected ions (CASI) and has been demonstrated with an FT-ICR MS instrument. Under normal imaging conditions, a wide range of ions introduced into to the ICR cell to be analyzed, but the presence of very abundant species can quickly fill the cell before lower abundance ions can accumulate. CASI can be implemented by selecting a specific *m/z* window to accumulate ions while the sample is analyzed at different regions. In this way, the sensitivity is increased for a selected *m/z* window.

A second instrumental approach to increase ion intensities is to introduce post-ionization strategies. Common post-ionization strategies include irradiation of the ion plume with either plasma, or with a secondary, lower wavelength UV laser, termed MALDI-2 [12–14]. In either case, post-ionization is delayed after the initial MALDI event to irradiate the MALDI plume above the sample (Fig. 7.3). MALDI-2 was shown to provide a 100-fold increase in intensities of selected ions, and a 7-fold increase in overall intensity from a spotted lipid homogenate [15]. The intensity increase provided by MALDI-2 allows for higher spatial resolution imaging while maintaining comparable signal-to-noise ratio with MALDI alone at a lower spatial resolution. MALDI-2 has been used with high numerical aperture objectives (NA = 0.95) in transmission geometry allowing for an ablation diameter of 1 μm [15] (Fig. 7.2).
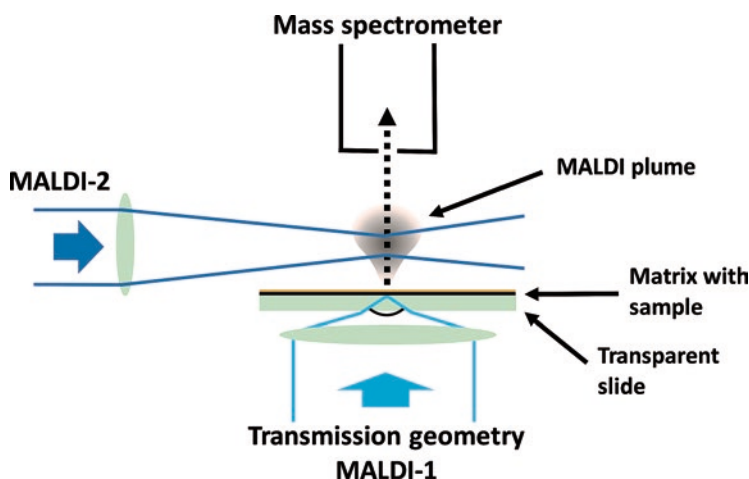
Fig. 7.2 MALDI-2 post-ionization shown with a transmission geometry optical setup for the primary MALDI event. The MALDI-2 laser beam is focused orthogonally to the sample surface above the sample. The lasers are synchronized such that MALDI-2 irradiates immediately following the MALDI plume formation. (Adapted with permission from McMillen et al. [16])

7.4 Unravelling Molecular Complexity Using IMS

The molecular complexity of biological tissues can pose a challenge to molecular identification by IMS. Even with a high mass resolution instrument such as an FT-ICR instrument, separation of closely isobaric species can considerably lengthen acquisition times. Ion mobility provides separations dependent on size, shape, and mass-to-charge ratio of the ions. One approach is to add a separation technology to help deconvolute the ion complexity. Ion mobility can be integrated with IMS and thereby enhance specificity and improve molecular coverage [17].

Multiple types of ion mobility separations exist, including drift tube ion mobility [18, 19], traveling-wave ion mobility spectrometry [20, 21], and field asymmetric waveform ion mobility spectrometry [22, 23]. These techniques have been coupled with imaging mass spectrometry for studying metabolites [24, 25], lipids [26], peptides [27, 28], and proteins [28, 29], improving the separation, specificity, and identification of molecular species. Trapped ion mobility spectrometry (TIMS) [30, 31] is a relatively new advancement in the field that provides increased ion mobility resolving power [32]. TIMS utilizes an electric field gradient (EFG) to trap and sequentially elute ions with ascending mobilities. TIMS separations are capable of resolving powers >200 for singly and multiply charged ions.

The recently developed MALDI timsTOF instrument incorporates a high throughput, high spatial resolution MALDI source with a high-performance TIMS platform [17]. The unique combination of spatial resolution and high-performance gas phase separations is critical for advanced molecular imaging applications, particularly for metabolite and lipid analysis where mass redundancy and structural isomers are prevalent [17].
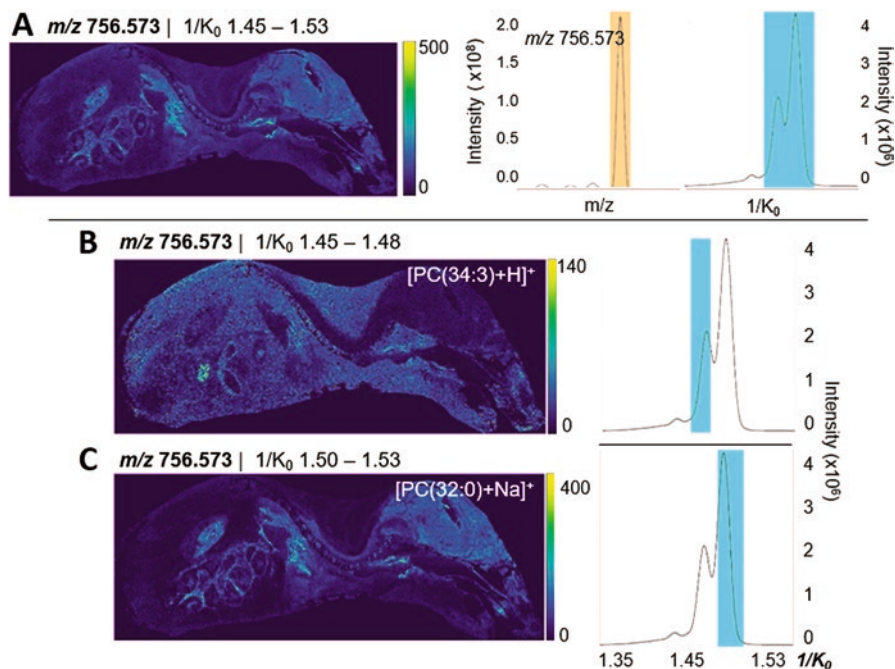
Fig. 7.3 Ion mobility IMS of a whole body mouse pup tissue collected at 50 μm spatial resolution and a 400 ms TIMS scan time. (**a–c**) Each panel highlights the positive ion mode images from selected mobility ranges for *m/z* 756.5517 and only one peak is detected in the selected mass window (orange) while multiple peaks are observed in the extracted ion mobilogram. (**a**) Ion image taken from 1/K0 1.45–1.53, is dominated by the higher intensity [PC(32:0) + Na]$^+$ similar to results from a non-ion mobility IMS experiment.(**b**) [PC(34:3) + H]$^+$ is found throughout the tissue except the brain and spinal cord. (**c**) [PC(32:0) + Na]$^+$ localizes in the brain, spine and intestines. (Adapted with permission from Ref. [17]. Copyright 2019 American Chemical Society)

MALDI TIMS imaging of a whole body mouse pup tissue was used to demonstrate TIMS capabilities. Positive ion mode TIMS lipid images were collected with a 50 μm spatial resolution and utilizing a 400 ms EFG scan time (Fig. 7.3). The extracted ion mobilogram for a single *m/z* value showed two different ions resolved across the tissue. One ion was detected throughout the animal but had lower intensity within the brain and brain stem. Conversely, the isobar was abundant within the brain, spine, and intestines. These ions can be differentiated with TIMS separation. Although these ions are not isomers, they require very high resolving power if they are to be resolved by a mass analyzer. High-field FTMS platforms require long scan times (~1.5–3 s) for the necessary resolving power, making the experiment impractical for most imaging applications. This example highlights the power of TIMS separations and ion mobility in general for imaging experiments to improve specificity and molecular coverage in direct tissue analysis.

7.5   Sample Preparation for IMS

IMS is highly dependent on the quality of sample preparation. Many factors must be taken into account when preparing a sample, including tissue stabilization or preservation, embedding material, the washing procedure, matrix choice, and matrix application method [34]. An example workflow consists of tissue sectioning, an optional washing procedure, matrix application, and an optional recrystallization procedure (Fig. 7.4). The primary goal of any sample preparation is to minimize analyte delocalization and degradation while maximizing sensitivity [35]. Sample preparation protocols are typically developed for specific tissue types and analytes of interest [36–40], although common methods and protocols can be established.

Sample preparation of formalin fixed tissue [41] begins by sectioning to 10–12 μm thickness and thaw mounting onto a conductive microscope slide (Fig. 7.4a). Fixation, offering the most accurate morphological tissue representation, is performed by incubating a harvested tissue in a paraformaldehyde solution for up to 7 days. Intramolecular crosslinks are formed between proteins during this incubation. The fixed tissue is then submerged in paraffin wax, and is termed formalin fixed paraffin embedded (FFPE) tissue. While this method allows ambient storage, the fixative can induce unwanted issues [42]. These can compromise analysis of metabolites, lipids, and intact proteins. However, some studies observe limited MS effects after paraffin removal or alternative procedures [43–45]. For proteins, developed protocols utilize proteolytic digestion of FFPE tissues and subsequent peptide analysis [37, 43, 45, 46]. Steps within these protocols allow more efficient enzyme digestion of proteins. Fresh frozen tissues are preferred for IMS [34]. However, freezing induces morphological changes and other artifacts to a tissue. Histological stains of fresh frozen tissue sections are typically inferior to those of FFPE sections.

For fresh frozen tissue, the preserved tissue is cryosectioned prior to thaw mounting onto the slide. Optimal cutting temperature (OCT) compound may be used to improve section quality. However, OCT is a polymer that introduces high intensity
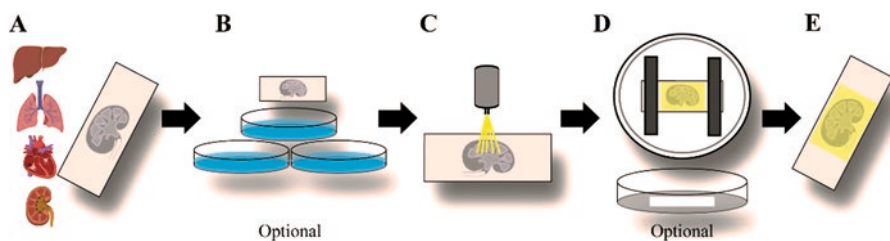
Fig. 7.4 MALDI IMS sample preparation workflow. (**a**) Biological tissues are thinly sectioned and thaw mounted onto conductive microscope slides. (**b**) Sections may undergo optional washing protocols to select for analytes of interest or lessen chemical interferences. (**c**) MALDI matrix is homogenously applied to a sample using a robotic aerosol sprayer. (**d**) An optional recrystallization procedure can be applied to samples when needed to ensure analyte-matrix layer co-crystallization. (**e**) Prepared samples are ready when needed for IMS analysis
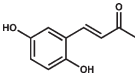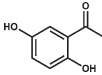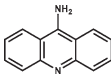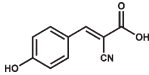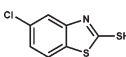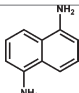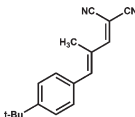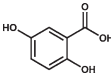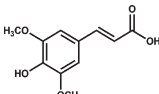
ions during MS analysis that can significantly complicate the mass spectra. Tissue washing procedures have been shown to lessen or remove OCT artifacts, but these washes may wash away compounds of interest as well [35]. Other materials have been purposed as embedding materials with limited MS effects, including carboxymethylcellulose (CMC) and gelatin [45, 46]. Use of these materials typically introduces minimal effects, while still assisting in sectioning.

Washing can remove potential chemical interferences and select for specific analytes (Fig. 7.4b) [35, 49, 50, 51]. Ammonium formate (AmF) buffer is used to remove salts from tissue for the analysis of lipids [49]. The ammonium cation of the buffer system is volatile and removed from tissue by the vacuum of MS instruments. In the positive ion mode, protonated ions dominate the spectra after AmF tissue washing. Decreased salt presence also increases sensitivity in the negative ion mode. Sensitivity for intact proteins can be increased by removing both lipids and salts from tissue using Carnoy's fluid (ethanol, chloroform, and acetic acid), water, and ethanol [35]. Recently washes have been developed to select for metabolites [48, 49]. Chloroform and acetone washes remove hydrophobic lipids, leaving behind many water soluble metabolites. Washes may delocalize some molecules, so care and validation are recommended. Some washes are being developed to either select or analytes of interest or eliminate chemical interferences [52–56].

7.6   MALDI Matrix Selection and Application
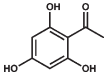
MALDI matrices are chosen based on their ability to provide sufficient ionization efficiency for a given analyte class (*e.g.* low molecular weight metabolites, lipids, proteins, polymers, or organometallics). A MALDI matrix is typically a small organic molecule consisting of a UV absorbing chemical moiety. Differences in observed analyte sensitivities can be attributed to the physical properties of a matrix such as molecular structure, pH, proton affinity, and peak wavelength absorbance [3, 57–64]. However, studies have successfully employed various inorganic materials such as nanoparticles or thin layers of metals [65]. 2,5-dihydroxybenzoic acid (DHB) is widely employed as a MALDI matrix, offering sufficient sensitives for many analyte classes in positive ion mode MS analysis [63, 66–69]. 9-Aminoacridine (9AA) is often used for the analysis of metabolites in negative ion mode and 1,5-diaminonaphthalene (DAN) for lipids with high sensitivity in both polarities [58, 64]. However, the energy transferred during the ablation process can result in analyte modification or fragmentation, complicating data interpretation [66, 70]. Volatility is also a consideration when selecting a MALDI matrix because the matrix layer must remain stable for lengthy acquisition times (hours) to avoid signal loss during an imaging experiment. 2,5-Dihydroxyacetophenone (2,5-DHA) is an excellent matrix for MS analysis of multiple analyte classes; however, its high volatility limits acquisition times [3]. (E)-4-(2,5-dihydroxyphenyl)but-3-en-2-one (2,5-cDHA) is a vacuum stable matrix providing high sensitivity for lipids, peptides, and intact proteins [57]. Table 7.1 lists many commonly used matrices.

Table 7.1 MALDI matrices and analyte applications

Matrix	Other names	Chemical structure	Application
(E)-4-(2,5-dihydroxyphenyl)but-3-en-2-one	2,5-cDHA		Lipids
			Peptides
			Proteins
			Positive and negative ionization modes
2,5-dihydroxyacetophenone	2,5-DHA		Lipids
			Peptides
			Proteins
			Positive and negative ionization modes
9-Aminoacridine	9-AA		Low molecular weight metabolites
			Lipids
			Negative ionization mode
α-Cyano-4-hydroxycinnamic acid	CHCA		Peptides
			Proteins
			Positive ionization mode
5-Chloro-2-mercaptobenzothiazole	CMBT		Lipids
			Peptides
			Positive and negative ionization modes
1–5,Diaminonapthalene	DAN		Lipids
			Positive and negative ionization modes
trans − 2-[3-(4-*tert*-Butylphenyl)-2-methyl-2-propenylidene]malononitrile	DCTB		Carbohydrates
			Polymers
			Inorganic materials
			Organometallics
			Positive and negative ionization modes
2,5-Dihydroxybenzoic acid	DHB		Low molecular weight metabolites
			Pharmacuticals
			Lipids
			Positive ionization mode
3,5-Dimethoxy-4-hydroxycinnamic acid	Sinapic acid		Peptides
			Proteins
			Positive ionization mode

Table 7.1 (continued)

Matrix	Other names	Chemical structure	Application
2′,4′,6′-Trihydroxyacetophenone	THAP		Carbohydrates
			Nucleic acids
			Lipids
			Peptides
			Positive and negative ionization modes

The protocol for application of a MALDI matrix to a tissue sample can dictate crystal size, analyte extraction, and analyte delocalization (Fig. 7.4c). MALDI matrices are most commonly applied by either aerosol spray or sublimation. Aerosol application can be accomplished using an airbrush sprayer or more homogenously and reproducibly using a robotic sprayer. Temperature, gas flow, and solvent composition can all influence analyte extraction and unwanted delocalization. Ideally, matrix application is wet enough to ensure analyte extraction yet not so wet to promote analyte delocalization. Optimal matrix concentration and deposition density are determined by resultant mass spectra, and delocalization is evaluated by MS acquisition off tissue [71]. When necessary, final assessment of a matrix application can be assessed using scanning electron microscopy to determine the matrix crystal size, an important factor when performing high spatial resolution IMS due to the need for crystals to be much smaller than the incident laser spot size [3]. Matrix application by sublimation has been shown to produce small crystal sizes [72]. However, sublimation does not provide the level of analyte extraction achieved by aerosol spray. A recrystallization procedure was developed to achieve efficient extraction after matrix application by sublimation (Fig. 7.4d) [35]. One issue with sublimation is the achievement of reproducible deposition amounts. Variation in the sublimation time or temperature will impact the amount of matrix deposited. Sublimation is generally not commonly used for large sample cohorts [3, 35, 49, 73]. Sample preparation and matrix selection are important considerations when developing a method for IMS analysis.

7.7 Application to Kidney Disease

The progression of chronic kidney disease often leads to a host of medical issues including vascular disease, blindness, and diabetic nephropathy. Kidney disease is characterized by damage to the many small sub-structures within the kidney such as the tubules and glomeruli and changes in the molecular profile of lipids, proteins, and peptides. Glomeruli, the central filtration units of the kidney, have a relatively small diameter (100–200 μm) and are distributed throughout the kidney. The untargeted nature of IMS is an ideal discovery tool for the detection of a range of intact biomolecules for the characterization of diseased tissue.
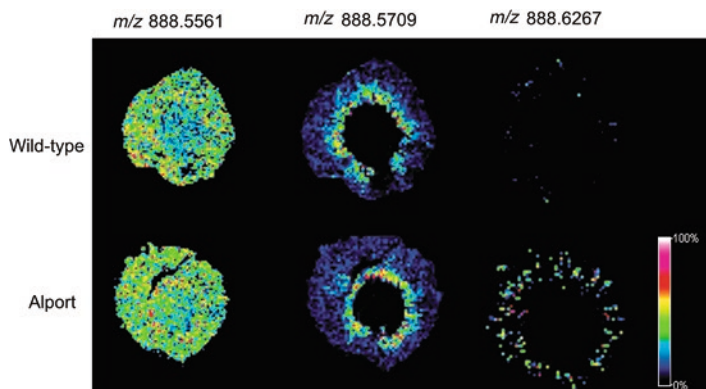
Fig. 7.5 Ion images of mice kidney comparing wild-type (top) to kidney from Alport model mouse (bottom). Three nominally isobaric ions are mapped showing no change in distribution for selected phospholipids (*m/z* 888.5561 and *m/z* 888.5709) whereas the sulfatide species SulfoHexCer (18:2/24:0) at *m/z* 888.6267 is increased in the Alport model compared to the wild-type. (Reprinted with permission from Ref. [75]. Copyright 2019 American Oil Chemists' Society)

One kidney disease of interest is Alport Syndrome that is caused by gene mutations and subsequent increase in laminin α1β1γ1 protein expression of adult mice, possibly facilitated by lipid dysregulation in lipid binding to the protein [74, 75]. IMS has recently been used for characterization of lipid species in mice in control and in an Alport model. Nominally isobaric lipid species are differentiated with high resolving power instrumentation. Three lipid species within 7 mDa of each other were identified and shown to have different spatial distribution within the mouse kidney (Fig. 7.5) [75]. Two ^{13}C isotopes of phospholipids (PI(36:4) and PI(36:3)) did not change between the kidneys of wild-type and Alport model mice. Interestingly, the sulfatide species SulfoHexCer(18:2/24:0) of *m/z* 888.6267 showed an increase in intensity in the kidney tubules of the Alport model, lending support to the hypothesis of the role of lipid changes in disease progression. Characterization of diseases such as Alport syndrome on a molecular level can lead to more informed and effective treatment strategies.

7.8   Applications to Infectious Disease

Due to the ability of IMS to molecularly probe complex tissue environments without the need for antigen-specific tags, this technology has been applied to a wide variety of biological and medical issues. For example, one such area is the application to the field of infectious diseases. Antibiotic-resistant bacteria exposure are not confined to healthcare settings. Isolated from many community settings, resistant strains of *Staphylococcus aureus* are a public health threat causing an estimated 20,000 deaths per year in the United States alone. Infections by *S. aureus* have the

ability to cause a broad range of life-threatening illnesses in a vertebrate host, ranging from soft tissue infections that present with abscess formation to systemic conditions such as sepsis. Abscess architecture consists of staphylococcal communities surrounded by layers of healthy and necrotic innate immune cells. Upon recognition of a pathogen, a vertebrate host will deploy mechanisms of innate immunity. These mechanisms vary from pathogen killing by oxidative stress to more specialized responses, such as nutrient metal sequestration in processes known as nutritional immunity [76–79]. Characterization of the host-pathogen interface in these infections by spatially-targeted molecular analysis technologies will enable a deeper understanding of bacterial pathogenesis and host defense mechanisms. IMS has been employed to investigate this interface, identifying both host and pathogen factors [80–84].

Advances in IMS instrumentation using Fourier transform ion cyclotron resonance mass spectrometry (FT-ICR MS) allow for the measurement of isotopically resolved protein species directly from tissue, Fig. 7.6a, b [82]. Previous research of protein distributions at the infectious interface focused on the heterodimer calprotectin (CP) constructed by S100A8 and S100A9 subunits [82, 83]. CP can bind manganese, zinc, calcium, and iron [83, 85, 86]. By decreasing the availability of necessary metal species, metalloproteins inhibit proliferation of pathogens by processes of nutritional immunity [79]. The resolving power provided by a 15 T FT-ICR MS results in the identification of post-translational modifications (PTMs) to S100A8 and S100A9. Modified S100A8 and S100A9 species were observed to form a spatial gradient from singly to triply oxidized species as distributions approached bacterial foci, Fig. 7.6d [83]. This observation can be explained by reactive oxygen species (ROS) used by a host to kill pathogens.

Application of IMS in tandem with multiple other imaging modalities such as laser ablation inductively coupled plasma imaging mass spectrometry (LA-ICP IMS), bioluminescent imaging, magnetic resonance imaging (MRI), and blockface imaging provided 3-dimensional (3D) distributions of protein and metal abundances at 50 μm spatial resolution [84]. Multimodal analysis revealed heterogeneous bacterial transcriptional responses and host inflammatory responses. Specifically, IMS allowed visualization of CP throughout a 3D volume of an *S. aureus* infected murine kidney, Fig. 7.6e. Use of genetically modified bacteria that produce a bioluminescent response to iron starvation allowed visualization of transcriptional response *in vivo,* Fig. 7.6e. LA-ICP IMS provided elemental distributions translocated by processes of nutritionally immunity, Fig. 7.6e. MRI provided a scaffold for 3D reconstruction of image data file. Finally, blockface image analysis provided visual context to imaging data as well as verification of signal localizations within tissue. A major discovery from this study is that abscesses within the same organ have heterogeneous molecular architectures despite having a homogeneous appearance by traditional microscopy. Consistent with this observation, bacterial pathogens exhibited heterogeneous responses both within and between tissue lesions. Collectively, IMS is a promising research tool for the label-free identification of tissue pathology characterized by altered protein or element abundance.
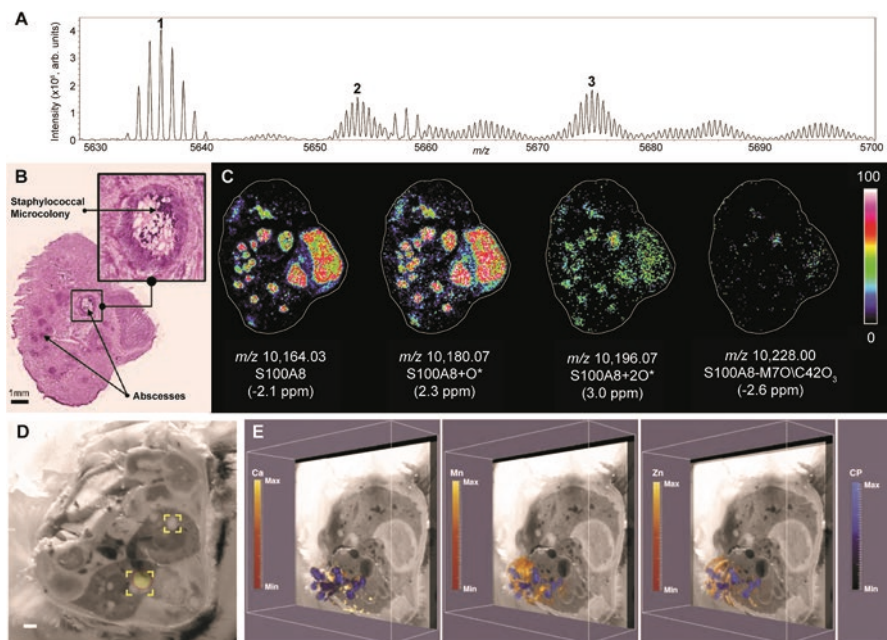
Fig. 7.6 MALDI FT-ICR IMS isotopic resolution of proteoforms and molecular context to the host-pathogen interface. (**a**) MALDI FT-ICR IMS of intact proteins from rat brain tissue (resolving power of ~40,000 at m/z 5000) provide isotopic resolution and allow ions of different charge states and modifications to be distinguished. The ion labeled 1 is singly charged and ions labeled 2 and 3 are examples of doubly charged ions. (**b**) A hematoxylin and eosin stained tissue section is annotated for *S. aureus* abscesses within a murine kidney tissue section. (**c**) Selected ion images of intact proteins from kidney tissue from a mouse infected with *S. aureus* collected using MALDI FTICR MS show advancing oxidation products localizing to the center of infectious foci. Ions were identified using mass accuracy to correlate imaging results with separate top-down proteomics experiments. (**d**) A blockface image of a *S. aureus* infected murine cross section overlaid with bioluminescent signal shows heterogeneous iron starvation of bacteria. The bioluminescent signal is depicted as a yellow sphere outlined in orange. Yellow boxes on the blockface images correspond to specific abscesses. (**e**) The MALDI IMS imaging volume for calprotectin encompassing the infected right kidney was co-registered to the LA-ICP-MS imaging volume for Ca, Mn, or Zn, displayed obliquely to delineate calprotectin and element distribution throughout the kidney. Heat maps depict minimum and maximum values in arbitrary units. (Adapted with permission from Ref. [82, 84]. Copyright 2015 American Society for Mass Spectrometry. Copyright 2018 Science Translational Medicine)

7.9 Data Analysis with IMS

IMS data is inherently complex and highly dimensional, requiring rigorous computational workflows to conduct effective analyses without losing valuable information. Data generated by IMS is also amenable to supplementation with other types of imaging, which further requires computational workflows to register and process
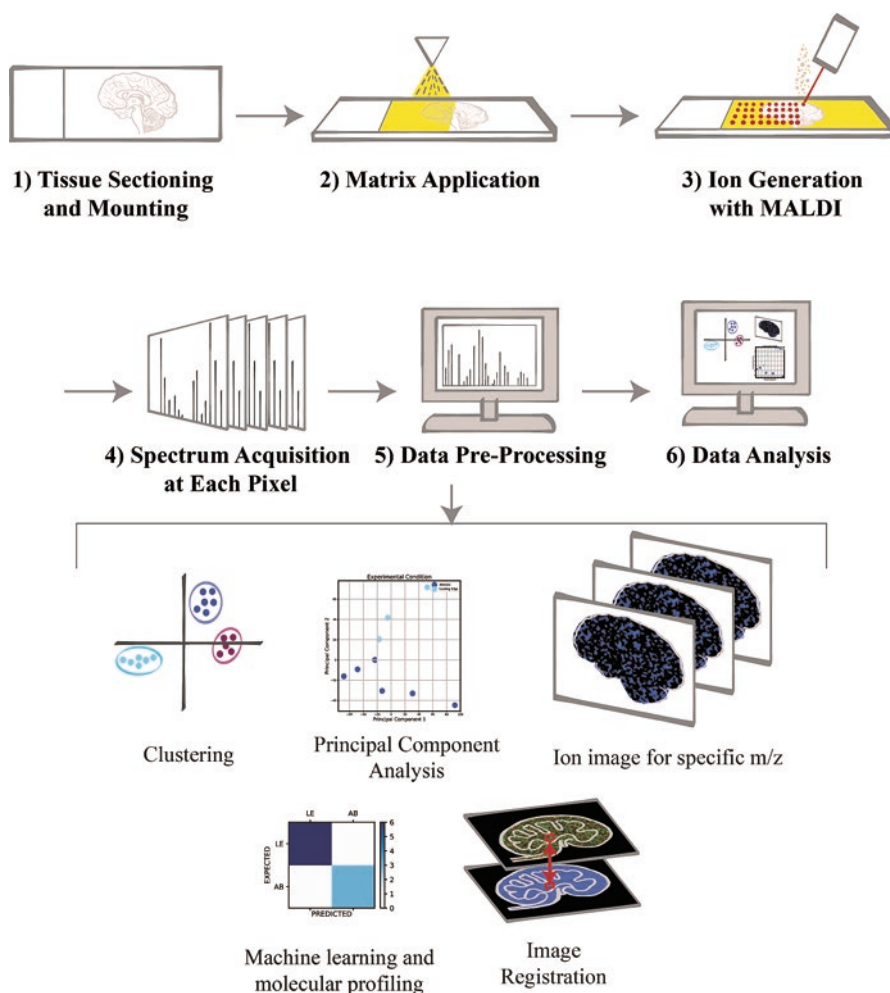
Fig. 7.7 Visual work-flow for IMS data analysis. (1) Tissues are embedded in a medium, sectioned, and mounted onto conductive glass slides. (2) A matrix, optimal for the tissue and experimental workflow, is applied uniformly across the slide. (3) Ions are generated via MALDI. (4) Individual spectra are collected at each pixel. (5) Data is pre-processed using methods such as baseline correction, peak detection and alignment, and normalization. (6) Data can be analyzed using a variety of techniques; these include statistical methods such as clustering and principal component analysis, visualization by specific m/z values, supervised and unsupervised machine learning for molecular profiling, and co-registration with other imaging modalities

the resultant multimodal imaging data set. Here we discuss computational approaches for data processing, which include pre-processing, visualization, statistical analysis, and multimodal data processing. A summary of a typical data analysis workflow can be seen in Fig. 7.7.

7.10 Data Import, Pre-Processing, and Visualization

Once IMS data are acquired, they are typically converted into imzML format, which is an open source format allowing for analysis with a variety of software applications. Data can then be pre-processed using normalization, baseline correction, peak detection, and peak alignment.

IMS data is high dimensional and large in terms of data size, often requiring a form of data compression to decrease the computational load. Common methods to compress data include binning mass spectra for each pixel or compressing based on regions of interest (ROI). One compression method based on regions of interest is image segmentation, which involves partitioning tissue into regions of homogenous spectral profiles and identifying co-localized *m/z* values. Another data compression approach uses unsupervised clustering to reduce dimensionality and extract features for statistical analysis. A common unsupervised approach is principal component analysis (PCA), which involves collapsing individual variables into groups that exhibit similar behavior.

These groups are known as "components" and explain the variance in data with far fewer dimensions. Because of its utility in dimensionality reduction, PCA is also often used for downstream statistical analysis of pre-processed IMS data. Other clustering approaches such as hierarchical clustering and k-means clustering can also be used to visualize potential groupings of the data. Resultant data can be visualized by selecting individual *m/z* values, extracting the intensity of that *m/z* value from each pixel's spectrum, and plotting the intensity values as a heat map showing the relative distribution of the *m/z* value across the tissue.

7.11 Statistical and Multivariate Analysis

Once the data have been processed and initial visualizations complete, a variety of statistical techniques can be applied to compare data. If the experimental hypothesis involves a direct comparison of relative *m/z* value intensities across regions of tissue, tests of significance such as t-tests and ANOVA can be applied. A t-test compares two groups of data, and ANOVA compares three or more. Unsupervised approaches such as PCA can also be used to process the data. For instance, if the regions of tissue are distinct in terms of their spectra, they should separate into components of the PCA, allowing distinct separations among the data. However, unsupervised approaches are usually applied to all *m/z* values identified in a tissue. If the purpose of the study is to compare how well a specific *m/z* value can be used to classify between groups or regions of tissue, a receiver operator characteristic curve (ROC) analysis can be used. An ROC analysis is a test of accuracy and involves plotting the true positive rate against the false positive rate. ROC analysis is often used to determine if a molecular species with an explicit *m/z* is specific to a region.

In the event that multiple species with multiple *m/z* values may be involved in a classification, a multivariate analysis can be applied.

Classification is often a goal with IMS data analysis, whether between regions of tissue, individual substructures within a tissue, or among tissue samples belonging to different experimental or biological groups. Although unsupervised approaches can offer some differentiation, supervised approaches can also be used, provided the data are "labeled", or the classes are known. The ultimate goal of any supervised approach is normally to classify new data into a given class using a classification model built using existing data. Machine learning algorithms such as support vector machines, neural networks, and random forest can be applied for dimensionality reduction and classification.

7.12 Common Software for IMS Data Analysis

Cardinal [87] and MSiReader [88] are commonly used open-source R package and MATLAB software, respectively, for analysis of imaging mass spectrometry datasets. Cardinal supports MALDI and Desorption Electrospray Ionization (DESI) IMS workflows. IMS data can be loaded into such software in imzML format, pre-processed, and analyzed using spatial segmentation, image classification, and statistical analysis functions. As they are open-source, they also support the development of new computational workflows. Users can create their own multivariate statistical modeling or model-based visualization using existing Cardinal functions. Commonly used commercially available software includes SCiLS and Data Analysis from Bruker, and ImageQuest from ThermoFisher Scientific.

7.13 Data Registration and Multimodal Approaches

IMS data alone can provide spatially resolved molecular information. However, coupled with other types of imaging modalities such as microscopy, it allows for even higher spatial and molecular resolution. For example, IMS provides highly resolved chemical specificity, but relatively low spatial resolution. Microscopy can provide a much higher spatial resolution, but relatively low chemical specificity. As such, combining an IMS dataset with a microscopy image, each obtained on serial sections of tissue can offer much higher resolution chemical and spatial resolution. Recent advances to couple these imaging modalities include multimodal image registration [89].

A combination of autofluorescence images, H&E stained images, and IMS images, pre and post-acquisition can be registered using explicit IMS pixel to laser ablation marks registration. This method (shown in Fig. 7.8 below) involves a series
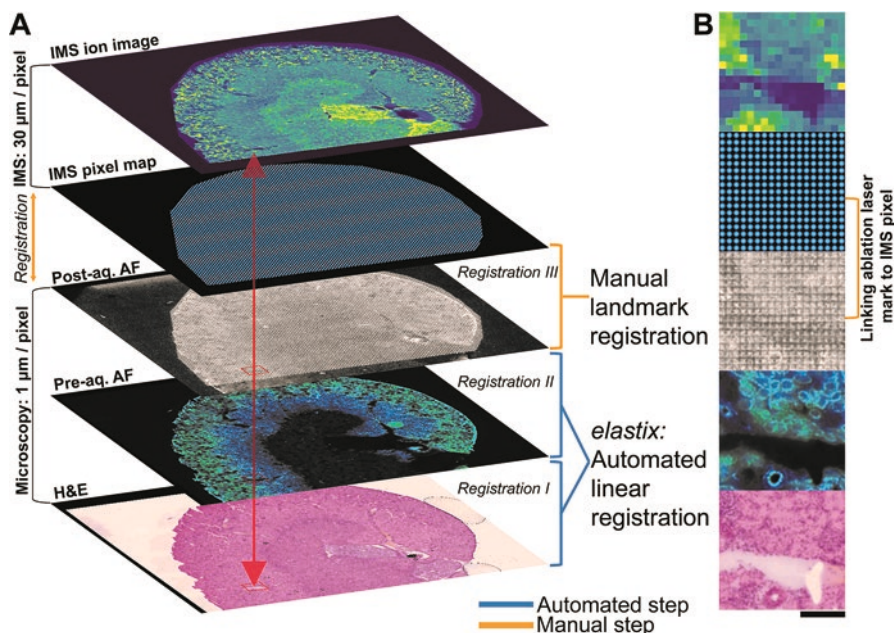
Fig. 7.8 Registration workflow between a multiplexed immunofluorescence microscopy image and an IMS-imaged tissue section. (**a**) Images of tissue sections. The registration process occurs from bottom to top, such that 'Registration I' is an automated linear registration between the H&E and pre-acquisition autofluorescence images. 'Registration II' is another automated linear registration between the registered image and post-acquisition autofluorescence, which includes laser ablation marks. 'Registration III' is a manual landmark registration between the registered image and corresponding IMS pixels. (**b**) High-magnification region of interest ROI representing single tile of the images for registration. Pre-acq: pre-acquisition. Post-acq: post-acquisition. (Reprinted with permission from Ref. [89]. Copyright 2018 American Chemical Society)

of three separate registration processes. First, automated linear registration is conducted between the H&E stained tissue and autofluorescence image before IMS acquisition using the *elastix* library with a stochastic gradient descent optimizer. Second, *elastix* is used for automated linear registration between the registered image and the autofluorescence image post IMS-acquisition. Third, manual landmark registration is used to register post-acquisition image with the IMS pixel map using ablation laser marks that correspond to the IMS pixels. Fourth and finally, the registered image is registered with the IMS ion image [89]. The resultant image now has much higher spatial resolution and molecular distributions across distinct tissue substructures can be compared with more granularity.

Another example of multimodal imaging can be seen with image fusion of IMS and microscopy images. This computationally driven process integrates IMS and microscopy, resulting in an image that is rich in chemical and spatial resolution using a statistical regression approach. Multivariate regression is applied to microscopy measurements to predict ion distributions, increasing ion image resolution by
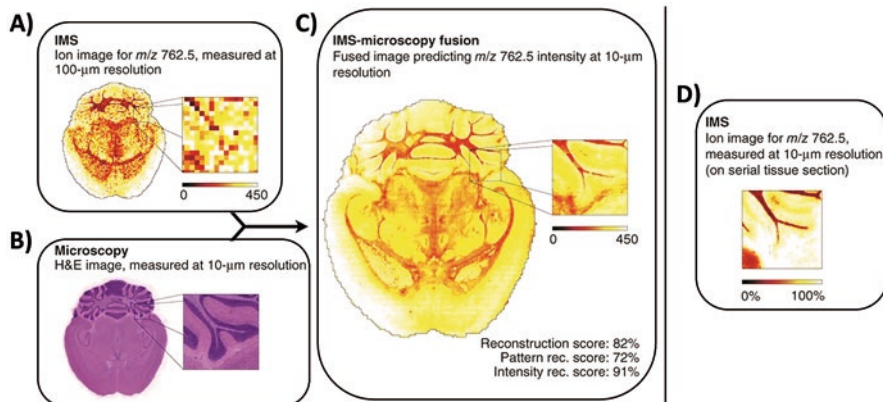
Fig. 7.9 Prediction of the ion distribution of *m/z* 762.5 in mouse brain at 10 μm resolution from 100 μm IMS and 10 μm microscopy measurements (sharpening). This example in mouse brain fuses a measured ion image for *m/z* 762.5 (identified as lipid PE(16:0/22:6)) at 100 μm spatial resolution (**a**) with measured H&E-stained microscopy image at 10 μm resolution (**b**), predicting the ion distribution of *m/z* 762.5 at 10 μm resolution (reconstruction Score 82%) (**c**). For comparison, (**d**) shows a measured ion image for 762.5 at 10 μm spatial resolution, acquired from a neighboring tissue section. (Adapted with permission from Ref. [90]. Copyright 2015 Springer Nature)

an order of magnitude. Not only does this lead to "sharper" IMS images, but it also allows prediction of ion distributions in areas not measured with IMS as well as enrichment of biological signals and attenuation of instrumental artifacts. Some dimensionality reduction methods discussed above, such as PCA, can help attenuate such artifacts, but since those are only done with IMS images, they can only identify IMS-related instrumental artifacts. By fusing multiple modalities, attenuation of such artifacts can be improved. An example of this workflow can be seen in Fig. 7.9 below. Figure 7.9a below shows an ion image for *m/z* 762.5 with a spatial resolution of 100 μm. Figure 7.9b shows a serial section of the same tissue stained using hematoxylin and eosin with a spatial resolution of 10 μm. Once the fusion method is applied to these images, a predicted ion image of *m/z* 762.5 is generated at a 10 μm spatial resolution (Fig. 7.9c) and is comparable to IMS of a serial section of the tissue obtained at 10 μm spatial resolution (Fig. 7.9d) [90].

7.14   Conclusion

Image registration and fusion are two methods that can be performed using IMS and other imaging modalities that offer higher chemical and/or spatial resolution. Ongoing efforts at the interface of hardware and software development seek to further improve chemical specificity, chemical coverage, and spatial resolution by improving IMS technology as well as incorporating other imaging modalities such as multiplexed immunofluorescence, transcriptomics, and elemental imaging.

References

 1. Caprioli RM, Farmer TB, Gile J (1997) Anal Chem 69:4751
 2. Norris JL, Caprioli RM (2013) Chem Rev 113:2309
 3. Zavalin A, Yang J, Hayden K, Vestal M, Caprioli RM (2015) Anal Bioanal Chem 407:2337
 4. Feenstra D, Dueñas ME, Lee YJ (2017) J Am Soc Mass Spectrom 28:434
 5. Kettling H, Vens-Cappell S, Soltwisch J, Pirkl A, Haier JR, Mü J, Dreisewerd K (2014) Anal Chem 86:3
 6. Kompauer M, Heiles S, Spengler B (2017) Nat Methods 14:90
 7. Zavalin A, Todd EM, Rawhouser PD, Yang J, Norris JL, Caprioli RM (2012) J Mass Spectrom 47:1473
 8. Niehaus M, Soltwisch J, Belov ME, Dreisewerd K (2019) Nat Methods 16:925
 9. Steven RT, Shaw M, Dexter A, Murta T, Green FM, Robinson KN, Gilmore I, Takats Z, Bunch J (2019) Anal Chim Acta 1051:110
10. McMillen JC, Prentice BM, Spivey EC, Zavalin A, Caprioli RM (2018). Transm. Geom. Instrum. Modif. Laser Energy Depos. Charact. High Spat. Resolut. MALDI Imaging Mass Spectrom. (Poster presentation at the American Society for Mass Spectrometry, San Diego, CA
11. Mowry D, Johnston MV (1993) Rapid Commun Mass Spectrom 7:569
12. Tsai S-T, Chen C-H, Lee YT, Wang Y-S (2008) Mol Phys 106:239
13. Soltwisch J, Kettling H, Vens-Cappell S, Wiegelmann M, Müthing J, Dreisewerd K (2015) Science (80–) 348:211
14. Ellis SR, Soltwisch J, Paine MRL, Dreisewerd K, Heeren RMA (2017) Chem Commun 53:7246
15. Spivey EC, McMillen JC, Ryan DJ, Spraggins JM Caprioli RM (2019) J Mass Spectrom 54:366
16. McMillen JC, Spivey EC, Ryan DJ, Spraggins JM, Caprioli RM (2019) MALDI Spat. Resolut. Improv. Using MALDI-2 Post-Ionization (Proceedings of the 67th ASMS Conference on Mass Spectrometry and Allied Topics, Atlanta, GA)
17. Spraggins JM, Djambazova KV, Rivera ES, Migas L, Neumann EK, Fuetterer A, Suetering J, Goedecke N, Ly A, Van de Plas R, Caprioli RM (2019) Anal Chem 91:14552
18. May JC, Goodwin CR, Lareau NM, Leaptrot KL, Morris CB, Kurulugama RT, Mordehai A, Klein C, Barry W, Darland E, Overney G, Imatani K, Stafford GC, Fjeldsted JC, McLean JA (2014) Anal Chem 86:2107
19. Valentine SJ, Koeniger SL, Clemmer DE (2003) Anal Chem 75:6202
20. Zhong Y, Hyung S-J, Ruotolo BT (2011) Analyst 136:3534
21. Shvartsburg AA, Smith RD (2008) Anal Chem 80:9689
22. Purves RW, Guevremont R (1970) Int J Mass Spectrom Ion Process 52:2346
23. Kolakowski BM, Mester Z (2007) Analyst 132:842
24. Chughtai K, Jiang L, Greenwood TR, Glunde K, Heeren RMA (2013) J Lipid Res 54:333
25. Yan C, Parmeggiani F, Jones EA, Claude E, Hussain SA, Turner NJ, Flitsch SL, Barran PE (2017) J Am Chem Soc 139:1408
26. McLean JA, Ridenour WB, Caprioli RM (2007) J Mass Spectrom 42:1099
27. Sans M, Feider CL, Eberlin LS (2018) Curr Opin Chem Biol 42:138
28. Towers MW, Karancsi T, Jones EA, Pringle SD, Claude E (2018) J Am Soc Mass Spectrom 29:2456
29. Kocurek KI, Griffiths RL, Cooper HJ (2018) J Mass Spectrom 53:565
30. Fernandez-Lima F, Kaplan DA, Suetering J, Park MA (2011) Int J Ion Mobil Spectrom 14:93
31. Michelmann K, Silveira JA, Ridgeway ME, Park MA (2015) J Am Soc Mass Spectrom 26:14
32. Fernandez-Lima FA, Kaplan DA, Park MA (2011) Rev Sci Instrum 82:126106

33. Spraggins J, Djambazova K, Rivera E, Migas L, Neumann E, Fuetterer A, Suetering J, Goedecke N, Ly A, Van de Plas R, Caprioli R (2019) Anal Chem 91:14552
34. Thomas A, Chaurand P (2014) Bioanalysis 6:967
35. Yang J, Caprioli RM (2011) Anal Chem 83:5728
36. Fujino Y, Minamizaki T, Yoshioka H, Okada M, Yoshiko Y (2016) Bone Reports 5:280
37. Judd AM, Gutierrez DB, Moore JL, Patterson NH, Yang J, Romer CE, Norris JL, Caprioli RM (2019) J Mass Spectrom 54:716
38. Dufresne M, Patterson NH, Norris JL, Caprioli RM (2019) Anal Chem 91:12928
39. Angel PM, Baldwin HS, Gottlieb Sen D, Su YR, Mayer JE, Bichell D, Drake RR (2017) Biochim Biophys Acta, Proteins Proteomics 1865:927
40. Powers TW, Neely BA, Shao Y, Tang H, Troyer DA, Mehta AS, Haab BB, Drake RR (2014) PLoS One 9:e106255
41. Thomas A, Chaurand P (2014) Bioanalysis 6:967
42. Fowler CB, O'Leary TJ, Mason JT (2013) Expert Rev Proteomics 10:389
43. Paine MRL, Ellis SR, Maloney D, Heeren RMA, Verhaert PDEM (2018) Anal Chem 90:9272
44. Ly A, Buck A, Balluff B, Sun N, Gorzolka K, Feuchtinger A, Janssen K-P, Kuppen PJK, van de Velde CJH, Weirich G, Erlmeier F, Langer R, Aubele M, Zitzelsberger H, McDonnell L, Aichler M, Walch A (2016) Nat Protoc 11:1428
45. Buck A, Ly A, Balluff B, Sun N, Gorzolka K, Feuchtinger A, Janssen K-P, Kuppen PJK, van de Velde CJH, Weirich G, Erlmeier F, Langer R, Aubele M, Zitzelsberger H, Aichler M, Walch A (2015) J Pathol 237:123
46. Angel PM, Mehta A, Norris-Caneda K, Drake RR (2018) In: Sarwal MM, Sigdel TK (eds) Tissue proteomics methods protoc. Springer New York, New York, pp 225–241
47. Gill EL, Yost RA, Vedam-Mai V, Garrett TJ (2017) Anal Chem 89:576
48. Stoeckli M, Staab D, Schweitzer A (2007) Int J Mass Spectrom 260:195
49. Angel PM, Spraggins JM, Baldwin HS, Caprioli R (2012) Anal Chem 84:1557
50. Sun C, Li Z, Ma C, Zang Q, Li J, Liu W, Zhao H, Wang X (2019) J Pharm Biomed Anal 176:112797
51. Yang H, Ji W, Guan M, Li S, Zhang Y, Zhao Z, Mao L (2018) Metabolomics 14:50
52. Grey AC, Chaurand P, Caprioli RM, Schey KL (2009) J Proteome Res 8:3278
53. Leinweber BD, Tsaprailis G, Monks TJ, Lau SS (2009) J Am Soc Mass Spectrom 20:89
54. Franck J, Longuespée R, Wisztorski M, Van Remoortere A, Van Zeijl R, Deelder A, Salzet M, McDonnell L, Fournier I (2010) Med Sci Monit Int Med J Exp Clin Res 16:BR293
55. Seeley EH, Oppenheimer SR, Mi D, Chaurand P, Caprioli RM (2008) J Am Soc Mass Spectrom 19:1069
56. Källback P, Shariatgorji M, Nilsson A, Andrén PE (2012) J Proteome 75:4941
57. Yang J, Norris JL, Caprioli R (2018) J Mass Spectrom 53:1005
58. Thomas A, Charbonneau JL, Fournaise E, Chaurand P (2012) Anal Chem 84:2048
59. Ulmer L, Mattay J, Torres-Garcia HG, Luftmann H (2000) Eur J Mass Spectrom 6:49
60. Stübiger G, Belgacem O (2007) Anal Chem 79:3206
61. Beavis RC, Chaudhary T, Chait BT (1992) Org Mass Spectrom 27:156
62. Strupat K, Karas M, Hillenkamp F (1991) Int J Mass Spectrom Ion Process 111:89
63. Xu NX, Huang ZH, Watson JT, Gage DA (1997) J Am Soc Mass Spectrom 8:116
64. Vermillion-Salsbury RL, Hercules DM (2002) Rapid Commun Mass Spectrom 16:1575
65. Shi CY, Deng CH (2016) Analyst 141:2816
66. Schröter J, Fülöp A, Hopf C, Schiller J (2018) Anal Bioanal Chem 410:2437
67. Groessl M, Graf S, Knochenmuss R (2015) Analyst 140:6904
68. Groseclose MR, Castellino S (2013) Anal Chem 85:10099
69. Li S, Zhang Y, Liu J, Han J, Guan M, Yang H, Lin Y, Xiong S, Zhao Z (2016) Sci Rep 6:37903
70. Fuchs B, Bischoff A, Süß R, Teuber K, Schürenberg M, Suckau D, Schiller J (2009) Anal Bioanal Chem 395:2479
71. Eriksson C, Masaki N, Yao I, Hayasaka T, Setou M (2013) Mass Spectrom (Tokyo, Japan) 2:S0022

72. Hankin JA, Barkley RM, Murphy RC (2007) J Am Soc Mass Spectrom 18:1646
73. Anderson MG, Ablonczy Z, Koutalos Y, Spraggins J, Crouch RK, Caprioli RM, Schey KL (2014) J Am Soc Mass Spectrom 25:1394
74. Li S, Liquari P, Mckee KK, Harrison D, Patel R, Lee S, Yurchenco PD (2005) J Cell Biol 169:179
75. Gessel MM, Spraggins JM, Voziyan PA, Abrahamson DR, Caprioli RM, Hudson BG (2019) Lipids 54:411
76. Russell DG (2008) Cell Host Microbe 3:115
77. Cheng AG, DeDent AC, Schneewind O, Missiakas D (2011) Trends Microbiol 19:225
78. Rigby KM, DeLeo FR (2012) Semin Immunopathol 34:237
79. Weinberg ED (1974) Science 184(80–.):952
80. Kehl-Fie TE, Zhang Y, Moore JL, Farrand AJ, Hood MI, Rathi S, Chazin WJ, Caprioli RM, Skaar EP (2013) Infect Immun 81:3395
81. Moore JL, Caprioli RM, Skaar EP (2014) Curr Opin Microbiol 19:45
82. Spraggins JM, Rizzo DG, Moore JL, Rose KL, Hammer ND, Skaar EP, Caprioli RM (2015) J Am Soc Mass Spectrom 26(947)
83. Wakeman CA, Moore JL, Noto MJ, Zhang Y, Singleton MD, Prentice BM, Gilston BA, Doster RS, Gaddy JA, Chazin WJ, Caprioli RM, Skaar EP (2016) 7:11951
84. Cassat JE, Moore JL, Wilson KJ, Stark Z, Prentice BM, Van de Plas R, Perry WJ, Zhang Y, Virostko J, Colvin DC, Rose KL, Judd AM, Reyzer ML, Spraggins JM, Grunenwald CM, Gore JC, Caprioli RM, Skaar EP (2018) Sci Transl Med 10
85. Kehl-Fie TE, Skaar EP (2010) Curr Opin Chem Biol 14:218
86. Nakashige TG, Zhang B, Krebs C, Nolan EM (2015) Nat Chem Biol 11:765
87. Bemis KD, Harry A, Eberlin LS, Ferreira C, van de Ven SM, Mallick P, Stolowitz M, Vitek O (2015) Bioinformatics 31:2418
88. Bokhart MT, Nazari M, Garrard KP, Muddiman DC (2018) J Am Soc Mass Spectrom 29:8
89. Patterson NH, Tuck M, Van de Plas R, Caprioli RM (2018) Anal Chem 90:12395
90. Van de Plas R, Yang J, Spraggins J, Caprioli RM (2015) Nat Methods 12:366

Chapter 8
Risks and Consequences of Hazard Agents to Human Health

Diana Coman Schmid

Abstract Human health, as a state of complete physical, mental and social well-being and not merely the absence of disease or infirmity, is under continuous threat posed by various factors, among which the environment plays an instrumental role. Biological, chemical and physical health hazard agents trigger adverse health effects on human health. Notably, the adverse effects of biological health hazards (biohazards) on people is further dependent on both the proximal and on the worldwide environment context, bringing the need of integrative, interdisciplinary and comprehensive approaches, such as One Health and Global Health, to provide sustainable public health strategies. To fight antimicrobial resistance, recognized now as one of the major public health threat, such integrative One and Global Health strategies will be instrumental. Furthermore, because of their versatility, biohazards can be weaponized for use in bioterrorism. In this context, critical and transparent risk analysis is of utmost importance to provide informed support for delineating priorities and for defining opportunities for research, prevention, and policy. Finally, preparedness (commitment to implement and continuously monitor the International Health Regulation, measures to foster research areas like biosurveillance and cyber-biosecurity) at global scale is paramount, as highlighted by the recent report of the Global Preparedness Monitoring Board (September 2019).

Keywords Agent · Biohazard · Biosurveillance · Cyberbiosecurity · Bioterrorism · Human health · Machine learning · Risk

D. C. Schmid (✉)
ETH Zurich, Zurich, Switzerland

8.1   Human Health and Disease

Human Health is defined, according to the World Health Organization (WHO) Constitution [1], as a state of complete physical, mental and social well-being and not merely the absence of disease or infirmity. Furthermore, an important aspect of human health is equality. Unequal development in different countries in the promotion of health and control of diseases, especially communicable disease, is a common danger. In this context, informed public opinion and active cooperation are of the utmost importance for improving the health of people, globally. The WHO definition may be regarded as idealistic but it does confer a holistic description of what characterizes human health. Furthermore, the concept of disease or disability cannot be simply defined as "non-health" or the opposite of health. Given an idealistic definition of health, it is likewise not trivial to define the threshold, for which deviation from perfection to be regarded as disease or disability requiring treatment [2, 3]. Here, we refer to disease as a particular abnormal condition that negatively affects the structure or function of parts or all of an organism, and that is not due to any external injury [4].

Diseases have usually multiple causes. For example, major possible causes of stroke include high blood pressure, heart disease, diabetes, tobacco use, and obesity. These in turn, can be influenced by other factors. One of the such major factor that can influence human health is the environment: clean air and water, safe and adequate food and in general, a stable global environment are promoters of human health. Yet, 23% of total global deaths were attributable to environmental factors in 2016. More than 6.7 million deaths due to respiratory disease, five million deaths due to infectious diseases, two million deaths due to neurological disorders were attributed to environmental factors such as air pollution, inadequate water sanitation or chemical agents [5]. Furthermore, unequal health is apparent, with nearly 92% of environmental pollution-related deaths (i.e., air and water pollution) occurring in low-and middle-income countries, distributed primarily in Africa, Asia, and Eastern Europe.

8.2   Environmental Disasters Impacting Human Health

Several prominent environmental disasters (i.e., catastrophic event due to human activity) impacted human health:

– 1950–1960 Minamata, Japan: methylmercury poisoning as effect of releasing polluted industrial wastewater. This lead to 2,265 victims with neurological syndrome symptoms, out of which 1,784 died.
– 1961–1971 Vietnam: one million people disabled or health impaired as a result of contamination with Agent Orange during the Vietnam War. Agent Orange is a herbicide containing dioxin (associated with cancer and birth defects) that was used by the U.S. military as defoliant agent during the Vietnam War.

– 1986 Chernobyl Ukraine: nuclear reactor accident resulting in the worst nuclear disaster in history. This accident reached the maximum severity on the International Nuclear Event Scale (level 7). The estimated number of deaths from the Chernobyl nuclear disaster ranges from thousands to tens of thousands [6].
– 2011 Fukushima Japan: nuclear disaster of level 7. Noteworthy, in the reports of United Nations Scientific Committee on the Effects of Atomic Radiation (UNSCEAR) from 2014, no significant correlation was found between exposure and increase in miscarriages, stillbirths or physical and mental disorders in babies born after the accident [7].
– 2014–2016 West Africa: the largest Ebola virus disease outbreak followed by the current 2018–2019 outbreak in eastern Democratic Republic of Congo (3,145 cases out of which, 1,992 resulted in death) reported as of September 2019 [8].
– Now, globally: antimicrobial resistance, recognized as one of the major Global Health challenges of the twenty-first century by all major regulatory, economic and political bodies (e.g. the International Monetary Fund, the WHO, the World Bank and the G8). If not tackled now, the predicted death toll could reach as far as one person dying every three seconds by 2050 [9].

8.3   Environmental Health

The environment (i.e., circumstances, objects, or conditions by which one is surrounded) is an important factor impacting the human health. Contrary to what the name implies, the field of environmental health is not focused on the health and well-being of the environment itself. Rather, it refers to human health and well-being as impacted by the environment. As such, the **environmental health** field comprises all the physical, chemical, and biological factors external to a person, and all the related factors impacting behaviors, with the main focus on preventing disease and creating health-supportive environments [10].

The **environmental health** field encompasses several individual study domains to contribute to the broad field of public human health: *environmental epidemiology* (focused on identifying associations between exposure to agents and disease), *environmental toxicology* (investigating causal mechanisms between exposure to agents and disease), *environmental engineering* (focused on reducing exposure), *preventive medicine* (focused on reducing disease development). Furthermore, specific laws and regulations support the field of environmental health by providing the frameworks for implementing appropriate public health strategies.

In the classical environmental health continuum, stressors or agents in air, water, soil, or food are transferred to exposed people by inhalation, ingestion, or absorption, and may produce adverse health effects as an outcome of the exposure [5]. In this context, the complex collection of all exposures and associated biological responses the individuals experience across their life is defined as the *exposome*. The exposome includes any factor of interest that may impact health, such as biological materials, noise, radiation, chemical substances, access to healthy foods, clean water.

Stressors or agents in the exposome that have an impact on human health are referred here to as **health hazard agents** and indicate any biological, chemical, physical or radiological stressor or agent that has the potential to cause harm to human health.

The level of exposures to health hazards ranges from high-level exposures, that may result in acute environmental catastrophes, to chronic low-level exposures and to indirect effects on health, attributed to global environmental change. Following exposure to health hazards, acute or delayed onset adverse effects on human health may be observed. These adverse effects may be reversible or irreversible and may display clinical or subclinical manifestations, such as lung disease, reproductive effects, teratogenic effects, neurologic effects, cancer. Noteworthy, an important factor is the genetic predisposition of individuals to diseases, which together with a combination of exposure to health hazards and duration of exposure, may trigger the manifestation of adverse effects and disease. As emphasized by Prof. Judith Stern, distinguished Professor Emerita of Nutrition and Agriculture & Environmental Sciences at University of California, Davis: "*Genetics loads the gun but environment pulls the trigger*".

8.4   One Health and Global Health

Humans, as part of the environment, are impacted by the co-existence in complex, interdependent relationships, with the companion, production, and wild animals we depend on for our food, livelihoods, and well-being. A notable consequence of sharing the environment between humans and animals, is the *zoonosis process*: a naturally occurring mechanism of disease originating in and being transmitted from animals to humans. As such, *zoonoses* may be of bacterial, viral, or parasitic origin and comprise a large percentage of all newly emerging infectious diseases (75%) as well as existing infectious diseases (60%) [11]. Importantly, *antimicrobial resistance* of human pathogens, currently one of the major public health threat, is partly impacted by use of antibiotics in animals raised for meat production and in agriculture [12]. Furthermore, 80% of the agents with potential bioterrorist use are zoonotic pathogens.

One Health is a broad framework for designing and implementing programs, policies, legislation and research to improve public health outcomes, with a major focus on zoonoses and antimicrobial resistance. One Health acts locally but involving humans and animals, addressing local transmission among connected habitats at cities or at region levels [11]. **Global Health** extends the One Health concept to the world-wide scale and focuses primarily on the corresponding influencing factors such as the communication among local ecosystems and the global conditions that facilitate the worldwide spread of diseases (e.g. through the global interchange of goods by travelling people, migrating animals etc.). An illustrative example for One and Global Health concerted efforts is the public health strategy for fighting antimicrobial resistance (AMR) [13]. Reduction of antibiotic consumption is insufficient

to control AMR. Instead, a coordinated One Health and Global Health approach may assist in controlling AMR by designing and implementing epidemiological and ecological AMR surveillance networks, applying multivariate analysis of AMR drivers (including sociodemographic and economic factors) and by realistically estimating the economic impact of interventions to reduce AMR.

8.5 Classification of Health Hazard Agents

Health hazards cover a wide range of agents, from **physical** (e.g. noise, radiation), **chemical** (e.g. pesticides, explosives) and to **biological agents** (e.g. viruses, bacteria, toxins). These agents may be contained in air, water, soil, or food. Humans are exposed to such health hazards via inhalation, ingestion, or skin absorption and as consequence, manifest adverse health effects with various degrees of severity (acute or delayed in onset, clinical or subclinical, reversible or irreversible).

Nanoparticles, engineered structures with diameters of <100 nm for which currently limited knowledge exists on the adverse effects they might have on human health, are not addressed here [14]. Nevertheless, appropriate evaluation and regulation of nanoparticle effects on health, fostered by transdisciplinary One Health approaches, is of great actuality in the context of the rapid developments in the field of nanotechnology [15].

8.5.1 Physical Health Hazard Agents

Physical health hazards include noise, temperature, vibration, radiation. Exposure to physical health hazard agents may be short or long term and can occur at home, school, work and in the community. Among physical hazard agents, *radiation* is outstanding and associates with carcinogenic effects on human health. Radiation is a natural part of our environment and as such, exposure to small doses of radiation is a casual and constant part of our environment. Radiation is defined as energy emitted in the form of waves or particles, transmitted through an intervening medium or space.

Depending on the capacity of removing electrons during its interaction with atoms, radiation classifies as: *ionizing* (has sufficient energy to remove electrons from atoms) and *non-ionizing* (cannot remove electrons from atoms). Examples of ionizing radiation are the radon gas (naturally occurring), the X-rays and the radiation from nuclear power plants (man-made). Examples of non-ionizing radiation include radio waves, microwaves, infrared, ultraviolet and visible light and radiation from ultrasound and magnetic resonance imaging devices.

Exposure to very high levels of radiation, such as being close to an atomic blast, can cause acute health effects such as skin burns, acute radiation syndrome and may lead to long-term health effects such as cancer and cardiovascular disease. Exposure to low levels of radiation encountered in the environment does not cause immediate health effects, but is a minor contributor to our overall cancer risk.

The average annual radiation dose per person in the U.S. is 6.2 millisieverts and most of the average annual dose comes from natural background radiation, with radon and thoron together amounting to 37% of all natural radiation sources [16].

Radon is a chemically inert, naturally occurring, radioactive gas with no smell, color, or taste, and is produced from the natural radioactive decay of uranium, which is found in rocks and soil. Radon gas escapes easily from rocks and soils into the air and tends to concentrate in enclosed spaces, such as underground mines, houses, and other buildings. Exposure to radon at home and at the workplace is one of the main risks of ionizing radiation causing tens of thousands of deaths from lung cancer each year globally [17]. Radon is the second most important cause of lung cancer after smoking and it is the primary cause of lung cancer among people who have never smoked. Furthermore, based on current observations no reliable threshold concentration below which radon exposure presents no risk can be defined [18].

Although radon is dangerous at high levels indoors, radon levels outdoor are generally very low. Strategies to reduce exposure to radon involve increasing house ventilation and performing radon measurements (with particular focus on quality assurance and quality control measures) using dedicated devices such as alpha-track detectors, electret ion chambers, activated charcoal detectors, electronic integrating devices and continuous radon monitors.

Based on the latest scientific data, the proposed reference level to be used for minimizing health hazards due to indoor radon exposure is 100 Bq/m^3. If this level is not reachable due to country-specific conditions, the chosen reference level should not exceed 300 Bq/m^3 [18, 19]. Exposure to radioactive health hazard agents has resulted from past nuclear weapons testing, nuclear waste disposal, accidents at nuclear power plants, as well as from transportation, storage, loss, and misuse of radioactive sources. While there are risks associated with exposure to radiation, the benefits of nuclear applications in medicine, industry and science are well established. Noteworthy, research reviewing scientific studies linking radiation exposure and cancer, published in a window spanning 40 years and covering over 300,000 nuclear workers from different countries, revealed that even the very lowest levels of radiation are harmful to life [20]. This raises awareness for objectively evaluating the benefits of radiation technology in comparison to the posed known risks. In this context, the WHO's radiation program is one of the international initiatives aiming to assure that the benefits far exceed any known risks of the radiation technology.

8.5.2 Chemical Health Hazard Agents

Chemical hazards can cause acute or chronic adverse health effects, as consequence of short- or long-term exposures. Manifestation of adverse effects range from skin and eye irritation, to chronic diseases (affecting the heart, lung, brain or other organs) and to cancer.

The top 10 categories of chemicals of major public health concern according to WHO are: air pollution, arsenic, asbestos, benzene, cadmium, dioxin and

dioxin-like substances, inadequate or excess fluoride, lead, mercury and highly hazardous pesticides. A total of 1.6 million lives and 45 million disability-adjusted life-years were lost in 2016 due to exposures to chemicals [21].

Pregnant women and children are particularly vulnerable to the adverse effects of chemical hazards, with the so called "intellectual robbers" (e.g. lead, mercury and polychlorinated biphenyl) as notable examples. Lead, is a toxic, cumulative metal that may trigger neurotoxic effects particularly in vulnerable categories such as children and pregnant women. Children are different from adults in several respects, including differences in metabolism, diets, patterns of behavior, growth and changes of organ systems and functions. For example, children absorb up to 4–5 times as much lead as adults. Furthermore, a systematic review found that a dose of 25 μg/kg body weight (Provisional Tolerable Weekly Intake, PTWI) is in fact associated with a decrease of at least 3 intelligence quotient (IQ) points in children and may cause learning disabilities, poor school performance, or violent behaviors [22, 23]. As consequence, the previously establish PTWI was retracted. Furthermore, it was not possible to establish a new PTWI for lead that would be health protective, while the recommendation resumed to using the dose-response analyses as guidelines for assessing the effect magnitude of dietary lead exposure in different populations [23]. Addressing lead exposure would prevent significantly deaths and disabilities. Recent reductions in the use of lead in petrol, paint, plumbing and solder resulted in substantial reductions in lead levels measured in the blood. However, significant sources of exposure to lead still remain, particularly in developing countries. Specifically, as of September 2018, only 36% of countries have legally binding controls on the production, import, sale and use of lead paints [23].

8.5.3 Biological Health Hazard Agents

Biological health hazard agents (**biohazards**) include bacteria, viruses, fungi, other microorganisms and their associated toxins. They can pose a threat to human health when they are inhaled, eaten or come in contact with skin. Biohazards can cause illness such as food poisoning, tetanus, respiratory infections or parasite infection. Biohazards are transmitted through food, air or water, from person to person or from vectors (e.g. animals) to people. The adverse effects of biohazards range from mild, allergic reactions, to serious medical conditions and even death. Furthermore, biohazards can be weaponized for use in bioterrorism.

Notable examples of biohazard agents include: *Bacillus anthracis* (bacterium that causes anthrax), human immunodeficiency virus (HIV), hepatitis B and C viruses (HBV and HCV), *Clostridium botulinum (*bacterium whose toxin causes botulism), Ebola virus (causes Ebola virus disease), *Yersinia pestis* (bacterium that causes plague), ricin (produced from *Ricinus communis*, is the most toxic and easily produced plant toxin), Variola virus (causes smallpox) or Zika virus (causes Zika virus disease).

Biohazards are classified according to the Centers for Disease Control and Prevention (CDC) [24] as:

– **category A:** includes biohazard agents that are easily disseminated or transmitted from person to person and lead to high mortality rates. They require special action for public health preparedness and might cause public panic and social disruption. As such, category A biohazards have the highest priority while having the potential to pose risk to national security. Examples are *Bacillus anthracis*, botulinum toxin, *Yersinia pestis* or Variola virus.
– **category B:** includes biohazards that are moderately easy to disseminate, have moderate morbidity rates and low mortality rates and require specific enhancements of diagnostic capacity and enhanced disease surveillance. A notable example is the ricin toxin.
– **category C:** includes emerging pathogens (e.g. Nipah virus, hantavirus) that could be engineered for mass dissemination and with potential for high morbidity and mortality rates resulting in major health impact.

Noteworthy, while the classification of biological agents is a basic requirement for both biosafety and biodefense strategies, different classification schemes for biohazards exist at international level. Several inconsistencies have been reported, for example the Influenza virus was listed in the highest threat group according to the Russian biodefense categorization, but was included in the second highest category by the European Union classification, and was not specifically listed by the U.S. CDC [25].

8.6   Biohazards and Bioterrorism

Diseases caused by biological health hazard agents are not only a public health issue but also a problem of national security. Biohazards can be weaponized for use in bioterrorism. **Bioterrorism** is the deliberate release of viruses, bacteria, toxins or other harmful agents to cause illness or death in people, animals, or plants [26]. Furthermore, bioterrorist attacks may cause mass panic and fear among the public, chaos in many spheres of life, economic losses and loss of faith in state authorities. A notable example is "*Amerithrax*" event in the U.S. (2011): soon after the terrorist attacks of 9/11, letters contaminated with anthrax spores were placed in the U.S. mail. Overall, 22 clinical anthrax cases and 5 deaths were reported. The ensuing investigation (one of the largest and most complex in the history of law enforcement) resulted in hundreds of million dollars spent on remediation, disruption of the mail service, fear and distrust in the government ability to protect its citizens.

Weapons of mass destruction in bioterrorism include devices produced for military or terrorist purposes, that can cause a large number of victims, or have a broad impact on human life. Such weapons may make use of chemical, biological, radiological and nuclear agents (CBRN) and are illegal to produce and stockpile, under the regulation of the Biological Weapons Convention enacted in 1975. Whereas

biological weapons are a mean applicable for military or other warfare purposes, containing the functional parts necessary for the stabilization and delivery of a pathogen or its toxin, **biological warfare agents** are biohazard agents (e.g., *Bacillus anthracis*, *Yersinia pestis*, botulinum toxin) that can be produced and spread by military or misused by terrorist groups [27]. Biological warfare agents can be legally produced and manipulated for the purpose of medical or other protective research (i.e., development of therapies, new drugs, decontamination means etc.). However, any offensive research programs are banned by the Biological Weapons Convention.

Biological warfare agents that can be weaponized for bioterrorism have several characteristics: they are easy to procure and inexpensive to acquire, simple to use, efficient in small amounts, disseminate easily and at great distance, difficult to detect (invisible, odorless, tasteless), overwhelm medical capabilities and create panic, perpetrators escape before effects. For example, *Bacillus anthracis* has 1–7 (up to 60) days incubation, a high fatality rate and according to WHO estimation, 50 kg Anthrax spores spread over 2 km in a major city may cause up to 95,000 deaths [28]. Botulinum toxin is another notable example, with 12 h to 5 days of incubation, a high fatality rate and lethal at a dose of only 0.001 micrograms/kg body weight [29].

8.7   Risk Assessment of Health Hazards

In this context, it is of utmost importance to analyze and determine the major risk factors that influence human mortality, including health hazard agents and specifically, biological warfare agents. An analysis of risk factors helps to delineate priorities and define opportunities for research, prevention, and policy.

Risk analysis activities include:

- *risk assessment*: the systematic characterization of potential adverse health effects resulting from human exposure to hazardous agents.
- *risk communication*: the process of making risk assessment and risk management information comprehensible to lawyers, politicians, judges, business and labor professionals, environmentalists, and public community groups.
- *risk management*: the process of weighing policy alternatives and selecting the most appropriate regulatory action based on the results of risk assessment and social, economic, and political concerns.

Risk is defined as the probability of an adverse health outcome to occur under specific exposure conditions. The opposite of "risk" is the concept of "safety", which may be interpreted as "without risk" if the probability of risk occurring is lower than one in a million. As such, performing a risk assessment, one is able to determine what level of a health hazard agent will produce an adverse effect in one individual out of one million exposed individuals [30].

Risk assessment processes have usually four main stages: (1) *hazard agent identification* (e.g. does a hazard agent i.e., chemical of concern, cause an adverse health effect, what is the lethal dose or LD50 of the agent, what is the specific form of toxicity e.g. neurotoxicity, carcinogenicity), (2) *exposure assessment* (e.g. hazard agent distribution, routes of exposure, number affected people, what is the intensity, frequency, and duration of exposure, etc.), (3) *dose-response assessment* (e.g. how is the identified adverse health effect influenced by the level of exposure or dose) and (4) *risk characterization* (i.e., estimation of the probability of an adverse health effect in a given population based on integrating the information gathered during the hazard identification, exposure assessment, and dose-response assessment stages). Based on the risk assessment, the public health risks can be estimated and the significance of the risk can be defined. Importantly, the underlying assumptions, uncertainties, and scientific judgements must be documented and communicated along with the outcome of the risk assessment analysis.

An important risk analysis activity is the *risk communication*, which should be an interactive process of exchanging information and opinions among individuals, groups and institutions, related to the nature of risk. Furthermore, other related information, not strictly about risk, expressing concerns, opinions, or reactions to risk or to legal and institutional actions for risk management must be included in the process of risk communication [31]. Finally, the *risk management* activity provides the framework for selecting the most appropriate regulatory actions based on the results of risk assessment and social, economic, and political concerns gathered during the risk communication activities.

Two strategies may be followed in a risk management process: *a risk-based approach* (i.e., define an acceptable level of risk and implement any action required to reduce the risk to the respective level) or a *risk-informed approach* (i.e., define an acceptable level of risk and assess whether or not the risk can be reduced to that level given economic, political, and social considerations). In both approaches, should a satisfactory solution not be identified, a revision and re-definition of the acceptable level of risk should be performed before repeating the risk management processes.

Finally, the risk analysis provides a systematic approach for understanding and designing strategies to reduce a risk. Whereas it considers objective factors (i.e., technical and scientific assessments, evidence based information), risk analysis also includes subjective information (i.e., human wants, societal values, population dichotomies like rich and poor), most of which is hard to quantitate. As result, while accommodating for uncertainty and with the aim of protecting human populations, risk assessments and analyses may tend to be conservative and overestimate risks.

8.7.1 Identification Methods for Biological Warfare Health Hazards

An instrumental activity in risk assessment as part of the risk analysis process, is the identification of health hazard agents. As such, the response to bioterrorism events requires fast analytical methods for identification, that can quickly and specifically detect the biological warfare agents used, allowing effective treatment of the exposed individuals and the implementation of appropriate decontamination measures. As the biological warfare agents are effective in very low quantities, identification methods must exhibit both a high degree of sensitivity and a high degree of selectivity to discriminate them from other interfering biological and non-biological material present in complex samples [32].

Direct identification methods, such as mass spectrometry methods, are instrumental in biological warfare agent analysis because they can address various and complex samples (e.g., air, water, culture medium, bodily fluids, and food), are quick and sensitive. For example, MALDI-TOF MS (Matrix-assisted Laser Desorption/Ionization Time-of-Flight Mass Spectrometry) was shown to reliably identify *B. anthracis* spores with a limit of detection of 2.5×10^6 spores within a 30 min long detection protocol) [32].

The application of direct detection may be hampered, particularly due to the biological agents being available at low concentrations in the samples. Because adverse health effects (i.e., diseases or infections) are linked to changes in physiological traits possibly involving new regulations and connections between molecular entities (e.g., genes, proteins or metabolites), it is plausible that such molecular networks emerging after exposure to agents could offer an indirect signature for the presence of specific hazard agents. In this context, indirect identification methods (e.g., proteomics, metabolomics, breathomics and microbiomics) are promising technologies that could complement the classical direct identification methods. For example, proteomics can be applied for assessing host interaction and discovery of therapeutic targets and markers or for identifying protein signatures of biological health hazards [32].

8.8 Concluding Remarks

The annual report on global preparedness for health emergencies published by the Global Preparedness Monitoring Board (GPMB, 2019) draws an actual and critical alarm signal on the current status of public health. Whereas the past and current efforts, as of 2019, are "grossly insufficient", the emerging and newly emerging disease are increasingly tough to manage (e.g. Ebola outbreak, flu, Zika, antimicrobial resistance) and a pandemic threat is real [33]. As such, the GPMB urges political action to prepare for and mitigate the effects of global health emergencies: (i) governments must commit to preparedness by fostering the implementation of the

International Health Regulations [34] to strengthen the health systems, (ii) adequate funding and incentives must be provided for research into new technologies (i.e., genomics combined with machine learning for biosurveillance, governed by cyber-biosecurity practices [35]) to foster preparedness for "the worst" (e.g. implement global, robust and secure near-live pathogen DNA sequence sharing), (iii) improve coordination and rapid communication systems, and finally, (iv) implement mechanisms for consistent and permanent monitoring of the preparedness progress.

References

1. World Health Organization (2014) BASIC DOCUMENTS Forty-eighth edition. Retrieved from http://apps.who.int/gb/bd/PDF/bd48/basic-documents-48th-edition-en.pdf#page=1. Accessed Oct 2019
2. Misselbrook D (2014) W is for well-being and the WHO definition of health. Br J Gen Pract 64(628):582
3. Scully JL (2004) What is a disease? EMBO Rep 5(7):650–653
4. Wikipedia. Disease. Retrieved from https://en.wikipedia.org/wiki/Disease. Accessed Oct 2019
5. Brusseau ML, Ramirez-Andreotta M, Pepper IL et al (2019) Environmental impacts on human health and well-being. In: Brusseau ML, Pepper IL, Gerba CP (eds) Environmental and pollution science., 3rd. Academic, pp 477–499
6. Our World in Data. Retrieved from https://ourworldindata.org/what-was-the-death-toll-from-chernobyl-and-fukushima. Accessed Oct 2019
7. UNSCEAR (2015). Retrieved from https://www.unscear.org/docs/reports/2015/Fuku-shima_WP2015_web_en.pdf. Accessed Oct 2019
8. World Health Organization (2019) Ebola virus disease – Democratic Republic of the Congo. Retrieved from https://www.who.int/csr/don/19-september-2019-ebola-drc/en/. Accessed Oct 2019
9. Review on Antimicrobial Resistance (2016) Tackling drug-resistant infections globally: final report and recommendations. Retrieved from https://amr-review.org/sites/default/files/160525_Final%20paper_with%20cover.pdf. Accessed Oct 2019
10. World Health Organization. (2019).. Environmental Health. Retrieved from http://www.searo.who.int/topics/environmental_health/en/. Accessed Oct 2019
11. World Organisation for Animal Health (2019) One Health. Retrieved from https://www.oie.int/en/for-the-media/onehealth/. Accessed Oct 2019
12. Rabinowitz P, Conti L (2013) Links among human health, animal health, and ecosystem health. Annu Rev Public Health 34:189–204
13. Hernando-Amado S, Coque TM, Baquero F et al (2019) Defining and combating antibiotic resistance from one health and Global Health perspectives. Nat Microbiol 4:1432–1442
14. Gwinn MR, Vallyathan (2006). Nanoparticles: health effects—pros and cons. Environ Health Perspect 114(12): 1818–1825
15. Lombi E, Donner E, Dusinska M et al (2019) A one health approach to managing the applications and implications of nanotechnologies in agriculture. Nat Nanotechnol 14:523–531
16. United States Environmental Protection Agency (2019) Radiation Sources and Doses. Re-trieved from https://www.epa.gov/radiation/radiation-sources-and-doses. Accessed Oct 2019
17. Mass.gov (2019) Six facts about Radon, the leading cause of lung cancer in nonsmokers. Retrieved from http://blog.mass.gov/blog/health/six-facts-about-radon-the-leading-cause-of-lung-cancer-in-nonsmokers/. Accessed Oct 2019

18. World Health Organization. (2009). Who handbook on indoor radon.. Retrieved from https://apps.who.int/iris/bitstream/handle/10665/44149/9789241547673_eng.pdf;jses-sionid=C24B1F444342DDD6DF1BDF97831913CC?sequence=1. Accessed Oct 2019
19. Radioactivity Environmental Monitoring (2018) Atlas of Natural Radiation. Retrieved from https://remon.jrc.ec.europa.eu/About/Atlas-of-Natural-Radiation. Accessed Oct 2019
20. Richardson DB, Cardis E, Daniels RD et al (2015) Risk of cancer from occupational exposure to ionising radiation: retrospective cohort study of workers in France, the United Kingdom, and the United States (INWORKS). BMJ 351:h5359
21. World Health Organization. (2016) The public health impact of chemicals: knowns and unknowns. Retrieved from https://apps.who.int/iris/bitstream/han-dle/10665/206553/WHO_FWC_PHE_EPE_16.01_eng.pdf?sequence=1. Accessed Oct 2019
22. Yaffe S (ed) (2000) Rational therapeutics for infants and children: workshop summary. Similarities and dissimilarities in physiology, metabolism, and disease states and responses to therapy in children and adults. National Academies Press, Washington, DC
23. World Health Organization (2010) Joint FAO/WHO expert committee on food additives. Retrieved from http://www.fao.org/3/a-at862e.pdf. Accessed Oct 2019
24. Centers for Disease Control and Prevention (2018) Bioterrorism agents/diseases. Retrieved from https://emergency.cdc.gov/agent/agentlist-category.asp. Accessed Oct 2019
25. Tian D, Zheng T (2014) Comparison and analysis of biological agent category lists based on biosafety and biodefense. PLoS One 9(6):e101163
26. Centers for Disease Control and Prevention (2018) Bioterrorism. Retrieved from https://www.cdc.gov/anthrax/bioterrorism/index.html. Accessed Oct 2019
27. Madad SS (2014) Bioterrorism: an emerging global health threat. J Bioterror Biodef 5:129
28. Riedel S (2005) Anthrax: a continuing concern in the era of bioterrorism. Proc (Bayl Univ Med Cent) 18(3):234–243
29. Janik E, Ceremuga M, Saluk-Bijak J et al (2019) Biological toxins as the potential tools for bioterrorism. Int J Mol Sci 20(5):1181
30. World Health Organization (2001) Acceptable risk. Retrieved from https://www.who.int/water_sanitation_health/dwq/iwachap10.pdf. Accessed Oct 2019
31. Frewer L (2004) The public and effective risk communication. Toxicol Lett 149(1–3):391–397
32. Duriez E, Armengaud J, Fenaille F et al (2016) Mass spectrometry for the detection of bioterrorism agents: from environmental to clinical applications. J Mass Spectrom 51:183–199
33. World Health Organization. (2019). Annual report on global preparedness for health emergencies. Retrieved from https://apps.who.int/gpmb/assets/annual_re-port/GPMB_annualre-port_2019.pdf. Accessed Oct 2019
34. World Health Organization. (2019). The international health regulations. Retrieved from https://www.who.int/ihr/about/en/. Accessed Oct 2019
35. Peccoud J, Gallegos JE, Murch R et al (2018) Cyberbiosecurity: from naive trust to risk awareness. Trends Biotechnol 36(1):4–7

Chapter 9
Bacterial Threats to Human Health and Food Supply

Vanessa Sperandio

Abstract Human health is constantly being threatened by bacterial pathogens. Foodborne pathogens are responsible for many health crisis and economic losses worldwide. Diarrheal diseases are the second leading cause of childhood mortality worldwide, and also constitute a severe health threat to adults. Most of the food-borne diseases can be prevented through sanitation. However, rapid pathogen evolution, antibiotic resistance and globalization, lead to the quick emergence or reemergence of enteric pathogens both in the developing and the developed world. Moreover, political and economic instability enhances the chances of a bioterrorism attack. Bacterial, virus, or toxins are all considered biological threat agents, and have been previously employed in attacks. Bacterial pathogens share several virulence strategies amongst themselves. They encode toxins that either kill or change signal transduction in mammalian cells. They also employ specialized secretion systems, "molecular syringes", which inject bacterial proteins called "effectors" that hijack host cell function. These virulence traits tend to be carried in mobile elements that can be quickly transferred between bacteria, leading to the rapid evolution of novel pathovars. Understanding bacterial pathogenic strategies is crucial to prevent or develop new treatments to infectious diseases.

9.1 Introduction

Bacterial pathogens have a huge impact in human health and the global economy. Food borne pathogens mainly cause diarrheal disease and impact food security. According to the WHO, diarrheal diseases are within the top 10 causes of mortality world wide [1]. The economic impact of these diseases is also significant, with decreased productivity due to sick workers, and recall of contaminated food items. It is also noteworthy the threat posed by bioterrorism involving bacterial agents and toxins. Political unrest and economic issues can drive the weaponization of

V. Sperandio (✉)
Department of Microbiology, UT Southwestern Medical Center, Dallas, TX, USA
e-mail: vanessa.sperandio@UTsouthwestern.edu

biothreat agents. Bacterial pathogens share similar strategies to cause disease. They produce toxins that either kill or highjack host cell function. They also have specialized secretory systems, akin to molecular syringes, which directly inject "effector" proteins that change mammalian cell signaling. In this chapter we will discuss some of the main food borne bacterial pathogens and biothreat agents, as well as focusing in the function of their toxins, and mode of action within the host cell.

9.2 Food-borne Pathogens

Bacterial food-borne pathogens are a major cause of gastroenteritis and diarrheal diseases worldwide. The three main species responsible for the majority of outbreaks worldwide are *Salmonella enterica*, *Campylobacter jejuni* and *E. coli*.

Salmonella enterica causes food poisoning and enteric fever [2]. Food poisoning by nontyphoidal *Salmonella* infections leads to diarrhea, fever, nausea, and cramps. These symptoms usually resolve without treatment in 4–7 days. However, nontyphoidal infections have a large public health impact resulting in ~1.4 million infections, 16,000 hospitalizations, and 400–600 deaths annually in the US alone. The economic impact has been estimated to be about $2.4 billion [3]. Most food poisonings are caused by *Salmonella enterica* serovar Typhimurium (*S*. Typhimurium) or *Salmonella enterica* serovar Enteritidis (S. Enteritidis). Typhoid fever is caused by *Salmonella enterica* serovar Typhi (*S.* Typhi) and although it is rare in the US, it is very common in developing nations. Typhoid fever leads to fever, stomach pain, weakness, cough, loss of appetite and mild diarrhea or constipation. An important public health concern is that people can become carriers of *S.* Typhi, even after they cease to have symptoms. Moreover, they can later relapse. It is also worrisome that *Salmonella* has become increasingly resistant to multiple antibiotics [4–8].

Salmonella invades intestinal epithelial cells and replicates within macrophages travelling from Payer's Patches to systemic organs such as spleen and liver. Its virulence repertoire includes expression of two type three secretion systems (T3SSs), which are molecular syringes that deliver several bacterial effector proteins within the host cells. These effectors mimic or highjack host cell function, leading to cytoskeleton rearrangement, changes in signaling and immune responses among others. The first T3SS promotes invasion of intestinal epithelial cells, which are nonphagocytic. The second T3SS allows for survival within macrophages through modifications of the vacuole. T3SS1 is involved in the intestinal phase, while T3SS2 is mostly involved in systemic disease [9] (Fig. 9.1).

Campylobacter jejuni is estimated to cause about 1.3 million illnesses in the US annually. C. jejuni is a food pathogen whose main reservoir is poultry. Infections are usually linked to consumption of raw or undercooked poultry meat. C. jejuni causes bloody diarrhea accompanied by fever and cramps. A severe and debilitating autoimmune complication known as Guillain-Barré syndrome may occur in some patients [10]. C. jejuni is a pathogen for humans but a commensal in poultry. Its

Fig. 9.1 *Salmonella enterica* invades intestinal epithelial cells using the type three secretion system 1 (T3SS1). *Salmonella* survives and replicates within the Salmonella containing vacuole (SCV) within macrophages through the T3SS2
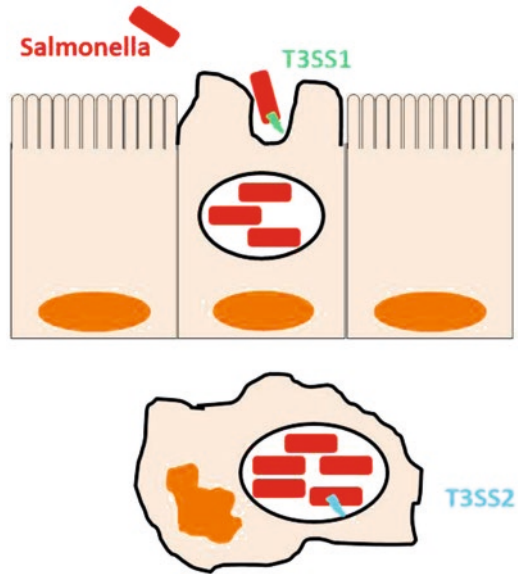
main virulence factor, which is its flagellum, a whip-like structure used for locomotion and cellular adhesion, is also required for colonization of chicks [11].

Diarrheagenic *E. coli* are subdivided in six pathovars according to their virulence repertoire and the disease they cause. Enterotoxigenic *E. coli* (ETEC) causes watery diarrhea mainly in developing nations, and is commonly known as the cause of travelers' diarrhea. ETEC uses afimbrial and fimbrial adhesins to attach to host cells, and delivers exotoxins that cause changes in signal transduction leading to diarrhea. Enteroaggregative *E. coli* (EAEC) is quickly becoming more prevalent as a diarrheal agent in developing countries than ETEC. EAEC adheres in a distinct honey-comb pattern to gut epithelial cells forming a biofilm. The delivery of enterotoxins combined with the biofilm adherence, leads to a longer term colonization and diarrheal disease of the host. Diffuse adherence E. coli (DAEC) is a cause of diarrheal disease in developing nations. Other than its diffuse adherence pattern to epithelial cells, not much is known about the mechanisms that this pathovar engenders to cause disease. Enteroinvasive *E. coli* (EIEC) is really similar to *Shigella*. It causes bloody diarrhea accompanied with inflammation, and high. EIEC and *Shigella* employ a T3SS to invade intestinal epithelial cells. They break free from the vacuole, replicating within the cytoplasm, and spreading in a horizontal manner through the intestinal epithelium. Enteropathogenic *E. coli* (EPEC) is an important cause of diarrhea in infants in developing countries. EPEC causes watery diarrhea by employing a T3SS that allows it to form attaching and effacing lesions on enterocytes. AE lesions are characterized by effacement of the microvilli and rearrangement of the host cell cytoskeleton to cup each bacterium forming a pedestal-like structure. Enterohemorrhagic *E. coli* (EHEC) or Shiga-toxin producing *E. coli* (STEC) cause outbreaks of bloody diarrhea throughout the world, being one of the
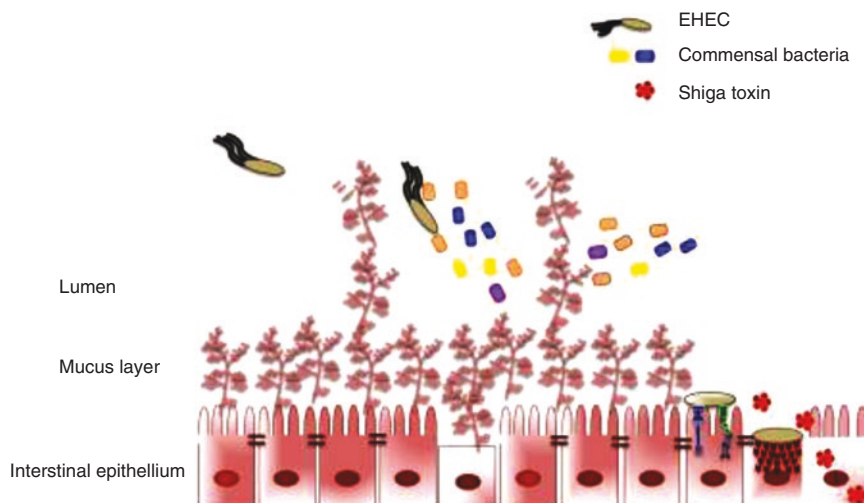
Fig. 9.2 Enterohemorrhagic E. coli (EHEC) has a low infectious dose of 50 bacteria. It colonizes the human colon that is highly populated with a commensal microbiota. EHEC destroys the mucus layer via mucinases to gain access to the epithelium. There through its T3SS it leads to the formation of the attaching and effacing (AE) ledions. It also secretes a toxin, Shiga toxin, which translocates through the intestine reaching the bloodstream and causing hemolytic uremic syndrome

major causes of gastroenteritis in developed nations. EHEC/STEC infections may lead to a complication known as hemolytic uremic syndrome (HUS) that leads to high levels of morbidity and mortality in the young and the elderly. EHEC also forms AE lesions on enterocytes through a T3SS. However, it encodes a potent toxin (Shiga-toxin) that leads to the development of HUS [12] (Fig. 9.2).

9.3   Biothreat Biological Bacterial Agents

The category A bacterial biothreat agents are classified based on the ease of transmission and dissemination, high mortality rates, and their ability to cause panic in the public. The tree bacterial pathogens classified within this class are *Bacillus anthracis* (anthrax), *Yersinia pestis* (plague) and *Francisella tularensis* (tularemia). The main use of these agents in bioterrorism is through their dissemination in the form of aerosols. Inhalation of these agents causes fever, muscle pain, and malaise, which are general symptoms that are hard to discern in time for efficient antibiotic treatment. Moreover, there is concern that several of these agents have been engineered to carry multi-antibiotic resistance [13].

Bacillus anthracis is a Gram-positive ubiquitous soil bacterium that forms spores. Weaponization of anthrax relies on aerosolization of spores. Inhalation of anthrax leads to lung colonization and systemic disease with a high mortality rate. It is noteworthy that anthrax does not spread from person-to-person but through

inhalation of spores. The disease is caused by the systemic effects of the anthrax toxins and a capsule that prevents phagocytosis of this pathogen. The 2011 anthrax attacks that followed the 9/11 terrorist attack in the US led to the rise of panic in the general public, and infusion of funds towards the discovery of novel therapeutics and vaccines [14].

Francisella tularensis causes tularemia, which is classically considered a zoonotic disease and the incidence of human infection is low. *F. tularensis* is a highly infectious pathogen, with as few as 10 organisms being capable of causing disease in humans [15]. The disease can have a number of clinical presentations, and does not spread from person-to-person [16–19].

Due to its high infectivity and lethality in humans, *F. tularensis* has been classified as a high-risk agent for bioterrorism. Furthermore, there is little information on *F. tularensis* pathogenesis, and the only vaccine; *F. tularensis* live vaccine strain, LVS, is not readily available and poorly characterized [20].

F. tularensis seems to employ a secretion system named type six secretion system (T6SS) to deliver effectors into the host cell, but the role of this system in pathogenesis is still not very well defined [21].

Yersinia pestis is the causative agent of bubonic plague that has a mortality rate of 30 to 60%. Unlike anthrax and tularemia, *Y. pestis* can spread from person-to-person. Pneumonic plague is fatal if left untreated, and is considered the main potential form of a. *Y. pestis* infects the host through flea bites (bubonic) or air droplets (pneumonic) biothreat. However, plague has a long history as being used as a biological weapon dating back to ancient China and medieval Europe [22] *Y. pestis* encodes a T3SS and a plasminogen activated protease that are necessary for virulence in pneumonic plague [23].

9.4   Bacterial Toxins at the Host/Bacterium Interface

The most recognizable bacterial virulence factors are toxins. These are bacterial proteins that damage host cells. Toxins have different modes of action, and tend to be classified according to their origin and mode of action. The lipopolysaccharide (LPS) that is a structural component of the bacterial outer membrane is known as endotoxin. The LPS from Gram-negative bacteria is highly toxic and is named endotoxin, given that it is embedded in the membrane. Most toxins, however, are exotoxins, which are not structural components of the bacterial cell and are secreted or exported. They comprise bacterial proteins that are toxic to mammalian cells. They are found in both Gram-positive and Gram-negative bacteria. Toxin nomenclature is based on their target (e.g.: neurotoxin, leukotoxin, hepatotoxin, etc), named according to the bacterial species that produces them or the disease they cause (e..g.: cholera toxin, Shiga toxin, botulinum toxin, tetanus toxin); based on the type of activity they have (e.g.: adenylate cyclase, lecithinase), or are designated by letters (e.g. exotoxin A of *Pseudomonas aeruginosa)*. The majority of bacterial toxins are encoded on mobile genetic elements such as bacteriophages (e.g.

diphteria toxin, cholerae toxin, Shiga toxin) and plasmids (e.g. heat stable toxin and heat labile toxin from enterotoxigenic *E. coli*).

There are three main types of bacterial toxins, classified in Toxins 1–3 according to the location of their target in the host cells:

Type I toxins bind to targets on cell surface and are not translocated into the cell. E.g. superantigens. Superantigens bind to the Major Histocompatibility Complex (MHC) class II of macrophages and the receptors on T cells that interact with MHC. In a normal scenario, macrophages process protein antigens by cleaving them into peptides and display one of these resulting peptides in a complex with MHC class II on the macrophage surface. This peptide-MHC class II complex is recognized by few helper T cells, which have receptors able to recognize it. Superantigens are not processed and since they bind indiscriminately to MHC class II and the T cells receptors, many more macrophage-T helper cell pairs are formed. Thus, instead of stimulating 1 in 10,000 T cells (normal response to an antigen), as many as 1:5 T cells can be stimulated by the bridging action of superantigens. This phenomena causes the release of excessive levels of cytokines (especially IL-2) giving rise to a variety of symptoms (nausea, malaise, vomiting, and fever) that culminate in toxic shock syndrome. E.g. Superantigens are important during streptococcal and staphylococcal infection (Fig. 9.3).

Type 2 toxins compromise the integrity of eukaryotic cell membranes. There are two types of membrane-disrupting toxins: a protein that forms channels in the membrane (because of differences in osmotic strength between the host cell cytoplasm and the environment, these holes in the membrane trigger a rush of water into the cell, rupturing the cell); and an enzyme (phospholipase) that degrades the
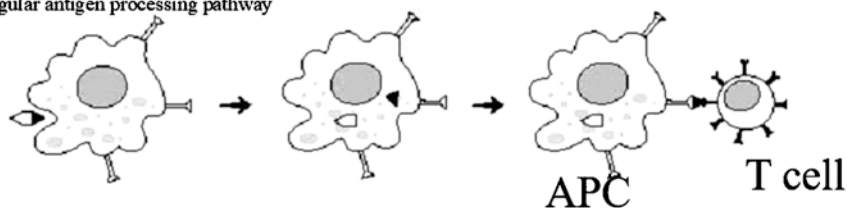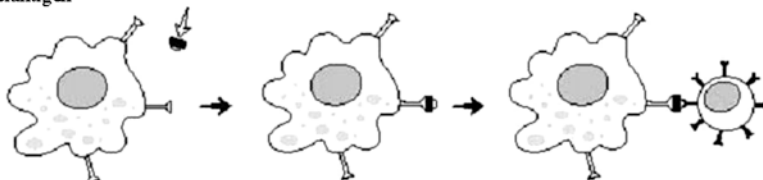
Fig. 9.3 Superantigens are bacterial toxins that bind to Major Histocompatibility Complex (MHC) of macrophages and the receptors on T cells that interact with MHC. This indiscriminant binding activates as many as 1 out of every 5 T cells (1: 10,000 normal response) leading to Toxic shock syndrome
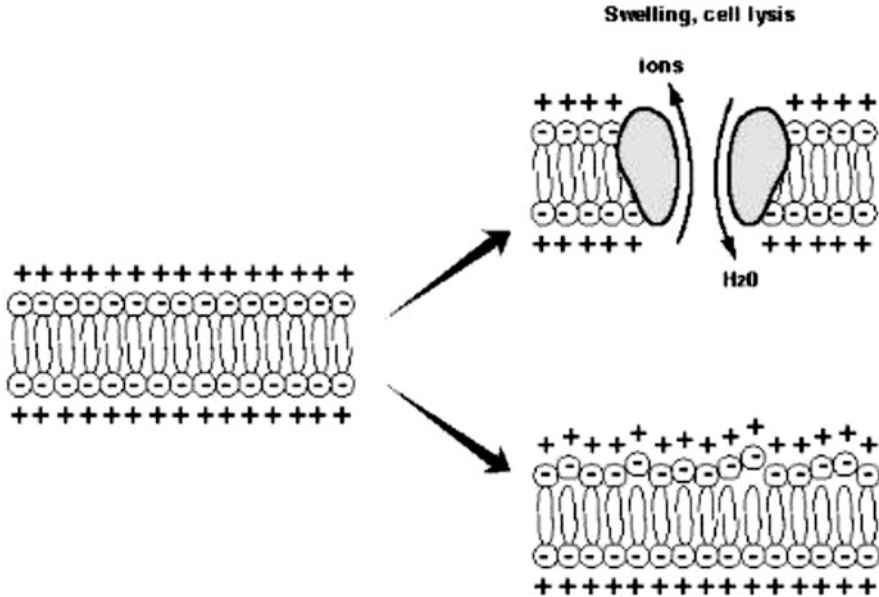
Fig. 9.4 Type II toxins destroy the integrity of eukaryotic membranes by either forming channels in the membrane (pore forming toxins, or by degrading phospholipids (Phospholipases)

phospholipids in the membrane removing the polar head group of the phospholipid. E.g. *Staphylococcus aureus* alpha-toxin is a pore forming toxin (Fig. 9.4).

Type 3 toxins are also known as A-B toxins. A-B toxins are composed of two types of subunits: a "B" subunit that recognizes and binds to the host cell receptor (usually a carbohydrate moiety), and an "A" subunit that has enzymatic activity. AB toxins can be simple having only one A and one B subunit, or can be composed of several B subunits and only one A subunit. The A and B subunits of such toxins are usually separated by a proteolytic cleavage event and they remain connected through a disulfide bond. Both the simple and compound toxins bind to and enter the host cell. The B subunit binds to the host receptor (which is what determines the host cell specificity of the toxin). Following this binding the toxin is endocytosed by the cell and the A subunit (active enzymatic subunit) translocated to the cytoplasm. The A subunit of different toxins enter different cell types according to the distribution of the receptors for the B subunit (which confers host cell specificity).

However, most A subunits catalyze the same reaction: they remove the ADP-ribosyl group from NAD and attach it covalently to a host cell protein. The effects of this reaction vary according to the host cell protein that has been ADP-ribosylated. E.g.: The A subunit of diphtheria toxin ADP-ribosylates elongation factor-2 (a protein that plays an essential role in host cell protein synthesis), therefore killing the host cell by stopping protein synthesis. The A subunit of cholera toxin ADP-ribosylates a regulatory enzyme that controls cyclic AMP levels in the host cell; this prevents the enzyme from being turned off causing the host cell to lose control of

Fig. 9.5 AB toxins are
compound toxins where
the B subunit binds to the
cellular receptor, and the A
subunit has the enzyme
activity. Most A subunits
are ADP-rybosylases, they
remove the ADP-ribosyl
group from NAD and
attach it covalently to a
host cell protein changing
signaling or affecting
protein synthesis
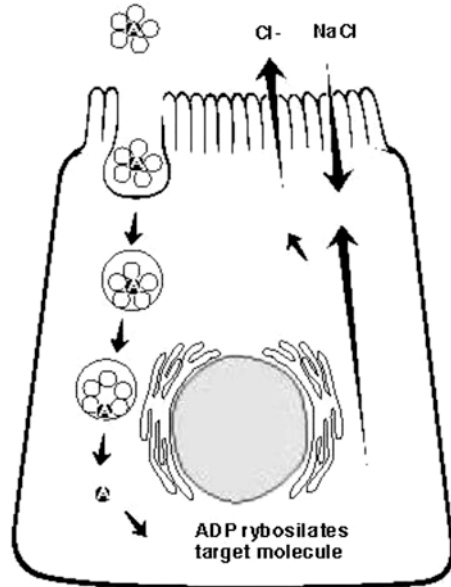
ion flow and resulting in a massive loss of host cell water, which is seen as diarrhea. Other A subunits have different activities, Shiga-toxin A subunit cleaves a host cell rRNA molecule preventing protein synthesis (Fig. 9.5).

References

1. https://www.who.int/news-room/fact-sheets/detail/the-top-10-causes-of-death
2. Boyle EC, Bishop JL, GrassL GA, Finlay BB (2007) Salmonella: from pathogenesis to therapeutics. J Bacteriol 189:1489–1495
3. Frenzen P (2006) Foodborne illness cost calculator [Online]. USDA Economic Research Service. Available: http://www.ers.usda.gov/Data/FoodborneIllness/. Accessed 2 Apr 2007
4. Davis MA, Hancock DD, Besser TE, Rice DH, Gay JM, Gay C, Gearhart L, Digiacomo R (1999) Changes in antimicrobial resistance among Salmonella enterica Serovar typhimurium isolates from humans and cattle in the Northwestern United States, 1982–1997
5. Crump JA, Barrett TJ, Neleson JT, AnguloLO FJ (2003) Reevaluating fluoroquinolone breakpoints for Salmonella enterica serotype Typhi and for non-Typhi salmonellae. Clin Infect Dis 37:75–81
6. Nakaya H, Yasuhara A, Yoshimura K, Oshihoi Y, Izumiya H, Watanabe H (2003) Life-threatening infantile diarrhea from fluoroquinolone-resistant Salmonella enterica typhimurium with mutations in both gyrA and parC. Emerg Infect Dis 9:255–257
7. Weill FX, Bertrand S, Guesnier F, Baucheron S, Cloeckaert A, Grimont PA (2006) Ciprofloxacin-resistant Salmonella Kentucky in travelers. Emerg Infect Dis 12:1611–1612

8. Samrakandi MM, Zhang C, Zhang M, Nietfeldt J, Kim J, Iwen PC, Olson ME, Fey PD, Duhamel GE, hinrichs SH, Cirillo JD, Benson AK (2004) Genome diversity among regional populations of Francisella tularensis subspecies tularensis and Francisella tularensis subspecies holarctica isolated from the US. FEMS Microbiol Lett 237:9–17

9. Galan JE, Wolf-Watz H (2006) Protein delivery into eukaryotic cells by type III secretion machines. Nature 444:567–573

10. https://www.cdc.gov/campylobacter/index.html

11. Burnham PM, Hendrixson DR (2018) Campylobacter jejuni: collective components promoting a successful enteric lifestyle. Nat Rev Microbiol 16:551–556

12. Kaper JB, Nataro JP, Mobley HL (2004) Pathogenic Escherichia coli. Nat Rev Microbiol 2:123–140

13. https://emergency.cdc.gov/agent/agentlist-category.asp

14. Moayeri M, Leppla SH, Vrentas C, Pomerantsev AP, Liu S (2015) Anthrax pathogenesis. Annu Rev Microbiol 69:185–208

15. Golovliov I, Ericsson M, sandstrom G, Tarnvik A, sjostedt a (1997) Identification of proteins of francisella tularensis induced during growth in macrophages and cloning of the gene encoding a prominently induced 23-kilodalton protein. Infect Immun 65:2183–2189

16. Prior RG, klasson L, Larsson P, Williams K, Lindler L, Sjostedt A, Svensson T, Tamas I, Wren BW, Oyston PC, Andersson SG, Titball RW (2001) Preliminary analysis and annotation of the partial genome sequence of Francisella tularensis strain Schu 4. J Appl Microbiol 91:614–620

17. Syrjala H, Sutinen S, Jokinen K, Nieminen P, Tuuponen T, Salminen A (1986) Bronchial changes in airborne tularemia. J Laryngol Otol 100:1169–1176

18. Pullen RL, Styuart BM (1945) Tularemia: analysis of 225 cases. JAMA 129:495–500

19. Stuart BM, Pullen RL (1945) Tularemic pneumonia: review of american literature and report of 15 additional cases. Am J Med Sci 210:223–236

20. Andstrom G (1994) The tularaemia vaccine. J Chem Technol Biotechnol 59:315–320

21. Clemens DL, Lee BY, Horwitz MA (2018) The Francisella type VI secretion system. Front Cell Infect Microbiol 8:121

22. https://www.who.int/news-room/fact-sheets/detail/plague

23. Athem WW, Price PA, Miller VL, Goldman WE (2007) A plasminogen-activating protease specifically controls the development of primary pneumonic plague. Science 315:509–513

Chapter 10
An Overview of Male Reproductive Toxicants: Facts and Opinions

Charles Pineau

Abstract A large variety of exogenous molecules such as therapeutic drugs, agriculture and industrial chemicals, food additives and cosmetics are present in our environment. The continuous exposure of humans to these chemicals raises crucial questions about its impact on health. The male reproductive system has emerged as one of the major toxicity targets of environmental toxicants. In industrialized countries, male infertility caused by exposure to environmental toxicants is becoming a crucial problem. In this review, we will discuss the anatomy of the male reproductive system, in particular that of the testis and epididymis, and reflect on the known mechanisms by which exposure to toxicants contribute to unwanted effects on spermatogenesis. Finally, we will present the relevance of Matrix-Assisted Laser Desorption/Ionization (MALDI) Imaging Mass Spectrometry for studying the distribution of small exogenous molecules such as drugs and their metabolites in male reproductive organs and perform whole-body distribution studies on animal models.

Keywords Testis · Epididymis · Endocrine disruptors · Imaging Mass Spectrometry · Reproductive toxicants

10.1   Introduction

A wide variety of exogenous molecules such as agriculture and industrial chemicals, food additives, cosmetics and therapeutic drugs are present in our environment, *i.e.,* in food, air, water and soil, but also in animals and plants. The continuous

C. Pineau (✉)
Université de Rennes, Inserm, EHESP, Irset (Institut de recherche en santé, environnement et travail) – UMR_S 1085, Rennes, France

Protim, Université de Rennes, Rennes, France
e-mail: charles.pineau@univ-rennes1.fr

exposure to these chemicals raises crucial questions about their impact on human health. Different effects on respiratory, neurological, immunological and endocrine systems are reviewed on a regular basis [1–6]. This recent awareness calls for the development of new analytical techniques that are able to provide rapid information on tissular, cellular and molecular targets of these chemicals and their metabolites. It is also important to study the biological processes implicated in their mechanisms of toxicity.

The risk assessment and characterization of adverse effects of environmental pollutants on human health has become a major issue. Since 1981, guidelines for the testing of chemicals are published and regularly updated by OECD, the Organization of Economic Cooperation and Development. This organism gathers internationally accepted methods used by governments, universities and industrial laboratories to determine the safety of chemicals by evaluating their physicochemical properties, degradation and accumulation in the environment, but also effects on biotic systems (ecotoxicity) and on human health (toxicity). Toxicity tests must evaluate the different adverse effects observed after oral administration, inhalation or contact via the skin of each studied molecule at different dose levels (*i.e.,* repeated, chronic or sub chronic doses) [7]. These effects are skin/eye irritation, mutagenicity, carcinogenicity, neurotoxicity, developmental toxicity, one- and two-generation reproduction, etc. As defined by the OECD test guidelines, toxicokinetic studies must also be conducted to provide information on the absorption, distribution, metabolization and excretion (ADME) of the tested molecule.

The population concerns about changes in our environment and the potential health consequences of these changes have increased over the past decades to become one of the major concerns of this new century. In the 2000's, this concern has seen developments with the release of results showing the increase in the frequency of various abnormalities affecting the reproductive system and/or the different functions controlled by hormones in male and female individuals, in different species, including Man. These results were immediately relayed throughout the world by major international media.

In humans, the concern and debate did crystallize on the fact that sperm production in some parts of the world was decreasing (dropping) and on the increase of genital tract pathologies such as testicular cancers. In women, it is the increase in the frequency of breast cancer and perhaps the possibility of an increase in the frequency of endometriosis, that is the subject of most debates. As a matter of fact, the scientific community now considers that each case of endometriosis can be attributed for half to genetic factors and half to environmental factors, among which endocrine disruptors. A recent study shows that prenatal exposure to Bisphenol A could contribute to the development of a disorder resembling endometriosis in female mice [8].

Several converging indices attribute the increase in the frequency of these abnormalities or conditions to changes in environmental conditions: epidemiological data on migrants between their country of origin and their host country, or between consumer groups for example; experimental biological data on the exposure of wild or laboratory animals to different physical or chemical agents.

In the male, the testis in which spermatogenesis takes place, is an organ which is very vulnerable to toxicants but also to radiations. Paradoxically, for decades, that organ had generally not been studied precisely by toxicologists although the situation has changed over the past ten years with the appearance and concept of endocrine disruptors. Recently, the US Food and Drug Administration has announced the availability of a final guidance for industry entitled "*Testicular Toxicity: Evaluation During Drug Development*". It addresses nonclinical findings that may raise concerns of a drug-related adverse effect on the testes, clinical monitoring of adverse testicular effects early in clinical development, and the design and conduct of a safety clinical trial assessing drug-related testicular toxicity (Center for Drug Evaluation and Research; FDA-2015-D-2306). Interestingly, environmental toxicologists can rely upon this highly valuable guidance when studying the adverse effects of environmental toxicants on male reproduction.

The function of the male reproductive system is to produce male gamete – spermatozoa - and transfer them into the female reproductive tract. The testis is a crucial component in this process, as it produces both spermatozoa, testosterone and other androgens that support male reproductive physiology. Accessory organs and ducts contribute to sperm maturation and transport, among which the epididymis.

10.2   The Testicular Function

The testis is one of the most complex organs because of its anatomical and functional organization. It is divided into two compartments: the interstitial tissue and the seminiferous tubules where spermatogenesis takes place. All of these structures are wrapped in a fibrous envelope called *Tunica albuginea* (Fig. 10.1).

The interstitial tissue is a connective tissue that occupies the space between the seminiferous tubules. It contains resident nerves, blood and lymphatic vessels, Leydig cells, macrophages, and occasionally other cells (*i.e.,* fibroblasts, lymphocytes and mast cells). The primary function of Leydig cells is to produce male steroid hormones, testosterone and it's 5α-reduced metabolites. Testosterone helps to differentiate and develop the male genital glands, as well as the establishment and maintenance of secondary sexual characteristics. On the other hand, together with follicle-stimulating hormone (FSH), testosterone has also essential paracrine functions since it ensures the initiation and maintenance of spermatogenesis.

The tightly coiled seminiferous tubules form the bulk of each testis and account for 60 to 80% of total testis volume in mammals. Seminiferous tubules are bordered by the peritubular cells and consist of an epithelium formed by Sertoli cells between which the germinal cells are dividing and differentiate at different stages of spermatogenesis. Peritubular cells co-secrete with Sertoli cells the extracellular matrix of the *Lamina propria* and are in contact with them. In rodents, peritubular cells form intercellular junctions and constitute one of the elements of the so-called blood-testis barrier (BTB).

Fig. 10.1 Once released from the seminiferous epithelium, spermatozoa are transferred to the epididymis through the *rete testis* and *efferent ductules*. During their transit through this organ, spermatozoa become motile. However, they are not yet competent for fertilization. Spermatozoa finally acquire the ability to fertilize eggs within the female reproductive tract, during a time-dependent process called capacitation. It makes it possible for them to undergo the so-called acrosomal reaction and to bind to the oocyte membrane
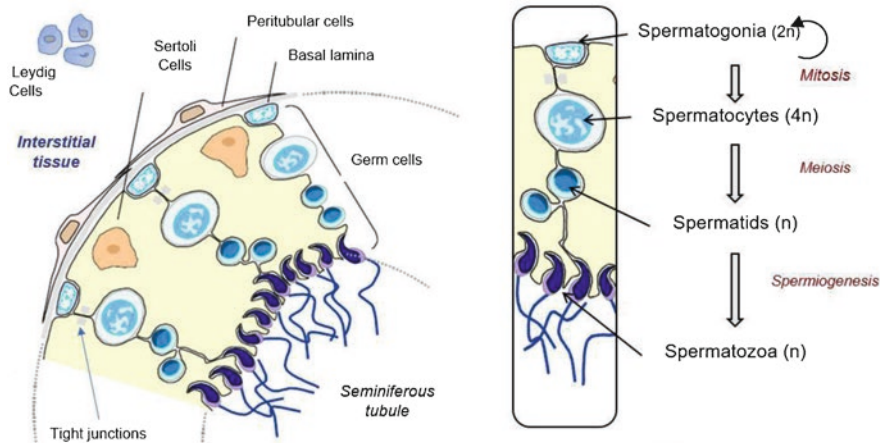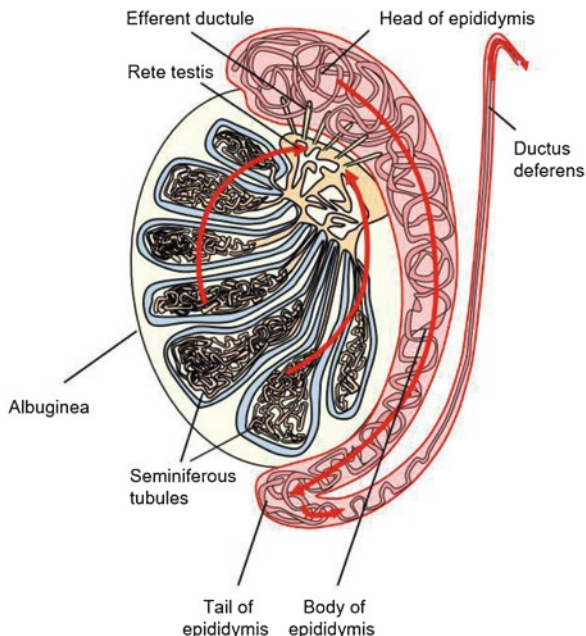
Fig. 10.2 Schematic organization of a seminiferous tubule

Sertoli cells form the wall of seminiferous tubules and extend from the base of tubules to the lumen. During the post-natal development of the testis, at the base of the tubules, Sertoli cells establish between them numerous tight junctions that make up the Sertoli cell barrier, the physical and one of the most important elements of the BTB. Nested between the Sertoli cells, germ cells migrate from the basal compartment of the tubules, where mitotic divisions of germ stem cells take place, to the adluminal compartment where meiosis and spermiogenesis take place (Fig. 10.2).

The process that allows the formation of sperm from germline stem cells is called spermatogenesis. In most mammals, this production continues throughout life, but in others, spermatogenesis is seasonal. This process takes place within the seminiferous tubules. In the first phase of spermatogenesis, differentiating germ cells progress between Sertoli cells, from the base to the lumen of the tubules. Three major steps can be identified: the proliferation of stem cells, spermatogonia, by successive mitosis allows their renewal; meiosis which allows, from spermatogonia, to obtain spermatocytes then round spermatids; and finally, the differentiation of spermatids into highly differentiated cells such as spermatozoa. This last step is called spermiogenesis. Eventually, the spermatozoa are released into the lumen by a process called spermiation. Spermatozoa are moved along a series of ducts in the testis toward a structure called the epididymis for the final steps of post-testicular maturation.

Spermatogonia Spermatogonia are dividing by mitosis and constitute a pool of cells for spermatogenesis. Spermatogonia are divided into two classes according to nuclear morphological criteria, *i.e.,* type A and type B spermatogonia. In order for spermatogenesis to be continuous, it is necessary that spermatogonia not only enter into meiosis, but also self-renew to maintain a constant stock of stem cells within the seminiferous tubules.

Spermatocytes Meiosis consists of two successive cell divisions and allows from a stem cell with 2n chromosomes, the spermatogonia, to obtain n chromosome cells, the spermatids. During the first meiotic division, primary spermatocytes will undergo numerous chromosomal rearrangements allowing a genetic mixing. At the end of the second meiotic division, the secondary spermatozoa will generate haploid cells, the spermatids.

Spermatids and Spermiogenesis The differentiation of spermatids into spermatozoa is called spermiogenesis. This process includes many morphological changes. Spermatids resulting from meiosis will grow longer, lose a lot of cytoplasm and acquire a locomotion structure, the flagella. The loss of cytoplasm is caused by the formation of residual bodies that will be phagocytosed by Sertoli cells at the moment when older spermatids are released into the seminiferous tubule lumen. Other changes also occur in the nucleus of spermatids. Chromatin condenses resulting in a complete repression of gene transcription.

10.2.1 The Cycle of the Seminiferous Epithelium

Depending on the development of the spermatid acrosome and the shape of the nuclei, Leblond & Clermont historically defined 14 stages or associations of germ cells whose composition is constant in the rat with spermiogenesis broken down further into 19 differentiation steps providing a striking and unique example of cell differentiation involving acrosome formation, nuclear condensation and flagellar biogenesis [8].

Another intriguing feature of spermatogenesis is the distinct ordering of cell associations along the length of the seminiferous tubules (segments), often referred to as the 'wave of the seminiferous epithelium' [9]. A segment is defined as a longitudinal portion of seminiferous tubule corresponding to a single cell association or stage (for review see [10, 11] . A wave encompasses all 14 segments in rat, 12 in mouse, and 6 in human (for review see reference [12], but the number of discernible stages in human has been suggested to be increased from 6 to 12, based on acrosome development [13]. At a given point in the tubules, the chronological succession of all stages constitutes a cycle of the seminiferous epithelium. The duration of a cycle corresponds to the interval of time separating two waves of entry of spermatogonia into spermatogenesis. A complete spermatogenesis requires four to five successive cycles. In the longitudinal direction of the tubule, the spermatogenic process is also coordinated because the cell associations succeed one another in an order corresponding to the numerical order of the stages of the cycle. That succession corresponds to the spermatogenetic wave [14].

10.2.2   The Sertoli Cell-Germ Cell Communication System

Due to its unique strategic position within the seminiferous tubules, the Sertoli cell is an orchestrator of the testicular microenvironment. It will play a key role in the paracrine control of spermatogenesis. The BTB established by the sustentacular Sertoli cells will divide the seminiferous epithelium into a basal and an adluminal compartment, thus fulfilling several functions such as the promotion of the seminiferous epithelium architecture; the formation of the environment required for both meiosis and spermiogenesis by preventing a numerous bloodborne substances entering the organ through the testicular blood and lymph streams from penetrating into the depths of the seminiferous epithelium and reaching germ cells; a segregation of the Sertoli cell plasma membrane into distinct regions (for review, see references [15, 16].

Sertoli cell also produce the seminiferous tubule fluid and secrete hundreds of proteins, peptides and steroids, most of which remain to be characterized. The tubule fluid is essential for the nutrition of germ cells, but also for transport of chemical substances, the release of spermatozoa and their transport to the epididymis. Most, if not all Sertoli cell products are destined to support the germ cell lineage through the entire spermatogenic process. These physical and chemical microenvironments are required for the completion of each of the different steps of spermatogenesis. Sertoli cell production can be classified as follows: transport or soluble binding proteins, components of the extracellular matrix, components of Sertoli cell membranes and junctional complexes, proteases, energy metabolites and factors involved in germ cell division, differentiation and metabolism. Interestingly, the seminiferous tubules are also considered an immune sanctuary as tight junctions between Sertoli cells keep surface antigens against developing germ cells from escaping into the bloodstream and prompting autoimmune responses [17].

10.2.3 Germ Cell Activity

Several decades ago, we have hypothesized that germ cell control Sertoli cell structure and function by three major mechanisms: i) morpho-regulatory mechanisms and the involvement of plasma membrane molecules; ii) the transfer of material and cell-shape changes; and iii) the production of germ cell soluble factors. Regarding the latter pathway, it has been demonstrated that germ cells can regulate the activity of Sertoli cell through the secretion of factors of proteinaceous nature (for a review see [18]. Changes in the composition of the germ cell complement and in germ cell size and shape, as well as germ cell divisions and migration, will profoundly affect Sertoli cell morphology and function.

10.2.4 The Peritubular Cell-Seminiferous Epithelium Communication System

The dialog between the myoid peritubular cells, which border the seminiferous epithelium and the Sertoli cells is very important during fetal and post-natal development of the testis The myoid cells contribute to the constitution of the BTB, insure the structural cohesion and contraction of the tubules, and produce, in cooperation with the Sertoli cells, the extracellular matrix, which separates Sertoli from myoid cells. This matrix is required for the promotion and maintenance of Sertoli cell polarity and migration, but also cord formation in the fetal testis.

10.2.5 The Sertoli Cell-Leydig Cell Communication System

Because the seminiferous tubules and the interstitium are anatomically distinct, cells inside the tubules and Leydig cells can only communicate through soluble signals. Indeed, this communication system is simpler than the intratubular communication network. The interdependence of Sertoli cells and Leydig cells, and the crucial role played by testosterone on peritubular and Sertoli cells, and thus on spermatogenesis are well established [19, 20], although, apart from testosterone, the identity of signals these cells may exchange remains poorly known.

10.2.6 Regulation of Spermatogenesis

Spermatogenesis is a very complex process controlled by juxtacrine, paracrine and endocrine factors and conditioned by the successive activation and/or repression of thousands of genes and proteins [21]. In this regard, the local regulation of

spermatogenesis can be considered as a particular cellular achievement. Thus, the testis is considered one of the most complex tissues in the body. This sophisticated communication network has a weak point, such that the dysfunction of one cell type spreads to all other cell types in cascade. This largely explains the particular vulnerability of the testis to exogenous molecules from the environment, and more specifically drugs and xenobiotics. It also explains the general difficulty encountered by the toxicologist in identifying the testicular cell target of a given toxicant and hence its precise mode of action. More or less complex culture systems of isolated testicular cells have been developed over the past decades which represent very useful tools for the toxicologist. Among the different testicular cell types, Sertoli and Leydig cells, have been the ones most usually used for the *in vitro* analysis of toxic compounds. While Sertoli cells are used *in vitro* for mechanistic toxicology studies, the extreme fragility of germ cells prevents their culture for that purpose. However, Sertoli and germ cells can be cultured together for short periods of time.

10.3   The Epididymal Function

The mammalian epididymis is major organ of the male excurrent duct system. It is a single, narrow, tightly-coiled tubule connecting the testis (*i.e.,* efferent ducts) to the *vas deferens.* Its unraveled length was estimated as 6-7 meters in humans with a gross anatomical structure consisting of three histologically and functionally distinct regions, *i.e.*, the *caput*, *corpus* and *cauda.* (for a review see refrence [22]. The epididymis fulfills major functions that are: (i) the storage of spermatozoa produced by the testis; (ii) the preservation of viability for these stored gametes; and (iii) the post-testicular maturation of sperm (for a review see reference [23]. Interestingly, the caput epididymis that is characterized histologically by a thick epithelium with long stereocilia, is involved in absorbing fluid to make the sperm more concentrated.

The epididymis is covered by a two layered pseudostratified epithelium separated from the connective tissue wall by a basement membrane. The two major cell types form the majority of the epithelium. The so-called **Principal cells** are columnar shaped and equipped in the *caput* with stereocilia, long cytoplasmic projections with an actin filament backbone that project into the lumen. Principal cells actively secrete numerous molecules into the lumen. Shorter and pyramid-shaped **Basal cells** which contact the basal lamina are thought to be undifferentiated precursors of principal cells. Stereocilia in the epididymis are non-motile. These membrane extensions aim at increasing the surface area of the cell, allowing for greater absorption and secretion capabilities.

Although morphologically complete, spermatozoa released from the testis are immotile and do not fulfill the requirements for a correct fertilization process (for a review see [23]. Thus, large volumes of testicular fluid are secreted by Sertoli cells to propel them to the epididymis. The core function of stereocilia is to resorb most of this fluid and to create a fluid current that will move immotile sperm deeper into the epididymis.

Highly polarized spermatozoa have eliminated most of its cytoplasm and organelles during spermiogenesis. Interestingly, nuclear gene transcription is switched off when DNA begins to condense in elongating spermatids and testicular sperm are generally considered transcriptionally inert although they retain a few specific coding and non-coding RNAs [24]. In such context, the post-testicular maturation of sperm cells is crucial and will take place during its transit through the epididymis [25]. When the spermatozoon transits from *caput* to *cauda,* numerous biochemical events occur at various subcellular parts of the male gamete, including post-translational modifications of proteins, proteolytic processing, protein redistribution and disappearance, and integration of new components (for a review see [23]. Epididymal sperm maturation events are inextricably linked to the complex epididymal luminal microenvironment [22, 26, 27].

It was demonstrated in the rat model that segmentation of the epididymis is a unique feature that occurs during postnatal development and prior to the appearance of spermatozoa in the epididymal lumen [28] . This segmentation coincides with dramatic changes in morphology of epididymal cells and with regionalized functions that are essential to the different steps of sperm maturation [26]. As a consequence, a plethora of epididymal genes are expressed on a spatially restricted manner along the organ [29]. This regionalized gene expression has been studied in various species (*i.e.,* Human, rat, mouse and boar) and the high degree of gene expression segmentation appeared to be a common feature shared between these species (for a review see [26]. It is now well described that in vertebrates, spermatozoa leaving the testis are unable to fertilize the egg. Thanks to numerous works in animal models, it became clear that the male gamete has to transit through a certain portion of the epididymis in order to do so (for a review see [Indeed, this strongly evidences a role of the epididymis in controlling and/or inducing the final maturation of the spermatozoa.

The mammalian epididymis holds an essential role in promoting the functional maturation of spermatozoa, in addition to their prolonged storage in a viable state. Both processes are supported by a highly specialized luminal microenvironment that is created, and maintained, by the combined secretory and absorptive activity of the lining epithelium. The molecular machinery it employs to regulate the tightly coupled processes of exocytosis and endocytosis remain poorly understood.

In the epididymis, the dominant number of proteins present in the epididymal fluid are synthesized by the epithelium in a region-specific manner and secreted into the tubule lumen [30, 31], for a review see reference [32]. These secretion-absorption events create a special microenvironment for sperm maturation and storage. Studies *in vitro* have also shown that epididymosomes, the vesicles formed after apocrine secretion, exchange material with immature spermatozoa [33, 34], for a review see [35].

Spermatozoa entering the caput epididymis, progress through the corpus and finally reach the cauda region, where they are stored. The transit through the coils of the epididymis takes about 2-3 days in humans (it is longer in other species) and the sperm can be stored in the cauda for another 2–3 days. During their transit in the epididymis, sperm undergo maturation processes necessary for them to acquire motility and fertility (Fig. 10.1). The final maturation of the male gamete, named *capacitation*, will be completed in the female reproductive tracts.

The daily production of testicular spermatozoa varies greatly from one species to another. In animal species used in reproductive toxicology such as the rat and mouse, the very high production of spermatozoa and the existence of a large epididymal reserve of male gametes may mask the reproductive toxicity of a compound at low doses [36]. In the mouse for example, the production of spermatozoa should be reduced by 80 to 90% to observe an impairment of fertility.

10.4 Toxicologic Evaluation of Environmental Chemicals on the Reproductive Sphere

Reproductive toxicity is defined as adverse impacts of chemical substances on sexual function/fertility in adult males and females, as well as developmental toxicity in the offspring. Such substances which interfere in some way with normal reproduction in humans and other species are called reprotoxic.

The evaluation of reproductive toxicity by exogenous molecules can be subdivided into two main sections. On one hand, we must consider direct effects on fertility that include the harmful effects on the libido, sexual behavior, on different aspects of gametogenesis in both sexes, hormonal activity or the physiological response that would disrupt the capacity of fertilization, the fertilization process itself, or development of the fertilized egg up to and including implantation. On the other hand, we will consider the toxicity on development in its broadest sense. That includes any effect disrupting normal development, also well before after birth. Are considered toxic effects on the embryo and the fetus (*e.g.,* abortion, death, reduction body weight, stunting and development, organ toxicity, functional, structural, peri- or post-natal abnormalities) and mental alteration or physical development after birth, up to and including normal pubertal development.

The embryo corresponds to the first period of life intrauterine fertilization at the end of organogenesis. The fetus corresponds to the period of intrauterine life including functional maturation and growth until birth. Relevant fertility studies on one or two generation(s) together with teratogenesis studies allow highlighting the toxic effects on reproduction and the calculation of different indexes used during the evaluation properties of a substance: (i) a fertility index that is the percentage of mating resulting in a pregnancy; (ii) a pregnancy index that is the percentage of gestations ending with the birth of living animals; (iii) a viability index that corresponds to the percentage of newborns who survive at least 4 days; and (iv) a lactation index that is the percentage of living animals at 4 days who are still alive at the time of weaning (*i.e.,* about 21 days in the mouse model).

The toxicologic literature is abounding with examples of environmental chemicals, including pharmaceutical drugs, with adverse and/or deleterious effects on the male reproductive sphere in laboratory animals. Indeed, unless proven otherwise, one can assume that similar effects (*i.e.,* greater, lesser or equal) are likely to occur in humans exposed to these molecules.

10.4.1   *Endocrine Disruptors*

Among the various environmental agents, chemical agents are the focus of attention, and among these, a particular class of agents, the endocrine disruptors (EDs). The most widely accepted definition of an ED is the one provided by the World Health Organization in 2002, according to which "*An endocrine disruptor is a substance or mixture of substances that alters the function of the endocrine system and thereby induces adverse effects in an intact organism, its offspring or within (sub) populations*". However, only very few substances fully meet this definition. As a result, WHO has further work on the definition of potential ED: "*A potential endocrine disruptor is a substance or mixture of substances whose properties could result in endocrine disruption in an intact organism, in its offspring, or within (sub) populations*".

Naturally occurring but also synthetic (*e.g.,* DBCP, PCBs, dioxin and organochlorine pesticides), xenohormones are found in the food chain where it could behave like sex steroid hormones. The first xenohormones studied were xeno-oestrogens, which can mimic the action of estradiol. These hormones exert effects via cellular receptors that can interact with other estrogens, but also with xeno-hormonal substances, because of the common characteristics of their structure. The xeno-estrogens may have been deliberately administered as drugs (*e.g.,* diethylstilbestrol in pregnant women). Xeno-estrogens can also be integrated by food, pollute the air or water or be present on professional sites. There are therefore of synthetic origin (drugs, chemicals and household, cosmetics) or biological, such as phytoestrogens or estrogens present in human waste (urinary estrogen).

In order for a xeno-estrogen to act on a receptor, its binding capacity to this receptor must be sufficient, that the quantity of molecules reaching the target tissue is much greater than that of estradiol, that it does not bind, or misbehave, to the steroid binding proteins present in the biological fluids that might trap it, and finally, that the target cells are exposed to specific moments of development or for a period of sufficient duration.

Of the tens of thousands of man-made chemicals, only a few agents have been tested for their xeno-hormonal activities; that its activities are estrogenic (or anti-), or androgenic (or anti-). But xeno-estrogens present in food and of synthetic origin constitute only a small part of the totality of xeno-estrogens; the rest consists of natural phytoestrogens, especially of plant origin.

In fact, there is very little data available on the possible effects of xeno-hormones on the male and female reproductive sphere in a so-called "normal" environment. On the other hand, experimentally, it was demonstrated yet twenty-five years ago that the administration of several xeno-estrogens at high concentrations, such as organochlorine pesticides (lindane, methoxychlore, polychlorobyphenyls (PCBs)) or alkylphenols (surfactants present in detergents or shampoos), induced alterations of reproductive function in vertebrates. The mechanisms of action of xeno-hormones can be diverse. Indeed, certain xeno-hormonal agents may interfere with the action of estrogens but by pathways not directly involving their binding to the estradiol receptor.

The term "endocrine disruptor", now part of the scientific and popular common language, raises concerns but also questions from practitioners faced with patient questions about environmental causes of their illnesses, or occupational physicians as part of the chemical risk prevention. The concept has now been extended to other hormonal systems than sex steroids, and his definition is still not unanimous in the scientific community [37].

10.4.2   The Testicular Dysgenesis Syndrome

In recent decades, concerns about changes in the environment and their possible consequences for human and animal reproduction have increased. Several studies have described a gradual decline in the production and quality of sperm over time in humans in Western countries. Indeed, in Northern Europe as well as in the United States, the number of spermatozoa per ejaculate has decreased by about 1% per year since the 1940s until today [38–43]. A very recent study conducted in France on a cohort of 26,609 men reports an even greater decrease in the number of spermatozoa and sperm quality [44].

In addition, an increase in the frequency of testicular cancers in Europe has also been described. This frequency increases regularly from 2 to 4% per year in adult men in the 25 to 40 age group The increase in testicular cancers is also described in the American population between 1975 and 2004 [45]. On the other hand, an increase in the incidence of two congenital abnormalities of the external genitalia has also been reported: cryptorchidism, or absence of testicular descent [46] and hypospadias, which is a morphological alteration of the urethra [47]. These correlations have allowed Sharpe and Skakkebaek to hypothesize that these different abnormalities are the symptomatic manifestations of the same syndrome, the TDS (testicular dysgenesis syndrome) which is caused by defects in testicular development during fetal life and may also be caused by genetic, environmental and lifestyle factors, or by a combination of these [48, 49] (Fig. 10.3).

10.5   Evaluation of the Male Reproductive Toxicity of a Substance

10.5.1   Understanding the REACH Regulation

REACH is a regulation of the European Union. It stands for Registration, Evaluation, Authorisation and Restriction of Chemicals. It entered into force on June 1st, 2007 and was adopted to improve the protection of human health and the environment from the risks that can be posed by chemicals, while enhancing the competitiveness of the chemicals industry in the European Union. This regulation also promotes
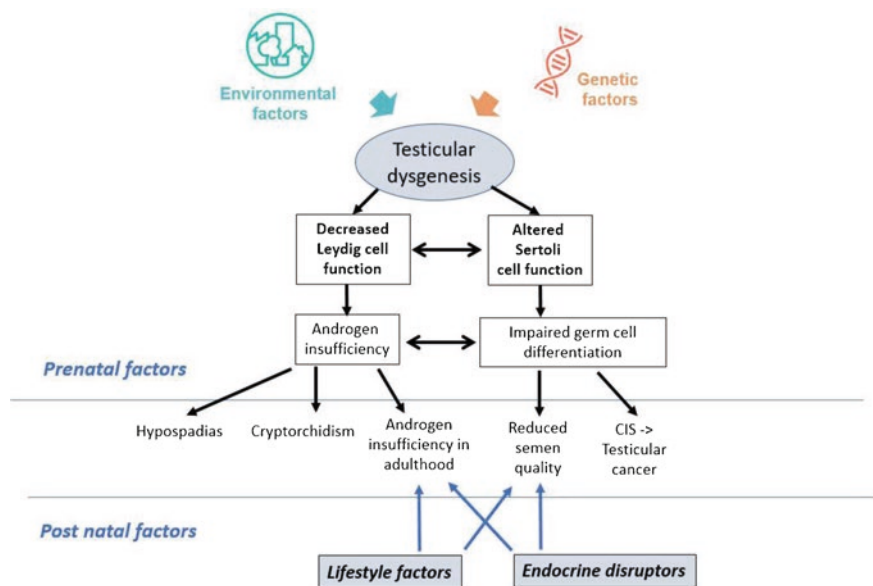
Fig. 10.3 Testicular dysgenesis syndrome (TDS). Adapted from Nordkap et al. (Nordkap, Joensen et al. 2012)[50] with permission. Copyright 2012 Molecular and Cellular Endocrinology

alternative methods for the hazard assessment of substances in order to reduce the number of tests on animals.

REACH applies to about 30,000 chemical substances produced in excess of 1 ton per year and used in industrial processes but also in our day-to-day lives (e.g., paints, cleaning products, cosmetics, electrical appliances, etc.). To comply with the regulation, companies must register their substances, identify and manage the risks linked to the substances they manufacture and market in the EU. They have to demonstrate to the European Chemicals Agency (ECHA) how the substance can be safely used, and must communicate the risk management measures to users. ECHA evaluates individual registrations of substances and the EU Member States evaluate selected substances to clarify initial concerns for human health or for the environment. Authorities and ECHA's scientific committees assess whether the risks of substances can be managed. If the risks cannot be managed, authorities can restrict the use of substances in different ways. In principle, in the long run, the most hazardous substances should be substituted with less dangerous ones.

10.5.2 *Tools for Male Reproductive Toxicity Evaluation*

For all molecules concerned by REACH, it will be necessary to perform a battery of physicochemical, ecotoxicity and toxicity tests. The animal testing required for such tests could result in the use of several million animals, which is difficult to justify. Although REACH and Directive 86/609/EEC2 encourage the use of alternative methods such as cellular models, the European Commission does not define exactly which alternative tests should be used. The assessment is therefore based on tests specified by the OECD, where animal testing is the rule since a few alternative methods have been validated by this organization.

There are several possible routes by which spermatogenesis can be affected by toxicants [19, 20]: (i) an alteration of the hypothalamic-pituitary axis; (ii) the alteration of other functions than that of the hypothalamus, the pituitary or the reproductive system, but which will secondarily lead to adverse effects on spermatogenesis; (iii) the direct disruption of the testicular vasculature or somatic cells in the testis (*i.e.,* Leydig, peritubular, and Sertoli cells); and (iv) a direct effect on the germ cell lineage. Indeed, many of the reproductive toxicants have a primary effect on the testis, which could overshadow the effects downstream on the efferent ducts and/or the epididymis (for a review reference [51]).

For evaluating the testicular toxicity of a substance, in vivo animal models are rare and not always appropriate for mechanistic studies. In vitro studies carried out so far relied on primary cultures of rodent testicular somatic cells (*i.e.,* Leydig or Sertoli cells) or of representative cell lines. However, such systems are not fully relevant to study the effects of potentially toxic compounds on spermatogenesis. Few studies have also used freshly isolated germ cells, grown alone on a short-term period or in the presence of Sertoli cells. But the short survival of germ cells in vitro greatly reduces the usefulness of these models (for a review see reference [52]). Germ cell-Sertoli cell cocultures in bicameral chambers have been developed by Weiss and coworkers [53]. These sophisticated systems reproduce the inter-Sertoli cells tight junctions that are the main physical counterpart of the blood-testis barrier. It thus makes it possible to study the effects and mechanism of action of reproductive toxicants on spermatogenesis, while reducing the number of animals required [53].

Effects of reproductive toxicants on the epididymis will depend upon the dose and time response. The design of specific experiments will be necessary to differentiate testosterone-dependent effects arising within the testis from direct effects on the epididymis and spermatozoa. As a matter of fact, from a toxicologic point of view the epididymis is inherently complicated as the organ structure and function can be altered, both indirectly and directly.

The most spectacular alteration of the epididymis has been described subsequently to a complete androgen withdrawal subsequent to exposure to Ethane dimethanesulphonate (EDS) a potent Leydig cell toxicant [54]. Androgen withdrawal rapidly leads to apoptosis of epithelial epididymal cells and to a reduction of the epididymal tube diameter in the different regions of the organ. Any chemical

altering the testosterone production by Leydig cells may cause androgen deprivation over time in the organ. Another feature of testosterone withdrawal is the appearance in the epididymal lumen of round spermatids that have been sloughed from the testis. However, germ cell loss from the seminiferous epithelium is also a feature of Sertoli cell toxicants, which complicates the evaluation. Testosterone deprivation will also reduce the number of qualitatively normal sperm that enter the epididymis and cause regression of the epididymal epithelium.

Toxicants with a direct effect on the epididymis will alter its structure and function. Effects on the epididymal epithelium may result in degeneration, necrosis and exfoliation of principal cells. An increase of epithelial cell height due to exposure to direct acting epididymal toxicants has also been documented, together with a disappearance in clear cells in the cauda epididymis, particularly the proximal cauda. All effects are commonly restricted to very specific segments of the epididymis, thus highlighting the importance of examining the entire length of the epididymis. To date there are about 20 known toxicants with a direct effect on the epididymis (*e.g.,* Cadmium, ethane dimethanesulphonate (EDS), diethylstilbestrol (DES), chloroethylmethasulfonate (CEMS), methyl chloride, epichlorohydrin, etc.) (for a review, see [51]).

In vitro systems have been developed for evaluating the effect of direct toxicants on the epididymis. Coculture of epididymal epithelial cells and sperm were developed [55, 56] that maintain all facets of normal sperm maturation during epididymal transit. This includes the morphological integrity of epithelial cells and cocultured sperm, but also the protein synthesis and secretion by the epididymal cells and the further association of these proteins to sperm membranes. These coculture systems also successfully promote the acquisition of the capacity for progressive motility of the cocultured sperm. In the early 2000s, a novel rat caput epididymis cell line was characterized [57]. It opens relevant possibilities to study the epithelial cell-cell and spermatozoa-epithelial cell interactions that are involved in sperm maturation.

There are only few examples of toxicants with a direct effect on spermatozoa within the epididymal lumen (*e.g.,* epi-chlorohydrin [58]. It must be noted that these effects are dose-dependent with direct effects on spermatozoa occurring at low dosages (*i.e.,* sperm velocity and fertility), while higher doses induce pathological changes in the epididymis.

These in vitro systems, together with recent advances in technologies, prompt the use of Omics strategies to identify *e.g.* transcriptome and proteome alteration signatures following exposure to reproductive toxicants. It should now provide an in-depth understanding of toxicants effects on the epididymis structure and function.

10.5.3   Key Characteristics of Male Reproductive Toxicants

The International Agency for Research on Cancer (IARC) has introduced the ten key characteristics of human carcinogens to provide a uniform and objective approach for identifying and organizing the mechanistic evidence to support cancer

hazard identification [59]. Recently, Arzuaga and collaborators [60], based on their knowledge of the mechanisms by which chemicals cause reproductive toxicity, have proposed a set of eight key characteristics of male reproductive toxicants that, in combination with male-specific end points, can be applied for the evaluation of toxicological and mechanistic evidence for male reproductive hazard identification [60] (Fig. 10.4).

Based on previous literature reviews and mechanistic analyses of toxicant-induced adverse male reproduction effects, Arzuaga and collaborators [60] have described each key characteristic in the context of mechanisms or pathways by which exposure to male reproductive toxicants (*e.g.,* environmental toxicants, pharmaceuticals, drugs of abuse) can lead to adverse health effects. Examples of toxicants known to affect male reproduction via mechanisms that fall under these eight key characteristics are presented in Table 1. In support of an evaluation of a chemical for male reproductive toxicity, this highly valuable initiative provides a structure for systematically identifying and organizing the relevant literature on mechanistic information.

10.5.4   *Imaging Mass Spectrometry: A Powerful Complementary Tool for Understanding Toxicity Mechanisms*

As defined by the OECD test guidelines, toxicokinetic studies must be conducted to provide information on the absorption, distribution, metabolization and excretion (ADME) of the tested molecule. Toxicokinetic studies are generally based on the use of radiolabeled compounds and on the analysis of tissue homogenates or biological fluids by liquid chromatography-mass spectrometry (LC-MS), gas chromatography–mass spectrometry (GC–MS) and nuclear magnetic resonance (NMR). Quantitative whole-body autoradiography (QWBA) is a commonly used reference technique for distribution studies that involves the administration of the radiolabeled molecule, providing robust, sensitive and quantitative information. However, as QWBA only monitors radioactivity, the parent molecule cannot be differentiated from its metabolites - if any - or degradation products in situ. Therefore, metabolites are generally identified from the analysis of tissue homogenates or biological fluids, leading to the loss of information concerning their *in situ* localization. Since the last decade, IMS [61] has appeared as a powerful alternative for distribution and metabolism studies of small molecules (<1 kDa) [62–65] and could be also useful for the toxicological assessment of chemicals released into the environment. Lagarrigue and coworkers have demonstrated that IMS could be used for the *in situ* absolute quantification of chlordecone, an organochloride pesticide and known endocrine disruptor, in the mouse liver [66]. Their quantification method combines the normalization by an internal standard added to the matrix solution, the correlation with an orthogonal technique (*e.g.,* GC), and the establishment of a correlation curve between the data from IMS and GC, to achieve *in situ* absolute quantification
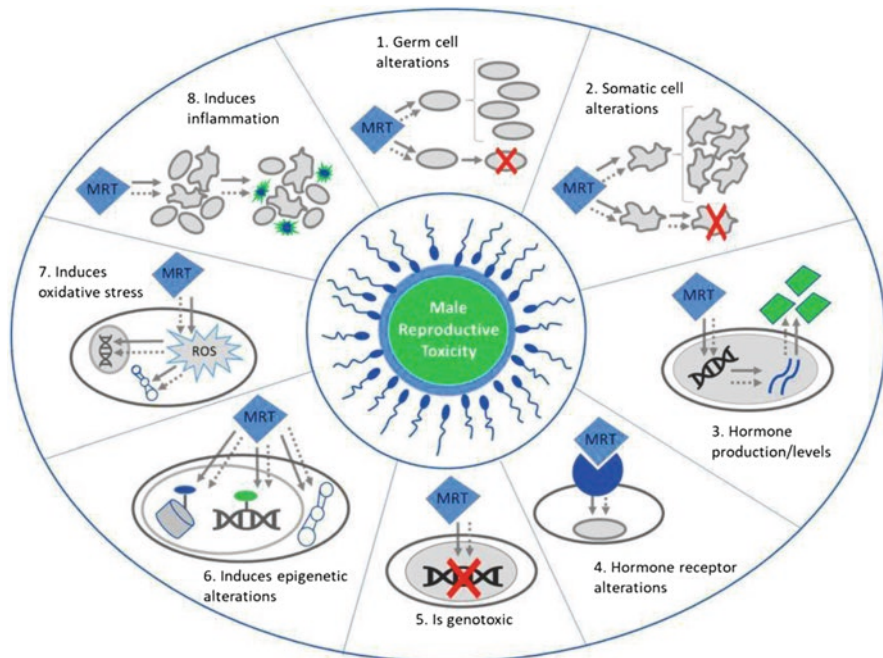
Fig. 10.4 Key characteristics of male reproductive toxicants. Exposure to male reproductive toxicants (MRT) resulting in (1) altered spermatogenesis, normal functions (*e.g.,* acrosome reaction), or increased cell death; (2) disruptions in somatic cell development (*e.g.,* increased or decreased proliferation), functions (*e.g.,* alterations in blood–testis barrier), or death; (3) changes in hormone production/levels; (4) modifies hormone receptor functions/cellular levels; (5) increases DNA damage; (6) epigenetic alterations of cellular macromolecules (DNA, RNA, and/or proteins); (7) reactive oxygen species (ROS)-induced cellular damage; and (8) increases inflammation (*e.g.,* elevated production/levels of pro-inflammatory cytokines and edema). Adapted from Arzuaga et al. (Arzuaga, Smith et al. 2019) with permission. Copyright 2019 Environmental Health Perspectives

(Fig. 10.5). In our hands, the sensitivity of this method is sufficient to detect several reproductive toxicants (*e.g.,* chlordecone, Bisphenol A, paracetamol) at doses conventionally used for toxicological studies in rodents. Moreover, as shown in other publications, IMS offers the advantage of being able to extract quantitative information at the pixel level [67].

Fig. 10.5 In situ absolute quantification of chlordecone in the mouse liver by IMS. (**a**) The quantification method was calibrated with different amounts of chlordecone manually spotted on a control section and normalized with an internal standard (13C10-chlordecone) added in the matrix solution. (**b**) In situ absolute quantification of chlordecone in the pathological liver of a chlordecone and CCl4 treated mouse with the microscopic image of a serial section stained with H&E and the MALDI image corresponding to chlordecone hydrate: the local absolute quantities measured in each necrotic areas are lower than that measured in the healthy tissue (381 μg/g). (**c**) Accumulation profile of chlordecone in the mouse liver after an exposure of 1, 2, 5, 10, or 25 days at 5 mg/kg bw. Adapted from Lagarrigue et al. [66] with permission. Copyright 2014 American Chemical Society

10.6 Conclusion

Both the male and female male reproductive systems appear to be one of, if not the key target of environmental toxicants. In the male, acute toxicants exposure will have an immediate effect leading to apoptosis and necrosis of testicular cells, but that stays relatively rare. The general public is rather exposed chronically to sub-lethal doses [68]. Thus, chronic and low-level exposure to toxicants with very long half-lives could cause long-term unwanted health effects in humans. Assessing the effects of a mixture of environmental toxicants on male reproductive functions is now becoming a priority for scientists. However, these studies are inherently difficult to perform. Thanks to recent developments in Omics technologies and quantification methods developed in IMS unique perspectives are now open for the discovery of alterations in molecular biomarkers (e.g., proteins, metabolites) that could help for a better understanding of toxicity mechanisms on

male reproduction. This priority also corresponds with a strong societal demand. Indeed, humans are exposed to an array of chemicals which might antagonize or agonize each other [69, 70]. Societies now aim at a full understanding of the impact of environmental toxicants on the reproductive system and scientists have legitimately seized the issue.

References

1. Dick S, Friend A, Dynes K, AlKandari F, Doust E, Cowie H, Ayres JG, Turner SW (2014) A systematic review of associations between environmental exposures and development of asthma in children aged up to 9 years. BMJ Open 4(11):e006554

2. Kabir ER, Rahman MS, Rahman I (2015) A review on endocrine disruptors and their possible impacts on human health. Environ Toxicol Pharmacol 40(1):241–258

3. Kalkbrenner AE, Schmidt RJ, Penlesky AC (2014) Environmental chemical exposures and autism spectrum disorders: a review of the epidemiological evidence. Curr Probl Pediatr Adolesc Health Care 44(10):277–318

4. Kravchenko J, Corsini E, Williams MA, Decker W, Manjili MH, Otsuki T, Singh N, Al-Mulla F, Al-Temaimi R, Amedei A, Colacci AM, Vaccari M, Mondello C, Scovassi AI, Raju J, Hamid RA, Memeo L, Forte S, Roy R, Woodrick J, Salem HK, Ryan EP, Brown DG, Bisson WH, Lowe L, Lyerly HK (2015) Chemical compounds from anthropogenic environment and immune evasion mechanisms: potential interactions. Carcinogenesis 36(Suppl 1):S111–S127

5. Thompson PA, Khatami M, Baglole CJ, Sun J, Harris SA, Moon EY, Al-Mulla F, Al-Temaimi R, Brown DG, Colacci A, Mondello C, Raju J, Ryan EP, Woodrick J, Scovassi AI, Singh N, Vaccari M, Roy R, Forte S, Memeo L, Salem HK, Amedei A, Hamid RA, Lowe L, Guarnieri T, Bisson WH (2015) Environmental immune disruptors, inflammation and cancer risk. Carcinogenesis 36(Suppl 1):S232–S253

6. Zeliger HI (2013) Exposure to lipophilic chemicals as a cause of neurological impairments, neurodevelopmental disorders and neurodegenerative diseases. Interdiscip Toxicol 6(3):103–110

7. Parasuraman S (2011) Toxicological screening. J Pharmacol Pharmacother 2(2):74–79

8. Jones RL, Lang SA, Kendziorski JA, Greene AD, Burns KA (2018) Use of a mouse model of experimentally induced endometriosis to evaluate and compare the effects of Bisphenol A and Bisphenol AF exposure. Environ Health Perspect 126(12):127004

9. Leblond CP, Clermont Y (1952) Definition of the stages of the cycle of the seminiferous epithelium in the rat. Ann N Y Acad Sci 55(4):548–573

10. Clermont Y (1972) Kinetics of spermatogenesis in mammals: seminiferous epithelium cycle and spermatogonial renewal. Physiol Rev 52(1):198–236

11. Parvinen M (1982) Regulation of the seminiferous epithelium. Endocr Rev 3(4):404–417

12. Hess RA, Renato de Franca L (2008) Spermatogenesis and cycle of the seminiferous epithelium. Adv Exp Med Biol 636:1–15

13. De Kretser DM, Kerr JB (1988) The cytology of the testis. In: Knobil E, Neill J (eds) The physiology of reproduction. Raven Press, New York, pp 837–932

14. Muciaccia B, Boitani C, Berloco BP, Nudo F, Spadetta G, Stefanini M, de Rooij DG, Vicini E (2013) Novel stage classification of human spermatogenesis based on acrosome development. Biol Reprod 89(3):60

15. Perey B, Clermont Y, Leblond CP (1961) The wave of the seminiferous epithelium in the rat. Am J Anatomy 108:47–77

16. Ploen L, Setchell BP (1992) Blood-testis barriers revisited. A homage to Lennart Nicander. Int J Androl 15(1):1–4

17. Jegou B (1993) The Sertoli-germ cell communication network in mammals. Int Rev Cytol 147:25–96
18. Kaur G, Mital P, Dufour JM (2013) Testisimmune privilege - Assumptions versus facts. Anim Reprod 10(1):3–15
19. Jégou B, Sharpe RM (1993) Chapter 8: Paracrine mechanisms in testicular control. In: de Kretser (ed) The molecular biology of the male reproductive system. Academic, New York, pp 273–310
20. Sharpe RM (1998) Toxicity of spermatogenesis and its detection. In: Korach KS (ed) Reproductive and developmental toxicology. Marcel Dekker, New York, pp 625–634
21. Calvel P, Rolland AD, Jegou B, Pineau C (2010) Testicular postgenomics: targeting the regulation of spermatogenesis. Philos Trans R Soc Lond Ser B Biol Sci 365(1546):1481–1500
22. Cornwall GA (2009) New insights into epididymal biology and function. Hum Reprod Update 15(2):213–227
23. Dacheux JL, Dacheux F (2014) New insights into epididymal function in relation to sperm maturation. Reproduction 147(2):R27–R42
24. Sendler E, Johnson GD, Mao S, Goodrich RJ, Diamond MP, Hauser R, Krawetz SA (2013) Stability, delivery and functions of human sperm RNAs at fertilization. Nucleic Acids Res 41(7):4104–4117
25. Cooper TG, Yeung C-H (2006) Sperm maturation in the human epididymis. In: De Jonge C, Barratt C (eds) The sperm cell production, maturation, fertilization, regeneration. Cambridge University Press, Cambridge, UK, pp 72–107
26. Belleannee C, Thimon V, Sullivan R (2012) Region-specific gene expression in the epididymis. Cell Tissue Res 349(3):717–731
27. Sullivan R, Mieusset R (2016) The human epididymis: its function in sperm maturation. Hum Reprod Update 22(5):574–587
28. Sun EL, Flickinger CJ (1979) Development of cell types and of regional differences in the postnatal rat epididymis. Am J Anat 154(1):27–55
29. Rodriguez CM, Kirby JL, Hinton BT (2001) Regulation of gene transcription in the epididymis. Reproduction 122(1):41–48
30. Dacheux JL, Belghazi M, Lanson Y, Dacheux F (2006) Human epididymal secretome and proteome. Mol Cell Endocrinol 250(1-2):36–42
31. Belleannee C, Labas V, Teixeira-Gomes AP, Gatti JL, Dacheux JL, Dacheux F (2011) Identification of luminal and secreted proteins in bull epididymis. J Proteome 74(1):59–78
32. Dacheux JL, Belleannee C, Jones R, Labas V, Belghazi M, Guyonnet B, Druart X, Gatti JL, Dacheux F (2009) Mammalian epididymal proteome. Mol Cell Endocrinol 306(1-2):45–50
33. Frenette G, Sullivan R (2001) Prostasome-like particles are involved in the transfer of P25b from the bovine epididymal fluid to the sperm surface. Mol Reprod Dev 59(1):115–121
34. Oh JS, Han C, Cho C (2009) ADAM7 is associated with epididymosomes and integrated into sperm plasma membrane. Mol Cells 28(5):441–446
35. Sullivan R, Saez F (2013) Epididymosomes, prostasomes, and liposomes: their roles in mammalian male reproductive physiology. Reproduction 146(1):R21–R35
36. Williams J, Reel JR, George JD, Lamb JC (1990) Reproductive effects of diethylene glycol and diethylene glycol monoethyl ether in Swiss CD-1 mice assessed by a continuous breeding protocol. Fundam Appl Toxicol 14(3):622–635
37. Multigner L (2012) Perturbateurs endocriniens : une exposition difficile à estimer en l'absence de définition claire. Le concours médical 134(10):2–4
38. Carlsen E, Giwercman A, Keiding N, Skakkebaek NE (1992) Evidence for decreasing quality of semen during past 50 years. BMJ 305(6854):609–613
39. Auger J, Kunstmann JM, Czyglik F, Jouannet P (1995) Decline in semen quality among fertile men in Paris during the past 20 years. N Engl J Med 332(5):281–285
40. Irvine S, Cawood E, Richardson D, MacDonald E, Aitken J (1996) Evidence of deteriorating semen quality in the United Kingdom: birth cohort study in 577 men in Scotland over 11 years. BMJ 312(7029):467–471

41. Swan SH, Elkin EP, Fenster L (2000) The question of declining sperm density revisited: an analysis of 101 studies published 1934–1996. Environ Health Perspect 108(10):961–966

42. Merzenich H, Zeeb H, Blettner M (2010) Decreasing sperm quality: a global problem? BMC Public Health 10:24

43. Sharpe RM (2012) Sperm counts and fertility in men: a rocky road ahead. Science & Society Series on Sex and Science. EMBO Rep 13(5): 398–403.+ Toppari J, Larsen JC, Christiansen P, Giwercman A, Grandjean P, Guillette LJ, Jr., Jegou B, Jensen TK, Jouannet P, Keiding N, Leffers H, McLachlan JA, Meyer O, Muller J, Rajpert-De Meyts E, Scheike T, Sharpe R, Sumpter J, Skakkebaek NE (1996) Male reproductive health and environmental xenoestrogens. Environ Health Perspect 104 (Suppl 4): 741–803

44. Rolland M, Le Moal J, Wagner V, Royere D, De Mouzon J (2013) Decline in semen concentration and morphology in a sample of 26,609 men close to general population between 1989 and 2005 in France. Hum Reprod 28(2):462–470

45. Holmes L Jr, Escalante C, Garrison O, Foldi BX, Ogungbade GO, Essien EJ, Ward D (2008) Testicular cancer incidence trends in the USA (1975-2004): plateau or shifting racial paradigm? Public Health 122(9):862–872

46. Toppari J, Kaleva M, Virtanen HE (2001) Trends in the incidence of cryptorchidism and hypospadias, and methodological limitations of registry-based data. Hum Reprod Update 7(3):282–286

47. Paulozzi LJ, Erickson JD, Jackson RJ (1997) Hypospadias trends in two US surveillance systems. Pediatrics 100(5):831–834

48. Skakkebaek NE, Rajpert-De Meyts E, Main KM (2001) Testicular dysgenesis syndrome: an increasingly common developmental disorder with environmental aspects. Hum Reprod 16(5):972–978

49. Sharpe RM, Skakkebaek NE (2008) Testicular dysgenesis syndrome: mechanistic insights and potential new downstream effects. Fertil Steril 89(2 Suppl):e33–e38

50. Nordkap L, Joensen UN, Blomberg Jensen M, Jorgensen N (2012) Regional differences and temporal trends in male reproductive health disorders: semen quality may be a sensitive marker of environmental exposures. Mol Cell Endocrinol 355(2):221–230

51. De Grava Kempinas W, Klinefelter GR (2014) Interpreting histopathology in the epididymis. Spermatogenesis 4(2):e979114

52. Pineau C, Dupaix A, Jegou B (1999) The co-culture of Sertoli cells and germ cells: applications in toxicology. Toxicol In Vitro 13(4-5):513–520

53. Weiss M, Vigier M, Hue D, Perrard-Sapori MH, Marret C, Avallet O, Durand P (1997) Pre- and postmeiotic expression of male germ cell-specific genes throughout 2-week cocultures of rat germinal and Sertoli cells. Biol Reprod 57(1):68–76

54. Klinefelter GR, Laskey JW, Roberts NL (1991) In vitro/in vivo effects of ethane dimethanesulfonate on Leydig cells of adult rats. Toxicol Appl Pharmacol 107(3):460–471

55. Klinefelter GR (1992) J Tissue Cult Methods 14:195–200

56. Chen YC, Bunick D, Bahr JM, Klinefelter GR, Hess RA (1998) Isolation and culture of epithelial cells from rat ductuli efferentes and initial segment epididymidis. Tissue Cell 30(1):1–13

57. Dufresne J, St-Pierre N, Viger RS, Hermo L, Cyr DG (2005) Characterization of a novel rat epididymal cell line to study epididymal function. Endocrinology 146(11):4710–4720

58. Slott VL, Jeffay SC, Dyer CJ, Barbee RR, Perreault SD (1997) Sperm motion predicts fertility in male hamsters treated with alpha-chlorohydrin. J Androl 18(6):708–716

59. Smith MT, Guyton KZ, Gibbons CF, Fritz JM, Portier CJ, Rusyn I, DeMarini DM, Caldwell JC, Kavlock RJ, Lambert PF, Hecht SS, Bucher JR, Stewart BW, Baan RA, Cogliano VJ, Straif K (2016) Key characteristics of carcinogens as a basis for organizing data on mechanisms of carcinogenesis. Environ Health Perspect 124(6):713–721

60. Arzuaga X, Smith MT, Gibbons CF, Skakkebaek NE, Yost EE, Beverly BEJ, Hotchkiss AK, Hauser R, Pagani RL, Schrader SM, Zeise L, Prins GS (2019) Proposed key characteristics of male reproductive toxicants as an approach for organizing and evaluating mechanistic evidence in human health Hazard assessments. Environ Health Perspect 127(6):65001

61. Caprioli RM, Farmer TB, Gile J (1997) Molecular imaging of biological samples: localization of peptides and proteins using MALDI-TOF MS. Anal Chem 69(23):4751–4760

62. Solon EG, Schweitzer A, Stoeckli M, Prideaux B (2010) Autoradiography, MALDI-MS, and SIMS-MS imaging in pharmaceutical discovery and development. AAPS J 12(1):11–26

63. Prideaux B, Stoeckli M (2012) Mass spectrometry imaging for drug distribution studies. J Proteome 75(16):4999–5013

64. Cobice DF, Goodwin RJ, Andren PE, Nilsson A, Mackay CL, Andrew R (2015) Future technology insight: mass spectrometry imaging as a tool in drug research and development. Br J Pharmacol 172(13):3266–3283

65. Arzuaga X, Smith MT, Gibbons CF, Skakkebaek NE, Yost EE, Beverly BEJ, Hotchkiss AK, Hauser R, Pagani RL, Schrader SM, Zeise L, Prins GS (2019) Proposed key characteristics of male reproductive toxicants as an approach for organizing and evaluating mechanistic evidence in human health Hazard assessments. Environ Health Perspect 127(6):65001

66. Lagarrigue M, Lavigne R, Tabet E, Genet V, Thome JP, Rondel K, Guevel B, Multigner L, Samson M, Pineau C (2014) Localization and in situ absolute quantification of chlordecone in the mouse liver by MALDI imaging. Anal Chem 86(12):5775–5783

67. Porta T, Lesur A, Varesio E, Hopfgartner G (2015) Quantification in MALDI-MS imaging: what can we learn from MALDI-selected reaction monitoring and what can we expect for imaging? Anal Bioanal Chem 407(8):2177–2187

68. Hauser R, Sokol R (2008) Science linking environmental contaminant exposures with fertility and reproductive health impacts in the adult male. Fertil Steril 89(2 Suppl):e59–e65

69. Moline JM, Golden AL, Bar-Chama N, Smith E, Rauch ME, Chapin RE, Perreault SD, Schrader SM, Suk WA, Landrigan PJ (2000) Exposure to hazardous substances and male reproductive health: a research framework. Environ Health Perspect 108(9):803–813

70. Wong EW, Cheng CY (2011) Impacts of environmental toxicants on male reproductive dysfunction. Trends Pharmacol Sci 32(5):290–299

Chapter 11
Defense Against Biological Terrorism: Vaccines and Their Characterizations

Mauro Bologna, Abanoub Mikhael, Ilaria Bologna, and Joseph H. Banoub

Abstract This chapter presents an introduction to infective diseases and potential biological agents that could potentially be used for bioterrorism. Technical brief description of the possible treatments and preventions of these biothreats is presented with emphasis placed on the principles of immunological defenses, vaccination, and preparation of vaccines. In principle, various types of vaccines that are commercially used as "antibacterial or anticancer vaccines" can be produced using various types of antigenic carbohydrate haptens containing relevant epitopes. This review highlights the strategies used for the characterization of such synthetic neoglycoconjugate vaccines used as a means of protection against biothreats. A complete mass spectrometry-based strategy for validating the preparations of the neoglycoconjugate vaccine is presented.

Keywords Biological agents · Toxins · Poisons · Immunology · Vaccines · Neoglycoconjugates · Mass spectrometry

M. Bologna · I. Bologna
General Pathology, Department of Medicine, Health, Life and Environmental Sciences, Medical School and Biological Sciences School, University of L'Aquila, L'Aquila, Italy

A. Mikhael
Department of Chemistry, Memorial University of Newfoundland, St John's, NL, Canada

J. H. Banoub (✉)
Department of Fisheries and Oceans Canada, Science Branch, Special Projects, St John's, NL, Canada

Department of Chemistry, Memorial University of Newfoundland, St John's, NL, Canada
e-mail: joe.banoub@dfo-mpo.gc.ca

11.1 Classification of Diseases Caused by Biological Terrorism

In the light of recent concern and interest about the potential for biological terrorism (biowarfare), there are several diseases and bacterial toxins that must be considered in particular, like anthrax [1, 2], smallpox [3, 4], plague [5], botulinum toxin [6], and tularemia [7]. A very detailed discussion of such diseases and other infectious diseases with similar risks in terms of bioterrorism goes beyond the scope of this concise chapter, but some features of these and other infectious diseases representing important threats in the biowarfare field will be mentioned. In this respect, we may distinguish in time diseases which are:

1. old diseases which are disappearing and sometimes returning, like smallpox and poliovirus infections (which are either extinct or close to be eradicated, thanks to planetary vaccination programs);
2. diseases still active at present times, like carbuncle (anthrax), plague, tularemia, tetanus, botulinum, TBC, etc.;
3. New diseases, which are appearing/spreading, like SARS (SevereAcute Respiratory Syndrome) and its more recent variety of MERS (Middle-East Respiratory Syndrome), infections by Ebola/Marburg viruses, hantavirus, filovirus, novel Flu virus strains and coronavirus COVID-19.

The next section is dedicated to the essential facts concerning these diseases. For a complete medical reference to all of them, see, for instance, the Merck Manual of Diagnosis and Therapy [8].

11.1.1 Old Infective Diseases

11.1.1.1 Smallpox (Variola)

Smallpox is a highly contagious disease (incubation 10–12 days) caused by the smallpox virus, an orthopoxvirus. It causes death in up to 30% of infected subjects. The indigenous infection has been eradicated (last case, Ethyopia, 1990 – WHO). The main concern for outbreaks of smallpox is today from bioterrorism. Smallpox is characterized by severe constitutional symptoms (fever, headache, extreme malaise) and a characteristic pustular rash. Treatment is supportive; prevention involves vaccination, which, because of its risks (eczema, encephalitis, etc.), is done selectively.

The pathogenesis of smallpox demonstrates that the virus is transmitted from person to person by direct contact or inhalation of droplet nuclei. Clothing and bed linens can also spread infection. Most contagions are in the first 7–10 days after the skin rash appears. Once crusts form, the infectivity declines. The virus invades the oropharyngeal and respiratory mucosa, multiplies in regional lymph nodes, causing viremia and localization in small blood vessels of the skin (rash) and rarely in CNS (encephalitis).

Officially, smallpox has been wiped out in the world. There are no longer cases detected in the world population since 1990. An ethical question remains concerning smallpox. Are we allowed to destroy old samples of smallpox virus (used as standard reference material), which are kept in some virology laboratories around the world? Certainly not [3], because we could no longer prepare proper vaccines without the live virus samples to start from. And without the vaccine, a small number of wild viruses could ignite a wide epidemic killing a large proportion of the human population since the vaccination is no longer mandatory in any country, and a large percentage of young populations have no longer been vaccinated after the early 1990s.

11.1.2   Existing Active Infective Diseases

11.1.2.1   Anthrax (Carbuncle)

Anthrax is caused by *Bacillus anthracis*, toxin-producing, encapsulated, aerobic or facultative anaerobic organisms. Anthrax, an often-fatal disease of animals, is transmitted to humans by contact with infected animals or their products (woolsorter's disease). In humans, infection typically occurs through the skin. Inhalation infection is less common; oropharyngeal, meningeal, and GI infections are rare. For inhalation and GI infections, nonspecific local symptoms are typically followed in several days by severe systemic illness, shock, and often death. Empiric treatment is with ciprofloxacin or doxycycline. A vaccine is available (antitoxin).

Pathogenesis of anthrax takes place since *Bacillus anthracis* readily forms spores when germs encounter a dry environment -a condition unfavorable for growth. Spores resist destruction and can remain viable in soil, wool, and animal hair for decades.

Spores germinate and multiply in favorable conditions (wet skin, tissue, blood) and can give human disease by contact (papules, black eschars, contagious also via fomites), ingestion (raw meat → fever, nausea, vomiting, diarrhea), and inhalation (flu-like illness, respiratory distress, cyanosis, shock, coma). Needless to say, that biothreats with anthrax attacks through mailings (using spores in powder form) have already taken place in the USA in 2001 (US Postal Service, Washington DC). This event highly sensitized the public to the global theme of bioterroristic attacks.

11.1.2.2   Plague (Pestis, Black Death)

Plague is caused by *Yersinia pestis* (formerly named *Pasteurella pestis*). Short bacillus with hairpin shape, infects wild rodents and can infect humans via tick bites. Symptoms are either severe pneumonia or massive lymphadenopathy with high fever, often progressing to septicemia. Diagnosis is epidemiologic and clinical, confirmed by culture and serologic testing. Treatment is with streptomycin or doxycycline. Unfortunately, a vaccine is not available for the plague.

11.1.2.3 Tetanus

Tetanus is an acute poisoning from a neurotoxin produced by *Clostridium tetani.* Symptoms are intermittent tonic spasms of voluntary muscles. The spasm of the masseters accounts for the name "lockjaw" (trismus). Incubation requires 2–10 days. The diagnosis is clinical. Treatment is with immune globulin and intensive support. The only unbound toxin can be neutralized. A vaccine is available, with a good extent of preventive protection.

11.1.3 New Infective Diseases

11.1.3.1 Ebola/Marburg Diseases

Marburg and Ebola are filoviruses that cause hemorrhage, multiple organ failure, and high mortality rates. Diagnosis is with enzyme-linked immunosorbent assay, PCR, or electron microscopy. Treatment is supportive. Strict isolation and quarantine measures are necessary to contain outbreaks. Incubation 5–10 days. Marburg virus has been identified in bats and primates. Human to human transmission occurs via skin and mucous membranes contact (humans/primates). Filoviruses can affect intestines (nausea, vomiting, diarrhea), respiratory tract (cough, pharyngitis), liver (jaundice), CNS (delirium, stupor, coma), and cause hemorrhagic phenomena (petechiae, frank bleeding) with high mortality rates (up to 90% with Ebola virus). Survivors recover very slowly and may develop long-lasting complications (hepatitis, uveitis, orchitis) with only supportive care available. No specific antivirals nor vaccines are available for filovirus infections.

11.1.3.2 Influenza Virus, with New Strains, Continuously Appearing

Last but not least, we must now mention influenza! Flu viruses are in nature among the most rapidly changing (mutating) organisms through their ability to infect a variety of hosts: birds (migrating waterfowl -ducks-, stantial poultry -chickens-), mammals (pigs, felines), and humans. In southeast Asia (mostly in China, but also in Viet-Nam, Laos, Thailand, etc.), it is widespread to have mixed farms of pigs, poultry and ducks, attended by humans. Every year, new strains appear in SE-Asia is favored by the reciprocal passage between migrating birds (mostly fowl), pigs, and chickens, with exposure of many humans in farms, markets, rooster fighting sports, and food preparation places.

A common say in China tells that "Anything with four legs (except chairs), and anything that flies (except airplanes) can be eaten." With this philosophy, there is generally a lot to be desired in food safety and general hygienic prevention in such geographical areas.

After the avian flu H5N1 of 2005–2006, highly lethal but unable to give human to human contagion, new combinations of flu strains are expected and feared, with high lethality and high human to human transmissibility.

11.1.4   New Virus Causing World Pandemic

Actually, concerning the world diffusion of new virus strains with pandemic potential, the world has been shaken by the recent coronavirus, also known as COVID-19, which has spread to all countries in the world. A new protocol to investigate the extent of COVID-19 infection in the population, as determined by positive antibody tests in the general population, has been developed. The protocol is titled the Population-based age-stratified seroepidemiological investigation protocol for COVID-19 virus infection.

11.1.5   General Considerations

In summary, we can see that continuous worldwide biomedical surveillance caused by perceived biotreats or actually new infective agents, is a primordial task that needs to be maintained and improved. For this reason, it is imperative that the worldwide appearance of new strains of viruses, like COVID-19, demands immediate and analytical precise isolation and characterization of the new viruses. This is required in order to isolate as soon as possible the potentially pandemic new strains and to prepare biological stocks suitable for massive vaccine preparations in due time to prevent the global spreading of potentially lethal new viruses. Examples in time recall the cases of the highly lethal pandemics known as "Spanish flu" in 1917–1918 (more than 40 million deaths worldwide), "Asian flu" in 1956 (over 100,000 deaths worldwide), "Hong Kong flu" in 1978 (in excess of 700,000 deaths worldwide) and finally COVID-19 [9].

Recently, a novel SARS-CoV-2 virus, also known as the COVID-19 virus, has shown to be highly contagious, pathogenic, and rapidly spreading. This novel SARS-CoV-2 has caused a global pandemic *COVID-19,* which has severely affected the health and economy of several countries. It was found that this novel COVID-19 virus can enter the host cell, by the specific binding resulting from the viral surface spike glycoprotein (S-protein) to the converting angiotensin enzyme 2 (ACE2). This specific virus molecular interaction with the host cell represents a promising therapeutic throughput virtual screening approach that was used to target for identifying SARS-CoV-2 (COVID-19) antiviral drugs.

To sum it up, the primary screening of any biological agents capable of causing a world pandemic needs to be identified as soon as possible, in order to find the promising drugs or immunotherapeutic agents.

11.2   Biothreats and Risk Level Assessment

The ability to identify counter bioterrorism depends on the information generated by researchers on the disease-causing microorganisms and also on understanding the immune system [10, 11]. It was shown that biothreat caused by biological agent weapons could be classified on the following four criteria:

 (i) the impending treat to cause morbidity and mortality in healthy individuals;
 (ii) the potential of the biological agent to spread within the community;
(iii) the potential to elicit fear or panic alleged by the biological agent threat and;
(iv) the capability of public health responders to counteract and control the biothreat

In response to the possible biological threat, a list of selected biological agents threat named the "Priority Pathogens" list was created for countermeasures, including vaccines. A complete list of these agents with their respective designations (Category A–C) is presented in Table 11.1 [10].

11.2.1   Category A Agents

The Category A biological agents comprise four highly infectious pathogens that can be transmitted as aerosols. Consequently, *Bacillus anthracis*, *Yersinia pestis*, smallpox (variola major), and *Francisella tularensis* were contemplated as being of the greatest threat to public safety, because of their highly pathogenic nature, ability to spread from person-to-person [12]. In addition, botulinum neurotoxin (BoNT), which can be aerosolized, belongs to Category A Agents, as it is one of the most lethal known biological toxins [13]. It should be repeated that smallpox and anthrax are the biothreats that pose the greatest risk for causing large numbers of casualties in the event of an effective release by a terrorist group.

11.2.2   Category B Agents

The Category B biological agents are known to have the capability to moderately disseminate, and are capable of inflicting moderate morbidity/low mortality. Category B biological agents require specific improvements to the known standard diagnostic capacity. The majority of the Category B agents attack the gastrointestinal tract and are introduced in the human system by food and water ingestion. Such Category B agents that pose safety threats include the Salmonella and *Shigella* species, pathogenic *Vibrios*, enterotoxigenic *E. coli*, as well as toxins such as ricin, staphylococcal enterotoxin B. In general, the Category B agents are not communicable from person to person but are rather easy to disperse to cause highly debilitating sicknesses that need immediate medical attention.

Table 11.1 Category A–C Bio threats. Copied from reference [10]

Toxins	Central European tick-borne encephalitis[a]
Botulinum neurotoxins[a,A]	Kyasanur forest disease[a,B]
Shigatoxin[a]	Omsk hemorrhagic fever[a]
Tetrodotoxin[a]	Far eastern tick-borne encephalitis[a]
T-2 toxin[a]	Russian spring/summer encephalitis[a]
Staphylococcal enterotoxins[a,B]	Avian influenza virus (highly pathogenic)[c]
Ricin[a,A]	Reconstructed 1918 influenza virus[a]
Diacetoxyscirpenol[a]	Cereopithecine herpesvirus 1 (Herpes B virus)[a]
Conotoxins[a]	
Abrin[a]	Severe acute respiratory syndrome (SARS)[C]
Saxitoxin[a]	Caliciviruses[B]
Shiga-like ribosome inactivating proteins[a]	Influenza[C]
Clostridium perfringens epsilon toxin[a,B]	West nile virus[B]
Viruses	Crimean-congo hemorrhagic fever[a,C]
Eastern equine encephalitis[a,B]	*Bacteria/rickettsia*
Hendra virus[b]	*Bacillus anthracis*[b,A]
Variola major (smallpox)[a,A]	*Brucella abortus*[b,B]
Variola minor (alastrim)[a,A]	*Brucella melitensis*[b,B]
Monkeypox[a,A]	*Brucella suis*[b,B]
Filoviruses	*Burkholderia mallei*[b,B]
Ebola virus[a,A]	*Burkholderia pseudomallei*[b,B]
Marburg virus[a,A]	*Coxiella burnetii*[a,B]
Arenaviruses	*Francisella tularensis*[a,A]
Junin[a,A]	*Yersinia pestis*[a,A]
Machupo[a,A]	*Rickettsia prowazekii*[a,B]
Guanarito[a,A]	*Rickettsia rickettsii*[a]
Flexal[a,A]	Pathogenic vibrios[B]
Sabia[a,A]	*Shigella* species[B]
Lassa[a,A]	*Salmonella* species[B]
Japanese encephalitis virus[B]	*Listeria monocytogenes*[B]
Venezuelan equine encephalitis[b,B]	*Yersinia enterolitica*[B]
Dengue[A]	*Campylobacter jejuni*[B]
LaCrosse[B]	Multi-drug resistant tuberculosis[C]
California encephalitis[B]	Other Rickettsia[C]
Western equine encephalitis[B]	*Chlamydia psittaci*[A]
Bunyaviruses	Diarrheagenic *E. coli*[B]
Hantaviruses[A]	Botulinum toxin-producing species of *Clostridium*[a]
Rift Valley Fever[b,A]	
Chikungunya[C]	*Protozoa*
Hepatitis A[B]	*Cryptosporidium parvum*[B]
Yellow fever[C]	*Cyclospora cayatanensis*[B]
Rabies[C]	*Entamoeba histolytica*[B]

Table 11.1 (continued)

Toxins	Central European tick-borne encephalitis[a]
Nipah virus[b]	Toxoplasma[B]
Tick-borne encephalitis complex (flavivirus)	*Giardia lamblia*[B]
Fungi	
Coccidioides posadasii[a]	
Coccidioides immitis[a]	
Microsporidia[B]	

Listing of the biological agents considered to be a threat to human health as a compilation from a number of sources including the (1) select agents and toxins provided by the U.S. Department of Health and Human Services (DHHS), Centers for Disease Control and Prevention (CDC) and the U.S. Department of Agriculture (USDA) and (2) the priority pathogens from the National Institutes of Health/National Institute of Allergy and Infectious Diseases (NIAID) (www3.niaid.nih. gov/topics/BiodefenseRelated/Biodefense/research/CatA.htm).
[a]Select Agents and Toxins designated by DHHS/CDC
[b]Overlap select agents and toxins that are designated and regulated by both DHHS/CDC and the U.S. Department of Agriculture (USDA)
[c]Select agents designated and regulated by the USDA
[A, B, C] NIH/NIAID priority pathogens group A, B or C

11.2.3 Category C Agents

Presently, Category C biological agents are not considered to be high risk, but rather as possible emergent diseases that could pose a threat to public health. The Category C comprises the Nipah virus and hantavirus, yellow fever, influenza, rabies, tick-borne encephalitis viruses, severe acute respiratory syndrome-associated coronavirus (SARS-CoV), as well as certain other types of drug/antibiotic-resistant pathogens, such as tuberculosis-causing mycobacteria.

In addition, the NIAID Category C agents include pathogens commonly found circulating in the general population as Hepatitis A and C and HIV.

11.3 Immunology: Origins and Development

Immunology is a rather young science (a little more than 60 years old, with this explicit name). However, the first information on the existence and validity of immune defenses go back indeed to Edward Jenner with his "vaccination" practices in the 1790s and probably to some older but analogous Chinese medicine practices [14].

The first "immunological" experiment by Jenner is something that would not be ethically feasible today by any medical deontological rules! He started from the observation that English milkmaids who caught cowpox (a benign form of skin eruptions from contacts with diseased cows) did not develop the human form of the smallpox disease; therefore, he voluntarily and deliberately exposed his gardener's son (James Phipps) to biological materials from cowpox pustules (causing a fever illness in the recipient); after recovery, Jenner challenged the boy with human smallpox, verifying his attained "immunity" also to the human disease [15].

Jenner is therefore considered the father of experimental "immunology." No mechanistic explanations of that experiment were, however, possible at that time: only about 100–150 years later we started discovering antibodies and immune system functions allowing us to understand what was biologically happening at that time in the milkmaids (and at any other time in "immune" individuals) and in the "vaccinated" individuals like Jenner's gardener's son.

All the developing "immunological" science, enriched later through microbiology, biochemistry, physiology and pathology studies in the following decades, recorded more and more details in the functioning of the defense mechanisms of mammals and humans, having the most complex and efficient forms of immunological defense against foreign agents entering the body.

The immune system is in fact like an "eye within" the body, controlling that nothing extraneous is biologically active in each individual organism, and therefore, recognizing effectively "self" from "not-self", so that replication of self-cells are not contaminated by "foreign" biological agents and that any extraneous biological entity will be eliminated by soluble "light" weapons (antibodies) and by "heavy" killers (immune cells and macrophages, interacting and collaborating in the task). The key steps of an immune reaction are substantially three: (a) internalization of foreign particles by macrophages (MPH) degrading and "presenting" them to T-helper lymphocytes (T_h-cells) which in turn start an elaborated attack, mostly through either (b) synthesis of soluble "light" weapons (antibodies, humoral response by B-cells) or (c) development of cellular "heavy" weapons (killer T-lymphocytes T-K cells, with cellular or cytotoxic response); in many cases, we observe the activation of both responses (b + c), depending on the needs. The key steps of an immune reaction are illustrated in the following Fig. 11.1.

Recently, it has been shown that activated T-cells tend to aggregate, like a swarm of bees, exchanging information, useful to coordinate the immune response (i.e., to elaborate coordinated defense plans): this is the visual demonstration of the complex molecular dialogue taking place within the various families of immune cells collaborating to the full enactment of defense mechanisms.

When invaders are present in body fluids or the extracellular domains, like most bacteria, they can be attacked by antibodies, through specific surface recognition. However, when the invaders are instead of the intracellular type, like viruses and some bacteria (like TBC), they must instead be attacked by special killer lymphocytes (cytotoxic TK-cells), which destroy all the self-cells harboring the intruders, together with their content. Nevertheless, viruses anyway can also transit the body fluids; consequently, also antibodies are produced against them.

In most responses, both humoral (antibodies) and cellular attacks are deployed. The immune response, moreover, is specific and potentiated by memory: therefore, a second (or further) encounter with the same foreign agent (antigen) produces a stronger and quicker defense reaction. Details of the immune mechanisms are continuously discovered. So, this discipline is still far from being completely described and understood. New details are continuously added and better focused by immunology researchers in time [16].
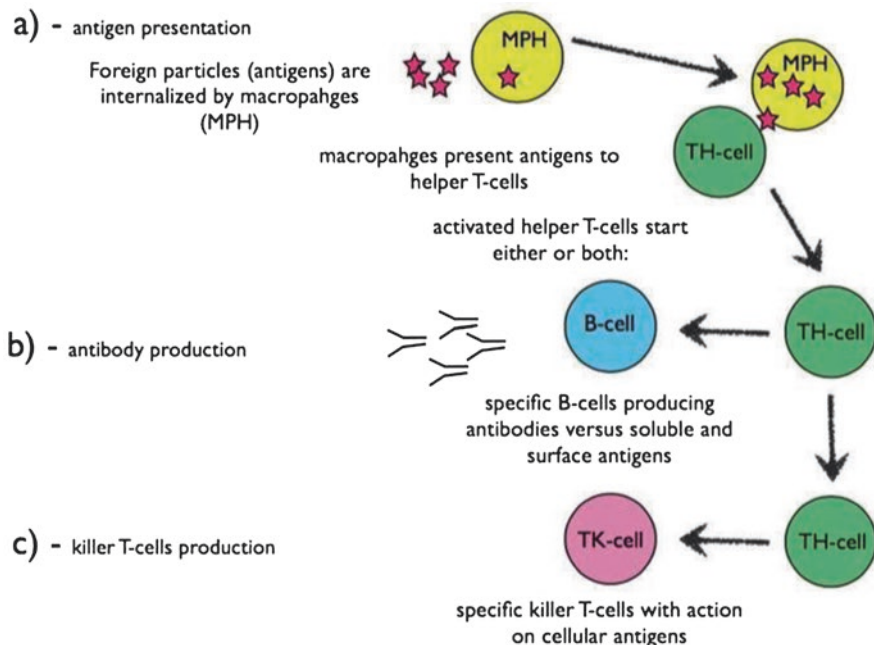
Fig. 11.1 Mechanisms of key steps of the Immunological System

11.4   Assessing Degrees of Mucosal Involvement

In order to develop a vaccine for biodefense, it is primordial to know the difference between biological agents that elicit mucosal infections, and the biological agents that simply exploit mucosal tissues as a means to gain access to the systemic compartment. Consequently, mucosal immunity likely plays an essential role in preventing and clearing infections. This is why vaccines against these agents have to involve mucosa-associated lymphoid tissues.

On the other hand, situations where the mucosa functions act solely as the port of entry, systemic immunity is likely to be sufficient to control infection. For example, we can consider the case of anthrax. Although the *B. anthracis* spores are highly infectious by aerosol, the vegetative bacteria generally do not multiply locally. Somewhat, after inhalation of the spores, the bacteria circulate systemically via the lymphatics and the circulatory system. Then, within the systemic compartment, *B. anthracis* germinates and produces two toxins, which account for the lethality associated with this infection [17]. For these reasons, protective immunity to *B. anthracis* is associated primarily with anti-toxin serum IgG antibodies. The mucosal defense is of little (if any) importance in con-trolling anthrax.

Contrary to protective immunity, mucosal immunity plays an important role in controlling infections caused by two other Category A bacterial pathogens, notably *Y. pestis* and *F. tularensis* that are the main cause of mucosal and systemic complications following inhalation [18].

For many of the other Category A–C agents, it should be noted that the route of infection transmission cannot occur via the respiratory tract. Thus, the actual participation of the mucosa in the pathogenesis of the infection process is not usually known. Therefore, the initial host interaction and the subsequent pathophysiology will follow known established clinical outcomes. In addition, there could be a lack of clinical data that defines the aerosol-related disease adequately. An example of one such agent is *Staphylococcal enterotoxin* B (SEB), which is a member of the superantigen family of toxin. Hence, SEB forms "bridges" between the Major Histocompatibility Class II molecules on antigen-presenting cells and T cell receptors on specific subsets of CD4+ and CD8+ T cells. And as a result of this SEB binding, the T cells start to release massive amounts of proinflammatory cytokines and undergo hyper-proliferation, which ultimately results in their depletion [19, 20].

For the alphaviruses, the infection and associated pathogenesis depend on the route of exposure. It is assumed that exposure to aerosols induce disease directly via the olfactory bulb, whereas experimental infection via ingestion causes a disseminated viremia prior to nervous system engagement and encephalitis.

11.5 Prevention to Favor Defense and Immunity Success

To control infections and favor human immune responses, it is essential to adhere to the following defenses:

1. to reduce microorganism proliferation (through the use of bacteriostatic drugs) or kill the germs (disinfection, use of bactericidal medications);
2. to control the vectors diffusing the infection (insects, arthropods, birds, rats, etc.);
3. to immunize the potential hosts (vaccinations) preventively: this requires public health planning, technology, costs and time;
4. to administer preformed antibodies (serotherapy): this also requires technology, costs, and time.

11.5.1 Actions Against Germs

Concerning prevention defense #1, the use of chemotherapeutic antibiotics, which have a multitude of modes of action mechanisms, is recommended. However, as germs tend to develop resistance to them, it is evident that fewer effective antibiotics are available today. It should be prevention defenses #2–4 require stringent and effective world operations against biological vectors, which could be transported by insecticides, biological competitors – fungi, bats, genetics can also be beneficial [21, 22]. But the best possible actions to combat biothreats are the use of vaccines (if available and if time allows) and of immune sera (if available).

A vaccine is always preferable because it induces an active response and an advantageous state of immune memory in the individual, with minimal side effects (active immunization). A serum specific for a given antigen can be life-saving (serotherapy, immediately active), but has some side effects (since it introduces heterologous proteins -for instance, horse immunoglobulins, which in turn will be immunologically eliminated-) and does not have lasting protection (passive immunization).

Modern life has created some extra occasions for germs and some "new" diseases [22]: air conditioning apparatuses for instance (if not properly cared and cleaned) are a new ideal environment for bacteria; because of dirt and humidity they can foster the growth of airborne bacteria never seen before as human pathogens: *Legionella pneumophyla*. The story of Legionaries disease (a fatal lung infection by *Legionella*) is very instructive for microbiologists and epidemiologists. Human behaviors (homosexual intercourses, exchange of syringes among intravenous drug users, and frequency of air travel) have extended the contagion of formerly rare infections like HIV. Also, in this case, the facts are dramatically instructive for medicine and epidemiology.

Transfusions of unscreened blood have also diffused hepatitis and HIV viruses. Centralized processing of foods has sometimes diffused a contagion of food-borne infections (*E. coli*) [21]. Airplanes have replaced ships for human travel and are at the center of attention for human communicable diseases spreading (Influenza, SARS, etc.). Many more people are traveling today to remote and tropical areas than before (forests, wilderness). This can expose more populations (even at home, on the return) to rare insects and microbes (see cases of malaria, Ebola virus, Marburg virus, etc.). In addition, economic development expands contacts: mining, forestry, agriculture in new tropical areas with recent deforestation.

Additionally, the increasing number of subjects with immunodeficiency diseases or immunosuppressant therapies (for transplants) strengthen the probability of new communicable agents to infect people, survive and propagate in modern societies (opportunistic infections, with possible mutations in progress.

This entire prospect of new possible pandemics constantly increases especially with the emerging new variety of infections such as new bacterial and viral pathogens as the Rotavirus, *Cryptosporidium parvum*, *Legionella pneumophyla*, *Ebola* virus, *Hantaan* virus, *Campylobacter jejuni*, HTLV virus, HIV, *Helicobacter pylori*, Herpesvirus-6 and -8, virus *Guanarito*, virus *Sabia,* nCoV-MERS virus, COVID-19, to name just some of the most relevant and recent [22].

11.6   Preparation of Vaccines

What is a vaccine? In a dangerous disease caused by microorganisms and "foreign" not-self substances (an "antigen"), it may be possible to raise a vaccine, that is an innocuous preparation of that "antigen" which can induce the production of an immune response and create immune memory in the subjects we want to protect.

A vaccine can be developed in many ways: using killed (denatured) or non-replicating pathogens (viruses), recombinant protein antigens, live, attenuated (less harmful) strains of pathogens (for instance cowpox virus to protect against smallpox).

Vaccines and their uses have shown to be very effective in eradicating smallpox. Indeed, the extinction of the smallpox disease on earth is one of the best success of global vaccine campaigns. Similarly, we can say the same thing concerning polio. Hence, the near extinction of disease in the world, except in some nomad populations and critical areas of today's world, like Syria and also, surprisingly, of remote China provinces [22].

11.6.1 Requirements for Vaccine Preparation

Requirements for vaccine preparation are the following:

(a) An innocuous preparation of the antigen (+/− adjuvants);
(b) a suitable biologic model in which to test the effectiveness of the immunization procedure;
(c) a reduced series of administrations able to induce a long-lasting response (number of boosters required): polio (very long-lasting), as opposed to tetanus (lasts only some years, many boosters required);
(d) an easy and affordable procedure for preparing quickly a large amount of product to use in case of necessity [22].

11.6.2 Different Method of Vaccinations

The most used method of vaccination generally can be divided as follows:

1. Using killed whole germ preparations (influenza; polio type Salk; Hepatitis A; rabies; pertussis; cholera);
2. Using live attenuated germ preparations (tuberculosis; mumps-parotitis-rubella; polio type Sabin; yellow fever; variola; typhus and lately also against Ebola and Marburg viruses);
3. Using purified antigens component of the infective diseases (meningitis –using antigenic subunits of *Haemophilus influenzae b*; acellular pertussis vaccine; tetanus-diphtheria anatoxins);
4. Using recombinant DNA vaccines (surface antigen of hepatitis B);
5. Using naked DNA vaccines (against many different germs, not yet widely used); and
6. Finally, using vaccines of genetically modified plants (against many different germs, not yet widely used) [22].

The technology of vaccine preparations is continuously evolving, in order to improve our capacity to prepare quickly enormous amounts of vaccinating doses from microorganisms soon after their isolation in newly appearing forms or strains. For viruses, for instance, an important step forward has been the technology of reproducing the organisms on cell cultures rather than on fertilized chicken eggs.

11.6.3   Vaccination Campaigns: How Best Use Vaccines

Mass vaccination campaigns have taken place several times in history, like those of 1947 against smallpox, in which the citizens of New York City stood in long lines to be vaccinated at a rate of eight persons per minute, and like those of several countries against polio (after the Sabin vaccine introduction, in 1960), with periodic vaccination days organized to reach many secluded groups of citizens living in remote areas [22].

The realities, however, are that the existence of a vaccine is not enough to prevent a worldwide pandemic; more testing is needed before a new vaccine may be offered to the public; for vaccines prepared on chicken eggs, the successful mass production depends on the availability of the eggs, indeed; obstacles include an organizational system for distribution and timely supply of doses, where and when they are needed.

Good news for scientists and biologists is that since the September 2001 terroristic attacks in the USA (anthrax spores in the mailings), the employment needs of biologists have increased remarkably (production of vaccines, enactment of protection plans, treatment schemes for infections, etc.) [21, 22].

The field of immunology, in particular for vaccine research and development, continues to be of high impact in modern medicine and high relevance in the contrast of bioterrorism.

To conclude, science is here to help; to be of use; to spread not infections but knowledge, across different cultures and nationalities. Our role of scientists is mostly that of being "pontifices" (Latin "pontes facientes," which means "bridge makers" across cultures and nationalities). For this reason, it has been a real pleasure to exchange our knowledge here and to discuss it together, among so many different people and so broad scientific expertise.

11.7   Development of Biothreat Vaccines

The development of vaccines and other countermeasures against the diverse biological agents that can be considered posing potential biothreats to public health is a daunting challenge for the scientific community. Licensed vaccines against both anthrax and smallpox that protect against aerosol transmission are available. An existing licensed plague vaccine is protective against flea - transmitted disease but not against aerosol challenge in animal experiments or pneumonic plague. This vaccine is in limited supply, and the manufacturer has recently ceased production.

11.7.1 Glycoconjugate Vaccines Used for Prevention from Biological Agents

As mentioned before in 1796, Edward Jenner discovered that the inoculation with cowpox was able to protect against smallpox infection. Since then, different vaccines were developed to prevent infectious diseases [23, 24]. It was found that the protection conferred by these vaccines was due to adaptive immunity (cellular and/or humoral immunity) [23–26]. Unlike adaptive immunity, innate immunity does not recognize every possible antigen. Instead, it is designed to recognize the microbial molecules that are essential for the survival of the pathogens. These unique microbial molecules are called pathogen-associated molecular patterns (PAMPS) [25, 26].

PAMPS include lipopolysaccharides (LPS, also called endotoxin) from the gram-negative cell wall, peptidoglycan lipoteichoic acid from the gram-positive cell wall, flagellin of bacterial flagella, the sugar mannose (a terminal sugar common in bacterial, viral or fungal glycolipid and glycoprotein), bacterial or viral unmethylated CpG DNA, double-stranded and single-stranded RNA from viruses and glucans from fungal cell wall [25, 26].

Several pathogens and tumor cells exhibit unique glycan structures on their cellular membrane surfaces. For example, bacteria, microbes, and viruses all possess a cell wall consisting of a plasma membrane and a capsule which were formed of glycoproteins or complex polysaccharides [27].

These carbohydrate antigens can be used as targets for the development of carbohydrate vaccines. In the case of pathogenic bacteria, one has to distinguish Gram-positive to Gram-negative bacteria that possess respectively, either capsular polysaccharides (CPS) and/or lipopolysaccharides (LPS) that are implicated in all virulence factors [28, 29]. The LPS are located on the outer membranes of Gram-negative bacterial cells. The study of the LPS revealed that it is composed of an amphiphilic macromolecule, corresponding to an external core oligosaccharide (O-specific chain, or hydrophilic antigen) and an internal core oligosaccharide covalently linked to the lipid A [30]. Knowing that the oligosaccharide portion confers the immunological properties to the bacteria, different portions of the LPS have been tested for vaccine development [31].

11.7.2 Lipopolysaccharide (LPS)

The lipopolysaccharides are located on the outer membranes of Gram-negative bacterial cells. Several studies on the isolation and structure and composition determination of LPS were reported [30, 32]. It was observed that LPS are composed an external polysaccharide consisting of repeating of identical sugar oligosaccharide units, called the *O* -specific chain, and an internal core oligosaccharide covalently attached to a lipid A. The lipid A is a glycolipid composed by a β-D-(1 → 6) GlcN

disaccharide in which O-3, O-3′, O-4′, C 2 -N and C 2 -N′ are acylated with different C:12 and C:14 fatty acids. The lipid A confers the toxicity to the LPS. In addition, it has to be noted that the *O* -specific oligosaccharide that corresponds to a sequence of oligosaccharide units is unique for each bacterial serotype and provides an immunological property to the bacteria. As a result, several studies involving different moieties of lipopolysaccharides were carried out for the development of vaccines and drugs [31, 33, 34].

11.7.3 LPS-Derived Vaccines or LPS-Protein Neoglycoconjugates

Various studies were carried out on the use of LPS derivatives as vaccines. It was found that the immune reaction relies mainly on the LPS, and it has been efficiently utilized for vaccination. However, the use of the LPS alone for vaccination is not efficient, as, because of its small size, it is not recognized by the immune system as it has resistance to non-specific host immunity such as complement system and resistance to specific host immunity (poor antibody response) [35, 36].

However, when conjugated to a protein carrier, the LPS is able to induce an immunological reaction and an extended immunity. Landsteiner's group was the first to utilize carbohydrate-protein conjugates as immunogens [37, 38], and lately, it was discovered that they could induce a strong antibody reaction [39]. Landsteiner's group was also first to refer to the carbohydrate-protein conjugate as a hapten [37, 38].

Figure 11.2 is representing the immune response generated by oligosaccharide antigen-carrier protein vaccines [40]. The interaction of the glycoconjugate vaccine (Fig. 11.2) with the B cell receptor (BCR) stimulates the lymphocytes and results in the activation of plasma B cells to secrete immunoglobulins, while the neoglyco-conjugate vaccine is recognized by the polysaccharide specific B cell receptors. The carrier protein will enter the B cell by phagocytosis. Then, the degradation of the protein carrier in B cells will be done by lysosomal enzymes into short peptides called epitopes. At that time these epitopes will be recruited by a special protein called major histocompatibility protein II (MHC II) that are presented at the cell surface of antigen-presenting cell (APC) or B cell and interact with the carrier-peptide-specific T cells (helper T cell) which send a signal to produce polysaccharide specific plasma cells and polysaccharide specific memory B cells [40].

The synthesis of efficient glycoconjugate vaccines has been challenging, since their efficacy relies on different factors, such as the saccharide size, the average number of saccharide chains per conjugate molecule, the nature of the carrier and the distance between the saccharide and the protein in the formed glycoconjugate (Fig. 11.3) [41–44].
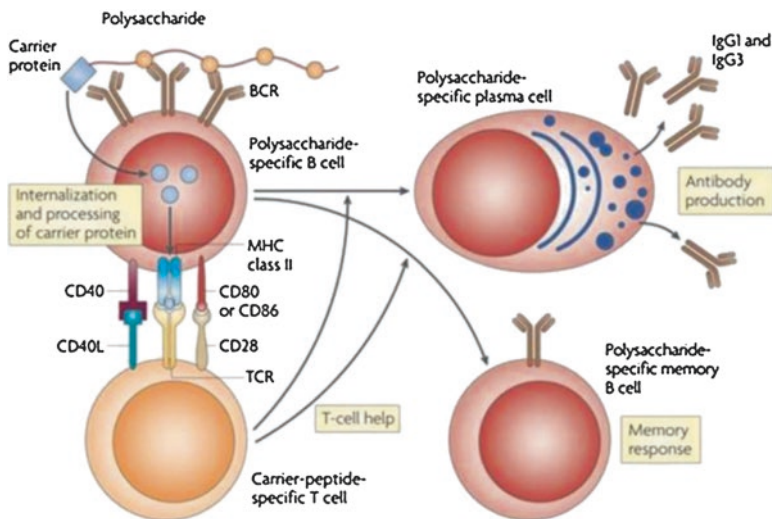
Fig. 11.2 Generation of the immune responses against oligosaccharide antigen-carrier protein conjugate vaccines [40]

Fig. 11.3 Composition of the neoglycoconjugate vaccine

Different methods have been used for the synthesis of carbohydrate antigen protein neoglycoconjugates. One of these methods consisted of the use of the squaric acid chemistry for the single-point attachment of carbohydrates to proteins [45–48]. Tietze et al. used squaric acid diethyl esters for the conjugation [46], while it has also been reported that squaric acid dimethyl esters [49, 50], as well as didecyl squarate [51], were used for the single point attachment of carbohydrates to proteins. In addition, Kamath et al. used squaric acid amide ethyl esters for the conjugation of oligosaccharides to protein. They monitored the conjugation using matrix-assisted laser desorption ionization-time of flight mass spectrometry (MALDI-TOF-MS) [52].

More recently, the group of Kováč also utilized the squaric acid chemistry to conjugate different carbohydrate antigens to a protein carrier [53–55]. They used this strategy to conjugate the synthetic tetrasaccharide side chain of the *Bacillus anthracis* exosporium to the bovine serum albumin (BSA) protein [54].

11.7.4   Molecular Weight and Carbohydrate-to-Protein Ratio Determination

The aim of determining the molecular weight and the carbohydrate-to-protein ratio of a carbohydrate-protein neoglycoconjugate is to define the number of carbohydrates that are incorporated in the protein carrier, as a result of the conjugation. Two main methods are currently used for the molecular weight determination carbohydrate-protein glycoconjugates: matrix-assisted-laser-ionization time-of-flight mass spectrometry (MALDI-TOF-MS) [56, 57] and surface-enhanced laser desorption ionization time-of-flight mass spectrometry (SELDI-TOF-MS) [53–55, 58–60]. Both of these methods allow determining the carbohydrate-to-protein ratio of the neoglycoconjugates by comparing the molecular weight of the protein before and after the conjugation to that of the neoglycoconjugate.

11.7.5   Mass Spectrometry Methods for the Characterization of Carbohydrate Vaccines

Mass spectrometry has emerged as a powerful technique for the characterization of different biomolecules ranging from small molecules to larger molecules. Thus, mass spectrometry is extensively used in proteomics [61], glycomics [62], metabolomics [63], lipidomics [64], and in oligonucleotides [65] analysis.

Initially, the exploring of MALDI-TOF-MS of the different hapten-BSA glycoconjugate vaccines allowed us to determine the hapten-to-BSA ratios. Then the glycoconjugate vaccine samples were then digested and analyzed by MALDI-TOF/TOF-MS/MS and LC-ESI-QqTOF-MS/MS for the determination of glycation sites.

The digestion was done by two different enzymes; trypsin, which will not be able to digest or react with the glycated lysines of the protein, and the other enzyme was GluC V8 endoproteinase which is known to digest proteins at C-terminus of the aspartic acid and glutamic acid residues. Finally, the MS/MS spectra will be submitted to the MASCOT library to get the matched and non-matched peptides.

11.7.6   MALDI-TOF-MS

Matrix-assisted laser desorption ionization mass spectrometry has been successfully used for the determination of the molecular weight of biomolecules, such as proteins, oligosaccharides, and glycoproteins [56–58]. Kamath et al. used MALDI-TOF-MS to characterize neoglycoconjugates formed by the conjugation of oligosaccharide amines to carrier proteins by the aim of diethyl squarate [59]. The MALDI-MS was recorded in linear mode and with positive ion detection. Figure 11.4 displays the MALDI-TOF-MS analysis of BSA (A) and the following

oligosaccharide-BSA glycoconjugates: (B) GlcNAc-BSA (carbohydrate- BSA ratio (n) = 8.4); (C) lactose-BSA (n = 3.5); (D) lactose-BSA (n = 8.2); (E) Fucal-2Galfl l-3[Fucal-4]GlcNAc- BSA (n = 11); (F) Fucal-2Fucal- 3GalNAc-BSA (n = 13). The MALDI-TOF-MS spectrum of BSA was used as a calibration standard. Then the analysis allowed to reveal the average carbohydrate-BSA ratios for the hapten-BSA neoglycoconjugates (Fig. 11.4).
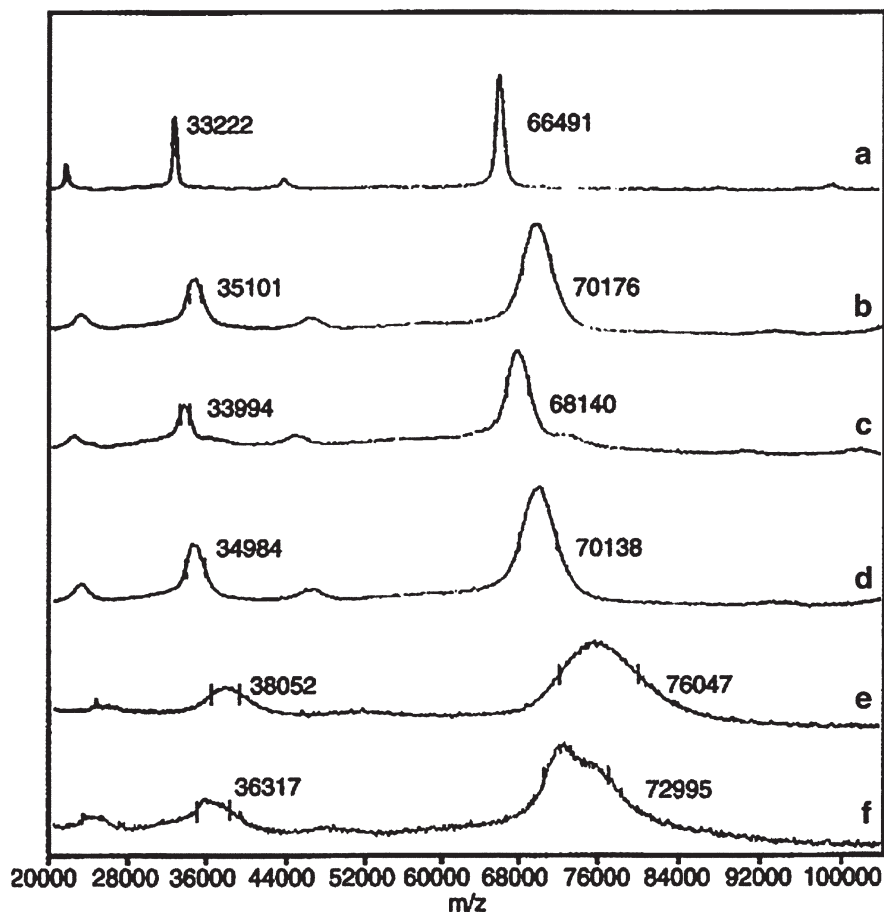

Fig. 11.4 MALDI-TOF spectra of: (a) BSA calibration standard; (b) GlcNAc-BSA (n = 8.4); (c) lactose-BSA (n = 3.5); (d) lactose-BSA (n = 8.2); (e) Fucal-2Galfl l-3[Fucal-4]GlcNAc-BSA (n = 11); (f) Fucal-2Fucal-3GalNAc-BSA (n = 13) [58]

11.7.7   SELDI-TOF-MS

Surface-enhanced laser desorption ionization time-of-flight mass spectrometry (SELDI-TOF-MS) has been extensively used for biomarkers discovery [59], and cancer diagnosis [60]. This technique consists in using a modified target for the immunoaffinity purification of proteins before analysis.

The group of Kováč successfully used this analytical method to monitor the conjugation of synthetic carbohydrate antigens to different protein carriers [53–55, 66]. Figure 11.5 shows the SELDI-TOF-MS analysis with a ProteinChip® System of a neoglycoconjugate prepared by the dialkyl squarate chemistry attachment of the hexasaccharide of *Vibrio cholerae* O:1 to the BSA [65]. This technology allowed the analysis of neoglycoconjugates at different reaction times by taking an aliquot of the reaction mixture, in the picomolar concentration range, and analyzing it without any purification step. In addition, this method was found to be fast, and only a small amount of sample is used for analysis. The same group followed the progress of conjugation of the hexasaccharide (exact mass: 1780.79 Da) to the BSA protein (molecular mass: 66,430 Da) at different reaction times [65]. It was observed that the conjugation rate increased with the reaction time. In addition, the SELDI-TOF-MS also allowed observing that after a reaction time of 7 h, the fine structure the peak of the neoglycoconjugate (Fig. 11.6) shows the polydispersity of the neoglycoconjugate formed from the hexasaccharide and BSA.

Moreover, after the conjugation is complete, the excess oligosaccharide can be recovered for further use, allowing an economy of labor and time for the preparation of synthetic oligosaccharides and their conjugation [66].

11.7.8   Glycation Sites Determination

The glycation site's determination of carbohydrates-protein neoglycoconjugates is usually carried out by first digesting the neoglycoconjugate using a protease, such as trypsin or GluC V8 endoproteinase, followed by MALDI-TOF-MS/MS or liquid chromatography-tandem mass spectrometry [67–72].

It has to be noted that during the tandem mass spectrometry analysis of the glycoconjugate digests, the identification of the glycated peptides is confirmed by the presence of diagnostic product ions of the carbohydrate in the mass spectrum.

In addition, the tandem mass spectrometry analysis also reveals the sequence of the peptide through diagnostic product ions of the peptide moiety of the glycated peptide. The combined information allows the unambiguous characterization of the carbohydrate-peptide and the glycation site identification. It has to be noted that during the tandem mass spectrometry analyses of the glycated peptides, the product ions corresponding to the fragmentation of the peptide portion were identified using the nomenclature established by Roepstorff et al. and lately modified by Johnson and coworkers [73, 74], and the product ions resulting from the fragmentation of the
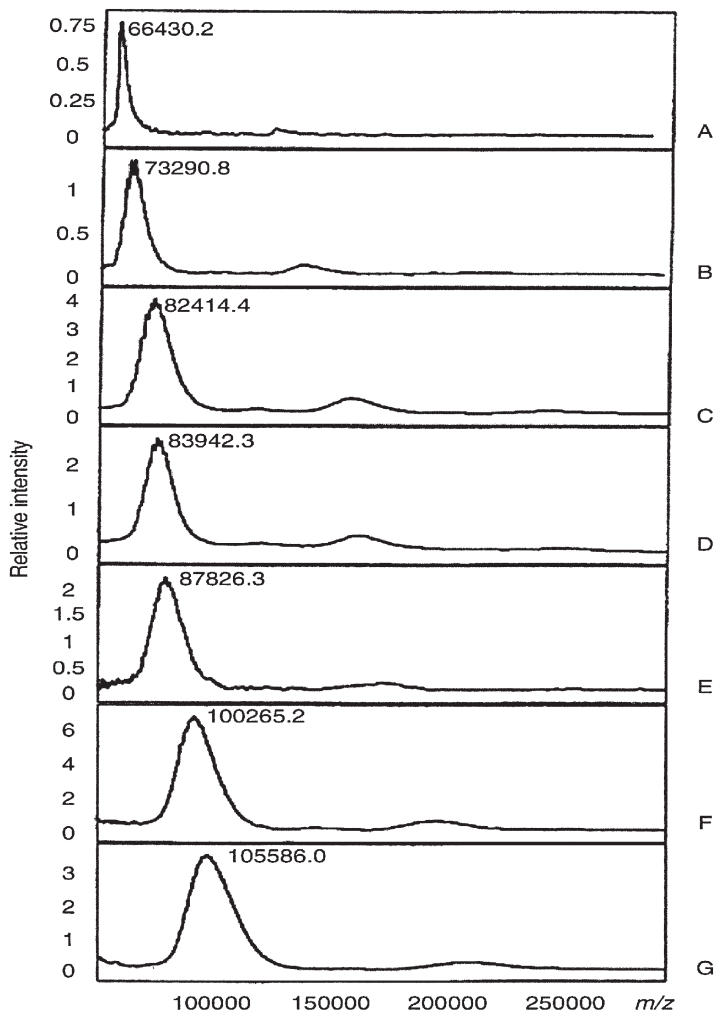
Fig. 11.5 The progress of conjugation of the hexasaccharide of Vibrio cholerae serotype Ogawa (exact mass, 1780.79 Da) and BSA (molecular mass, 66,430 Da) as revealed by monitoring the reaction by SELDI-TOF MS. Spectrum A was taken at the onset of the reaction (t-0); spectra B-G were taken at 1, 3, 7, 9, 27, and 54 h, respectively [66]

carbohydrate moiety was assigned using the nomenclature introduced by Domon and Costello, as A, B, C, X, Y, and Z [75]. An example of the mass spectrometry characterization of neoglycoconjugate vaccines is discussed in the next section.
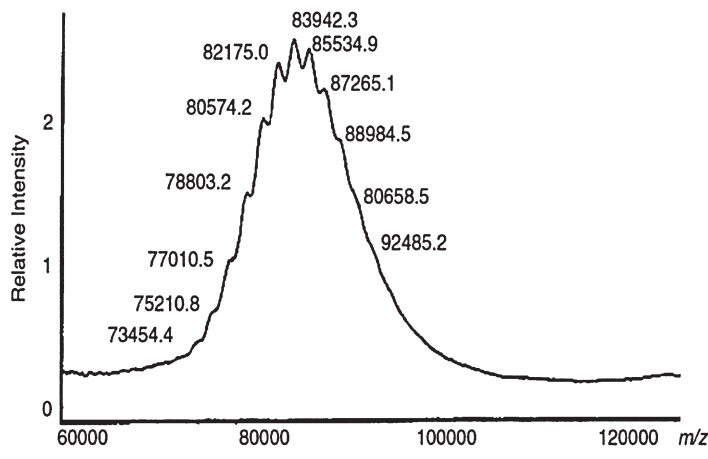
Fig. 11.6 The fine structure of the peak D (Fig. 11.5) showing the polydispersity of the neoglyco-conjugate formed from the hexasaccharide 4 and BSA after 7 h of reaction time. For further details, see text [66]

11.8 A Typical Example of the Mass Spectrometry Characterization of an Anthrax Biothreat

Bacillus anthracis is a Gram-positive bacterium that causes anthrax to both humans and animals [76]. The formation of endospores [77] at the maturity stage of the bacterium allows protection against severe conditions, such as extreme temperatures, radiations, physical damages, and chemicals [78]. *Bacillus anthracis* is the etiologic agent of anthrax that can be used as a biological weapon [79, 80].

Indeed, *Bacillus anthracis* a pathogen that is lethal in most cases for both humans and animals. There are different *Bacillus anthracis* strains, among those, 89 of them were identified, such as the Sterne strain [81], the Vollum strain [82], the Ames strain [80, 83], and the H9401 strain [84]. The last one has also been studied for the development of anthrax vaccine [84]. In addition, *Bacillus anthracis* has been extensively studied to understand its pathogenesis, identifying new biomarkers and vaccines design [85]. The capsular polypeptide (polyglutamic acid) of the *Bacillus anthracis* has been targeted for the development of synthetic vaccines [86].

Daubenspeck et al. reported the structure of the tetrasaccharide side chain of the collagen-like region of the major glycoprotein of the *B. anthracis* exosporium [87]. Their findings were that the upstream terminal of the tetrasaccharide corresponds to the sugar anthrose [4,6-dideoxy-4-(3-hydroxy-3-methylbutyramido)-2-O-methyl-D-glucopyranose].

The group of Kováč prepared a vaccine composed of a synthesized tetrasaccharide side chain of the collagen-like region of the major glycoprotein of the *B. anthracis* exosporium (MW = 950.43 Da) attached to the BSA using the squaric acid chemistry [54]. The conjugation led to the formation of vaccines with different carbohydrate: BSA ratios.

11.8.1 Carbohydrate: BSA Ratio

MALDI-TOF-MS analysis of one of these synthetic vaccines allowed to observe the following protonated molecular ions: $[M + H]^+$ at m/z 71,448.36 and $[M + 2H]^{2+}$ at m/z 35,730.08. The molecular weight of this vaccine was thus found to be 71,447.36 Da. As the molecular weight of the synthetic tetrasaccharide side chain of the collagen-like region being 950.43 Da, the carbohydrate: protein ratio of the synthetic vaccine was determined to be 5.4:1.

11.8.2 Glycation Sites Determination

The determination of the glycation sites of the hapten-BSA vaccine neoglycoconjugate was carried out by enzymatic digestion with the trypsin and/or GluC V8 proteases, followed by the MALDI-MS/MS and LC-MS/MS analysis of the digests.

The enzymatic digestion of the hapten-BSA glycoconjugate and MALDI-MS/MS, as well as LC-MS/MS analyses, were carried out as previously described [67–71].

11.8.2.1 MALDI-TOF/TOF-MS/MS

The spectra obtained during the MALDI-TOF/TOF-MS /MS analysis of the tryptic and GluC V8 digests (Fig. 11.7) were submitted to the MASCOT library to identify by PMF the peptides matching to the BSA. Two Serum Albumin protein isoforms from the *Bos taurus* species were identified for the tryptic and GluC V8 digests: the serum albumin precursor (gi|1,351,907) and the serum albumin (gi|74,267,962). The detected peptides that were not identified in the database were analyzed by tandem mass spectrometry. The MALDI-MS/MS analysis of the tryptic digests allowed to identify three glycated peptides corresponding to BSA peptides with an increment of 950 Da to their original molecular mass, namely: ALK*AWSVAR at m/z 1951.0130 (Fig. 11.8), VTK*CCTESLVNR at m/z 2416.1372, and QNCDQFEK*LGEYGFQNALIVR at m/z 3478.6429 (glycation represented with an asterisk on the lysine residue).

The high-energy CID-MS/MS analysis of the glycopeptide ALK*AWSVAR (Fig. 11.8) at m/z 1951.0130 afforded a series of product ions corresponding to the entire precursor ion that losses different carbohydrate portions, the monosaccharide B_1 (−259 Da), disaccharide B_2 (−405 Da), trisaccharide B_3 (−551 Da) and/or the tetrasaccharide B_4 (−697 Da), leading respectively to the formation of the following productions: Y_3^+ at m/z 1691.8829, Y_2^+ at m/z 1545.8376, Y1$^+$ at m/z 1399.7768 and Y0$^+$ at m/z 1253.7010 (Fig. 11.8). The mass difference between Y_3^+ and Y_2^+, Y_2^+ and Y_1^+, Y_1^+, and Y_0^+ were found to correspond to one α-L-rhamnopyranosyl unit (146 Da). Moreover, product ions resulting from the fragmentation of the same
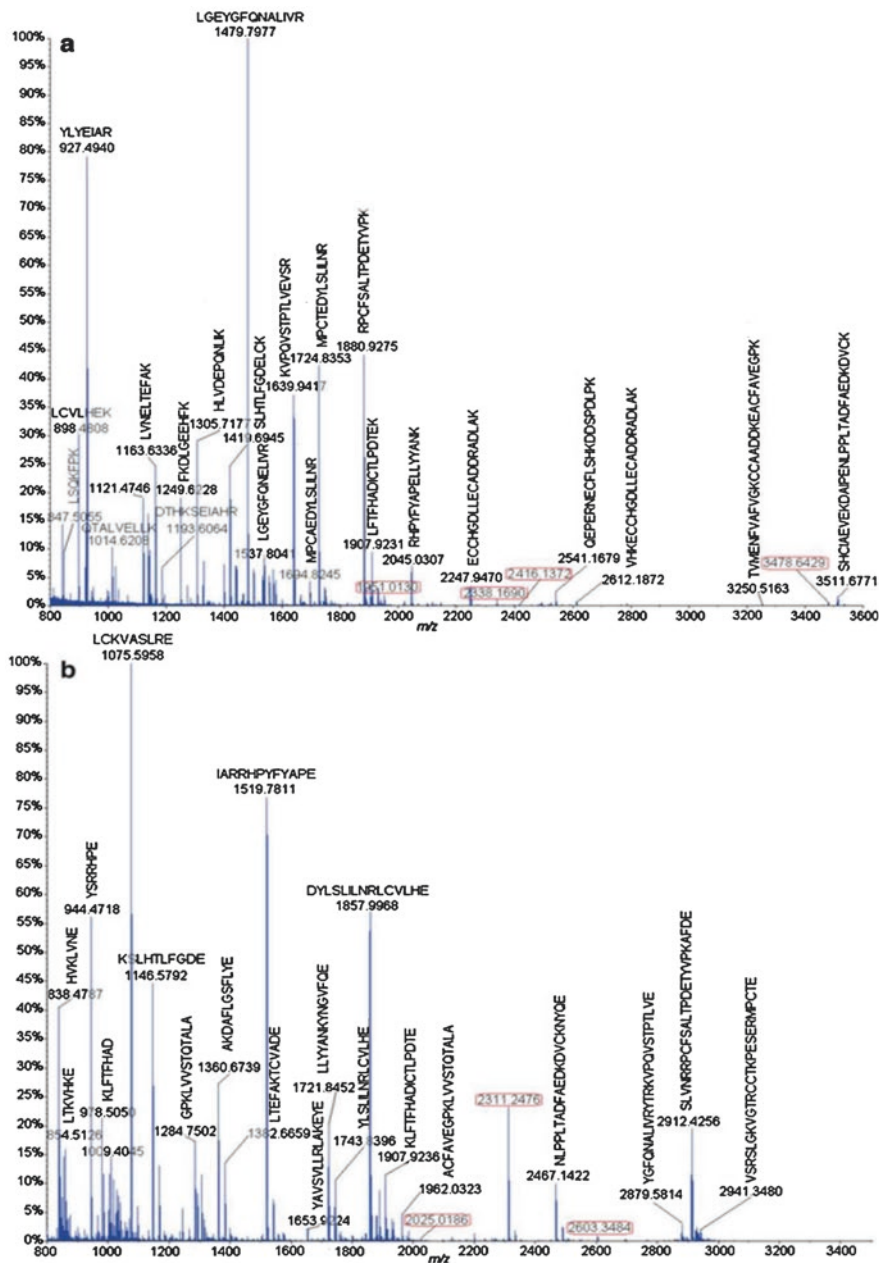
Fig. 11.7 MALDI-MS analysis of the glycoconjugate trypsin digests (**a**) and GluC V8 endopro-teinase digests (**b**) [69]

tetrasaccharide were observed: $C_{17}H_{26}N_3O_4^+$ at m/z 336.1242, B_1^+ at m/z 260.0739, $[B_1 - H_2O]^+$ at m/z 242.0709, $^{2,5}A_1^+$ at m/z 230.0719, $C_{11}H_{16}N_3O_2^+$ at m/z 222.0670 and $[C_1 - C_5H_{11}NO_2]^+$ at m/z 159.0486 (Fig. 11.8). Accordingly, the fragmentation of the carbohydrate portion allowed to confirm its structure and contributed to
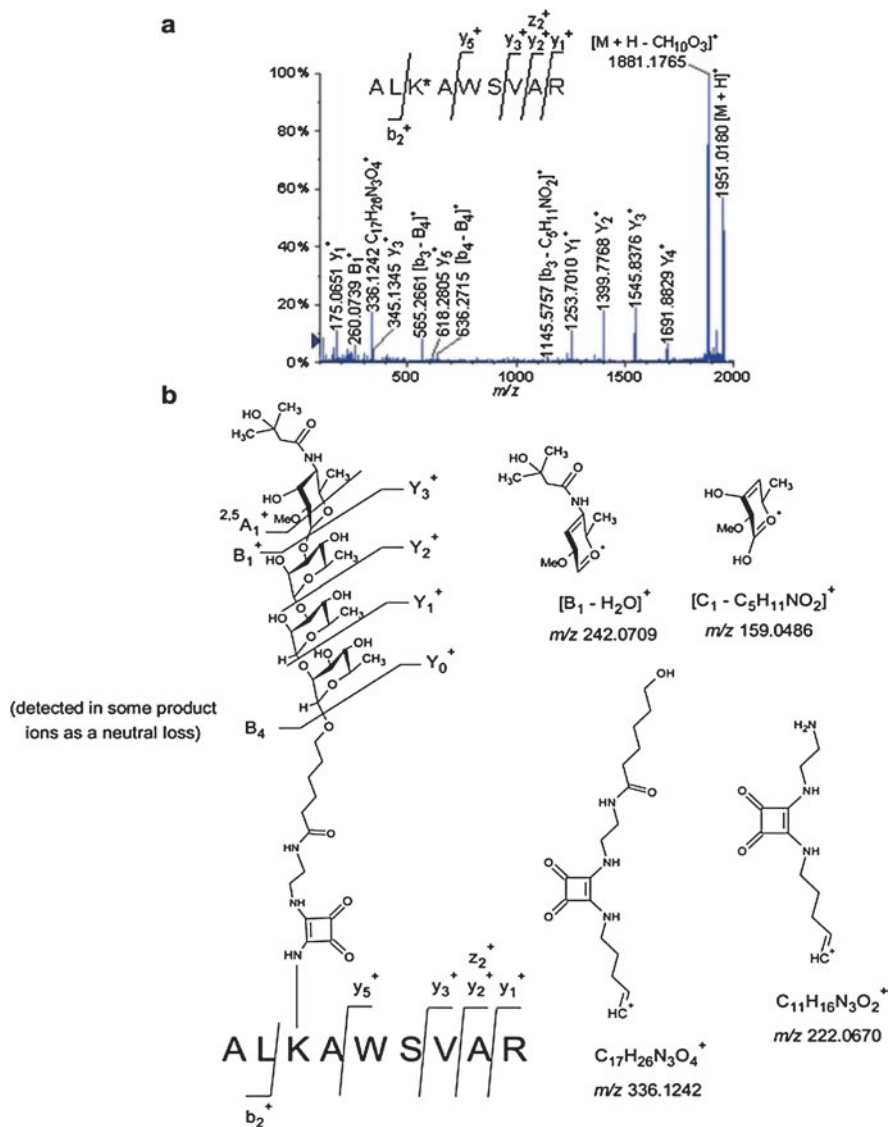
Fig. 11.8 (**a**) MALDI-TOF/TOF-MS/MS spectra of the glycated peptide ALK*AWSVAR (Lys 265) at m/z 1951.0130. (**b**) Different product ions involving the fragmentation of the carbohydrate hapten observed during the MALDI-TOF/TOF-MS/MS analysis of the glycated peptide ALK*AWSVAR (Lys 235) at m/z 1951.0130 [69]

establishing a diagnostic fragmentation signature of the synthetic tetrasaccharide. In addition, the fragmentation of the peptide portion led to the formation of b- and y- product ions that allowed the determination of the sequence of the glycated peptide.

However, some peptide product ions had the particularity to have lost the carbo- hydrate portion but were still attached to the spacer-squaric acid chain: $[b_3 - B_4]^+$ at m/z 565.2661, $[b_4 - B_4]^+$ at m/z 636.2715 and $[y_7 - B_2]^+$ at m/z 1361.7265. Thus, the identified glycated peptides ALK*AWSVAR at m/z 1951.0130, VTK*CCTESLVNR at m/z 2416.1372, and QNCDQFEK*LGEYGFQNALIVR at m/z 3478.6429 allowed to determine the glycation site on the following lysine residues: Lys 235, Lys 498 and Lys 420, respectively.

Similarly, the MALDI-MS/MS analysis of the GluC V8 digests afforded differ- ent glycated peptides: LCK*VASLRE at m/z 2025.0186, YAVSVLLRLAK*E at m/z 2311.2476 and YAVSVLLRLAK*EYE at m/z 2603.3484, allowing to identify the following glycation sites on lysine residues: Lys 100 and Lys 374. To sum it up, only five glycation sites were identified during the MALDI-MS and MS/MS analy- ses of the tryptic and GluC V8 digests of the hapten-BSA glycoconjugate: Lys 100, Lys 235, Lys 374, Lys 420 and Lys 498.

11.8.2.2   LC-MS/MS

The second approach for the determination of the glycation sites of the vaccine neoglycoconjugate was the LC-MS/MS analysis of the tryptic and GluC V8 digests. It was noted that the LC-MS/MS analysis of peptides has the advantage of minimiz- ing the ionization suppression effect comparing to the MALDI-MS/MS analysis [88, 89].

The data of the LC-MS/MS analysis of the tryptic and GluC V8 digests were submitted to the MASCOT library and matched two serum albumin protein iso- forms: the serum albumin precursor (gi|1,351,907) and serum albumin (gi|74,267,962) from *Bos taurus*.

For the tryptic digests, the BSA sequence coverage was found to be 57% for the serum albumin precursor from *Bos taurus* (gi|1,351,907) and 58% for serum albu- min protein from *Bos taurus* (gi|74,267,962). The LC-MS/MS analysis of the hap- ten- BSA tryptic digests allowed the identification of 18 glycated peptides, reported in Table 11.2.

The low-energy CID-MS/MS analysis of the extracted precursor ions of the gly- cated peptides allowed to localize the glycation sites on the following 18 lysine resi- dues: Lys 140, Lys 155, Lys 156, Lys 204, Lys 211, Lys 228, Lys 235, Lys 304, Lys 374, Lys 401, Lys 420, Lys 437, Lys 455, Lys 463, Lys 495, Lys 498, Lys 547 and Lys 559.

The LC-MS/MS analysis of the hapten-BSA vaccine GluC V8 digest allowed the identification of the serum albumin from *Bos taurus* (gi|74,267,962) with a sequence coverage of 42% and the precursor serum albumin from *Bos taurus* (gi|1,351,907) with a sequence coverage of 45%, in the MASCOT database. Table 11.3 displays the identified glycated peptides during the LC-MS/MS analysis of the GluC V8

Table 11.2 Tryptic glycopeptides identified of the bovine serum albumin protein by LC-ESI-QqTOF-MS/MS analysis of the hapten-BSA glycoconjugate [69]

Precursor ion					
m/z			Deviation	Missed	
(Charge)	Mr (expt)	Mr (calc)	Da	Cleavage	Peptide
729.8826 (+2)	1457.7506	1457.7389	0.0117	1	KHK*P (Lys 559)
733.3170 (+2)	1464.6194	1464.7698	−0.1504	1	QIK*K (Lys 547)
770.3757 (+2)	1538.7369	1538.7338	0.0031	1	ADEK*K (Lys 155)
807.9138 (+2)	1613.8129	1613.7964	0.0165	0	K*FWGK (Lys 156)
828.0811 (+3)	2481.2213	2481.2005	0.0208	2	LKECCDK*PLLEK (Lys 304)
832.7770 (+3)	2495.3092	2495.3146	−0.0054	1	LK*HLVDEPQNLIK (Lys 401)
863.7965 (+3)	2588.3677	2588.3572	0.0105	0	K*VPQVSTPTLVEVSR (Lys 437)
883.9655 (+2)	1765.9164	1765.9085	0.0079	1	SLGK*VGTR (Lys 455)
922.0941 (+3)	2763.2605	2763.2493	0.0112	1	LAK*EYEATLEECCAK (Lys 374)
969.5086 (+2)	1937.0026	1936.9868	0.0158	1	TPVSEK*VTK (Lys 495)
970.4900 (+2)	1938.9738	1938.9772	−0.0034	1	EK*VLTSSAR (Lys 211)
976.0173 (+2)	1950.0201	1950.0085	0.0116	1	ALK*AWSVAR (Lys 235)
990.4710 (+3)	2968.3911	2968.3886	0.0025	2	LK*PDPNTLCDEFKADEK (Lys 140)
1073.0144 (+2)	2144,0143	2144.0082	0.0061	1	CASIQK*FGER (Lys 228)
1058.4652 (+2)	2114.9159	2114.9123	0.0036	1	CCTK*PESER (Lys 463)
1208.5857 (+2)	2415.1569	2415.1284	0.0285	1	VTK*CCTESLVNR (Lys 498)
1160.2172 (+3)	3477.6297	3477.6385	−0.0088	1	QNCDQFEK*LGEYGFQNALIVR (Lys 420)
1169.5978 (+2)	2337.1810	2337.1583	0.0227	1	GACLLPK*IETMR (Lys 204)

digests. Thus, the CID-MS/MS analysis of theses glycated peptides allowed to discover 17 glycation sites, localized on the following lysine residues: Lys 65, Lys 75, Lys 88, Lys 100, Lys 117, Lys 151, Lys 183, Lys 197, Lys 256, Lys 266, Lys 304, Lys 309, Lys 336, Lys 374, Lys 420, Lys 455 and Lys 495.

Table 11.3 Glycopeptides identified in the bovine serum albumin protein by LC-ESI-QqTOF-MS/MS analysis of the hapten-BSA glycoconjugate digested with the endoproteinase GluC V8 [69]

Precursor ion m/z (charge)	Mr (expt)	Mr (calc)	Deviation Da	Missed Cleavage	Peptide
698.3598 (+2)	1394.7051	1394.6803	0.0248	0	K*LGE (Lys 420)
790.3774 (+2)	1578.7403	1578.7288	0.0115	1	K*QEPE (Lys ll7)
844.3721 (+2)	1686.7297	1686.7499	−0.0202	1	EFK*ADE (Lys 151)
894.4637 (+2)	1786.9128	1786.8976	0.0152	0	HVK*LVNE (Lys 65)
862.9539 (+2)	1723.8933	1723.8754	0.01179	1	VTK*LVTD (Lys 256)
897.4200 (+2)	1792.8255	1792.8176	0.0079	0	K*SHCIAE (Lys 309)
902.4801 (+2)	1802.9456	1802.9289	0.0167	0	LTKVHK*E (Lys 266)
962.1552 (+2)	2883.4439	2883.4093	0.0346	0	VSRSLGK*VGTRCCTKPE (Lys 455)
987.9658 (+2)	1973.9171	1973.8949	0.0222	0	K*VTKCCTE (Lys 495)
989.9697 (+2)	1977.9248	1977.9154	0.0094	2	K*QEPERNE (Lys 117)
992.4568 (+2)	1982.8989	1982.884	0.0149	1	CCDK*PLLE (Lys 304)
995.4702 (+2)	1988.9258	1988.8912	0.0346	1	FAK*TCVADE (Lys 75)
1013.0142 (+2)	2024.0138	2024.0123	0.0015	0	LCK*VASLRE (Lys 100)
1048.5225 (+2)	2095.0305	2094.9984	0.0321	1	K*SLHTLFGDE (Lys 88)
1097.0595 (+2)	2192.1045	2192.0909	0.0136	0	DK*GACLLPKIE (Lys 197)
1124.5018 (+2)	2246.9890	2246.9876	0.0014	1	DK*DVCKNYQE (Lys 336)
1336.1446 (+2)	2670.2746	2670.2728	0.0018	0	LLYYANK*YNGVFQE (Lys 183)
1156.132 (+2)	2310.2495	2310.2345	0.0150	0	YAVSVLLRLAK*E (Lys 374)

In summary, the LC-MS/MS analysis of both tryptic and GluC V8 digests allowed the identification of a total of 30 glycation sites on the lysine residues (Fig. 11.9a). Mapping these glycation sites on the 3D representation of the BSA (Fig. 11.9b, lysines highlighted in red) permitted to observe that they correspond to lysine residues located at the outer surface of the BSA. In addition, the number of

a
```
   1 MKWVTFISLL LLFSSAYSRG VFRRDTHKSE IAHRFKDLGE EHFKGLVLIA
  51 FSQYLQQCPF DEHVK*LVNEL TEFAK*TCVAD ESHAGCEK*SL HTLFGDELCK*
 101 VASLRETYGD MADCCAK*QEP ERNECFLSHK DDSPDLPKLK* PDPNTLCDEF
 151 K*ADEK*K*FWGK YLYEIARRHP YFYAPELLYY ANK*YNGVFQE CCQAEDK*GAC
 201 LLPK*IETMRE K*VLTSSARQR LRCASIQK*FG ERALK*AWSVA RLSQKFPKAE
 251 FVEVTK*LVTD LTKVHK*ECCH GDLLECADDR ADLAKYICDN QDTISSKLKE
 301 CCDK*PLLEK*S HCIAEVEKDA IPENLPPLTA DFAEDK*DVCK NYQEAKDAFL
 351 GSFLYEYSRR HPEYAVSVLL RLAK*EYEATL EECCAKDDPH ACYSTVFDKL
 401 K*HLVDEPQNL IKQNCDQFEK* LGEYGFQNEL IVRYTRK*VPQ VSTPTLVEVS
 451 RSLGK*VGTRC CTK*PESERMP CAEDYLSLIL NRLCVLHEKT PVSEK*VTK*CC
 501 TESLVNRRPC FSALTPDETY VPKAFDEKLF TFHADICTLP DTEKQIK*KQT
 551 ALVELLKHK*P KATEEQLKTV MENFVAFVGK CCAADDKEAC FAVEGPKLVV
 601 STQTALA
```

b
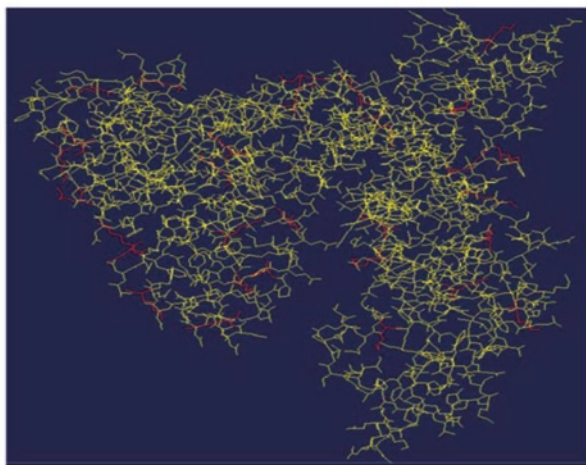
Fig. 11.9 (**a**) BSA sequence where the glycation sites are indicated by an *asterisk* (*red* = identified. on tryptic digests, *blue* = identified on GluC V8 digests and *red* and *underlined* = identified on both tryptic and GluC V8 digests) and (**b**) 3D structure of the BSA. The glycated lysine residues are highlighted in *red* (Swiss-Pdb Viewer software) [69]

the identified glycation sites (30 lysine residues) being higher than the determined (hapten: BSA ratio 5.4:1) of the tetrasaccharide-BSA neoglycoconjugate, it was concluded that the vaccine is composed of a mixture of glycoforms.

11.9 Conclusion

The systematic investigations presented herein constitute a series of versatile examples for the identification of accurate quality control necessary in commercial production of glycoconjugate vaccines against infectious diseases. The glycopeptides isolated and fully characterized during this work may well represent useful reference compounds to be used in standardization analyses.

Moreover, although BSA usually serves a universal model carrier protein for novel conjugation chemistry, we found it perfectly legitimate as a vaccine in mouse

experiments since the monoclonal antibodies isolated from the above conjugates were the basis for fully synthetic carbohydrate-based vaccines [24–27]. This would be particularly true when performed on other more immunogenic protein carriers such as tetanus toxoid and KLH.

References

1. Inglesby TV, Henderson DA, Bartlett JG, Ascher MS, Eitzen E, Friedlander AM, Hauer J, McDade J, Osterholm MT, O'Toole T, Parker G, Perl TM, Russell PK, Tonat K (1999) Anthrax as a biological weapon: medical and public health management. Working group on civilian biodefense. JAMA 281(18):1735–1745
2. Inglesby TV, O'Toole T, Henderson DA, Bartlett JG, Ascher MS, Eitzen E, Friedlander AM, Gerberding J, Hauer J, Hughes J, McDade J, Osterholm MT, Parker G, Perl TM, Russell PK, Tonat K (2002) Anthrax as a biological weapon, 2002: updated recommendations for management. JAMA 287(17):2236–2252
3. Henderson DA, Inglesby TV, Bartlett JG, Ascher MS, Eitzen E, Jahrling PB, Hauer J, Layton M, McDade J, Osterholm MT, O'Toole T, Parker G, Perl T, Russell PK, Tonat K (1999) Smallpox as a biological weapon: medical and public health management. Working group on civilian biodefense. JAMA 281(22):2127–2137
4. Lovinger S (2002) Addressing the unthinkable: preparing to face smallpox. JAMA 288(20):2530
5. Inglesby TV, Dennis DT, Henderson DA, Bartlett JG, Ascher MS, Eitzen E, Fine AD, Friedlander AM, Hauer J, Koerner JF, Layton M, McDade J, Osterholm MT, O'Toole T, Parker G, Perl TM, Russell PK, Schoch-Spana M, Tonat K (2000) Plague as a biological weapon: medical and public health management. Working group on civilian biodefense. JAMA 283(17):2281–2290
6. Arnon SS, Schechter R, Inglesby TV, Henderson DA, Bartlett JG, Ascher MS, Eitzen E, Fine AD, Hauer J, Layton M, Lillibridge S, Osterholm MT, O'Toole T, Parker G, Perl TM, Russell PK, Swerdlow DL, Tonat K (2001) Botulinum toxin as a biological weapon: medical and public health management. JAMA 285(8):1059–1070
7. Dennis DT, Inglesby TV, Henderson DA, Bartlett JG, Ascher MS, Eitzen E, Fine AD, Friedlander AM, Hauer J, Layton M, Lillibridge SR, McDade JE, Osterholm MT, O'Toole T, Parker G, Perl TM, Russell PK, Tonat K (2001) Tularemia as a biological weapon: medical and public health management. JAMA 285(21):2763–2773
8. Porter RK (ed) (2011) The Merck manual of diagnosis and therapy, 19th edn. Merck Sharp & Dohme Corp., Whitehouse Station
9. Choudhary S, Malik YS, Tomar S (2020) Identification of SARS-CoV-2 cell entry inhibitors by drug repurposing using in Silico structure-based virtual screening approach. ChemRxiv Preprint. https://doi.org/10.26434/chemrxiv.12005988.v1
10. Mantis NJ, Morici LA, Roy CJ (2011) Mucosal Vaccines for Biodefense. In: Kozlowski P (ed) Mucosal vaccines. Current topics in microbiology and immunology, vol 354. Springer, Berlin, Heidelberg
11. Rotz LD, Khan AS, Lillibridge SR et al (2002) Public health assessment of potential biological terrorism agents. Emerg Infect Dis 8:225–230
12. Artenstein AW (2008) New generation smallpox vaccines: a review of preclinical and clinical data. Rev Med Virol 18:217–231
13. Sobel J, Khan AS, Swerdlow DL (2002) Threat of a biological terrorist attack on the US food supply: the CDC perspective. Lancet 359:874–880
14. Bottaccioli F (2002) Il sistema immunitario: la bilancia della vita – Com'Ã¨ fatto, come funziona in salute e in malattia. Tecniche Nuove. ISBN 8848109462, www.tecnichenuove.com

15. Actor J (2014) Introductory immunology. 1st edition - basic concepts for interdisciplinary applications. Academic. ISBN: 9780124200302
16. Abbas A, Lichtman AH, Pillai S (2014) Cellular and molecular immunology, 8th edn, Saunders, ISBN: 9780323316149
17. Leppla SH, Robbins JB, Schneerson R et al (2002) Development of an improved vaccine for anthrax. J Clin Invest 110:141–144
18. Metzger DW, Bakshi CS, Kirimanjeswara G (2007) Mucosal immunopathogenesis of Francisella tularensis. Ann N Y Acad Sci 1105:266–283
19. Kappler J, Kotzin B, Herron L et al (1989) V beta-specific stimulation of human T cells by staphylococcal toxins. Science 244:811–813
20. White J, Herman A, Pullen AM et al (1989) The V beta-specific superantigen staphylococcal enterotoxin B: stimulation of mature T cells and clonal deletion in neonatal mice. Cell 56:27–35
21. Murphy K (2011) Janeway's immunobiology, 8th edition. Garland Science. ISBN-10: 0815342438
22. Abbas AK, Lichtman AH (2010) Basic immunology, 3rd edn. Saunders Kindle Edition ISBN-10: 141605569X
23. Plotkin SA (2008) Vaccines: correlates of vaccine-induced immunity. Clin Infect Dis 47:401–409
24. Heidelberger M, Avery OT (1923) The soluble specific substance of pneumococcus. J Exp Med 38:73–79
25. Ausubel FM (2005) Are innate immune signaling pathways in plants and animals conserved? Nat Immunol 6:973–979
26. Rumbo M, Nempont C, Kraehenbuhl J-P, Sirard J-C (2006) Mucosal interplay among commensal and pathogenic bacteria: lessons from flagellin and toll-like receptor 5. FEBS Lett (12):2976–2984
27. Shetty N, Aarons E, Andrews J (2009) Structure and functions of microbes. In: Shetty N, Tang JW, Andrews J (eds) Infectious disease: pathogenesis, prevention, and case studies. Wiley, London, p 15
28. Corbett D, Hudson T, Roberts IS (2010) Bacterial polysaccharide capsules. In: Konig H (ed) Prokaryotic cell wall compounds. Springer, Heidelberg, p 111
29. Monack DM, Mueller A, Falkow S (2004) Persistent bacterial infections: the interface of the pathogen and the host immune system. Nat Rev Microbiol 2:747–765
30. Westphal O, Liideritz O, Bister F (1952) Ueber die Extraktion von Bakterien mit Phenol/Wasser. Z Naturforsch. 7B:148–155
31. Pupo E, Aguila A, Santana H, Núnez JF, Castellanos-Serra L, Hardy E (1999) Mice immunization with gel electrophoresis-micropurified bacterial lipopolysaccharides. Electrophoresis 20:458–461
32. Davis MR Jr, Goldberg JB (2012) Purification and visualization of lipopolysaccharide from Gram-negative bacteria by hot aqueous-phenol extraction. J Vis Exp 28:e3916, 1–3
33. Nagy G, Pál T (2008) Lipopolysaccharide: a tool and target in enterobacterial vaccine development. Biol Chem 389:513–520
34. Reisser D, Pance A, Jeannin JF (2002) Mechanisms of the antitumoral effect of lipid
35. Bowden RA, Cloeckaert A, Zygmunt MS, Dubray G (1995) Outer-membrane protein- and rough lipopolysaccharide-specific monoclonal antibodies protect mice against *Brucella ovis*. J Med Microbiol 43:344–347
36. Fulop M, Mastroeni P, Green M, Titball RW (2001) Role of antibody to lipopolysaccharide in protection against low- and high-virulence strains of *Francisella tularensis*. Vaccine 19:4465–4472
37. Ada G, Isaacs D (2003) Carbohydrate-protein conjugate vaccines. Clin Microbiol Infect 9:79–85
38. Landsteiner K (1945) The specificity of serological reactions. Harvard University Press, Cambridge

39. Avery OT, Goebel WF (1929) Chemo-immunological studies on conjugated carbohydrate-proteins. II Immunological specificity of synthetic sugar-protein antigens. J Exp Med 50:533–550

40. Pollard AJ, Perrett KP, Beverley PC (2009) Maintaining protection against invasive bacteria with protein-polysaccharide conjugate vaccines. Nat Rev 9:213–220

41. Daum RS, Hogerman D, Rennels MB, Bewley K, Malinoski F, Rothstein E, Reisinger K, Block S, Keyserling H, Steinhoff M (1997) Infant immunization with pneumococcal CRM 197 vaccines: effect of saccharide size on immunogenicity and interactions with simultaneously administrated vaccines. J Infect Dis 176:445–455

42. Lefeber DJ, Kamerling JP, Vliegenthart JFG (2001) Synthesis of Streptococcus pneumoniae type 3 neoglycoproteins varying in oligosaccharide chain length, loading, and carrier protein. Chem Eur J 7:4411

43. Paoletti LC, Kasper DL, Michon F, DiFabio J, Jennings HJ, Tosteson TD, Wessels MR (1992) Effects of chain length on the immunogenicity in rabbits of group B Streptococcus type III oligosaccharide-tetanus toxoid conjugates. J Clin Invest 89:203

44. Chernyak A, Kondo S, Wade TK, Meeks MD, Alzari PM, Fournier JM, Taylor RK, Kováč P, Wade WF (2002) Induction of protective immunity by synthetic *Vibrio cholerae* hexasaccharide derived from *V. cholerae* O1 Ogawa lipopolysaccharide bound to a protein carrier. J Infect Dis 185:950–962

45. Dick WE Jr, Beurret M (1989) A survey and consideration of design and preparation factors. In: Cruse JM, Lewis RE Jr (eds) Glycoconjugates of bacterial carbohydrate antigens, vol 10. Krager, Basel, pp 48–114

46. Tietze LF, Arlt M, Beller M, Glüsenkamp KH, Jähde E, Rajewsky MF (1991) Anticancer agents, 15. Squaric acid diethyl ester: a new coupling reagent for the formation of drug biopolymer conjugates. Synthesis of squaric acid ester amides and diamides. Chem Ber 124:1215–1221

47. Glüsenkamp KH, Drosdziok W, Eberle G, Jähde E, Rajewsky MFZ (1991) Naturforsch C Biosci 46:498–501

48. Tietze LF, Schröter C, Gabius S, Brinck U, Goerlach-Graw A, Gabius HJ (1991) Conjugation of p-aminophenyl glycosides with squaric acid diesters to a carrier protein and the use of the neoglycoprotein in the histochemical detection of lectines. Bioconjug Chem 2:148–153

49. Cohen S, Cohen SG (1966) Preparation and reactions of derivatives of squaric acid. Alkoxy-, hydroxy-, and aminocyclobutenediones 1. J Am Chem Soc 88:1533–1536

50. Grünefeld J, Bredhauer G, Zinner G (1985) Zur reaktion von quadratsäuredimethylester mit N, *N*-disubstituierten hydrazin-derivaten. Arch Pharm (Weinheim) 318:984–988

51. Bergh A, Magnusson BG, Ohlsson J, Wellmar U, Nilsson UJ (2001) Didecyl squarate – a practical amino-reactive cross-linking reagent for neoglycoconjugate synthesis. Glycoconj J 18:615–621

52. Kamath VP, Diedrich P, Hindsgaul O (1996) Use of diethyl squarate for the coupling of oligosaccharide amines to carrier proteins and characterization of the resulting neoglycoproteins by MALDI-TOF mass spectrometry. Glycoconj J 13:315–319

53. Hou S-J, Saksena R, Kováč P (2008) Preparation of glycoconjugates by dialkyl squarate chemistry revisited. Carbohydr Res 343:196–210

54. Saksena R, Adamo R, Kováč P (2007) Immunogens related to the synthetic tetrasaccharide side chain of the *Bacillus anthracis* exosporium. Bioorg Med Chem 15:4283–4310

55. Bongat AFG, Saksena R, Adamo R, Fujimoto Y, Shiokawa Z, Peterson DC, Fukase K, Vann WF, Kováč P (2010) Multimeric bivalent immunogens from recombinant tetanus toxin HC fragment, synthetic hexasaccharides and a glycopeptide adjuvant. Glycoconj J 27:69–77

56. Aebersold R, Mann M (2003) Mass spectrometry-based proteomics. Nature 422:198–207

57. Morelle W, Michalski JC (2005) Glycomics and mass spectrometry. Curr Pharm Des 11:2615–2645

58. Dettmer K, Aronov PA, Hammock BD (2007) Mass spectrometry-based metabolomics. Mass Spectrom Rev 26:51–78

59. Blanksby SJ, Mitchell TW (2010) Advances in mass spectrometry for lipidomics. Annu Rev Anal Chem 3:433–465

60. Banoub JH, Newton RP, Esmans E, Ewing DF, Mackenzie G (2005) Recent developments in mass spectrometry for the characterization of nucleosides, nucleotides, oligonucleotides, and nucleic acids. Chem Rev 105:1869–1915

61. Zhang Y, Go EP, Desaire H (2008) Maximizing coverage of glycosylation heterogeneity in MALDI-MS analysis of glycoproteins with up to 27 glycosylation sites. Anal Chem 80:3144–3158

62. Laštovičková M, Chmelik J, Bobalova J (2009) The combination of simple MALDI matrices for the improvement of intact glycoproteins and glycans analysis. Int J Mass Spectrom 281:82–88

63. Kamath VP, Diedrich P, Hindsgaul O (1996) Use of diethyl squarate for the coupling of oligosaccharide amines to carrier proteins and characterization of the resulting neoglycoproteins by MALDI-TOF mass spectrometry. Glycoconj J 13:315–319

64. Issaq HJ, Conrads TP, Prieto DA, Tirumalai R, Veenstra TD (2003) SELDI-TOF MS for diagnostic proteomics. Anal Chem 75:148A–155A

65. Liu C (2011) The application of SELDI-TOF-MS in clinical diagnosis of cancers. J Biomed Biotechnol 6:245821

66. Chernyak A, Karavanov A, Ogawa Y, Kováč P (2001) Conjugating oligosaccharides to proteins by squaric acid diester chemistry: rapid monitoring of the progress of conjugation, and recovery of the unused ligand. Carbohydr Res 330:479–486

67. Jahouh F, Saksena R, Aiello D, Napoli A, Sindona G, Kováč P, Banoub JH (2010) Glycation sites in neoglycoconjugates from the terminal monosaccharide antigen of the O-PS of *Vibrio cholerae* O1, serotype Ogawa, and BSA revealed by matrix-assisted laser desorption- ionization tandem mass spectrometry. J Mass Spectrom (10):1148–1159

68. Jahouh F, Saksena R, Kováč P, Banoub JH (2012) Revealing the glycation sites in synthetic neoglycoconjugates formed by conjugation of the antigenic monosaccharide hapten of *Vibrio cholerae* O1 serotype Ogawa with the BSA protein carrier using LC-ESI-QqTOF-MS/MS. J Mass Spectrom 47:890–900

69. Jahouh F, Hou SJ, Kováč P, Banoub JH (2011) Determination of the glycation sites of *Bacillus anthracis* neoglycoconjugate vaccine by MALDI-TOF/TOF-CID-MS/MS and LC-ESI-QqTOF-tandem mass spectrometry. J Mass Spectrom 46:993–1003

70. Jahouh F, Hou SJ, Kováč P, Banoub JH (2012) Determination of glycation sites by tandem mass spectrometry in a synthetic lactose-bovine serum albumin conjugate, a vaccine model prepared by dialkyl squarate chemistry. Rapid Commun Mass Spectrom 26:749–758

71. Jahouh F, Xu P, Vann WF, Kováč P, Banoub JH (2013) Mapping the glycation sites in the neoglycoconjugate from hexasaccharide antigen of *Vibrio cholerae* , serotype Ogawa and the recombinant tetanus toxin C-fragment carrier. J Mass Spectrom 48:1083–1090

72. McCarthy PC, Saksena R, Peterson DC, Lee CH, An Y, Cipollo JF, Vann WF (2013) Chemoenzymatic synthesis of immunogenic meningococcal group C polysialic acid-tetanus Hc fragment glycoconjugates. Glycoconj J 30:857–870

73. Roepstorff P, Fohlman J (1984) Proposal for a common nomenclature for sequence ions in mass spectra of peptides. Biol Mass Spectrom 11:601

74. Johnson RS, Martin SA, Biemann K, Stults JT, Watson JT (1987) Novel fragmentation process of peptides by collision-induced decomposition in a tandem mass spectrometer: differentiation of leucine and isoleucine. Anal Chem 59:2621–2625

75. Domon B, Costello C (1988) A systematic nomenclature for carbohydrate fragmentations in FAB-MS/MS spectra of glycoconjugates. Glycoconj J 5:397–409

76. Mock M, Fouet A (2001) Anthrax. Annu Rev Microbiol 55:647–671

77. Pries FG (1993) In: Sonenshein AL, Hoch JA, Losick R (eds) Bacillus subtilis and other gram-positive bacteria: biochemistry, physiology, and molecular biology. American Society for Microbiology, Washington, DC, p 3

78. Nicholson WL, Munakata N, Horneck G, Melosh HJ, Setlow P (2000) Resistance of *Bacillus* endospores to extreme terrestrial and extraterrestrial environments. Microbiol Mol Biol Rev 64:548–572
79. Boutiba-Ben Boubaker I, Ben Redjeb S (2001) *Bacillus anthracis* : causative agent of anthrax. Tunis Med 79:642–646
80. Read TD, Salzberg SL, Pop M, Shumway M, Umayam L, Jiang L, Holtzapple E, Busch JD, Smith KL, Schupp JM, Solomon D, Keim P, Fraser CM (2002) Comparative genome sequencing for discovery of novel polymorphisms in *Bacillus anthracis*. Science 296:2028–2033
81. Turnbull PCB (1999) Defi nitive identifi cation of *Bacillus anthracis* -a review. J Appl Microbiol 87:237–240
82. Reed LJ, Muench H (1938) A simple method for estimating fifty percent endpoints. Am J Hyg 27:493–497
83. Hoffmaster AR, Fitzgerald CC, Ribot E, Mayer LW, Popovic T (2002) Molecular subtyping of *Bacillus anthracis* and the 2001 bioterrorism-associated anthrax outbreak, United States. Emerg Infect Dis 8:1111–1116
84. Chun J-H, Hong K-J, Cha SH, Cho M-H, Lee KJ, Jeong DH, Yoo C-K, Rhie G-e (2012) Complete genome sequence of *Bacillus anthracis* H9401, an isolate from a Korean patient with anthrax. J Bacteriol 194:4116–4117
85. Williams DD, Benedek O, Turnbough CL Jr (2003) Species-specifi c peptide ligands for the detection of *Bacillus anthracis* spores. Appl Environ Microbiol 69:6288–6293
86. Chabot DJ, Scorpio A, Tobery SA, Little SF, Norris SL, Friedlander AM (2004) Anthrax capsule vaccine protects against experimental infection. Vaccine 23:43–47
87. Daubenspeck JM, Zeng H, Chen P, Dong S, Steichen CT, Krishna NR, Pritchard DG Jr, Turnbough CL (2004) Novel oligosaccharide side chains of the collagen-like region of BclA, the major glycoprotein of the *Bacillus anthracis* exosporium. J Biol Chem 279:30945–30953
88. Burkitt WI, Giannakopulos AE, Sideridou F, Bashir S, Derrick PJ (2003) Discrimination effects in MALDI-MS of mixtures of peptides-analysis of the proteome. Aust J Chem 56:369–377
89. Kratzer R, Eckerskorn C, Karas M, Lottspeich F (1998) Suppression effects in enzymatic peptide ladder sequencing using ultraviolet – matrix assisted laser desorption/ionization – mass spectrometry. Electrophoresis 19:1910–1919

Chapter 12
Environmental Impacts of Air Pollution on Human Health in Annaba Region (Northeast of Algeria)

Aissa Benselhoub and Ali Ismet Kanlı

Abstract Nowadays, the protection of environment and in particular the preservation of human health is one of the major concerns of policymakers over the world. Annaba region offers the most favorable conditions for economic development, through multiple possibilities, landscape diversity, basic infrastructure and an industrial potential. Facing the severity of environmental problems in Annaba due to the dense industrial activities, an environmental health survey was conducted in order to highlight the specific morbidity of air pollution in the region. The obtained results show that 30% of consultations and are for respiratory diseases, 40% of infant mortality (children under 1 year) is caused by respiratory diseases and 600000 asthmatics suffer permanently. A sustainable control, periodic monitoring and the establishment of a database connecting with air pollution, can play a key role to effective assessment and reducing the negative impacts of air pollution in the study area.

Keywords Air pollution · Regulation · Environmental protection · Health risks · Annaba

A. Benselhoub
Dnipro State Agrarian and Economic University, Dnipro, Ukraine

A. I. Kanlı (✉)
Department of Geophysical Engineering, Istanbul University-Cerrahpasa, Istanbul, Turkey
e-mail: benselhoub@yahoo.fr

12.1   Introduction

The air we breathe today is a mixture more or less polluted depending on where we are. Whether near or far from sources, this mixture of pollutants generates significant and long-lasting damage to human health, particularly respiratory problems, so air pollution is currently a major concern of health organizations for the protection of the environment and in particular the preservation of human health [1, 2].

In the absence of limit values of pollution and stricter environmental legislation, it is difficult in term of assessment and management of environmental problems on national scale, particularly in the industrial cities [3].

The control of air quality would have a positive impact on the health of workers, which would be altered by the air generated by the steel industry, and would make it possible to locate the sectors requiring interventions that are specific to the process or under form of setting up clean technology [4].

Air pollution in the air of Annaba, as a coastal and industrial city (steel, Asmidal), is neither identified nor quantified. In fact, the environmental situation in this region is a curiosity for residents who are the first targets of significant environmental impacts, especially since respiratory diseases have reached their maximum in this region [5].

The present work aims to study the environmental impacts of air pollution in Annaba region located at the eastern part of Algeria, especially in the absence of database on air pollution.

12.2   Study Area

The province of Annaba is located in the northeast of Algeria (Fig. 12.1), on the Mediterranean coastline. Annaba is located at 581 km east from the capital Algiers. The province covers an area of 1420 km^2.

The population's data of Annaba municipalities of the study area is presented in Table 12.1.

This region offers the most favorable conditions for economic development, through multiple possibilities it contains. A landscape diversity, basic infrastructure, accessibility consistent, academic, and interdisciplinary research infrastructures, industrial potential consists of leaders in the export of seasoned managers and a skilled workforce, notwithstanding the tourist attractions and bewitching Agrofood. The development potential is undeniable, their implementation will revolve around the orientations and fundamental engineering by a local proactive strategy (heavy public investment) reinforced with an oriented strategy (private investment). The studied area is characterized by a major industries, which are subdivided into heavy industry that are Arcelor Mittal, Sider, and Ferrovial (metallurgy and boiler); chemical industry such as the complex of phosphate and nitrogen fertilizers
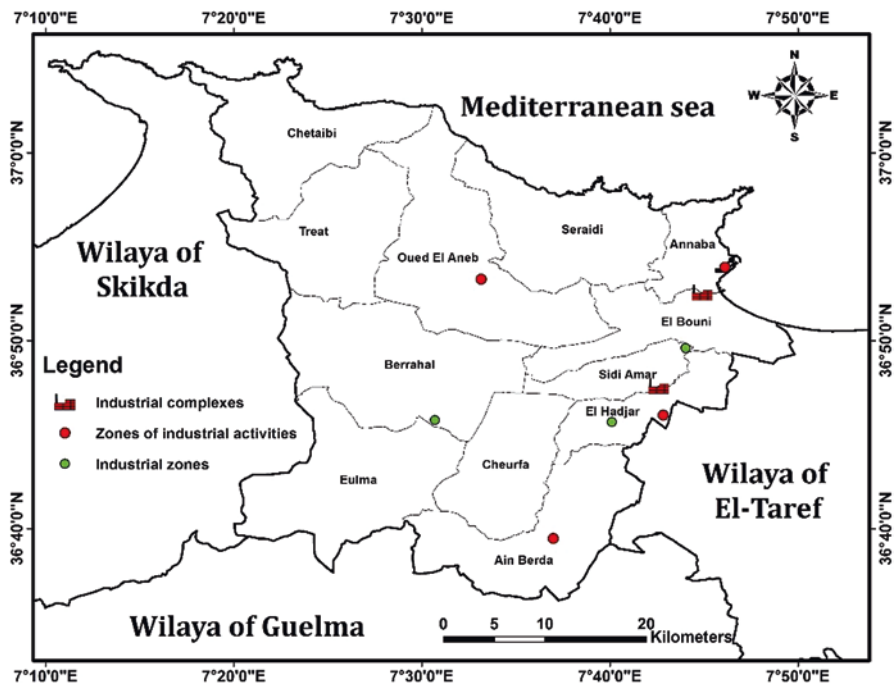
Fig. 12.1 Geographical location of the study area

Table 12.1 Population's data of municipalities of the study area

Municipality	Number of population (inhabitants)	Population nature
Annaba Center	269309	Urban
El Hadjar	38436	Sub-urban
El Bouni	130568	Urban
Sidi Amar	81313	Sub-urban

(FERTIAL). Additionally light manufacturing (ORELAIT) and several food industries or processing represented by small businesses [6].

12.3   Limit Values for Parameters of Atmospheric Emissions in Algeria

Any industrial operation may create risks or cause pollution or nuisance in particular for safety and the health of residents is a classified facility. Activities under the legislation on classified installations are listed in a schedule, which shall give an authorization or declaration depending on the significance of the risks or disadvantages that may be generated.

Table 12.2 Atmospheric emissions limits and liquid effluents for the industry

No	Parameters	Unit	Limit values	Tolerance of limit values of the old industries
1	Total dust	mg/Nm³	50	100
2	Sulphur oxides (expressed as sulfur dioxide)	''	300	500
4	Nitrous oxide	''	300	500
5	Hydrogen chloride and other inorganic gaseous compounds of chlorine (expressed as HCl).	''	50	100
7	Volatile organic compounds (total rejection of volatile organic compounds excluding methane)	''	150	200
8	Metals and metal compounds (gaseous and particulates)	''	5	10
10	Rejects of arsenic, selenium and tellurium and their compounds other than those mentioned among the releases of carcinogenic substances	''	1	2
11	Antimony releases, chromium, cobalt, copper, tin, manganese, nickel, vanadium and zinc, and their compounds other than those referred among the release of carcinogenic substances	''	5	10

The Algerian industry is required to make progress to overcome the challenges it faces. Meanwhile upgrading old industrial plants within five (5) years, the limit values for discharges of liquid and airborne effluents from industry support the antiquity of these Industrial installations by determining a tolerance concerning discharges from industrial liquid and atmospheric effluents from these facilities. In addition and due to the peculiarities of the technologies used, specific tolerance limit values are also granted by the relevant industrial categories [7].

For this purpose, the Executive Decree *n° 06–138 of 15 April 2006* aims to regulate the emission into the atmosphere of gases, fumes, vapor, liquid or solid particles, as well as the conditions under which exerted their control. Executive Decree *n° 06–141 of 19 April 2006* is for object to define the limit values for discharges of industrial liquid effluents. Atmospheric emissions limits and liquid effluents for the industry are listed below (Table 12.2) [8].

12.4 Air Quality Monitoring in Annaba Region

Overall, air quality in the Annaba area varies from excellent to fairly good with a rate of 81%. The poor quality is due in most cases to dust levels and to a lesser extent to photochemical pollution during the summer season.

The setting up of monitoring network and its exploitation allowed us to determine the potential for pollution in the pre-selected sites and to establish a data bank to improve the living environment of the citizen by correcting land-use planning and occupation of the land.

Reading the measurements given by the network reveals the following diagnosis:

Fig. 12.2 Air quality of
Annaba and its
agglomeration
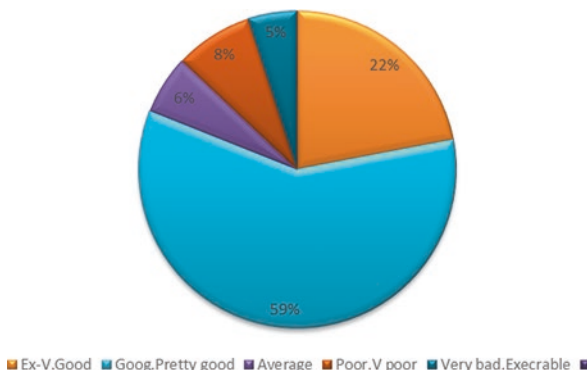
The presence of sediment pollution resulting from industrial activity, road traffic and lack of greening.

The sustainable operation of this network requires periodic monitoring either of the management of the data bank or of the maintenance of the various components. This last point emphasizes the availability of consumable materials essential to its sustainability [9]. Figure 12.2 shows the air quality in Annaba and its agglomeration.

12.5 Health Impact of Pollution in Annaba

According to the study conducted by the program of Technical Assistance of the Mediterranean Environment (METAP), the degradation of environment in Algeria costing $ 1.7 billion per year, or 3.6% of GDP. Furthermore, national report on the state of environment shown that 30% of consultations are for respiratory diseases, 40% of infant mortality (children under 1 year) is caused by respiratory diseases and 600000 asthmatics suffer permanently [10].

Considering the serious nature of the air pollution in Annaba, a health survey of the wilaya of Annaba was conducted by the Department of Epidemiology and Preventive Medicine of the University Hospital of Annaba (investigation four passages on a sample of 1000 households representing 6404 individuals). The results of the acute illness and chronic disease obtained after this survey were compared to those of the national survey. This comparison allowed to highlight the specific morbidity as described in Table 12.3.

12.6 Correlation Between Particulate Matter Concentrations and the Number of Asthma Crisis

Table 12.4 shows that the number of asthma varies from one municipality to another. It depends directly on the level of PM, where we recorded 360 cases of asthma crisis in 2006 at Annaba city, which corresponds to the PM content of 76.45 mg / m³. This number has increased to 4197 at El Hadjar. Wheras in 2009, the number of asthma

Table 12.3 Results on the epidemiological survey of Annaba

Disorders	National survey (Percentage %)	Survey in Annaba (Percentage %)
Acute disorders	16.7	18.4
Respiratory disorders	37.7	42.3
Cardiovascular disorders	02.1	05.2
Chronic disorders	07.0	16.3
Respiratory disorders	(9.2 Asthma)	(10.4 Asthma)
Cardiovascular disorders	22.5	23.2

Table 12.4 .Correlation between PM concentrations (for 2006) and asthma crisis (in 2006 and 2009)

City	PM 10 (μg/m^3)	Asthma crisis (case) 2006	Asthma crisis (case) 2009
Annaba City	76.45	360	1820
El Bouni	116.42	1920	4851
Sidi Amar	89.25	900	2084
El Hadjar	–	4197	9457

in the city of Annaba increases by 13 times compared than that in 2006 and reaching 4851 cases, although for the other municipalities this number was almost doubled (El Bouni 2084 cases, Sidi Amar 1820 and El Hadjar 9457 cases). Indicating a strong dust pollution during this year.

12.7 Relation Between Dust Concentrations and the Number of Other Respiratory Emergencies

The Fig. 12.3 indicates that the number of different respiratory emergencies is related to the dust level and varies from one municipality to another, from which there is a significant number of respiratory emergencies. The maximum cases was recorded at El Hadjar with 2123 cases and the minimum at the city of Annaba with 1030 cases. This number increased for the four municipalities during 2009, reaching 1614 cases for Annaba city cities, cases of Annaba, 3844 cases for El Bouni, 2403 cases for Sidi Amar and 6169 cases for El Hadjar. The increase in the number of different respiratory emergencies proves the increase in dust pollution during this year.

12.8 Conclusions

From the interpretation of the obtained results in this study, the following points should be highlighted:

– The environmental situation in Annaba region as a coastal and industrial city (steel) is a curiosity for residents who are the first targets of significant environ-
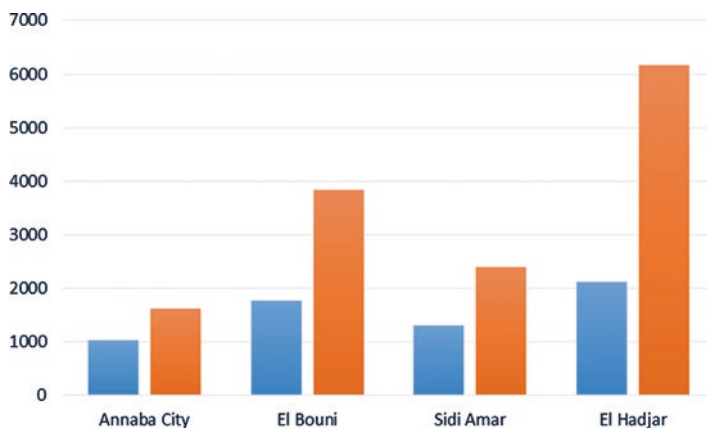
Fig. 12.3 Relation between dust concentrations and the number of other respiratory emergencies

mental impacts, especially since respiratory diseases have reached their maximum in this region.

– Air quality in the Annaba area varies from excellent to fairly good with a rate of 81%. The poor quality is due in most cases to dust levels and to a lesser extent to photochemical pollution during the summer season.
– The degradation of environment in Algeria costing $ 1.7 billion per year, or 3.6% of GDP.
– The state report on environment shown that 30% of consultations are for respiratory diseases, 40% of infant mortality (children under 1 year) is caused by respiratory diseases and 600000 asthmatics suffer permanently.
– The increase in the number of different respiratory emergencies proves an increasing of PM pollution.

A sustainable control, periodic monitoring and the establishment of a database connecting with air pollution, can play a key role to effective assessment and reducing the negative impacts of air pollution in the study area.

References

1. Benselhoub A, Kharytonov M, Bouabdallah S, Bounouala M, Idres A, Boukelloul ML (2015) Bioecological assessment of soil pollution with heavy metals in Annaba (Algeria). Studia Universitatis "Vasile Goldiş", Seria Ştiinţele Vieţii 25(1):77–22
2. Abedghers MT, Bouhamla K (2002) Internal environmental report: monitoring and evaluation of air quality at El-Hadjar metallurgical plant, CERSIM, DRA, SIDER
3. Kharytonov M, Benselhoub A, Klimkina I, Bouhedja A, Idres A, Aissi A (2016) Air pollution mapping in the Wilaya of Annaba (NE of Algeria). Min Sci 23:183–189
4. Benselhoub A, Kharytonov M, Bounouala M, Chaabia R, Badjoudj S (2015) Estimation of soil's sorption capacity to heavy metals in Algerian megacities: case of Algiers and Annaba. INMATEH-Agri Eng 46(2):147–154

5. Benselhoub A, Kharytonov M, Bounouala M, Chaabia R, Idres A (2015) Airborn soils pollution evaluation with heavy metals in Annaba region (Algeria). Metall Min Ind 7:32–35
6. Plan Directive d'Aménagement Urbain, 2008
7. Ramdane A (2011) la politique de protection de l'environnement en Algérie: réalisations et échecs. Disponible sur: http://elwahat.univghardaia.dz
8. Decree No. 06–141 of 19 April 2006
9. Samasafia. Bilan annuel sur la qualité de l'air pour l'année (2007). Techrep Réseau de surveillance de la qualité l'air d'Alger 2008
10. Kharytonov M, Benselhoub A, Krivakovska R, Zaichenko A, Aissi A, Bouabdallah S, Chaabia R, Vasilyeva T (2017) Risk assessment of aerotechnogenic pollution generated by industrial enterprises in algeria and ukraine, Studia Universitatis Vasile Goldis Seria Stiintele Vietii. Life Sci Ser 27:3
11. Benselhoub AM, Kharytonov MM, Zaichenko AO, Stankevich SA (2015) Environmental risks of man-made air pollution in Grand Algiers. J Georgian Geophys Soc 18(19):43–51
12. Benselhoub A (2017) Peculiarities of airborne soil pollution in the industrial regions of Algeria and Ukraine. PhD thesis, Dnipro, Ukraine

Chapter 13
New Insight into Idiopathic Nephrotic Syndrome: Strategy Based on Urinary Exosomes

Elisa Barigazzi, Lucia Santorelli, W. Morello, F. Raimondo, B. Crapella, L. Ghio, C. Tamburello, G. Montini, and M. Pitto

Growing interest regards the use of minimally invasive "liquid biopsies" to identify new biomarkers. Urinary exosomes (UE) are membranous nanovesicles released into urine by cells facing the urinary space. Their molecular composition depends upon the type of the producer cell; in that way, they provide a snapshot of the donor cell, capable to monitor its status. Their presence in urine makes them readily accessible, giving the possibility to investigate eventually pathological conditions especially related to kidney [1].

While exosomes research has flourished, few studies have specifically targeted the role of UE in the Nephrotic Syndrome (NS). As a rule, NS is a manifestation of many underlying renal disease processes. Most often in children, however, the NS is Idiopathic (INS), constituting the major childhood glomerular disease, with an incidence of 2-7/100.000 children <16 years old. Response to initial treatment with corticosteroids is an indicator of long-term prognosis, as resistant patients often present progressive disease [2].

The aim of the study is to verify the possibility to use UE of INS patients as a source of predictive markers of response to the corticosteroid treatment, and/or to clarify the disease etiopathogenesis. Thus, we investigated the UE protein content of a paediatric cohort of 30 patients, classified in three clinical classes, according to

---

E. Barigazzi (✉) · L. Santorelli · F. Raimondo · M. Pitto
School of Medicine and Surgery, University of Milano – Bicocca, Milan, Italy
e-mail: e.barigazzi@campus.unimib.it; l.santorelli@campus.unimib.it

W. Morello
School of Medicine and Surgery, University of Milano – Bicocca, Milan, Italy

Paediatric Nephrology, Dialysis and Transplant Unit, Fondazione IRCCS Ca' Granda-Ospedale Maggiore Policlinico, Milan, Italy

B. Crapella · L. Ghio · C. Tamburello · G. Montini
Paediatric Nephrology, Dialysis and Transplant Unit, Fondazione IRCCS Ca' Granda-Ospedale Maggiore Policlinico, Milan, Italy

the corticosteroids response: steroid-Dependent, (D), steroid-Sensitive (S) and steroid-Resistant (R).

Firstly, a characteristic SDS-PAGE protein profile emerged to be associated with each class, which preserves its peculiarity also when compared to UE protein content of non-INS patients (orthostatic proteinuria, hereditary tubulopathies) and healthy age-matched controls. Through a hierarchical clustering, we confirmed the imprints provided by the gel analysis: the UE of INS patients divided the cohort according to the clinical classifications.

Secondly, by immunoblotting, we also pinpointed different levels of specific glomerular membrane proteins (PgP, CD10, Podocin), described as involved in the INS development. Moreover, we observed that each protein above mentioned showed a major band located at the expected molecular weight (MW) and at least one other located at the higher MW, both significantly varied among the three classes, especially in the case of CD10.

These evidences confirmed the feasibility to use a UE approach to intercept the pathophysiological differences underlying the response to therapy. At the present time, we are proceeding in performing mass spectrometric analysis to more in depth comprehend the emerged differences in the UE proteome of the pilot cohort. Simultaneously, we are enlarging the sample size in order to develop a robust classification model, able to use UE as predictive parameter of long-term prognosis to treatment response.

References

1. Morrison EE, Bailey M, Dear JW (2016) Renal extracellular vesicles: from physiology to clinical application. J Physiol (20):5735–5748
2. Pasini A, Benetti E, Conti G, Ghio L, Lepore M, Massella L, Molino D, Peruzzi L, Emma F, Fede C, Trivelli A, Maringhini S, Materassi M, Messina G, Montini G, Murer L, Pecoraro C, Pennesi M (2017) The Italian Society for Pediatric Nephrology (SINePe) consensus document on the management of nephrotic syndrome in children: part I – diagnosis and treatment of the first episode and the first relapse. Italian J Pediatr 43:41

Chapter 14
Synthesis of Long-Chain Esters Under Continuous Flow Conditions

Daniela Caputo, Michele Casiello, Amelita Grazia Laurenza, Francesco Fracassi, Caterina Fusco, Angelo Nacci, and Lucia D'Accolti

In recent years, flow chemistry has rapidly gained interest due to the numerous improvements introduced in synthetic processes such as automation, safe reproducibility, improved safety, and process reliability [1]. Furthermore, reaction parameters settled for laboratory-scale fluidic processes can be used in the up-scaled flow reactors without the need for special optimization procedures [2].

In this study, the synthesis of biowax esters under flow conditions is reported [3], in order to obtain a convenient procedure for industrial applications. A simple way of access to these compounds is the Fisher-type esterification of long-chain acids with fatty alcohols to obtain wax esters with chains longer than C30 [4].

The flow chemistry procedure for the esterification of margaric, stearic, oleic and palmitic acids with an array of alcohols to produce the corresponding ester waxes, is developed. Three reaction factors (temperature, residence time, and wt % of catalyst) were optimized using the Box−Behnken design and the optimized parameters can be visualized in Fig. 14.1 (55 °C, 30 mins, 9.54 wt% of catalyst).

These milder conditions brought significant benefits in terms of energy consumption, cost efficiency, and eco-sustainability. All these benefits indicate that the preparation of biowax esters in continuous flow conditions has a good potential for industrial applications.

D. Caputo (✉) · A. Nacci · L. D'Accolti
Dipartimento di Chimica, Università degli studi di Bari "Aldo Moro", Bari, Italy

CNR, Istituto di Chimica dei Composti Organometallici (ICCOM), Bari, Italy
e-mail: daniela.caputo@uniba.it

M. Casiello · A. G. Laurenza · F. Fracassi
Dipartimento di Chimica, Università degli studi di Bari "Aldo Moro", Bari, Italy

C. Fusco
CNR, Istituto di Chimica dei Composti Organometallici (ICCOM), Bari, Italy
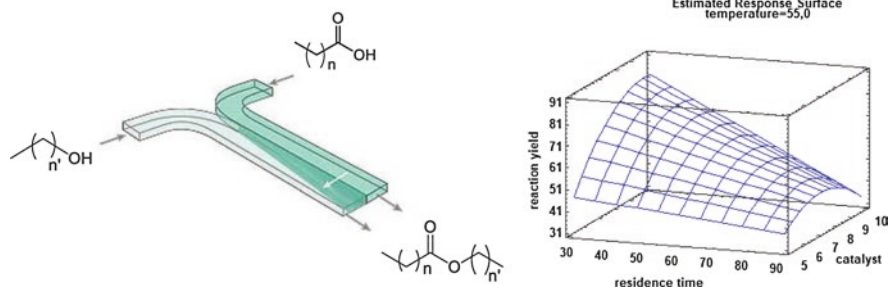
Fig. 14.1 Fisher-type esterification of long-chain acids with alcohols under flow conditions optimized by response surface methodology

References

1. Hartman RL, McMullen JP, Jensen KF (2011) Angew Chem Int Ed 50(2011):7502–7519
2. Wegner J, Ceylan S, Kirschning A (2011) Chem Commun 47:4583–4592
3. Caputo D, Casiello M, Laurenza AG, Fracassi F, Fusco C, Nacci A, D'Accolti L (2019) ACS Omega 4:12286–12292
4. Fei T, Wang T (2017) Curr Opin Food Sci:167–14

Chapter 15
Data Independent Acquisition Mass Spectrometry for Proteomic Advances into Isolated Methylmalonic Acidemia

Michele Costanzo, Marianna Caterino, Armando Cevenini, Laxmikanth Kollipara, Olga Shevchuk, Chi D. L. Nguyen, Albert Sickmann, and Margherita Ruoppolo

This reaction is normally supported by adenosylcobalamin which is the MUT cofactor. The result of this enzymatic block is the accumulation of methylmalonyl-CoA that is hydrolyzed to form methylmalonic acid. As a biomarker of the disease, methylmalonic acid is identified and quantified in patients' body fluids, i.e., urine and blood by liquid chromatography - tandem mass spectrometry (LC-MS/MS) or gas chromatography - mass spectrometry (GC-MS) to make a diagnosis. Other metabolites dosed for the diagnosis and the clinical monitoring of methylmalonic acidemia are propionylcarnitine, 3-OH-propionic acid, methylcitric acid, and the amino acids glycine and alanine. Since the first month of the newborn period, patients can show neurologic manifestations and metabolic instability with

M. Costanzo (✉) · M. Caterino · M. Ruoppolo
Dipartimento di Medicina Molecolare e Biotecnologie Mediche, Università degli Studi di Napoli "Federico II", Naples, Italy

CEINGE – Biotecnologie Avanzate scarl, Naples, Italy

Associazione Culturale DiSciMuS RFC, Casoria, Naples, Italy
e-mail: michele.costanzo@unina.it

A. Cevenini
Dipartimento di Medicina Molecolare e Biotecnologie Mediche, Università degli Studi di Napoli "Federico II", Naples, Italy

CEINGE – Biotecnologie Avanzate scarl, Naples, Italy

L. Kollipara · O. Shevchuk · C. D. L. Nguyen
Leibniz-Institut für Analytische Wissenschaften – ISAS – e.V., Dortmund, Germany

A. Sickmann
Leibniz-Institut für Analytische Wissenschaften – ISAS – e.V., Dortmund, Germany

Medical Proteome Centre, Ruhr Universität Bochum, Bochum, Germany

Department of Chemistry, College of Physical Sciences, University of Aberdeen, Aberdeen, UK

long-term complications, including severe neuronal impairment, developmental delay, kidney and liver disease, coma, and death. Also, acute metabolic decompensation and cardiac crises are frequent in these patients, so that early intervention is required.

No therapeutic treatment actually exists for MMA, so that the only recommended guideline subscribes limitation in the dietary propiogenic amino acids assumption and, in the case of vitamin B12-responsive patients, supplementation with vitamin B12 [1-3].

In order to study altered molecular mechanisms representative of the damage induced by the disease in patients, two HEK293 cell models were developed. The first one is a CRISPR/CAS9-based *MUT* gene knock out (MUT-KO). The knocking-out process was monitored by fluorescence and, after collection of the positive clones, protein signals were (not) detected by western blot. Then, the second cell model derived from a MUT-KO cell line, engineered to rescue the stable expression of MUT protein (MUT-RES). As control, a wild type HEK293 cell line (MUT-WT) was used for the following experiments.

To track the quantitative changes in the global proteome of MUT-KO and MUT-RES cells, a Data Independent Acquisition mass spectrometry-based proteomics experiment was performed.

A total number of 5278 proteins were accurately identified (≥ 2 unique peptides, 1% False Discovery Rate) and quantified by LC-MS/MS, throughout the above-mentioned cell conditions. Data analysis was performed using Spectronaut Pulsar software and the KO/WT and KO/RES ratios were analyzed to retrieve the relative quantitative abundances of proteins in KO samples. As expected, MUT protein was not detected in the KO cell line. Then, the list of both KO/WT and KO/RES differentially regulated proteins was managed in order to visualize the trend of abundances in protein levels through the three experimental conditions. Thus, proteins with a similar trend of abundance within the three conditions were extrapolated from the list and analyzed by gene ontology enrichment.

The high confidence of these results, obtained with the latest high resolution-accurate mass proteomic technologies, can be helpful in determining novel and unknown molecular pathways affected in cellular models recapitulating the general features of isolated methylmalonic acidemia. The perturbed biological processes highlighted in this dataset are related to cell survival and organization, supposing an unbalance between cell division and apoptosis.

The alterations described could be the trigger for the damage in patients and, thus, this represent the starting point for the identification of potential targets of therapy to be translated in the clinical practice.

References

1. Costanzo M, Caterino M, Cevenini A, Jung V, Chhuon C, Lipecka J, Fedele R, Guerrera IC, Ruoppolo M (2020) Proteomics reveals that methylmalonyl-CoA mutase modulates cell architecture and increases susceptibility to stress. Int J Mol Sci 21(14):4998
2. Costanzo M, Cevenini A, Marchese E, Imperlini E, Raia M, Vecchio LD, Caterino M, Ruoppolo M (2018) Label-free quantitative proteomics in a methylmalonyl-CoA mutase-silenced neuroblastoma cell line. Int J Mol Sci 19(11):3580
3. Fraser JL, Venditti CP. Methylmalonic and propionic acidemias. Curr Opin Pediatr 28(6):682–693

Chapter 16
Deposition Strategies of Nano-TiO$_2$ Photocatalyst for Wastewater Applications

Massimo Dell'Edera, Francesca Petronella, Teresa Sibillano, Cinzia Giannini, Angela Agostiano, Maria Lucia Curri, and Roberto Comparelli

Nowadays the increase of human activities also related to increase of the world population causes harmful consequences for the environment. In this context, water resources are gaining increasing attentions due to the occurrence of emerging pollutants including dyes, pharmaceutical and personal care products (PPCP), endocrine disruptors, pathogens; for this type of pollutants traditional methods show limited performances [1]. Recently the interest of the scientific community has been focusing on alternative methods as the Advanced Oxidation Processes (AOPs) [2, 3]. Among AOPs, TiO$_2$-based photocatalysis has recently emerged as a promising water treatment. In particular, nanosized TiO$_2$ demonstrated improved performances with respect to its bulk counterpart, thanks to its extremely high surface-to-volume ratio which can greatly increases the density of active sites available for adsorption and catalysis. In addition, the size-dependent band gap of nanosized semiconductors allows tuning the red-ox potentials to achieve selective photochemical reactions. The immobilization of nano-photocatalyst onto solid surface is the main goal for real applications [4]. In the present work, we studied two type of deposition techniques, namely doctor blade method and a purposely developed dip coating procedure (here referred to as "inverted dip coating"), to coat TiO$_2$ NPs first on glass substrates, and successively the more performing method was used to coat on unconventional substrates stainless steel mesh. To this end, a batch of TiO$_2$ NPs was synthesized by suitably modifying a reported approach, specifically selected for its

M. Dell'Edera (✉) · A. Agostiano · M. L. Curri
Dipartimento di Chimica, Università degli studi di Bari 'Aldo Moro', Bari, Italy

CNR-IPCF, Istituto per i Processi Chimico-Fisici, Bari, Italy
e-mail: m.delledera@ba.ipcf.cnr.it

F. Petronella · R. Comparelli
CNR-IPCF, Istituto per i Processi Chimico-Fisici, Bari, Italy

T. Sibillano · C. Giannini
CNR-IC, Istituto di Cristallografia, Bari, Italy

scalability [5]. UV-Vis absorption spectroscopy, X-ray diffraction analysis and TEM microscopy were used to characterized the obtained product. TiO_2NPs-based coatings were obtained by means of the *doctor blade* technique and the *inverted dip coating* method, from isopropanol suspensions of TiO_2 NPs, at a concentration of 6,5%, 13% and 26% by weight, respectively. The morphology of the resulting coatings was investigated by SEM analysis and allowed to detect significant differences between the coatings fabricated by using the two deposition techniques. The difference between the substrates produced by the two techniques is linked to the homogeneity of the film: with *doctor blade* method appear inhomogeneous with presence of superficial cracks. On the contrary, more homogeneous coatings, without cracks were obtained by using the *inverted dip coating* method. The photocatalytic activity of the prepared coating was assessed by monitoring the decolouration of a model target molecule, Methylene Blue (MB), in aqueous solution under UV light irradiation. The inverted dip coating is the most versatile deposition method for real applications. The TiO_2 NPs were then deposited on stainless steel mesh by using isopropanol suspensions at 6,5% and 13%. TiO_2 NPs content. Also, the films deposited onto the stainless steel meshes were thoroughly investigated by SEM microscopy and by measuring their photoactivity. The experimental results revealed that the coatings obtained by inverted dip coating method at 13% TiO_2 NPs contents onto stainless steel mesh result to be the most promising for real applications, due to photocatalytic performance and the quality of the films.

References

1. Ebele AJ, Abdallah MA-E, Harrad S (2017) Pharmaceuticals and personal care products (PPCPs) in the freshwater aquatic environment. Emerg Con 3:1–16
2. Truppi A, Petronella F, Placido T, Striccoli M, Agostiano A, Curri ML, Comparelli R (2017) Visible-light-active TiO_2-based hybrid nanocatalysts for environmental applications. Catalysts 7(4):33
3. Petronella F, Truppi A, Dell'Edera M, Agostiano A, Curri ML, Comparelli R (2019) Scalable synthesis of mesoporous TiO_2 for environmental photocatalytic applications. Materials 12(1853):1–21
4. Petronella F, Diomede S, Fanizza E, Mascolo G, Sibillano T, Agostiano A, Curri ML, Comparelli R (2013) Photodegradation of nalidixic acid assisted by TiO_2 nanorods/Ag nanoparticles based catalyst. Chemosphere 91(7):941–947
5. Ancora R, Borsa M, Cassar L (2009) Titanium dioxide based photocatalytic composites and derived products on a metakaolin support. Google Patents

Chapter 17
Tri-Modal MALDI-MS Imaging on the Same Tissue Section: Deeper Molecular Insights of Disease

Vanna Denti, Sonia Guarnerio, Andrew Smith, Isabella Piga, Clizia Chinello, and Fulvio Magni

17.1 Introduction

Matrix-assisted laser desorption/ionization (MALDI) mass spectrometry imaging (MSI) is a unique technology that enables the *in-situ* detection of a broad range of biomolecules, including lipids, N-glycans, and proteins. In particular, combining multilevel molecular data can potentially improve the detection of novel disease signatures and lead to improved stratification of patients. Here, we present a workflow that highlights the feasibility of detecting lipids, N-glycans, and proteins from the same formalin-fixed paraffin embedded (FFPE) tissue section.

17.2 Methods

For each section of FFPE clinical specimens, MALDI-MSI was performed in three modalities using a Bruker rapiflex™ MALDI tissuetyper™. Initially, deparaffinization, tissue rehydration and antigen retrieval were performed. Thus, lipids were analysed within the *m/z* 400 to 1200 range. Subsequently, N-glycans, that were cleaved following digestion with PNGase-F, were analysed within the *m/z* 1000 to 3000 range. Finally, tryptic peptides obtained following enzymatic digestion were analysed within the *m/z* 700 to 3000 range. All image acquisitions were performed using a laser beam scan of 44 μm and a raster setting of 50 μm in both *x* and *y* coordinates.

V. Denti (✉) · S. Guarnerio · A. Smith · I. Piga · C. Chinello · F. Magni
Clinical Proteomics and Metabolomics Unit, Department of Medicine and Surgery, University of Milano-Bicocca, Milano, Italy
e-mail: v.denti@campus.unimib.it

17.3   Results

Initially, we detected a limited number of lipids within FFPE tissue sections, as expected, whose lateral distribution was in accordance with the morphological structures present within the tissue. Furthermore, we noticed that lateral diffusion of the N-glycans and tryptic peptides in the subsequent analysis was limited, despite the numerous tissue washes and matrix applications. Finally, comparing the spatial distribution of key signals detected at these multi-molecular levels, complementary information could be obtained, and regions of tissue with altered molecular profiles could be highlighted.

17.4   Conclusions

The tri-modal approach presented here would be the first of its kind to consecutively detect lipids, N-Glycans and tryptic peptides on the same FFPE tissue section. In conclusion, the workflow described here may be useful for a deeper understanding of complex diseases, where both lipids and proteins pathways are involved, and for assisting the pathologist in the diagnosis and stratification of patients, that maybe not possible when considering a single group of analytes.

Chapter 18
Fabrication of QDs Dimers with Sub-Nanometer Interparticle Distance

Carlo Nazareno Dibenedetto, Elisabetta Fanizza, Annamaria Panniello, Angela Agostiano, Maria Lucia Curri, and Marinella Striccoli

The semiconductor devices industry is constantly looking for a better control at the nanoscale. Efforts to miniaturize electronic devices point towards the exploitation of new materials and the use of chemical assembling strategies [1] that enables a control on the construction of solid structures at the atomic scale. Among the advanced materials, colloidal semiconductor quantum dots (QDs) are promising materials for the fabrication of nanoscale devices used for the implementation of optoelectronic, photonic and sensing application [2]. At such a scale, assemblies of colloidal semiconductor quantum dots (QDs) show original electronic collective properties, due to the QD coupling, depending on the number of connected nano-objects and their interparticle distance [3]. While most device implementations use disordered QD aggregates, here the fabrication and characterization of nanostructures composed of a low number of QDs with precise stoichiometry and defined nanometric and sub-nanometric particle-particle spacing are described. Dimers of CdSe QDs in solution are fabricated by engineering QD surface chemistry with ligand treatments that reduce the surface steric hindrance and promote the connection between two QDs by means of alkyl dithiols bifunctional molecules [4]. Alkyl dithiols with different chain lengths are selected to tune the interparticle distance from few nanometers down to sub-nanometers, where strong coupling is expected to be achieved.

C. N. Dibenedetto (✉) · E. Fanizza · A. Agostiano · M. L. Curri
Dipartimento di Chimica, Università degli studi di Bari 'Aldo Moro', Bari, Italy

CNR-Istituto per i Processi Chimico-Fisici SS Bari, Bari, Italy
e-mail: c.dibenedetto@ba.ipcf.cnr.it

A. Panniello · M. Striccoli
CNR-Istituto per i Processi Chimico-Fisici SS Bari, Bari, Italy

References

1. Naaman R (2011) Phys Chem Chem Phys 13:13153–13161
2. Klein DL, Roth R, Lim AKL, Alivisatos AP McEuen PL (1997) Nature 389(1997):699–701
3. Crisp RW, Schrauben JN, Beard MC, Luther JM, Johnson JC (2013) Nano Lett 13:4862–4869
4. Dibenedetto CN, Fanizza E, Brescia R, Kolodny Y, Remennik S, Panniello A, Depalo N, Yochelis S, Comparelli R, Agostiano A, Curri ML, Paltiel Y, Striccoli M (2019) Under submission

Chapter 19
Mapping Molecular Interactions in the *Clostridioides difficile* Infected Gastrointestinal Tract Using Multimodal Imaging Mass Spectrometry

Emma R. Guiberson, Aaron G. Wexler, William J. Perry, Eric P. Skaar, Richard M. Caprioli, and Jeffrey M. Spraggins

19.1 Introduction

Clostridioides difficile is a spore-forming pathogen that impacts half a million people annually in the United States alone [1]. *C. difficile* infections are characterized by the release of toxins that attack the intestinal linings, disrupting the normal gut flora [2]. Previous *C. difficile* studies utilized primarily histological techniques such as hematoxylin and eosin-stained slides, imaging limited to photomicrographs, and mass spectrometry techniques serving only for identification. Quantification techniques were limited to spore counts in feces. Matrix-assisted laser desorption/

E. R. Guiberson (✉) · W. J. Perry
Mass Spectrometry Research Center, Vanderbilt University, Nashville, TN, USA

Department of Chemistry, Vanderbilt University, Nashville, TN, USA
e-mail: emma.r.guiberson@vanderbilt.edu

A. G. Wexler · E. P. Skaar
Department of Pathology, Microbiology, and Immunology, Vanderbilt University, Nashville, TN, USA

R. M. Caprioli
Mass Spectrometry Research Center, Vanderbilt University, Nashville, TN, USA

Department of Chemistry, Vanderbilt University, Nashville, TN, USA

Department of Biochemistry, Vanderbilt University, Nashville, TN, USA

Departments of Pharmacology and Medicine, Vanderbilt University, Nashville, TN, USA

J. M. Spraggins
Mass Spectrometry Research Center, Vanderbilt University, Nashville, TN, USA

Department of Chemistry, Vanderbilt University, Nashville, TN, USA

Department of Biochemistry, Vanderbilt University, Nashville, TN, USA

ionization imaging MS (MALDI IMS) is a technology that allows the molecular mapping of potentially thousands of analytes from a tissue's surface [3]. Spatial molecular studies leveraging MALDI IMS during *C. difficile* infections will provide insight into both the mechanisms and effects of colonization on the gastrointestinal environment.

19.2   Methods

C57BL/6 mice were orally infected with *C. difficile* to an endpoint at three days. Mice were sacrificed and intestines were harvested and wrapped in a spiral manner, termed a 'swissroll', followed by freezing on liquid nitrogen. Intestines were sectioned at 10 µm thickness and thaw mounted onto conductive ITO coated slides or vinyl slides. Fluorescence microscopy images were acquired prior to preparation for IMS analysis. Samples were washed to remove salts and/or lipids and coated with (E)-4-(2,5-dihydroxyphenyl)but-3-en-2-one (2,5-cDHA) using an aerosol sprayer. High spatial resolution lipid and small molecule images were acquired using a prototype MALDI timsTOF Pro MS. Protein images were acquired using 15 T FT-ICR MS. Post-processing included a second collection of fluorescence microscopy images for accurate registration of data from different modalities.

19.3   Preliminary Data

MALDI MS, laser ablation inductively-coupled plasma MS, fluorescent, and bright field microscopy imaging data have been generated from a control mouse as proof of principle experiments. LA-ICP IMS data shows distinctions in localization of key nutrient metals and elements between the luminal content and tissue in control intestine samples. IMS data of lipids and proteins from the small intestine contain species that clearly localize to either the host epithelium or the luminal contents. Specifically, signals at *m/z* 1549.93 and *m/z* 1522.41 from positive ionization mode data localize to the luminal contents, while peaks at *m/z* 810.55 and *m/z* 895.73 localize to the epithelium. *C. difficile* infected cecum samples also showed strong epithelial localization at *m/z* 885.57 and *m/z* 936.62. However, lipids at *m/z* 741.54 were observed to localize primarily at the distal end. The proof-of-concept lipid imaging experiments were collected using a prototype MALDI timsTOF platform operated in Q-TOF mode. This platform allowed for rapid collection (20 pixels/s) of high spatial resolution ion images (10 µm). MALDI FT-ICR protein images showed similar trends to lipid images within localization substructures. Signals at *m/z* 4279.08 and *m/z* 8565.11 both show localization to the epithelium of the host. Ubiquitin, with a signal at *m/z* 8565.11, was also identified to localize exclusively to the epithelium. Higher-mass proteins, however, generally localized only to the luminal contents. Additionally, taurocholic acid (*m/z* 514.29), a primary bile acid

associated with inducing germination of *C. difficile* spores [4], has been shown at high intensity in infected luminal contents while lacking in control tissue. Distinctions between the epithelium and luminal contents were clearly demarcated in imaging data, with confidence that this demarcation will continue in infected samples.

Future work will apply a similar workflow to murine *C. difficile* infection models for small molecule and elemental analysis. We anticipate the generation of data from multiple imaging modalities with similar, robust qualities as those from control murine samples. Acquired data from control and infection models will then be compared, deducing molecular changes associated with *C. difficile* colonization of the gastrointestinal tract.

19.4   Novel Aspect

Imaging MS technology can be utilized to map molecular and elemental interactions in the gastrointestinal tract caused by *C. difficile* infection.

References

1. Abt MC, McKenney PT, Pamer EG (2016) Clostridium difficile colitis: pathogenesis and host defence. Nat Rev Microbiol 14:609–620
2. Fischetti Vincent A, Novick Richard P, Ferretti Joseph J, Portnoy Daniel A, Rood JI (2000) Gram-positive pathogens, pp 551–563
3. Cornett DS et al (2007) MALDI imaging mass spectrometry: molecular snapshots of biochemical systems. Nat Methods 4:828–833
4. Sagar NM, Cree IA, Covington JA, Arasaradnam RP (2015) The interplay of the gut microbiome, bile acids, and volatile organic compounds. Gastroenterol Res Pract

Chapter 20
Detection, Identification and Monitoring of Chemical Warfare Agents: a Comparison Between on-Field and in-Lab Approach

Matteo Guidotti, Massimo C. Ranghieri, and Stefano Econdi

When toxic chemical warfare agents, CWAs are used in criminal acts (terrorism, assassination, sabotage) or in warfare, they represent a non-negligible threat to the life of professionals and first responders (firefighters, law-enforcement or armed forces, healthcare service, etc.) involved in civil protection and emergency operations [1]. Detection, identification and monitoring, DIM, procedures are an essential step in responding to events involving CWAs, in order to obtain information on the (supposedly) contaminated incident scene and prevent undesired exposure or any form of direct contact between the operators and the toxic agent. In fact, not only the recent alleged use of CWAs in the civil war scenario in the Middle East or in targeted attacks in Europe, but also the permanent risk of accidental release of industrial highly hazardous and/or toxic materials in major incidents have highlighted the key role of an early and effective on-site detection of harmful agents [2, 3].

For this purpose, a prompt and on-site detection capability is crucial to: (i) detect the presence of life- or health-threatening levels of hazardous contaminants; (ii) set off a contamination alarm; (iii) gather information about the nature of the risk; (iv) identify the concentration and the diffusion of the toxic agent; (v) provide a mapping of hazardous areas; (vi) define the personal protection and decontamination requirements; and, eventually, (vii) declare the end of the emergency and give the 'all-clear' signal.

A broad variety of simple manual and conventional detection systems, such as colorimetric hand-held reaction tubes, test papers, enzymatic assays and wet-chemistry-based kits, is available on the market and, thanks to their limited cost, it

M. Guidotti (✉) · M. C. Ranghieri
CNR – SCITEC, Istituto di Scienze e Tecnologie Chimiche "Giulio Natta", Milan, Italy

Unità CBRN, Corpo Militare Ordine di Malta Italia, Milan, Italy
e-mail: matteo.guidotti@scitec.cnr.it

S. Econdi
CNR – SCITEC, Istituto di Scienze e Tecnologie Chimiche "Giulio Natta", Milan, Italy

can be the first choice for non-specialised responders and professionals. However, although undemanding and cheap, some of these systems show a limited specificity towards a desired analyte and may give rise to several false positive cases. Moreover, when completely unknown contaminants have to be detected and identified, the responder needs to use a very large number of test kits (which are often designed to give a feedback for one analyte compound only) before having a clear view of the situation.

For these reasons, electronic devices and/or automatic portable detectors based on advanced physico-chemical techniques, *i.e.* mass spectrometry, Fourier-transform infrared or Raman spectrophotometry, photoionization detection, flame photometry or high-performance (micro)-gas-chromatography, find now a well-established preferential use by first responders and specialist haz-mat teams who operate in potentially contaminated and hazardous environments. This kind of detection instruments is versatile and can cover a quite broad range of hazardous species, spanning from CWAs, to toxic industrial materials as well as environmental pollutants, with a good level of reliability and selectivity against false positive responses. As main drawbacks, their use is relatively complex, they are expensive and typically require an adequate know-how and training level by the operators, in order to obtain reliable and clear results.

However, it is worth highlighting the main differences in the approach to detection for a haz-mat first responder operating at an incident site or for an analytical chemist working in a conventional laboratory. First of all, the time scale and the level of expected and accepted accuracy are different [4]. A rescuer needs to understand if life-threatening amounts of toxic chemicals are present or not, in a very short time and, even, with a relatively low accuracy on quantification (*i.e.*, often a rapid identification and a semi-quantitative evaluation of the threat level is enough: low, moderate, high, according to acute exposure guideline levels, AEGLs [5]). On the contrary, a classical analytical laboratory, fulfilling all of the widely-accepted quality and reliability standards imposed by the international scientific community, is the optimal place devoted to a deeper evaluation on the nature and the amount/concentration of contaminant with well-established procedures, often requiring complex pre-treatment operations, costly and bulky desktop instruments and skilled specialised personnel (Table 20.1). Indeed, confirmative and/or forensic analyses about the contaminant is generally carried out in conventional reach-back laboratory facilities only [6].

In addition, a further series of differences has to be evidenced by comparing how civilian and military first responders face a CWA-related event. Civilian responders' absolute priority is to save lives, with a strict zero-risk approach. Conversely, armed forces' approach is mission-oriented and risks, such as entering a contaminated area, performing a task with scarcely adequate protective equipment or, even, under life-threatening conditions, might be possible and considered acceptable, under extreme conditions.

Other aspects, however, make the approach of civilian and military haz-mat teams different and, in some sense, complementary: military operators seldom have the necessity and the capability to carry out a thorough forensic investigation

Table 20.1 Most remarkable difference between on-field and in-lab detection of CWAs and highly toxic chemical contaminants

On-field	In-lab
Portable, light-weight apparatus	Benchtop standard apparatus
Speed, fast response	Possible delay
Robustness to decontamination from CWA	Decontamination of the entire instrument not required
Rough identification of CWA family	Confirmative identification of CWA
Qualitative, semi-quantitative DIM	Qualitative and quantitative identification
Suitable for pre-defined analytes (based on in-built databases: CWA, hazardous agents, toxic industrial materials)	Versatile and open to analytes of different type (hazardous materials, environmental pollutants, etc.)
Non-specialised personnel	Specialised high-qualified personnel
No/minimal pre-treatment	Possible complex pre-treatment
Fixed/close analytical protocols	Versatile/open protocols

aiming at pointing out the perpetrator of the criminal act, whereas the correct safeguard of the incident scene is a must for civilian haz-mat specialists working in close contact with police forces. These remarkable differences often lead to dissimilar standard operating procedures, SOPs, and this is frequently a problem, when major emergency events occur and a joint effort by civilian and military organizations is required.

Anyway, notwithstanding such fundamentally diverse approaches, detection systems and tools used for on-site DIM operations are essentially the same. Lightweight deployable gas-chromatograph mass-spectrometry (on-field GC-MS) instruments, photoionization-based detectors (PID) and ion mobility spectrometry devices (IMS; either with open-loop or closed-loop technology) proved to be among the most reliable and effective instruments for the on-site detection of hazardous chemicals and are all now widely employed. Although most of them were designed and developed in the last Cold War period for military use to reveal the use of CWAs on battlefields, this class of portable instruments was then successfully adapted to be detectors for civilian haz-mat specialists of the fire brigade, police forces, civil protection or emergency medical service. This shift from military to civilian application had, in particular, a relevant boost after the attacks to the Twin Towers in 2001, when the increasing threat of use of CWAs or highly toxic chemicals for terrorist attacks, sabotage actions or illicit purposes started to attract a major attention by governmental first response agencies.

As in other fields, also in the selection of the most suitable detection equipment and tools, a unique approach and only one class of instruments cannot provide a solution for all cases. It is, however, crucial that civilian and military on-field operators as well as academic researchers are all aware of these major gaps, especially when a multi-agency response to emergency situations is needed and a clear and timely exchange of expertise, scientific results and technical data is required from all of the actors involved in the response, in order to provide professionals and wide population with the most reliable and correct information.

References

1. Guidotti M, Trifirò F (2015) Chemical risk and chemical warfare agents: science and technology against humankind. Toxicol Environ Chem 98(9):1018–1025
2. Krykorkova J, Capoun T (2014) The equipment of Czech firefighters for the detection and field analyses of chemical warfare agents. Toxics 2:247–257
3. Nepovimova E, Kuca K (2018) Chemical warfare agent Novichok; mini-review of available data. Food Chem Toxicol 121:343–350
4. Cekovic B, Rothbacher D (2017) A fresh approach: review of the production development of the CBRN/HAZMAT equipment. In: Martellini M, Malizia A (eds) Cyber and chemical, biological, radiological, nuclear, explosives challenges. Terrorism, security, and computation. Springer, Cham
5. US Environmental Protection Agency. https://www.epa.gov/aegl/access-acute-exposure-guide-line-levels-aegls-values#chemicals. Accessed on July 2020
6. NATO Standardization Office, AJP-3.8, Allied Joint Doctrine for Comprehensive Chemical, Biological, Radiological and Nuclear Defence (Ed. B), August 2018

Chapter 21
New Tools for Rapid and Sensitive Detection of Water Contamination: Whole-Cell Biosensors and Cell-Free TX-TL Systems

Antonia Lopreside, Maria Maddalena Calabretta, Laura Montali, Xinyi Wan, Baojun Wang, Aldo Roda, and Elisa Michelini

Abstract Rapid, sensitive and user-friendly detection of water contaminants is a key factor for on-site response to terrorist attack or accidental toxic release. To this end, we developed and compared different biosensors based on living cells and transcriptional-translational cell-free system (TX-TL) using different optical reporter genes. Analytical performances such as response time, limit of detection and dynamic range of the different combinations were profiled to assess the best candidate of this application. To date, bioluminescent NanoLuc luciferase proved to be the best reporter gene for both the configurations independently from target analyte.

Real time routine monitoring of water for chemical and biological threat agents is one of the major concerns of our society. A rapid response to a terrorist attack, as well as to an accidental release of toxic environmental pollutants, requires the ability to rapidly detect chemical and biological agents so that an early warning can be raised, potential health risks defined, and proper countermeasures are employed. In this field cell-based biosensors have been widely used as they provide useful information (such as bioavailability and general toxicity) and they are suitable for on field application. During the last decade, thanks to the implementation of

A. Lopreside (✉) · M. M. Calabretta · L. Montali
Department of Chemistry "G. Ciamician", University of Bologna, Bologna, Italy
e-mail: antonia.lopreside2@unibo.it

X. Wan · B. Wang
School of Biological Sciences, University of Edinburgh, Edinburgh, UK

A. Roda · E. Michelini
Department of Chemistry "G. Ciamician", University of Bologna, Bologna, Italy

INBB, Istituto Nazionale di Biostrutture e Biosistemi, Rome, Italy

239

smartphones and other light detectors, cell-based biosensors have been also integrated into compact analytical devices. However, the scarce robustness of living cells still represents an issue and several immobilization methods have been developed for improving cell's shelf-life and obtain ready-to-use biosensors. More recently, cell-free transcription-translation (TX-TL) systems have been proposed as an alternative to cell-based biosensors. Conversely to whole-cell biosensors, TX-TL systems do not rely on living cells but rather include the biological machinery and energy source to express a reporter protein as consequence of target activation.

Whole-cell and cell-free biosensors have become preferential alternatives to conventional analytical methods for rapid detection of analytes of environmental interest as they are cost effective and easy to implement into portable devices. The choice of reporter genes in biosensors, is also a key factor especially for on-site monitoring. A reporter gene is a gene which can be easily and quantitatively distinguished over a background of endogenous proteins. Several reporter genes have been widely employed to monitor cellular events associated to signal transduction, including the application in biosensors.

We report a side-by-side investigation of whole-cell and cell-free transcriptional and translational system for rapid detection of heavy metal and bacterial contamination in water [1].

A comprehensive profile of diverse optical reporter genes (with fluorescent, colorimetric and bioluminescent detection) has been reported. Particularly, green fluorescent reporters (GFP and deGFP), red fluorescent reporters (mCherry and mScarlet-I), colorimetric reporter (LacZ) and bioluminescent reporters (NanoLuc luciferase and lux operons from Aliivibrio fischeri and Photorhabdus luminescens) have been analysed. A comparison of the analytical performance, in terms of limit of detection (LOD), sensitivity, input/output dynamic ranges and response time, have been obtained with diverse optical reporters (Fig. 21.1).

According to our results, NanoLuc luciferase is the best candidate to our purpose, as it shows the lowest LOD (50.0 fM for $HgCl_2$ and 0.4 pM for $3OC_6HSL$) within the shortest response time (30 min), proving its eligibility as reporter gene for fast and sensitive on field monitoring. Moreover, TX-TL cell-free systems have proven
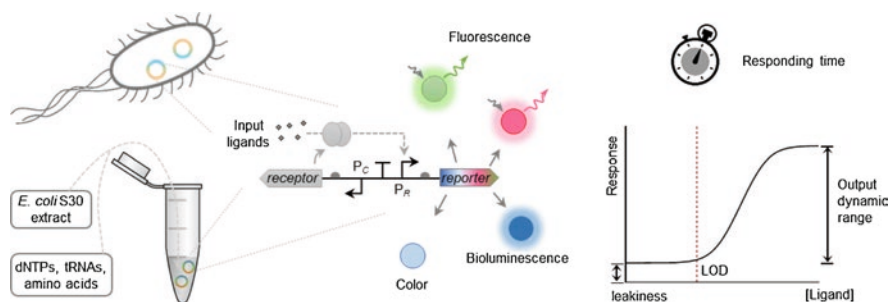

Fig. 21.1 Schematic representation of the comparison of different reporter genes in whole cell and cell-free system [1]. Reproduced by permission of ACS, further permissions related to the material excerpted should be directed to the ACS(https://pubs.acs.org/doi/10.1021/acs.analchem.9b04444)

to be excellent alternatives to whole-cell biosensors, particularly for rapid detection and on-site application, though their analytical performances are up-to-now not as sensitive as whole-cell biosensors. Despite this, the selection of reporters needs to be a balanced compromise with other important factors, including the cost of the assay and ease of use, especially for point of care and point of need applications.

Reference

1. Lopreside A, Wan X, Michelini E, Roda A, Wang B (2019) Comprehensive profiling of diverse genetic reporters with application to whole-cell and cell-free biosensors. Anal Chem 91(23):15284–15292

Chapter 22
A Novel Origami Paper-Based Chemiluminescent Biosensor Integrated with a Smartphone Device for Organophosphorus Compounds Detection

Laura Montali, Maria Maddalena Calabretta, Antonia Lopreside, M. Guardigli, Elisa Michelini, and Aldo Roda

Abstract The study presents the development and optimization of a novel origami paper-based chemiluminescent (CL) biosensor for measuring the acetylcholinesterase activity detection and its implementation into portable analytical devices as proof-of-principle of low-cost point-of-care applications.

Global security threats have become a major worldwide concern, and their early and sensitive detection represents a major challenge to current detection technologies. The routine monitoring of water, food, and the environment for chemical and biological threat agents is often hampered by the fact that available techniques usually require clean samples and sophisticated equipment based on high-performance liquid chromatography-tandem mass spectrometry and are thus unsuitable for real-time, cost-effective, and on-field routine monitoring.

The possibility of implementing enzymatic assays with bio-chemiluminescence detection in smartphones has been very successful over the years, as well as the possibility of creating ad hoc analytical devices manufactured with an easy and economical 3D printing technology. Here, we report the development and optimization

L. Montali (✉) · M. M. Calabretta · A. Lopreside · M. Guardigli
Department of Chemistry "G. Ciamician", University of Bologna, Bologna, Italy
e-mail: laura.montali2@unibo.it; antonia.lopreside2@unibo.it

E. Michelini · A. Roda
Department of Chemistry "G. Ciamician", University of Bologna, Bologna, Italy

INBB, Istituto Nazionale di Biostrutture e Biosistemi, Rome, Italy

of a novel origami paper-based chemiluminescent (CL) biosensor for acetylcholinesterase activity detection and its implementation into portable analytical devices as proof-of-principle of low-cost point-of-care applications. This biosensor is based on the inhibition process of acetylcholinesterase (AChE) by molecules such as organophosphate pesticides, nerve gases, and some drugs. The AchE activity is measured through a series of coupled enzymatic reactions leading to light emission. When acetylcholinesterase is inhibited, there is a decreased production of hydrogen peroxide, and consequently, a reduction in light emission. In particular, three different enzymes, AChE, choline oxidase (ChOx), and Horse Radish Peroxidase (HRP), are adsorbed on a paper pad obtained by wax printing. The origami technique allows to add reagents in separate steps and trigger the reactions to occur sequentially.

In the perspective of using our smartphone-based assay for rapid and on-field analysis of environmental samples, Reldan 22 (chlorpyrifos-methyl 21.4% v/v), a broad-spectrum insecticide for control of insects and pests that infest grain and grain stores, has been used as model analyte. As proof of concept, different spiked concentrations of Reldan 22 have been tested in the work concentration range of 0.5% v/v for direct application and 0.03–0.12% v/v for large area application. Signal acquisition was carried out by OnePlus 6 photocamera placing the 3D paper PAD cartridge inside a 3D-printed dark box and integrating CL signals for 30 sec with ISO800.

The device setup is shown in Fig. 22.1, the three different enzymes were absorbed on the paper PAD, a 3D printed cartridge with internal magnets allows to keep the origami in the folded state and a dark box printed with 3D printer enables interfacing with the smartphone (One Plus 6) [1].
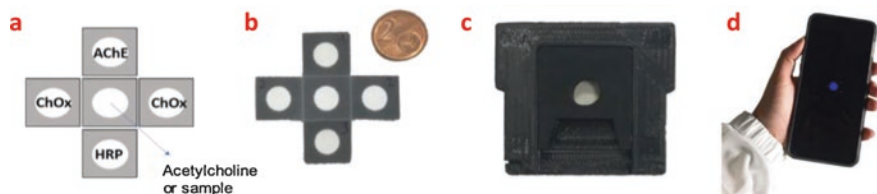

Fig. 22.1 (**a**) Schematic representation of AChE, choline oxidase (ChOx) and Horse Radish Peroxidase (HRP) adsorbed on PAD; (**b**) Origami PAD printed by wax printer; (**c**) 3D printed cartridge obtained with black ABS with internal magnets able to keep the PAD origami folded; (**d**) OnePlus 6 screen with chemiluminescent image

Reference

1. Montali L, Calabretta MM, Lopreside A, D'Elia M, Guardigli M, Michelini E (2020) Multienzyme chemiluminescent foldable biosensor for on-site detection of acetylcholinesterase inhibitors. Biosens Bioelectron 162:112232. https://doi.org/10.1016/j.bios.2020.112232

Chapter 23

Solid-Phase Microextraction Combined with Microwave-Assisted Extraction Using Eco-friendly Solvents as a New Approach for the Analysis of Toxic Compounds from Environmental Solid Matrices

Check for updates

Attilio Naccarato, Antonella Tassone, Sacha Moretti, Francesca Sprovieri, Nicola Pirrone, and Antonio Tagarelli

Abstract Generally, Soxhlet extraction is still the most used technique in the official methods of analysis for solid matrices. This traditional approach is expensive, time-consuming, and environmentally unfriendly. For some years, a great effort has been made to develop alternative and high-throughput analytical methods for the pollutant extraction from solids in compliance with the basic requirements of Green Analytical Chemistry (GAC). One of the most interesting approaches is the microwaveassisted extraction (MAE) because it allows for the rapid extraction of target molecules from solid matrices with low solvent consumption; besides, the working parameters can be controlled and properly optimized by univariate or multivariate approaches.

Keywords Solid-phase microextraction · Particulate matter · Pollutants · Gas chromatography · Design of experiment · Tandem mass spectrometry

A. Naccarato (✉) · A. Tassone · S. Moretti · F. Sprovieri · N. Pirrone
CNR-Institute of Atmospheric Pollution Research, Rende, Italy
e-mail: attilio.naccarato@iia.cnr.it

A. Tagarelli
Dipartimento di Chimica e Tecnologie Chimiche, Università della Calabria, Rende, Italy

23.1   Introduction

Until a few decades ago, sample preparation was carried out using traditional techniques, such as liquid-liquid extraction (LLE) and solid-liquid extraction (SLE), which use large volumes of organic solvents. Although with the advent of solid-phase extraction (SPE) much less solvent has been used compared to LLE, the volume can still be significant. However, this approach is not applicable to solid matrices for which the Soxhlet extraction is still the most used technique in the official methods of analysis. These preparation methods are expensive, time-consuming and environmentally unfriendly. Since some years, a great effort has been made to develop alternative and high-throughput analytical methods for the pollutant extraction from solid matrices. Among these approaches, one of the most interesting is the microwave-assisted extraction (MAE). In recent years this methodology has attracted growing interest as it allows for the rapid extractions of target molecules from solid matrices, with extraction efficiency comparable to that of the classical techniques [1]. In addition, compared to other extraction techniques, optimization of MAE experimental conditions is rather easy owing to the low number of influential parameters (i.e. matrix moisture, nature of the solvent, time, power, and temperature in closed vessels) [2].

The analysis of toxic agents in solid matrices is usually carried out by combining the extraction step, often followed by a clean-up and pre-concentration procedure, with a final determination using gas or liquid chromatography coupled to suitable detection system such as tandem mass spectrometry. In this respect, although the modern and advanced analytical techniques allow for the analysis of a broad range of organic compounds, to maximize the method performance in terms of sensitivity, specificity, and robustness, a proper sample preparation step is mandatory [3–6].

In this chapter, we focus our attention on a combined strategy for the analysis of toxic chemical compounds in solid matrices. This new approach provides for the use of MAE for the extraction of the target molecules followed by a solid-phase microextraction (SPME) analysis. The key point of the method is the use of an eco-compatible hydroalcoholic mixture, instead of the traditional organic solvents, which is compatible with the use of solid-phase microextraction in direct immersion mode (DI-SPME) and can be analyzed without any other clean-up step. SPME is an established sample preparation technique that has many advantages over the traditional approaches including the simultaneous extraction, pre-concentration, and direct introduction of analytes into the gas chromatographic system [7]. As a result, SPME has demonstrated to be a simple, solvent-free, reliable and flexible tool to analyze molecules with different physicochemical properties in various matrices [5, 8, 9]. As a case study, we present the application of the proposed approach to the analysis of organophosphate esters (OPEs) from airborne particulate matter (PM) [10]. OPEs are synthetic derivatives of phosphoric acid with a wide range of physical-chemical properties and several applications that in recent years led to a sharp increase in global consumption. OPEs are relatively stable toward biodegradation, and several studies report that once in the environment, OPEs may undergo

long-range atmospheric transport to even remote regions of the world. Their ubiquitous distribution in both indoor and outdoor environments make them of emerging toxic chemical compounds, thus motivating the development of methods for their reliable quantification.

23.2 Analytical Strategy

The proposed protocols provide for the microwave-assisted extraction (MAE) of the analytes from the solid matrix using a green hydroalcoholic mixture. Afterward, the MAE extract is properly diluted and analyzed using solid-phase microextraction and a convenient chromatographic technique (Fig. 23.1).

In our case study, the extraction of organophosphate esters from particulate matter was carried out in 10 mL of a water-ethanol mixture (50,50, v/v) using a microwave extraction system. A single MAE run allowed for the simultaneous extraction of up to 15 samples with a negligible environmental impact because of the use of ethanol, an eco-friendly organic solvent widely used in green chemistry. Design of Experiment (DoE) was used for the multivariate optimization of the parameters affecting both the MAE extraction and the SPME analysis, thereby achieving the optimal working conditions.

Extraction mixture volume, extraction time, heat-up time, extraction temperature and percentage of ethanol in the hydroalcoholic extraction mixture were identified as the variables affecting the MAE.

A fractional factorial design (FFD) was first performed to determine which of the surveyed factors had a significant influence on the extraction performance and then a central composite design (CCD) was carried out for the final optimization of the statistically significant factors.

The samples obtained after MAE were submitted to direct immersion analysis by solid-phase microextraction (DI-SPME). SPME is a technique devised to be used in aqueous solution and in these conditions provides the best analytical performance. As a consequence, since our method provided for the extraction of the analytes in a mixture with 50% ethanol, the sample had to be diluted before SPME. At this regards, the extraction performance of five SPME fibers was evaluated in samples with different percentage of ethanol. In the experimental conditions where the analytes have a different level of hydrophobicity and there is competition between the
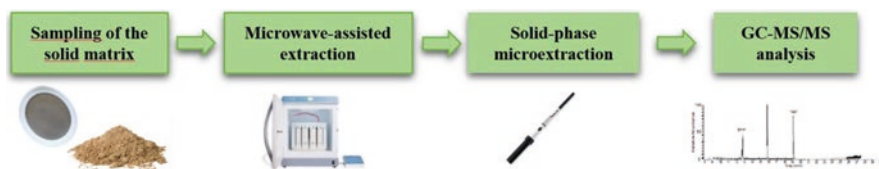

Fig. 23.1 The workflow of the proposed analytical strategy

hydroalcoholic solution and the fiber coating the selection of the coating necessarily entailed a compromise between the amount of extracted analytes and reproducibility. The best working conditions were obtained by using the 50/30 μm divinylbenzene/carboxen/polydimethylsiloxane coating and 5% ethanol. The experimental variables affecting the SPME were optimized using a CCD. Extraction time, extraction temperature, and percentage of sodium chloride were selected as the most critical factors. The outcomes of the optimization procedure indicate that the maximum value was achieved by setting the extraction time 45 min, extraction temperature 80 °C, and NaCl percentage 10% (w:w). In particular it was observed a substantial improvement in terms of precision at 80 °C which could be due to the depletion of the ethanol from the aqueous solution.

The assay of the analytes was performed by using tandem mass spectrometry in selected reaction monitoring (SRM) acquisition mode. The proposed method was carefully validated in terms of linearity, accuracy, precision (intra- and interday) and limit of quantification.

The method was applied to a real case scenario by analyzing PM10 samples collected at the monitoring station of the CNR-IIA in Rende. The results showed the presence of some of the investigated pollutants at a concentration above the lower limit of quantification of the method. These findings can be due to the closeness of the sampling area to the industrial area of Cosenza and the motorway, which crosses the area at about 1 Km east of the measurements site.

23.3   Conclusions

We set-up a new approach for the determination of the toxic chemicals from solid matrices. We base the analytical strategy on an MAE extraction of the analytes from the solid matrix using an eco-friendly hydroalcoholic mixture followed by the analysis using suitable instrumental equipment. Compared to the protocols generally used, which mainly use Soxhlet as extraction technique, the developed approach does not provide for the use of damaging organic solvents, is faster and automatable. As a case study, we presented the new approach through the analysis of OPEs from particulate matter. The final protocol reached satisfactory values in terms of linearity, sensitivity, lower limit of quantification, matrix effect, accuracy, and precision.

References

 1. Camel V (2000) TrAC – trends anal. Chem 19:229–248
 2. Sanchez-Prado L, Garcia-Jares C, Llompart M (2010) J Chromatogr A 1217:2390–2414
 3. Naccarato A, Gionfriddo E, Elliani R, Pawliszyn J, Sindona G, Tagarelli A (2018) J Sep Sci 41:929–939
 4. Cavaliere B, Monteleone M, Naccarato A, Sindona G, Tagarelli A (2012) J Chromatogr A. 1257:149–157

5. Naccarato A, Pawliszyn J (2016) Food Chem. 206:67–73
6. Naccarato A, Furia E, Sindona G, Tagarelli A (2016) Food Chem. 206:217–222
7. Pawliszyn J (2012) Handbook of solid phase microextraction. Elsevier, Waltham, USA
8. Naccarato A, Elliani R, Cavaliere B, Sindona G, Tagarelli A (2018) J Chromatogr A 1549:1–13
9. Naccarato A, Gionfriddo E, Sindona G, Tagarelli A (2014) J Chromatogr A 1338:164–173
10. Naccarato A, Tassone A, Moretti S, Elliani R, Sprovieri F, Pirrone N, Tagarelli A (2018) Talanta 189:657–665

Chapter 24
Recent Advances in MALDI Mass Spectrometry Imaging: A Cutting-Edge Tool for the Diagnosis of Thyroid Nodules

Isabella Piga, Giulia Capitoli, Francesca Clerici, Stefania Galimberti, Fulvio Magni, and Fabio Pagni

Abstract This study presents the implementation of a MALDI-MSI statistical tool that could be used to assist pathologists in the diagnosis of indeterminate cases.

24.1 Introduction

Approximately 20% of thyroid nodules Fine Needle Aspiration (FNA) are diagnosed as "indeterminate for malignancy", and these patients undergo diagnostic thyroidectomy, often unnecessary. MALDI-MSI represents a suitable tool to distinguish benign/malignant cases in different *ex-vivo* cytological smears taken from surgical thyroid nodule [1].

I. Piga (✉) · F. Clerici · F. Magni
Department of Medicine and Surgery, Proteomic and Metabolomic Unit, University of Milano-Bicocca, Monza, Italy
e-mail: isabella.piga@unimib.it

G. Capitoli · S. Galimberti
Bicocca Bioinformatics Biostatistics and Bioimaging B4 Center, School of Medicine and Surgery, University of Milano-Bicocca, Monza, Italy

F. Pagni
Department of Medicine and Surgery, Pathology Section, University of Milano-Bicocca, Monza, Italy

24.2   Results and Discussion

Moving forwards from these first results, we then applied MALDI-MSI proteomics approach on *real* FNAB. At a first instance, challenging technical aspects of this approach, such as the interference of hemoglobin and the morphological and proteomic stability of samples, were overcome [2]. Then, in accordance with the primary aim of the study [3], we are now working on the implementation of a MALDI-MSI statistical tool that could be potentially used to assist pathologists in diagnosis of indeterminate cases. *Real* thyroid FNAs from hyperplastic and papillary thyroid cancer (PTC) nodules, were collected from patients (San Gerardo Hospital, Monza, Italy) and transferred into CytoLyt solution, centrifuged and resuspended in PreservCyt solution. Cytospin spots have been positioned onto conductive slides and intact proteins MALDI-MSI analysis was performed within the *m/z* 3000–20,000 range. Regions of interest (ROIs) containing pathological areas (thyrocytes clusters) were comprehensively annotated by pathologist. This pilot study underlines the feasibility of the MALDI-MSI approach to spatially localize proteins in cancer cells area and its ability to discriminate, based on the proteomic profile, hyperplastic and PTC *real* FNA [4].

The present study introduces an original methodological approach to build a proteomic diagnostic tool in thyroid cytopathology by taking advantage of MALDI-MSI technology for the characterization of indeterminate for malignancy thyroid nodules.

References

1. Mosele N, Smith A, Galli M, Pagni F, Magni F (2017) MALDI-MSI analysis of cytological smears: the study of thyroid cancer. Methods Mol Biol 1618:37–47. https://doi.org/10.1007/978-1-4939-7051-3_5
2. Piga I, Capitoli G, Denti V, Tettamanti S, Smith A, Chinello C, Stella M, Leni D, Garancini M, Galimberti S, Magni F, Pagni F (2019) The management of haemoglobin interference for the MALDI-MSI proteomics analysis of thyroid fine needle aspiration biopsies. J Anal Bioanal Chem 411(20):5007–5012. https://doi.org/10.1007/s00216-019-01908-w
3. Piga I, Capitoli G, Tettamanti S, Denti V, Smith A, Chinello C, Stella M, Leni D, Garancini M, Galimberti S, Magni F, Pagni F (2019) Feasibility study for the MALDI-MSI analysis of thyroid fine needle aspiration biopsies: evaluating the morphological and proteomic stability over time. Proteomics Clin Appl 13(1):e1700170. https://doi.org/10.1002/prca.201700170
4. Capitoli G, Piga I, Galimberti S, Leni D, Pincelli AI, Garancini M, Clerici F, Mahajneh A, Brambilla V, Smith A, Magni F, Pagni F (2019) MALDI-MSI as a complementary diagnostic tool in cytopathology: a pilot study for the characterization of thyroid nodules. Cancers 11(9):pii: E1377. https://doi.org/10.3390/cancers11091377

Chapter 25
Luminescent Polymeric Nanovectors Loaded with Darunavir for Treatment of HIV-Associated Neurological Diseases

F. Rizzi, T. Latronico, A. Panniello, V. Laquintana, N. Denora, I. Arduino, A. Fasano, C. M. Mastroianni, E. Fanizza, M. Striccoli, A. Agostiano, G. M. Liuzzi, M. L. Curri, and N. Depalo

Human Immunodeficiency Virus (HIV)-associated neurocognitive disorders (HAND) are worrying comorbidities of various severity in HIV-infected patients over long term, arising from the invasion of HIV into the central nervous system (CNS). Currently, antiretroviral therapy (ART) represents the more effective therapeutic approach to HAND. Darunavir (DRV) is an antiretroviral drug of the class of HIV protease inhibitors and it has been approved for treatment of HIV-infected patients in combination with other antiretroviral drugs. MMP-2 and MMP-9 are two members of the family of matrix metalloproteinases (MMPs), that represent factors responsible for the development of HIV-related neurological disorders. The ability

F. Rizzi (✉) · A. Panniello · M. Striccoli · N. Depalo
Istituto per i Processi Chimico-Fisici-CNR SS Bari, Bari, Italy
e-mail: f.rizzi@ba.ipcf.cnr.it

T. Latronico · I. Arduino · A. Fasano · G. M. Liuzzi
Dipartimento di Bioscienze, Biotecnologie e Biofarmaceutica, Università degli Studi di Bari Aldo Moro, Bari, Italy

V. Laquintana
Dipartimento di Farmacia-Scienze del Farmaco, Università degli Studi di Bari Aldo Moro, Bari, Italy

N. Denora
Istituto per i Processi Chimico-Fisici-CNR SS Bari, Bari, Italy

Università degli Studi di Bari Aldo Moro, Dipartimento di Farmacia, Scienze del Farmaco, Bari, Italy

C. M. Mastroianni
Dipartimento di Sanità Pubblica e Malattie Infettive, Università degli Studi di Roma "Sapienza", Rome, Italy

E. Fanizza · A. Agostiano · M. L. Curri
Istituto per i Processi Chimico-Fisici-CNR SS Bari, Bari, Italy

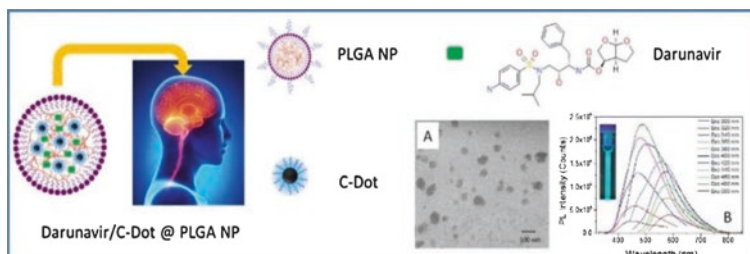Dipartimento di Chimica, Università degli studi di Bari 'Aldo Moro', Bari, Italy

255

Fig. 25.1 Transmission electron microscopy micrograph (**a**) and photoluminescence spectra as a function of excitation wavelength (**b**) of luminescent PLGA-based nanovectors for the delivery of DRV to CNS

of DRV to inhibit *in vitro* gelatinases A (MMP-2) and B (MMP-9) in astrocytes has been demonstrated [1]. However, owing to its low bioavailability when administered orally, poor water solubility and intermediate CNS penetration effectiveness score, innovative DRV formulation could improve its effectiveness to cross the blood brain barrier (BBB) and ability to reach the targets. The use of optically traceable nanoparticles (NPs) able to encapsulate and deliver specific therapeutic agents may not only enhance drug transport through the BBB and target relevant regions in the brain, but also provide an effective optical monitoring of the process. For this purpose, biodegradable poly (D,L-lactide-co-glycolide) (PLGA)-based NPs were used as nanovectors for the delivery of biocompatible luminescent Carbon Dots (C-Dots) and DRV. The resulting nanoformulations were extensively investigated in terms of their optical and morphological properties. PLGA-based NPs offers drug improved stability, high loading capacity, sustained drug release, non-immunogenic property, reduced drug toxicity and enhanced bioavailability, while C-Dots are promising candidate for imaging-guided therapy [2]. The prepared NPs with an average hydrodynamic diameter of ~130 nm, resulted characterized by high colloidal stability in aqueous medium, high drug encapsulation efficiency and emission properties in the visible region. The *in vitro* study on astrocytes demonstrated the high biocompatibility of the NPs and, remarkably, proved their ability to cross an *in vitro* model of BBB [3] and to modulate the expression of MMP-9. The overall results highlight the great promise hold by the luminescent nanoformulations as traceable delivery nanovectors of DRV for the treatment of HAND (Fig. 25.1).

References

1. Latronico T et al (2018) *In vitro* effect of antiretroviral drugs on cultured primary astrocytes: analysis of neurotoxicity and matrix metalloproteinase inhibition. J Neurochem 144(3):271–284
2. Panniello A et al (2018) Luminescent oil-soluble carbon dots toward white light emission: a spectroscopic study. J Phys Chem C 122(1):839–849
3. Liuzzi GM et al (2004) Anti-HIV drugs decrease the expression of matrix metalloproteinases in astrocytes and microglia. Brain 127(2):398–407

Chapter 26
Investigation of the N-Glycoproteome in the Urinary Exosomes: Technical Challenges

Lucia Santorelli, Elisa Barigazzi, M. Pitto, and F. Raimondo

Abstract Urinary Exosomes (UE) are membranous nanometer-sized vesicles that can originate from endothelial cells, podocytes or tubular epithelial cells. Their molecular composition depends upon the type, and even status, of the producer cell. Their presence in urine makes them readily accessible, representing a *liquid biopsy*, non-invasive modality capable to provide diagnostic and prognostic information about kidney health state. Additionally, the UE proteome includes many species that are N-glycomodified. N-glycosylation is one of the most complex and frequent protein post-translational modifications, playing diverse biological roles. Additionally, it is reported that disease-specific glycosylation profiles of circulating microvesicles were detected in autosomal dominant polycystic kidney disease and ovarian carcinoma. This study is set in this context. Our aim is to provide the best MS-sample preparation protocol to study the UE glycosylated protein content, focusing our efforts on the enrichment of the glycosylated species and simultaneously depleting the most abundant contaminant protein (Uromodulin).

Protein N-glycosylation is a biologically important post-translational modification (PTM), often altered on both glycosites and glycans. Its aberrant changes are closely associated with several diseases, including renal dysfunction and urologic malignancies [1].

In this context, Urinary Exosomes (UE), nanovesicles representing a molecular snapshot of the parental cell, are enriched in glycosylated renal proteins; in particular, their surface presents a complex glycoprotein pattern that can be considered a specific glycan signature [2]. While it is widely known the connection between UE and the pathophysiologic status of the origin cell, the characterisation of their glycoprotein content requires the development of new analytical procedures.

L. Santorelli (✉) · E. Barigazzi · M. Pitto · F. Raimondo
School of Medicine and Surgery, University of Milano – Bicocca, Milan, Italy
e-mail: l.santorelli@campus.unimib.it; e.barigazzi@campus.unimib.it

Current MS approaches for the UE glycoproteome investigation are limited by the low amount of UE proteins; furthermore, the presence of Uromodulin (UMOD), the most abundant glycoprotein in urine, hampers the UE recovery and the study of the other glycoproteins. These evidences arise a double technical challenge: primarily, the reduction of UMOD contamination, and secondly the search of a suitable strategy to investigate the UE glycoproteome. Thus, we tested different experimental procedures, starting from normal urine specimens, in order to improve the sample preparation and achieve a better MS analysis.

First, we performed the UE isolation through multistep differential centrifugations, trying to reduce UMOD presence by exploiting some chemical-physical features of this protein (oxidative state, solubility, size). The best compromise between the UE yield and the UMOD depletion emerged to be the addition of ZnSO4 to frozen urine specimens prior to UE purification. Then, we set up an optimised N-Glyco-FASP (Filter Aided Sample Preparation), a recently developed MS approach based on lectin-enrichment able to capture UE glycoproteins [3]. We compared the efficiency of different types of filters (Microcon vs Amicon) in order to improve the UE peptides and glycopeptides recovery.

Despite the small amount of starting sample (urine volume <40 ml; UE proteins <100 μg), we confirmed the correct glycopeptides enrichment, highlighting that our combined approach is suitable for the study of the UE glycoproteome. It would be interesting to glyco-characterise UE from patients affected by different type of kidney pathologies (Renal Cell Carcinoma and Idiopathic Nephrotic Syndrome), to bring out the remarkable impact of this PTM within the pathological mechanism of these diseases.

References

1. Taniguchi N, Kizuka Y (2015) Glycans and cancer: role of N-glycans in cancer biomarker, progression and metastasis, and therapeutics. Adv Cancer Res 126:11–51
2. Williams C, Royo F, Aizpurua-Olaizola O, Pazos R, Boons G, Reichardt N, Falcon-Perez JM (2018) Glycosylation of extracellular vesicles: current knowledge, tools and clinical perspectives. J Extracell Vesic 7(1):1442985
3. Deeb S, Cox J, Schmidt-Supprian M, Mann M (2014) N-linked glycosylation enrichment for in-depth cell surface proteomics of diffuse large B-cell lymphoma subtypes. Mol Cell Proteomics 13(1):240–251

Chapter 27
Fluoroquinolones in Water: Removal Attemps by Innovative Aops

Laura Scrano, Luca Foti, and F. Lelario

27.1 Introduction

Water pollution is becoming dramatic because of increasingly invasive and deleterious anthropic activities.

A significant number of contaminants called "Emerging Pollutants" (EPs) resulting from point and diffuse pollution are present in the aquatic environment.

These compounds, belonging to pharmaceuticals, industrial chemicals, surfactants, personal care products, analgesics, antibiotics, hormones and a whole range of other pharmaceutical compounds including anti-inflammatory, anti- diabetic, and antiepileptic drugs, are not commonly monitored but have the potential to enter the environment and cause adverse ecological and human health effects [1].

The threat lies in the fact that the environmental and human toxinology of most of these compounds has not been well addressed yet and many of these compounds are not removed by the conventional WasteWater Treatment Plants (WWTPs). Moreover, when these contaminants pass through the drinking water treatment systems undergo trasformations that generate derivative substances whose chemical properties remain undetermined. For this reason, it is necessary to try to find low-cost and easy-to-handle alternative methods to solve this vast problem.

Fluoroquinolones, which are powerful antibiotics used in human and veterinary medicine for the treatment of diseases and infections are among the drugs most frequently found in environmental waters along with sulfonamides, tetracyclines and macrolides. The synergistic action of these drugs can cause what is known as "bacterial resistance", which is the cause of 700,000 annually people death in worldwide due to resistant infections according to Joint Research Center (JRC)

L. Scrano (✉) · L. Foti · F. Lelario
University of Basilicata, Potenza, Italy
e-mail: c.alaura.scrano@unibas.it; luca.foti@unibas.it

2018 report.. This means that if no action is taken the estimated annual deaths attributable to bacterial resistance will be 10 million by 2050.

Adsorption by using porous materials (like activated carbon, polymeric resins, natural clay and organoclay complex adsorbents) was found to be one of the most simple, efficient, cost-effective, flexible methods to remove fluoroquinolonesin the wastewater treatment process. However, this technique does not lead to the complete removal of parent chemicals and their degradation products and, consequently, other treatments are needed for their mineralization.

Advanced Oxidation Processes (AOPs) can be a good choice because, basically, involve the generation of highly reactive free radicals, which convert the organic contaminants into final non-toxic by-products.

Among the various semiconductors employed, TiO_2 is the most preferable material for the photo-catalytic process (high photosensitivity, non-toxic nature, large band gap, chemical stability and low cost).

In this research the photocatalytic activity of this semiconductor immobilized onto the surface of glass borosilicate tubes was evaluated on levofloxacin (trade name Levaquin and other), which is an antibiotic used to treat a number of bacterial infections including acute bacterial sinusitis, pneumonia, urinary tract infections, chronic prostatitis, and some types of gastroenteritis. Kinetics of photoreactions were determined in ultrapure and ground water samples spiked with levofloxacin and photoproducts where identified by liquid chromatography coupled with micrOTOF-Q-II-Mass Spectrometer (LC-MS, Bruker Daltonik GmbH, Bremen).

27.2   Material and Methods

Levofloxacin (MW, 361,37 g mol^{-1}) pure standard (purity, 98%) was purchased from HPC (High Purity Compounds, Cunnersdorf, Germany), all solvent for HPLC analysis grade were purchased from Sigma Aldrich (Munich, Germany).

All the solutions were daily prepared and to avoid microbial contamination, all glass apparatus were heat sterilized by autoclaving for 60 min at 121 °C before use. Aseptic handling materials and laboratory facilities were used throughout the study to maintain sterility.

The groundwater was characterized according to standard methods (APHA, 2005).

The solar experiments were performed using a solar simulator device Heraeus Suntest CPS+ (Atlas, Chicago, USA), equipped with a 1500 W xenon arc lamp protected with a quartz filter (total passing wavelength: 280 nm < λ < 800 nm). The irradiation chamber was maintained at 20 °C by both circulating water from a thermostatic bath and through a conditioned airflow.

The irradiation system was dynamic: the solutions of levofloxacin (dissolved in ultrapure water or groundwater) was passed through the borosilicate tube, coated with TiO_2 on the internal and external surfaces, closed into the photoreactor and irradiated with the xenon arc (Fig. 27.1) [2]. At predetermined times aliquots of
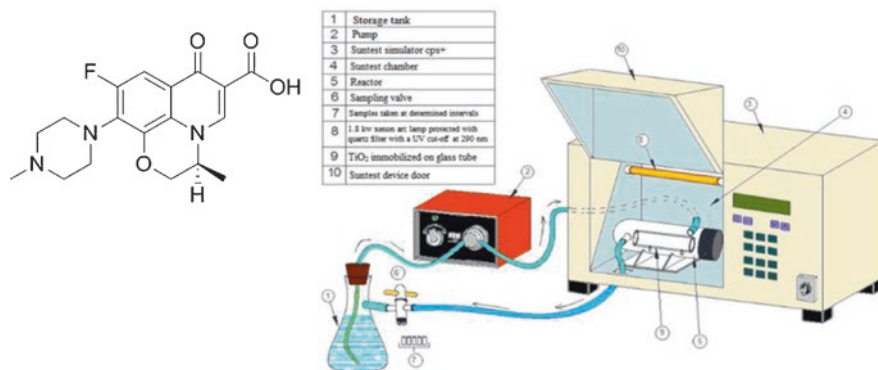
1	Storage tank
2	Pump
3	Suntest simulator cps+
4	Suntest chamber
5	Reactor
6	Sampling valve
7	Samples taken at determined intervals
8	1.5 kw xenon arc lamp protected with quartz filter with a UV cut-off at 290 nm
9	TiO₂ immobilized on glass tube
10	Suntest device door

Fig. 27.1 Levofloxacin structure and dynamic system of irradiation

solution were collected for the subsequent analytical determinations. The behaviour of this pharmaceutical in the dark was tested too.

Levofloxacin concentrations were monitored using High Performance Liquid Chromatography (HPLC) (1200 series, Agilent Technologies, USA) equipped with a C-18 column (SUPELCOSIL Discovery 5 micron-C18, 250 × 4.6 mm) and a diode array detector (DAD); λ, 295 nm.

The isocratic mobile phase was 75% formic acid (0.05%) and 25% methanol. The flow rate was 1.0 mL min^{-1}.

The identification of photoproducts was performed using micrOTOF-Q-II-Mass Spectrometer (LC-MS, Bruker Daltonik GmbH, Bremen). Mass spectrometric conditions were optimized by direct infusion of standard solutions. The instrument was tuned to facilitate the ionization process and to achieve the highest sensitivity.

27.3   Results and Discussion

The chemical characteristics of the groundwater used in the experiments are reported in Table 27.1.

Kinetic data calculated considering three replicates for each experiment are summarized in Table 27.2 (Table 27.3).

The levofloxacin fates in ultrapure and in groundwater seem to follow the same kinetic behaviour and the same photo-intermediates were detected and identified until the complete mineralization of the parent compound. During the photoreactions samples were collected to test the remaining toxicity of the solution by using official environmental assays (*Daphnia magna and Vibrio fischeri*) and phytotoxicity assays as seed germination (SG) and radical elongation (RE) of *Solanum lycopersicum* L. (tomato) and *Lepidium sativum* L. (garden cress).The toxicological data shows that the products of intermediate degradation are more toxic than the parent compound. Therefore, it is necessary to complete the reaction up to the

Table 27.1 Chemical and microbiological characteristics of ground water samples used for the photodegradation assays

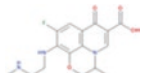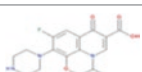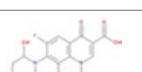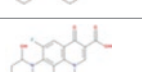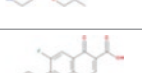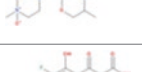| Parameters	Units	Data
pH	pH unit	7,98
Conductivity	µS/cm a 20 °C	332
Alkalinity	mg L^{-1}CaCO3	187
Bicarbonate	g L^{-1}	207
Ca	mg L^{-1}	61
Residual chlorine	mg L^{-1}	0,20
Chloride	mg L^{-1}	7,98
Na	mg L^{-1}	8,55
Settable solids (180 °C)	mg L^{-1}	264
Fecal streptococci	CFU/100 ml	<1
Escherichia Coli	CFU /100 ml	<1
Pseudomonas Aeruginosa	CFU /250 ml	0
Total microbial loads at 22 °C	CFU /1 ml a 22 °C	1
Total microbial loads at 37 °C	CFU /1 ml a 37 °C	1
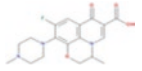
Table 27.2 Kinetic parameters of Levofloxacin degradation: n, reaction order; $t_{1/2}$, half-life; k, kinetic constant; R^2, determination coefficient of the linearized kinetic equation. Values were obtained on the basis of three replicate experiments

Samples	Method of degradation	Apparent kinetic order	k(L mol^{-1} min^{-1})	$t_{1/2}$(min)	R^2
Levofloxacin in distilled water	Xenon lamp + TiO$_2$-coated borosilicate tube	Second order $C_t = C_0 t_{1/2}/$ $(t + t_{1/2})$	0.06119	272	0.9954
Levofloxacin in ground water			0.10978	152	0.9985

mineralisation of the contaminant and its derivatives to avoid the diffusion of more toxic products to the environment. In any case, the developed photocatalysis system solves two fundamental problems:

1. eliminates the contaminant that with the filtration and adsorption systems would only be moved from one environment to another;
2. eliminates the need to recover titanium dioxide powder once the process is complete

Table 27.3 Structure and molecular formula of photo products obtained and identified during the photodegradation assays

Structure	Molecular formula [M+H]$^+$	Accurate m/z [M+H]$^+$	Error (ppm)	Sunligth + Tube	Sunlight + Tube (G.W.)
	$C_{18}H_{21}FN_3O_4^+$	362.1511	−3.4	x	x
	$C_{16}H_{19}FN_3O_4^+$	336.1354	−4.3	x	
	$C_{17}H_{19}FN_3O_4^+$	348.1354	−7.9	x	x
	$C_{16}H_{17}FN_3O_5^+$	350.1147	−4.9	x	x
	$C_{17}H_{19}FN_3O_5^+$	364.1303	−9.4	x	x
	$C_{18}H_{21}FN_3O_5^+$	378.1460	−9.7	x	x
	$C_{18}H_{21}FN_3O_6^+$	394.1409	−13.1	x	x

References

1. Zuccato E, Castiglioni S, Fanelli R (2005) Identification of the pharmaceuticals for human use contaminating the Italian aquatic environment. J Hazard Mater 122(3):205–209
2. Khalaf S, Shoqeir JH, Scrano L, Karaman R, Bufo SA (2019) Photodegradation using TiO2-activated borosilicate tubes. Environ Sci Pollut Res 26(19):19025–19034

Chapter 28
Evaluation of Surface Second Harmonic Generation SSHG for Detection of Antibody-Antigen Interactions

Abdel Mohsen Soliman

Abstract Surface Second Harmonic Generation (SSHG) is an optical non-linear analytical technique that has been applied to various biological and non-biological systems. Its application to biological systems has been limited to imaging and studies of molecular structures. However, its potential as a label-free method to detect bio-molecular interactions was not thoroughly investigated. This study explored, probed and evaluated the potential of SSHG as a viable biosensing technique.

The present study is undertaken to investigate the application of SSHG technique as a viable biosensing technique. This work probed immunoassays of a protein antigen (Ag), namely bovine serum albumin (BSA). The Ag-Ab interactions were detected using (ELISA). BSA was selected to represent natural non-glycoslated proteins. The optimization processes were trial and error experimentation with various Ag and its Primary Antibody (PAb) concentrations. Application of SSHG spectroscopy on these immunoassays and comparing them with the reference method, i.e. ELISA.

Keywords SSHG · BSA · Laminin · PAb · Biosensor · ELISA

28.1 Materials and Methods

28.1.1 Bovine Serum Albumin (BSA) Model

BSA was used as an Ag and purified rabbit anti-BSA was used as PAb.

A. M. Soliman (✉)
National Research Centre of Egypt, Cairo, Egypt

265

28.1.2   Indirect Enzyme-Linked Bioassays on 96-Microwell Format Plate

Indirect enzyme-linked bioassay of Ag-Ab was used as a reference test methods for 96-microwell formats

28.1.3   SSHG Spectroscopy Sampling and Analysis Procedure for 96-Microwell Format

The aim of this stage of the study is reproducing several replicates of the optimised immunoassays. The objective of this stage is to investigate the application of SSHG spectroscopy on biomolecular interactions by comparing SSHG modulation to the reference method readings.

The following SSHG readings were recorded during this phase of study as follows:

1. From empty surfaces, i.e. prior to depositing Ag, denoted as $SSHG_e$.
2. After depositing Ag and washing excessive deposited biomolecules and drying phase, denoted as $SSHG_{wd}$.
3. After forming Ag-Ab complex, denoted as $SSHG_{pb}$.

SSHG Readings
The general procedure for SSHG spectroscopy on immunoassays and DNA bioassays is summarised as follows:

1. Prepare replicates of the optimised enzyme-linked bioassay following the procedure described. NB. Only dilution steps for which the best linear fit is observed are needed to prepare these replicates in this step.
2. Prior to step 1, programme the scanner to select five random selected spots from each microwell and record $SSHG_e$ (Namely, the centre of each microwell and other four radial points located at 0.25 mm from the centre were selected). At step 2 of the preparation procedure, programme the scanner to scan the spots selected in 2 and record $SSHG_{wd}$.
3. At step 5 of the preparation procedure, programme the scanner to scan the spots selected in 2 and record $SSHG_{pb}$ values.

Analysis of SSHG Readings
1. Compute SSHG modulation due to Ag deposition, denoted as $\Delta SSHG_{depos\text{-}empty} = SSHG_{wd}\text{-}SSHG_e$.
2. For $\Delta SSHG_{depos\text{-}empty}$ compute the following statistical parameters: mean, median, standard deviation, variance and test the data for normal distribution using parametric tests. These parameters are used to examine central tendency and variance of data.

3. Compute SSHG modulation due to the biomolecular interaction denoted as $\Delta SSHG_{interact.} = SSHG_{pb}\text{-}SSHG_{wd}$.

4. Apply Passing and Bablok Regression analysis to compare $\Delta SSHG_{interact}$ values to their corresponding enzyme-linked ODs values to examine agreement between the two test methods.

5. Application of SSHG Spectroscopy to BSA using eight replicates of the optimised ELISA BSA plates.

28.2   Results

28.2.1   SSHG Spectroscopy for BSA Model

The results of this analysis are shown in (Figs. 28.1, 28.2, 28.3 and 28.4). Both the intercept and slope 95%CI revealed a null hypothesis, i.e. the intercept 95%CI did not include 0 (0.297–1.702) and the slope 95%CI did not include 1 (−2.398 to −0.481), indicating that there is disagreement between the two methods.

28.3   Discussion

Proteins are classified either as "soft" such as BSA or "hard" such as myoglobin and cytochrome [1]. BSA was selected as a representative for natural soft non-glycosylated proteins. Conformational studies of BSA and its closely-related human serum albumin (HSA) showed that they tended to retain their native conformation immediately after being deposited on a solid surface [2]. Thus, BSA was selected as a flexible protein as its activity is not likely to be influenced by deposition on solid surfaces. In the present investigation the Passing and Bablok regression analysis
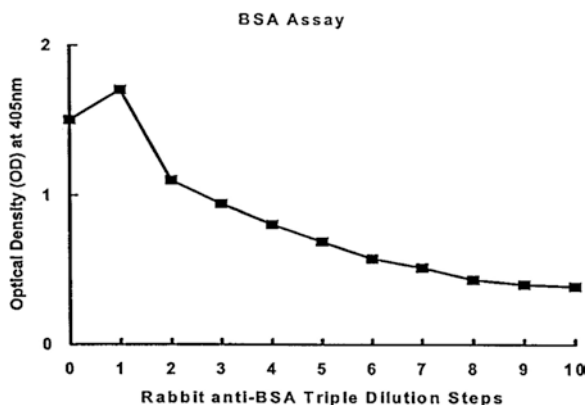

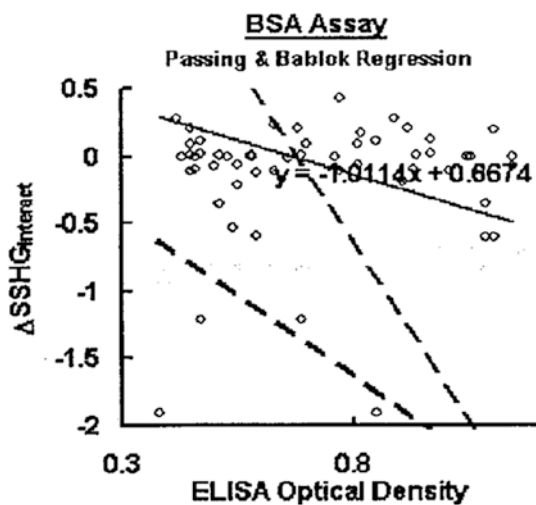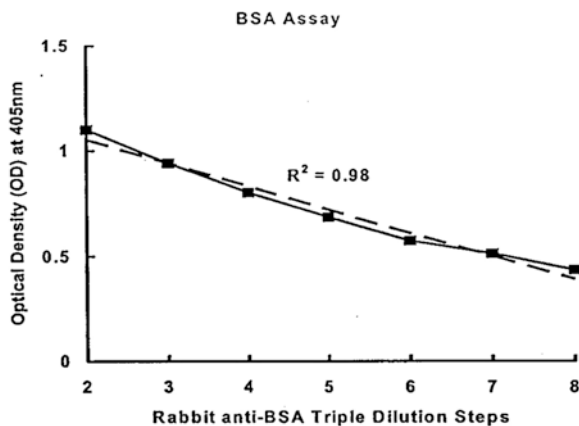**Fig. 28.1**   Optical densities for BSA ELISA plate

Fig. 28.2 Best linear fit
for BSA ELISA plate

Fig. 28.3 Passing and Bablok Regression comparing ELISA optical density with ΔSSHGinteract
of the SSHG spectroscopy for BSA

results for BSA indicate that for SSHG modulation, i.e. $\Delta SSHG_{interact}$, to be associated exclusively with Ag-Ab complex formation, it should show a compatible trend (whether increasing or decreasing) with that of PAb concentration. The lack of observing this indicates that the detected SSHG modulation is not exclusively linked to the formation of Ab and Ag complex. It had been reported that several

Fig. 28.4 Residuals and cumulative sum (cusum) of Passing and Bablok regression analysis for comparing ELISA Optical Density to $\Delta SSHG_{interact}$ of the SSHG spectroscopy
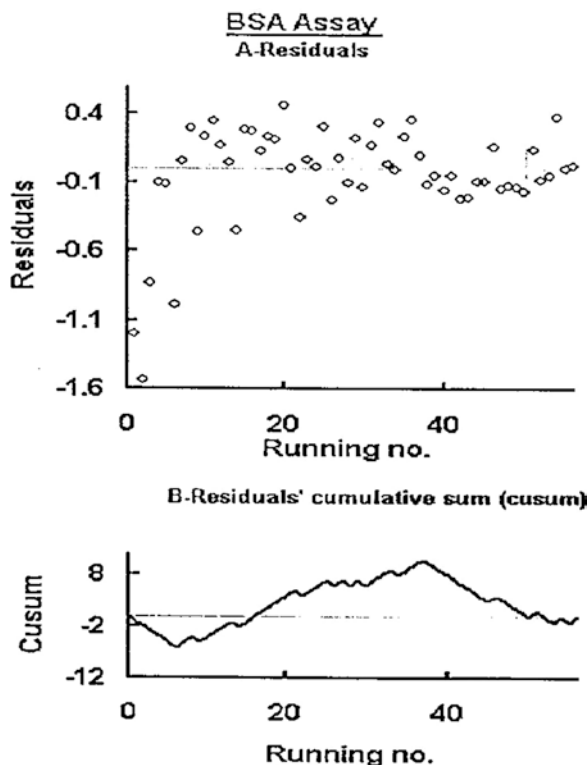
experimental factors influence SSHG spectroscopy results. These include the pulse width, average power, wavelength and polarization of the laser, the numerical aperture of the microscope objective, the length of interaction, the detection geometry of the imaging system, as well as inter-dependences between these factors [3]. Moreover, one of identified flaws in this study was complication introduced by random immobilisation of biomolecules. This is in agreement with other workers [4-5]. who identified the problem facing implementing optical biosensing techniques as difficulty of obtaining a reproducible, well-defined sensor surface, due to random immobilisation of biomolecules. Thus, it is more likely that recorded SSH signals during each stage were attributed to the aggregate effect of bioassays including sources within the microwell materials [6-7]. So to ensure reproducibility within the data, experiments should be designed on media or substrates with uniform SSHG characteristics. Also this phase of the study indicated clearly that there is a need to record SSHG data from different stages of assay preparation. This would enable monitoring of SSHG susceptibility introduced by each stage. It is worth noting that in an optimal configuration, it would be expected that most of protein molecules in the upper monolayer would contribute to the signal sensor. Therefore it would be very interesting to experiment with diversified surfaces that would produce aniso-tropic and oriented immobilisation of protein. The use of diversified surfaces that

meet such criterion has been widely reported in the literature [8-9]. Such surfaces might produce surfaces with minimal background interference.

28.4   Conclusions and Recommendations

1. SSHG signal modulations were detected by the modified SSHG experimental system. This indicated the ability of the SSHG experimental setup to distinguish between different deposited layers.
2. Passing & Bablok Regression analysis between the ELISA optical densities for segments (showing linear correlation with dilution steps) and corresponding $\Delta SSHG_{interact}$, indicated that the modulations in SSHG signals were not linked to the bio interaction between Ag and their PAbs.
3. Possible reasons for the lack of agreement between SSHG spectroscopy ELISA, could be due to the lack of homogeneity within the matrix of microwells, lack of precision of sampling by SSHG or random orientation of biomolecules, in addition to experimental errors.
4. To further investigate SSHG capability, the use of oriented immobilisation would be highly recommended.

References

1. Cao T, Wang G, Han WH et al (2012) Valley-selective circular dichroism of monolayer molybdenum disulphide. Nat Commun 3(887):1–5
2. Mak KF, He K, Lee CGH, et al (2013) Tightly bound trions in monolayer MoS2. Nat Mater 12:207–211
3. Radisavljevic B, Radenovic A, Brivio J, Kis VGA (2011) Single-layer MoS2 transistors. Nat Nanotechnol 6:147–150
4. Yin Z, Li H, Li HL, et al (2012) Single-Layer MoS2 Phototransistors. ACS Nano 6:74–80
5. Tran RJ, Sly KL, Conboy JC (2017) Determination of multivalent protein–ligand binding kinetics by second-harmonic correlation spectroscopy. Annu Rev Anal Chem 12:387–414
6. Kato N (2019) Optical second harmonic generation microscopy: application to the sensitive detection of cell membrane damage. Biophys Rev 11(3):399–408
7. Wang W, Wu B, Liu P, Liu J, Tan J (2019) Calculations of second harmonic generation with radially polarized excitations by elliptical mirror focusing. J Microsc 273(1):36–45
8. Wang W, Wu B, Lin S, Li X, Liu J, Tan J (2019) Rigorous modelling of second harmonic generation imaging through stratified media focused by radially polarized beams. Opt Express 27(14):19737–19748
9. Sun J, Wang X, Chang S, Zeng M, Shen S, Zhang N (2016) Far-field radiation patterns of second harmonic generation from gold nanoparticles under tightly focused illumination. Opt Express 24(7):7477–87

Chapter 29
Impact of Asbestos-Related Toxicity on Italian Working Population: Preliminary Incidence Data from the Last 5 Years across the Whole Country

Antonio Vinci, F. Ingravalle, S. Mancinelli, M. D'Ercole, F. Lucaroni, and L. Palombi

Abstract During the last years Italy showed an overall decreasing tendency of asbestos-related diseases, following the general trend happening in all the high-income countries because of the ban of the asbestos compounds.

There is significant distribution gradient between northern and southern Italian provinces. Further studies could be aimed at investigating whether this gradient is attributable to a real gap in incidence, due to the highest industrialization process affecting Northern Italy, or to an underreporting phenomenon in the South. Therefore, a detailed surveillance of the problem, for instance by case finding methods, could be an effective tool to assess new emerging cases. Identifying workers at risk would indeed allow public health servants to manage large-scale primary, secondary and tertiary prevention programs targeted on occupational risks.

29.1 Introduction

Asbestos is a group of naturally occurring silica minerals consisting of long and thin fibrous crystals, each one composed of minuscule volatile units named "fibrils" [1]. Asbestos fibrils interaction with human biology is well-known and documented, and asbestos is a notorious health hazard, being the sole aetiologic agent of asbestosis and mesothelioma [2]. It has also been linked to an increased risk for ovaries, larynx and gastro-intestinal cancer [3].

Asbestos is nowadays banned in more than 55 countries [4], because of its ascertained toxicity and carcinogenicity, as the result of a process begun in 1973 [5]. However, it still represents a global hazard because of its widespread use during the

A. Vinci (✉) · F. Ingravalle · M. D'Ercole
School of Hygiene and Preventive Medicine, Tor Vergata University of Rome, Rome, Italy

S. Mancinelli · F. Lucaroni · L. Palombi
Department of Biomedicine and Prevention, Tor Vergata University of Rome, Rome, Italy

last century. Indeed, asbestos was commonly utilized in construction industry (for building insulation and roofs), for water supply lines, or to build automotive parts [6].

Although no longer used in the most part of high-income countries, some of the developing nations, as India and China, still include it in various products, using hundreds of thousands of metric tons each year. Inevitably, asbestos-containing products are yet shipped to Western countries [7].

Because of the massive use of asbestos compounds during the past and the long latency of asbestos-related diseases (e.g. up to 47 years for mesothelioma development since first exposure), it emerged as a major health concern only during the last decades, especially among the working population [8]. For this reason, the attention to the occupational risk of asbestos chronic exposure has significantly increased.

In Italy, a national registry for asbestos-related diseases was set up. According to Italian law [9], the employer must report to the local office of the Italian National Agency for Insurance Against Work Injuries (INAIL) the occurrence of occupational asbestos-related diseases, within 5 days from the initial diagnosis, as certified by the General Practitioner.

29.2   Research Goal

Aim of the study is to draw the trend of asbestos-related diseases in Italian workers during the 2014–2018 period.

29.3   Materials and Methods

Ascertained diagnoses of asbestos-related diseases among workers were collected from the INAIL public registry [10] from 1st January 2014 to 31st December 2018.

Yearly incidence rate of asbestos-related diseases among workers was estimated by province, as the number of incident cases per million workers, and mapped by year.

Distribution Data regarding workforce population from open data provided by the Italian National Institute of Statistics (ISTAT) [11].

Yearly map sources of administrative repartitions were retrieved from official ISTAT source [12].

29.4   Results

Incidence rate rapidly increased from 2014, peaking at 7.2 new cases per 100.000 workers in 2015. Afterwards, the number of ascertained cases decreased by nearly 2 in 100,000 during the next 3 years, bottoming at 5.1 cases in 2018 (Fig. 29.1).
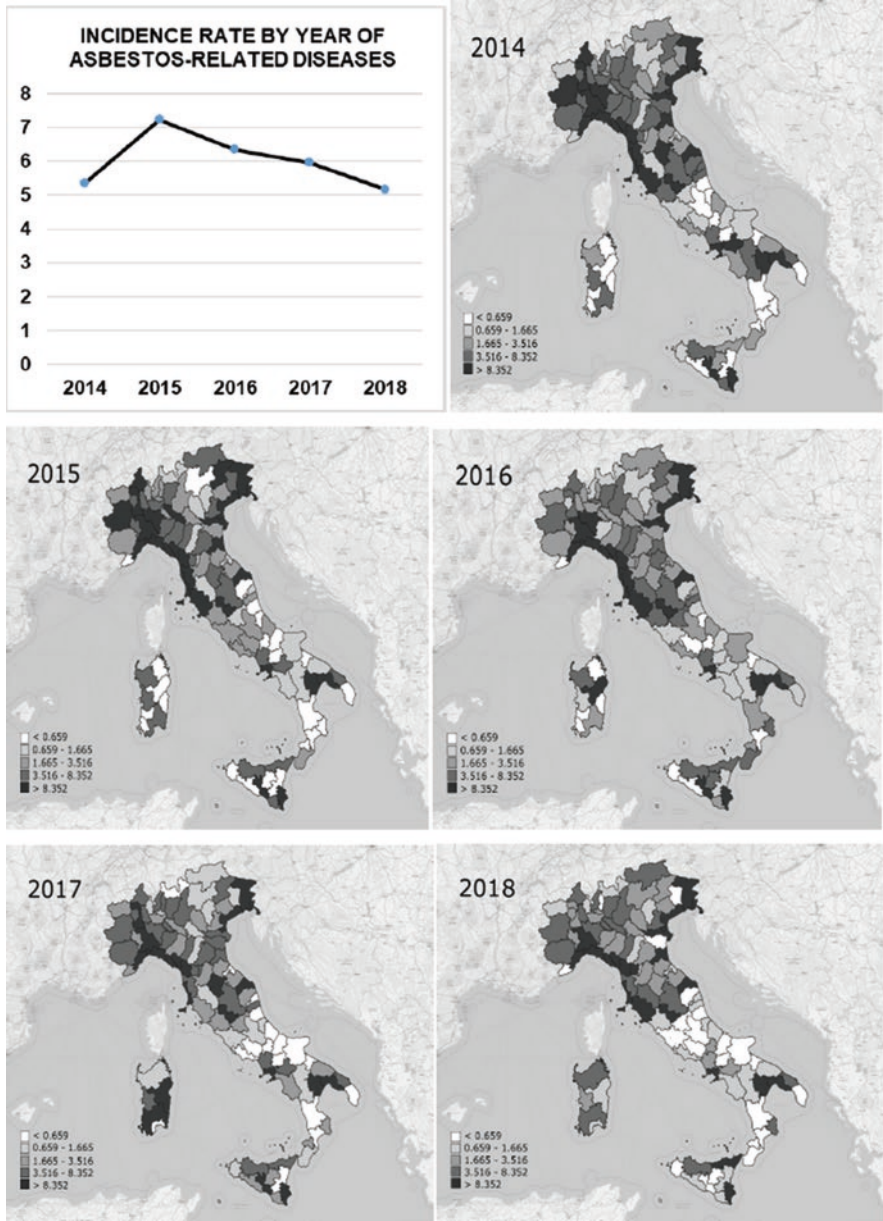
Fig. 29.1 Incidence rate of Asbestos-related diseases in Italy (per 100,000 workers)

Furthermore, there was a clear gradient distribution of incidence rate, with the highest rates in Northern Italy, as shown in Fig. 29.1. This is particularly evident for the year 2014 and declines over the time.

Gorizia province had the highest number of ascertained diagnoses every year, with a peak at 19.9 new cases by 100,000 workers in 2015.

Concerning disease types, mesothelioma, in its different variants (pleura, peritoneum, other sites or unspecified), was the most common one, with 2995 ascertained cases (35% of the sample). It was followed in the ranking by pleural plaques (2955 cases, 34%), pneumoconiosis (1327 cases, 15%) and lung cancer and cancer of the respiratory tract (1298 cases, 14%). These disorders together represent almost 99% of the retrieved cases.

29.5   Discussion and Conclusions

During the last years Italy showed an overall decreasing tendency of asbestos-related diseases, following the general trend happening in all the high-income countries because of the ban of the asbestos compounds.

Another noticeable feature is the significant difference between northern and southern Italian provinces. Further studies could be aimed at investigating whether this gradient is attributable to a real gap in incidence, due to the highest industrialization process affecting Northern Italy, or to an underreporting phenomenon in the South.

Therefore, a detailed surveillance of the problem, for instance by case finding methods, could be an effective tool to assess new emerging cases. Identifying workers at risk would indeed allow public health servants to manage large-scale primary, secondary and tertiary prevention programs targeted on occupational risks.

References

1. Young GJ, Healey FH (1954) The physical structure of asbestos. J Phys Chem 58:881–884
2. International Agency for Research on Cancer (IARC) IARC Monographs. Arsenic, metals, fibres and dusts. 2012 Volume 100C. A Review of Human Carcinogens. Available online: http://monographs.iarc.fr/ENG/Monographs/vol100C/mono100C.pdf. Accessed 11 Sep 2019
3. Henley SJ, Peipins LA, Rim SH, Larson TC, Miller JW (2019) Geographic co-occurrence of mesothelioma and ovarian cancer incidence. J Womens Health (Larchmt). https://doi.org/10.1089/jwh.2019.7752. [Epub ahead of print]
4. Lin RT, Chien LC, Jimba M, Furuya S, Takahashi K (2019, Aug) Implementation of national policies for a total asbestos ban: a global comparison. Lancet Planet Health 3(8):e341–e348. https://doi.org/10.1016/S2542-5196(19)30109-3
5. Frank AL, Joshi TK (2014) The global spread of Asbestos. Ann Glob Health 80(4):257–262. https://doi.org/10.1016/j.aogh.2014.09.016
6. Walton WH (1982) The nature, hazards and assessment of occupational exposure to airborne asbestos dust: a review. Ann Occup Hyg 25(2):117–119. https://doi.org/10.1093/annhyg/25.2.117

7. International Agency for Research on cancer. *Asbestos (Chrysontile, Amosite, Crocidolite, Tremolite, Actinolite, and Anthophyllite) – IARC MONOGHRAPHS – 100C*. 6 2018. Retrieved from https://monographs.iarc.fr/wp-content/uploads/2018/06/mono100C-11.pdf. Accessed 11 Sept 2019

8. Marsh GM, Ierardi AM, Benson SM, Finley BL (2019, Aug) Occupational exposures to cosmetic talc and risk of mesothelioma: an updated pooled cohort and statistical power analysis with consideration of latency period. Inhal Toxicol 5:1–11. https://doi.org/10.1080/08958378.2019.1645768

9. D.P.R. n. 1124 30 June 1965, Art. 53, comma 5, "Testo Unico delle disposizioni per l'assicurazione obbligatoria contro gli infortuni sul lavoro e le malattie professionali" e successive modifiche ed integrazioni

10. INAIL Open Data warehouse. Retrieved from https://dati.inail.it/opendata/default/Qualidati/index.html. Accessed 10 Sept 2019

11. ISTAT Open Data warehouse. Retrieved from http://dati.istat.it/. Accessed 10 Sept 2019

12. ISTAT Open Data warehouse. Retrieved from https://www.istat.it/it/archivio/222527. Accessed 8 Sep 2019

Chapter 30
Magnetically Targeted Delivery of Sorafenib Through Magnetic Solid Lipid Nanoparticles Towards Treatment of Hepatocellular Carcinoma

F. Vischio, N. Depalo, R. M. Iacobazzi, M. P. Scavo, S. Villa, F. Canepa, S. Hee Lee, B. Chul Lee, E. Fanizza, I. Arduino, V. Laquintana, A. Lopalco, A. Lopedota, A. Cutrignelli, M. Striccoli, A. Agostiano, N. Denora, and M. L. Curri

Sorafenib is an anticancer drug with multikinase inhibitor activity and it is only that has proved to significantly prolong the survival time in patients with advanced hepatocellular carcinoma (HCC). However, sorafenib is characterized by severe toxic

F. Vischio (✉) · E. Fanizza · A. Agostiano · M. L. Curri
Istituto per i Processi Chimico-Fisici-CNR SS Bari, Bari, Italy

Università degli Studi di Bari Aldo Moro, Dipartimento di Chimica, Bari, Italy
e-mail: f.vischio@ba.ipcf.cnr.it

N. Depalo · M. Striccoli
Istituto per i Processi Chimico-Fisici-CNR SS Bari, Bari, Italy

R. M. Iacobazzi
Istituto Tumori IRCCS Giovanni Paolo II, Bari, Italy

M. P. Scavo
National Institute of Gastroenterology "S. De Bellis", Personalized Medicine Laboratory, Bari, Italy

S. Villa · F. Canepa
Dipartimento di Chimica e Chimica Industriale, Università di Genova, Genoa, Italy

S. H. Lee · B. C. Lee
Seoul National University College of Medicine, Seoul National University Bundang Hospital, Seongnam, Republic of Korea

I. Arduino · V. Laquintana · A. Lopalco · A. Lopedota · A. Cutrignelli
Università degli Studi di Bari Aldo Moro, Dipartimento di Farmacia, Scienze del Farmaco, Bari, Italy

N. Denora
Istituto per i Processi Chimico-Fisici-CNR SS Bari, Bari, Italy

Università degli Studi di Bari Aldo Moro, Dipartimento di Farmacia, Scienze del Farmaco, Bari, Italy

277

side effects limiting the possible therapeutic response [1, 2]. Nanoparticle (NP) based approaches offer a valuable alternative for cancer drug delivery, functioning as a carrier for entry through fenestrations in tumor vasculature, thus allowing direct cell access and ensuring the accumulation of high concentrations of drug to the targeted cancer cell, with a concomitant reduced toxicity of healthy tissue. In this contest, superparamagnetic iron oxide NPs (SPIONs) are very attractive for delivery of therapeutic agents as enhance the drug delivery to specific locations in the body through the application of an external magnetic field [3, 4]. To make more biocompatible and protect the drug, solid lipid NPs (SLN) has been used to contain sorafenib and SPIONs by means of hot homogenization technique using cetyl palmitate as lipid matrix and polyethylene glycol modified phospholipids (PEG lipids), in order to achieve a PEG-based anti-fouling coating on SLN surface. These nanoformulations, thoroughly investigated by means of complementary techniques, have finally resulted effective drug delivery magnetic nanovectors with good stability in aqueous medium and high drug encapsulation efficiency (>90%). In addition, the magnetic relaxometric characterization has proven that the SLN loaded with sorafenib and SPION are also very efficient contrast agents, with a great potential in magnetic resonance imaging (MRI) technique. Cellular uptake on HepG2 cell line shows a better effectiveness of antitumoral action of sorafenib when it is encapsulated in SLN and subjected to magnetic field. The proposed magnetic SLNs loaded with sorafenib represent promising candidates for image guided and magnetic targeting of sorafenib to liver towards an efficacious treatment of HCC.

References

1. Villanueva A et al. (2011) Gastroenterology 140:1410–1426
2. El-Serag HB et al. (2008) Gastroenterology 134:1752–1763
3. Depalo N et al. (2017) Nanoresearch 5:1909–1917
4. Hervault A et al. (2014) Nanoscale 6:11553–11573

Chapter 31
Identification of Some Organic Solvents During Regular Forensic Determination of Alcohols in Blood and Bioliquids

Igor Winkler, Nataliia Burkun, and Iryna Lebedintseva

Abstract Some mixed organic solvents (MOS) can be detected preliminary during regular gas-chromatography (GC) forensic analysis of alcohols content in human blood. Some alcohols present in MOS can form detectable concentrations of volatile esters during the pre-treatment of blood samples according to the alcohol content determination protocol and then they can manifest themselves through the corresponding GC responses recorded in the chromatogram. The '646' and '647' MOS form quite different patterns of GC, which can bring an expert to an assumption of their possible presence in the samples, which then should be verified by the corresponding more specific and quantitative methods.

Determination of alcohols in the 'alive' or corpse blood or other bioliquids is a routine part of forensic investigations and road police practice. Gas chromatography (GC) is one of reliable methods recognized in the juridical practice according to the legislation of many countries including Ukraine. Using this highly selective and sensitive method, alcohol contents can be determined and identified up to the tenth of pro mille.

According to the officially approved lab method, the sample that may consist of some traces of alcohols should be treated with trichloroacetic acid and then with the solution of potassium nitrite. As a result, nitrous acid is formed (31.1) and then it interacts with the alcohols immediately after formation, transforming them into corresponding nitrite ethers (31.2) (see the example below representing chemical reactions running in case of ethanol).

I. Winkler (✉)
Bucovinian State Medical University, Chernivtsi, Ukraine
e-mail: winkler@bsmu.edu.ua

N. Burkun · I. Lebedintseva
Chernivtsi Regional Department of Forensic Medicine, Chernivtsi, Ukraine
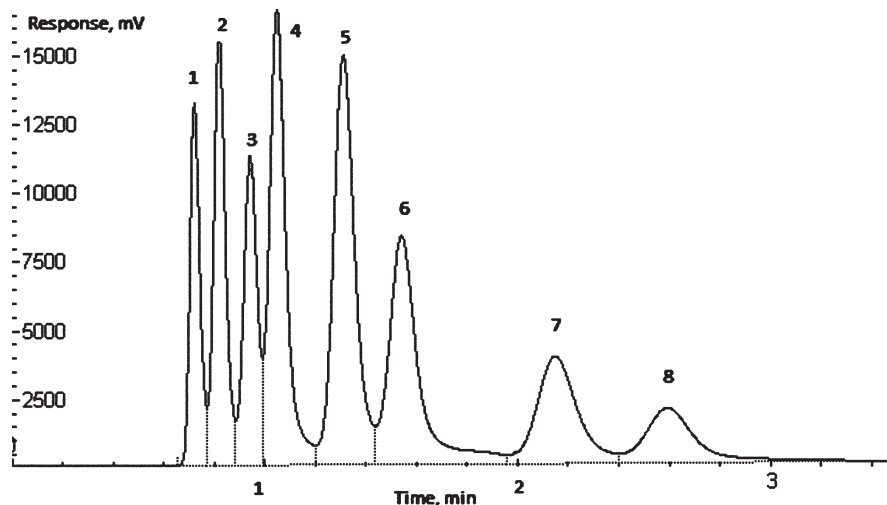
279

Fig. 31.1 Typical GC image of the eight homological alcohols (1 – methanol; 2 – ethanol; 3 – isopropyl; 4 – propyl; 5 – isobutyl; 6 – butyl; 7 – isoamyl; 8 – amyl acohols) manifesting themselves through the corresponding nitrite ethers

$$CCl_3COOH + KNO_2 \rightarrow KCCl_3COO + HNO_2 \tag{31.1}$$

$$HNO_2 + C_2H_5OH \rightarrow C_2H_5ONO_2 + H_2O \tag{31.2}$$

All these reactions should be performed in a tightly capped vessel to keep the just-formed alkyl nitrites inside. The ethers are highly volatile, they evaporate actively and a probe taken from the gas section of the vessel will contain a mixture of the ethers composed by the alcohols present in the sample. Being injected in a GC device they will manifest themselves by the corresponding peaks (see Fig. 31.1).

This method is fast, quite sensitive, comparatively simple and highly reliable. In the context of wide utilization of the above mentioned method in the everyday forensic medicine practice, it is interesting to investigate how other volatile compounds that could be present in the samples would manifest themselves in GC results.

There are multicomponent organic solvents available on the market under commercial brand names "646" and "647." These mixtures are used widely in construction and repair practices for cleaning surfaces before painting and/or for thinning paints. Insufficient ventilation of the working area or failure to keep the necessary time pause between the completion of the painting works and the beginning of regular usage of the just-painted items or rooms may cause inhalation of the solvent components followed by more or less severe intoxication. Such accidents are reported regularly in many countries.

Both compositions are in fact mixed distillates obtained from some oil products. They consist of toluene (40–50%), butyl, propyl, ethyl and some other alcohols

Table 31.1 GC peak areas (conventional units) and relative areas (%)

Alcohols	Control mixture	Control + 646	Control + 647
Methanol	36,480 (0.4091)	47,894 (0.5677 + 39%)	119,208 (0.9749 + 138%)
Ethanol	51,946 (0.5826)	80,729 (0.9570 + 64%)	171,388 (1.4016 + 140%)
Isopropanol	41,997 (0.4709)	64,215 (0.7612 + 61%)	127,701 (1.0443 + 122%)
Propanol	78,329 (0.8784)	85,922 (1.0186 + 16%)	157,817 (1.2906 + 46%)
Isobutanol	89,167 (1)	84,354 (0%)	122,281 (0%)
Butanol	69,182 (0.7759)	59,201 (0.7018–10%)	92,347 (0.7552–9.7%)
Isoamyl alc.	44,164 (0.4953)	47,756 (0.5661 + 14%)	55,595 (0.4556–9.2%)
Amyl alcohol	29,085 (0.3262)	29,528 (0.3500 + 7%)	34,207 (0.2797–15%)

(10–20%), acetate esters, acetone (below 5%) and some other minor admixtures. Each of these components can potentially be identified by GC but the corresponding experimental procedures differ from those used for identification of the alcohols. Therefore, it should be clarified how can these solvents manifest themselves in the samples during the alcohols identification and, in case any components actually provide some GC responses, which of them do they correspond to?

In order to clarify this issue, the regular mixture of eight alcohols (from methanol to amyl alcohol) has been used to obtain the reference chromatogram and then some amount of each solvent was added to the mixture. The chromatograms obtained after 'poisoning' of the mixture with the solvents has been compared with the reference one for identification of changes and/or extra peaks present at the former records.

No extra peaks appeared in the chromatograms but some obvious changes were registered for analytical responses of all low molecular alcohols (Table 31.1).

Table 31.1 represents all measured peak areas for the eight alcohols in the pure control mixture and in the same mixture with additions of '646' and '647' solvents. The percentage deviations for the '646' and '647' peak areas were calculated basing on the following. Isobutanol has been selected as the 'inner standard' since this homolog is not mentioned as a component of neither '646' nor '647' compositions. Therefore, it can be chosen as the one, for which the peak area should be taken as the base by which all other peak areas are normalized. To do that, all the peak areas should be divided by the isobutanol's area and, finally, the normalized areas of same representatives should be compared to calculate a percentage they increase or decrease in comparison with the control mixture. For example, the normalized ethanol peak areas are 0.4091, 0.5677 and 0.9749 for the control mixture and the mixtures containing '646' and '647' solvents correspondingly. Comparing the normalized '646' and '647' areas with the control mixture value, one can find that the '646' and '647' areas are 39% and 138% larger than that of the control mixture.

It can also be seen that the peak areas reveal some difference even for the heavy representatives (butanol, isoamyl and amyl alcohols) although their contents in the solvents are expected comparatively low or even too low to be mentioned. Therefore, such deviations can be considered as experimental errors, which, according to the data from Table 31.1 do not exceed ±15%.

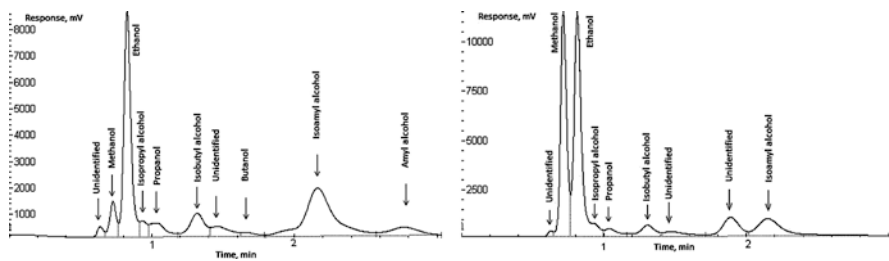**Fig. 31.2** GC images of the '646' (left) and '647' (right) solvents and the peaks of their components revealed according to the officially approved alcohol content determination method

All other alcohols showed an obvious and quite strong rise in their contents for both solvents. However, it has to be verified if their contents can be sufficient to form a representative GC peaks in case the solvents are present in the samples alone, without the eight alcohols control mixture.

This assumption has been checked by the GC investigation of the aqueous mixtures containing both solvents with the volumetric dilution ratio 1:1000. As seen in Fig. 31.2, both solvents form their own unique chromatographic patterns.

The two confident peaks of ethanol and isoamyl alcohol can be seen in case of the '646' solvent while in case of the '647' solvent two other components: methanol and ethanol form the strong peaks while the peak of isoamyl alcohol remains less reliable. All other components form less distinct peaks.

These results lead us to the conclusion that the traces of both solvents can be detected in course of the routine investigation of the human blood or other bioliquids for ethanol content. Detection of abnormal ethanol and isoamyl alcohol presence in the blood should attract the expert's attention to the fact of possible intoxication with the '646' solvent while abnormal presence of the methanol and ethanol peaks – of intoxication with the '647' solvent. This suspicion should be considered as especially probable in case the blood samples were obtained from the individuals for whom the probability of regular alcohol intoxication was not likeable (i.e. massive intoxication of schoolchildren because of possible inhalation of the contaminated air in the just-painted classrooms).